UNIVERSITY OF LEEDS

The ice-nucleating activity of fertile soils and crop pathogens

by

Kathleen Anna Thompson

Supervisors: Benjamin Murray and Catherine Noakes

Submitted in accordance with the requirements for the degree of Doctor of Philosophy

University of Leeds

School of Chemical and Process Engineering

School of Earth and Environment

March 2024

Declaration

I confirm that the work submitted is my own and that appropriate credit has been given where reference has been made to the work of others.

Acknowledgements

I want to start by thanking my main supervisors, Ben Murray and Cath Noakes, whose support and guidance have been invaluable throughout my PhD experience. I am also grateful for the additional supervisory support of Nadine Borduas-Dedekind, my Canadian supervisor for my Mitacs Globalink project, and Jon West, my industrial supervisor. I would also like to thank the team behind the Aerosol Science CDT; Jonathan Reid, Rachel Miles, Kate Lucas, Yaelle Hartley and everyone else involved in making the CDT what it is.

I was lucky enough to work with a variety of different research groups throughout my PhD; including the Ice Nucleation Group at the University of Leeds, the NBD Group at the University of British Columbia, Canada and the Protecting Crops and the Environment Group at Rothamsted Research in Harpenden, UK. I want to acknowledge the help and support received from the members of these groups, in particular, Paul Bieber, Anna Zeleny, Nicole Link, Kevin King and Gail Canning. I acknowledge the help and support from lab technicians at the University of Leeds, in particular, Andrew Hobson and Rachel Gasior. I am also grateful for the friendships I have made along the way and would like to thank Ashar Aslam, Ross Herbert, Nina Kinney and Sam Clark for sticking by me and supporting me through the rough times.

Finally, I would like to thank my close family and friends, whose unwavering support has been vital to my ability to make it through this thesis unscathed. Thanks go to my dad, for helping to proofread my introduction despite the science being somewhat beyond his remit of knowledge. A special thanks goes to my wonderful partner, Joanna. Thanks for believing in me, being there for me and providing joy in moments of despair.

This PhD was funded by the Engineering and Physical Sciences Research Council (Grant No.: EP/S023593/1). I would also like to respectfully acknowledge that the work completed in Chapter 3 was carried out on the traditional, ancestral and unceded territory of the Musqueam people.

Abstract

Atmospheric ice formation plays a key role in controlling the radiative properties and lifetimes of supercooled clouds. Ice-nucleating particles, which initiate the heterogeneous nucleation of ice in supercooled clouds, are rare in the atmosphere and crucial for the formation of ice in clouds. Therefore, our understanding of the sources and atmospheric concentrations of ice-nucleating particles is critical for our understanding of the impact of clouds on the climate. Biological aerosol particles have been identified as potentially important ice nucleators, particularly at temperatures above $-10\,^{\circ}\mathrm{C}$. However, our current understanding of the relative contribution of biological material to regional and global ice-nucleating particle populations remains poor. In particular, crop agriculture contributes up to 25% of global dust emissions, creating a potentially important source of biological ice-nucleating particles which is yet to be fully understood. This thesis investigated different agricultural sources of ice-nucleating particles with the overall goal of determining the extent to which agriculture influences regional and global ice-nucleating particle populations. Agricultural soil samples from the UK and Canada were extracted to examine the ice-nucleating activity of the submicron entities within the soil. This analysis revealed that the ice-nucleating activity of agricultural soils from different locations varied significantly but this variation was not attributable to concentrations of surfactants within the soil. The ice-nucleating activity of two common fungal crop pathogens was also analysed to determine the relative influence of crop agriculture on the regional ice-nucleating particle populations, which indicated that the ice-nucleating activity of these spores was stable when stored. Finally, the size-resolved ice-nucleating particle concentrations of agricultural soil samples were analysed using a lab-based aerosol chamber technique which showed that the ice-nucleating activity of agricultural soils is evenly distributed across its size distribution. Through these techniques, we have been able to unpick some of the complexities in understanding agricultural sources of ice-nucleating particles by highlighting the potential importance of biological, macromolecular substances to the ice-nucleating activity of these soils.

Contents

List of Figures

List of Tables

List of Abbreviations

APS	Aerodynamic Particle Sizer
CCN	Cloud Condensation Nuclei
CFU	Colony-Forming Unit
CPC	Condensation Particle Counter
DMA	Differetial Mobility Analyser
$FINC$	Freezing Ice Nuclei Counter
IBP	Ice-Binding Particle
INA	Ice Nucleation Active
INM	Ice-Nucleating Macromolecule
INP	Ice-Nucleating Particle
LW	Long-wave radiation
SML	Sea Surface Microlayer
$SMPS$	Scanning Mobility Particle Sizer
SSA	Sea Spray Aerosol
SW	Short-wave radiation
$\mu L - NIPI$	Microlitre Nucleation by Immersed Particle Instrument
CNT	Classical Nucleation Theory
WBF	Wegener-Bergeron-Findeisen

1 Introduction

1.1 Clouds and their Importance

Clouds are a significant part of the climate system; playing a key role in regulating the Earth's radiative energy balance (Ceppi et al., 2017). The radiative effect of clouds depends on several factors, including altitude, total cloud cover and optical thickness. The total cloud cover and optical thickness determine the percentage of incoming, short-wave (SW) solar radiation reflected from the Earth's surface (Hartmann et al., 1992). For example, optically thicker clouds, with greater overall cloud cover, will reflect more SW radiation back into space. This increased reflectivity reduces the amount of radiation reaching the Earth's surface, therefore creating a cooling effect on the climate. On the other hand, the altitude of a cloud determines the amount of outgoing, long-wave (LW) radiation that the cloud can trap (Hartmann et al., 1992). For example, high-altitude clouds are much colder than low-altitude clouds, meaning they absorb more LW radiation at the top of the atmosphere, creating a warming impact on the climate. The phase of a cloud also plays a role in its radiative effect.

Clouds can exist in liquid, ice or mixed-phase (which contains a mix of liquid and ice) states. The phase of a cloud is predominately driven by altitude, as higher clouds exist in much colder conditions, which generally tend to contain more ice. For example, cirrus clouds, are thin, wispy clouds composed entirely of ice. Cirrus clouds are optically very thin, meaning that they transmit the majority of SW radiation. Since cirrus clouds occur at very low temperatures and very high altitudes, they tend to trap more LW radiation, creating a net warming effect on climate. Mixed-phase clouds, which are of greatest relevance to this thesis, and liquid clouds, have a net cooling effect as they exist at much lower altitudes and tend to be optically thicker than ice clouds. The combined radiative effect of aerosols on clouds has been shown to have a net cooling effect of -1.0 $\pm$ 0.7 W m^{-2} (Forster et al., 2021) with the radiative effect of mixed-phase clouds having a global net radiative effect of -3.4 W m^{-1} (Matus and L'Ecuyer, 2017).

Cloud radiative feedback is the change in the radiative flux at the top of the atmosphere due to changes in cloud properties as a result of a warming climate (Ceppi et al., 2017; Storelvmo et al., 2015; Storelvmo, 2017) and describes how atmospheric warming impacts the radiative flux of clouds. In a warming climate, we will likely see a decrease in the total low-level cloud cover, leading to reduced reflection of SW radiation and further

exacerbation of climate warming. This scenario would be described as a positive feedback mechanism. Convection will also increase in a warming world, especially in tropical and subtropical regions, leading to an increase in cloud top height (Ceppi et al., 2017). As the temperature of clouds decreases with altitude, increases in cloud top heights will lead to an increase in the amount of LW radiation trapped by clouds at the Earth's surface. Therefore, increasing cloud heights resulting from atmospheric warming creates a positive feedback mechanism which leads to further warming of the climate. Another possible feedback mechanism pertains to the formation of ice in mixed-phase clouds creating shifts in cloud dynamics (Murray et al., 2021). In a warming climate, the amount of ice formation within mixed-phase clouds will likely decrease, creating a shift to more liquid cloud droplets in these mixed-phase clouds. This change in the ratio of ice crystals to liquid cloud droplets will likely lead to increased cloud lifetimes and reflectivity (more details in Section 1.2) due to the overall increase in the optical thickness of the cloud. Therefore, we will likely observe an increase in the reflection of SW radiation, which dampens the effect of the increasing temperatures, forming a negative feedback response (Murray et al., 2021).

Increases in total aerosol concentrations will impact the microphysical properties of clouds, also impacting the radiative properties of clouds (Haywood and Boucher, 2000). Increasing concentrations of cloud condensation nuclei (CCN) leads to a greater number of smaller cloud droplets, increasing the amount of SW radiation reflected by the cloud. This creates a cooling impact on the climate by reducing the amount of SW radiation reaching the Earth's surface (Haywood and Boucher, 2000). Additionally, an increase in CCN in clouds will lead to a reduction in the growth of liquid cloud droplets, restricting their ability to grow large enough for precipitation to be initiated. As a result of this precipitation suppression, the atmospheric lifetimes of clouds will increase, further increasing the amount of SW radiation reflected. The suppression of precipitation will also lead to an increase in cloud thickness, which leads to an increase in the amount of LW radiation trapped in the Earth's atmosphere, as described above.

1.2 Atmospheric Ice Formation

Atmospheric ice formation is an important microphysical process within clouds. Ice formation in clouds can affect their macrophysical properties; impacting their radiative effects and lifetimes in the atmosphere. When clouds are cooled below 0 °C, pure liquid cloud droplets have the potential to remain in a supercooled, metastable state until tem-

peratures are as low as approximately −35 °C (Murray et al., 2012; Herbert et al., 2015). Once ice formation is initiated, rapid glaciation of the supercooled cloud can occur as the ice crystal grows at the expense of the surrounding liquid water droplets by a process known as the Wegener-Bergeron-Findeisen (WBF) process (Korolev, 2007).

Cloud condensation nuclei, or CCN, are atmospheric particles that activate the formation of cloud liquid water droplets. CCN are very common in the atmosphere, with concentrations ranging from 10 to 100 cm^{-3} over remote marine locations, and from 100 to 1000 cm^{-3} in continental regions (Pruppacher and Klett, 2010). Atmospheric particles that initiate the formation of ice in the atmosphere, also known as ice-nucleating particles or INP, are much rarer in the atmosphere by contrast and constitute only a very small fraction of the background aerosol concentrations in the atmosphere (Rosinski et al., 1986; Rogers et al., 1998). Only approximately 1 in 10^3 to 1 in 10^6 aerosol particles act as INP in the atmosphere (DeMott et al., 2010; Murray et al., 2012). Given the rarity of INPs in the atmosphere, clouds can persist in a supercooled state for extended periods, which exacerbates the WBF process once INPs are present at their activation temperature (Lohmann and Feichter, 2005). The WBF process and the associated rapid growth of ice crystals within clouds can trigger cloud precipitation and lead to the dissipation of the cloud. Furthermore, this rapid glaciation of clouds can reduce their optical thickness, impacting their radiative properties (see Section 1.1). Since INPs play an important role in this process, our understanding of these particles is vital for our understanding of cloud radiative effects and lifetimes.

1.2.1 Pathways of Ice Nucleation

There are two main pathways for atmospheric ice formation; homogeneous nucleation and heterogeneous nucleation (as shown in Figure 1.1). Homogeneous nucleation is the formation of ice in the absence of any particles or surfaces. In these pristine conditions, cloud liquid water droplets persist in a supercooled, metastable state until temperatures reach approximately −35°C (Kanji et al., 2017; Murray et al., 2012; Herbert et al., 2015). However, heterogeneous nucleation occurs only in the presence of INPs (Lohmann and Feichter, 2005; Murray et al., 2012), by providing a surface on which ice formation can occur. Heterogeneous nucleation can take place at temperatures higher than the homogeneous freezing temperature via one of four different modes described below.

The most common mode of heterogeneous nucleation in mixed-phase clouds is im-

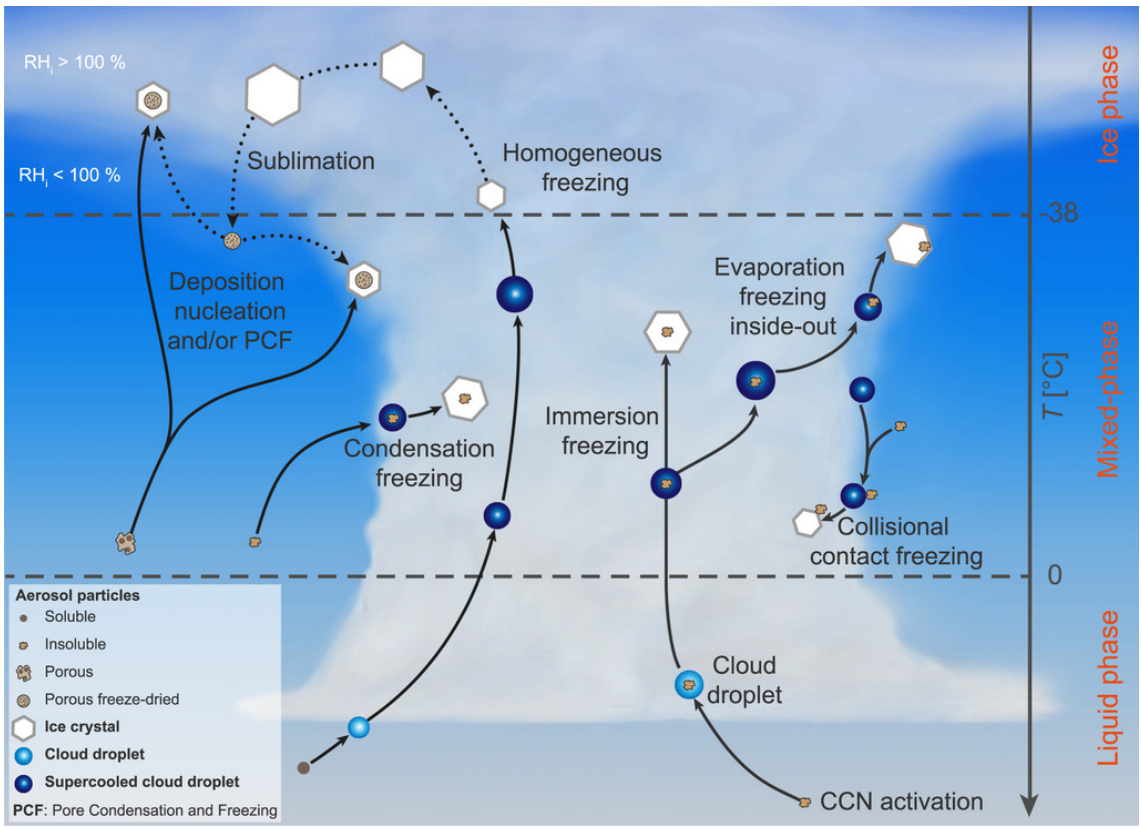

Figure 1.1: Illustration of the different ice nucleation pathways in the atmosphere. *Figure taken from Kanji et al. (2017).*

mersion freezing (Lohmann and Diehl, 2006). Immersion freezing occurs when particles immersed in the cloud droplet become activated as INPs. The INPs will initiate freezing in the cloud droplet when its characteristic freezing temperature is reached, which varies depending on the type and composition of INP (see Section 1.2.3). Commonly, the particle responsible for freezing will first act as a CCN, which activates the formation of the cloud droplet. The particle will later become activated as an INP when supercooling allows it to reach its activation temperature. However, the CCN is not always responsible for the activation of immersion freezing as other particles within the droplet may be activated as INPs.

Condensation freezing differs from the immersion freezing mode in that the entire process occurs within a supercooled cloud. In condensation freezing, the activation of the CCN, which initiates the formation of the water droplet, occurs at the same time as the initiation of the ice formation. Therefore, water forms within a supercooled cloud and then rapidly freezes and grows into an ice crystal. Contact freezing occurs when aerosol particles come into direct contact with the surface of a supercooled cloud droplet, meaning ice formation occurs at the air-water interface of the cloud droplet.

When water vapour deposits directly onto an aerosol particle as ice, this is known as deposition nucleation (Vali et al., 2015), meaning bulk water does not need to be present for ice formation to occur, as ice formation occurs as a gas-to-solid phase process. Deposition nucleation occurs at much lower temperatures compared to other nucleation modes, meaning that this nucleation mode tends to be of secondary importance in mixed-phase clouds but may be the dominant pathway of nucleation in cirrus clouds. There has been some debate as to whether true deposition freezing occurs in the atmosphere. Instead, it is thought that microscopic quantities of liquid water first form in the cracks and pores of aerosol particles and that this water then goes on to freeze either homogeneously or heterogeneously, in a process called pore condensation freezing (Marcolli, 2014; David et al., 2019).

1.2.2 Classical Nucleation Theory

Classical nucleation theory, or CNT, is usually used to describe the rate of nucleation of particles as a result of a phase change from the vapour phase into liquid or solid particles (Seinfeld and Pandis, 2016). This theory can be used to predict the formation of ice in clouds from supercooled liquid cloud droplets and the role of other substances within the cloud to increase ice formation efficiency through heterogeneous ice nucleation (Ickes et al., 2015). The theory uses the assumption that nucleation is a time-dependent and stochastic process, with an even distribution of nucleation probabilities across the homogeneous liquid.

1.2.2.1 Homogeneous Ice Nulceation

As detailed above, homogeneous ice nucleation describes the formation of ice crystals from supercooled water droplets. Ice formation can be triggered in this way from the formation of stable ice embryos within the water. These ice embryos are clusters of water molecules which are initially very unstable and likely to be redissolved back into the supercooled water. The Gibbs Free energy of the system (ΔG) between the ice embryo and the bulk liquid water is the energy barrier for the formation of ice embryos within the system. ΔG can be described by the sum of the Gibbs free energy of the surface (ΔG_{S}) and the Gibbs free energy of the volume (ΔG_{V}) between the cluster and the bulk (Eq. 1) (Mullin, 2001).

$$\Delta G = \Delta G_{\mathrm{S}} + \Delta G_{\mathrm{V}} \tag{1}$$

Assuming that the ice cluster is spherical with a radius of r and an interfacial tension between the supercooled water and ice of γ, ΔG_{S} represents the energy barrier to forming the surface of the ice cluster and can be described by:

$$\Delta G_{\mathrm{S}} = 4\pi r^2 \gamma \tag{2}$$

For the same ice cluster, the volume term, ΔG_{V}, is the energy barrier per unit volume of the phase change from liquid water to ice and can be described as:

$$\Delta G_{\mathrm{V}} = -\frac{4\pi r^3}{3v} k_{\mathrm{B}} T \ln S_{\mathrm{i}} \tag{3}$$

where r is the raduis of the cluster, v is the volume of the water molecule, k_{B} is the Boltzmann constant (1.38×10^{-23} J K^{-1}), T is the temperature of the system and S_{i} is the supersaturation with respect to ice. Since the surface term, ΔG_{S}, is positive and the volume term, ΔG_{V}, is negative (Figure 1.2) with increasing cluster sizes, there is a critical cluster radius (r^*) at which the Gibbs free energy is at its maximum. This r^* is the size that the ice cluster needs to be for ice growth to become thermodynamically favourable and for it to become stable. The critical cluster radius can be described as follows:

$$r^* = \frac{2v\gamma}{k_{\mathrm{B}} T \ln S_{\mathrm{i}}} \tag{4}$$

To find the value for the Gibbs free energy of the formation of the critical cluster, or ΔG^*, we can substitute Eq. 2 and Eq. 3 into Eq. 1 and then further substitute in Eq. 4, as follows:

$$\Delta G^* = \frac{16\pi v^2 \gamma^3}{3(k_{\mathrm{B}} T \ln S_{\mathrm{i}})^2} \tag{5}$$

Since CNT determines the rate of formation of these critical clusters, this critical Gibbs free energy can be used to determine the rate of homogeneous nucleation, J_{hom} (cm^{-3} s^{-1}), shown as follows:

$$J_{\mathrm{hom}} = A_{\mathrm{hom}} \exp\left(-\frac{\Delta G^*}{k_{\mathrm{B}} T}\right) \tag{6}$$

$$J_{\mathrm{hom}} = A_{\mathrm{hom}} \exp\left(-\frac{16\pi v^2 \gamma^3}{3k_{\mathrm{B}}^3 T^3 \ln {S_{\mathrm{i}}}^2}\right) \tag{7}$$

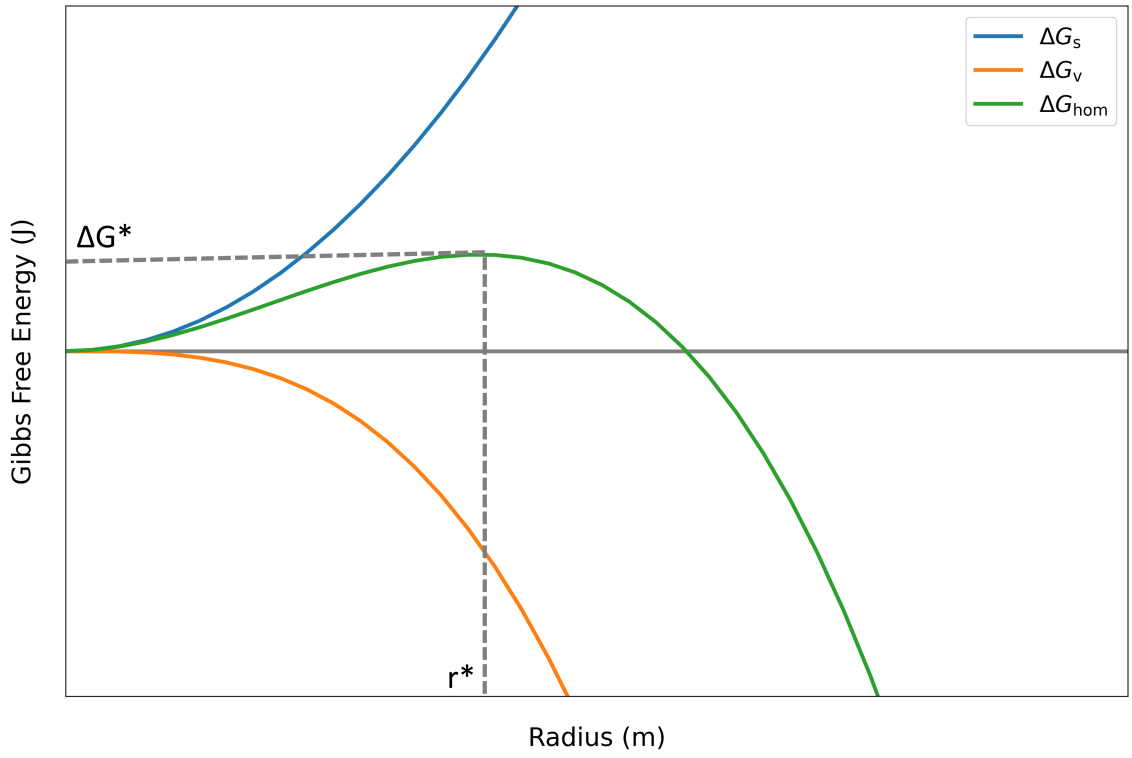

Figure 1.2: The change in Gibbs Free Energy (ΔG) for the homogeneous nucleation of ice from supercooled water *showing the volume term (ΔG_V), the surface term (ΔG_S), the critical energy barrier for nucleation (ΔG^*) and the critical radius (r^*).*

where A_{hom} is a pre-exponential factor mostly related to the self-diffusion of water. Since J_{hom} is an exponential term, the rate of formation of critical ice embryos within supercooled water is highly sensitive to the temperature of the system and the factors influencing the value of ΔG^*.

1.2.2.2 Heterogeneous Ice Nulceation

Heterogeneous ice nucleation requires the presence of a surface, which acts to lower the free energy barrier to critical cluster formation (ΔG^*). This surface is often in the form of a particle, as an INP, which lowers the free energy for critical cluster formation (Ickes et al., 2015). The degree to which an INP can lower the free energy barrier to the formation of critical ice clusters depends on the interactions with the particle at the surface, which can be described as follows:

$$\phi = \frac{(2 + \cos\theta)(1 - \cos\theta)^2}{4} \tag{8}$$

where ϕ is the reduction factor applied to ΔG^* to alter the free energy compared to homogeneous nucleation conditions and $\cos\theta$ is the contact angle between the ice embryo and the nucleating surface (or INP). Therefore, the contact angle between the ice embryo

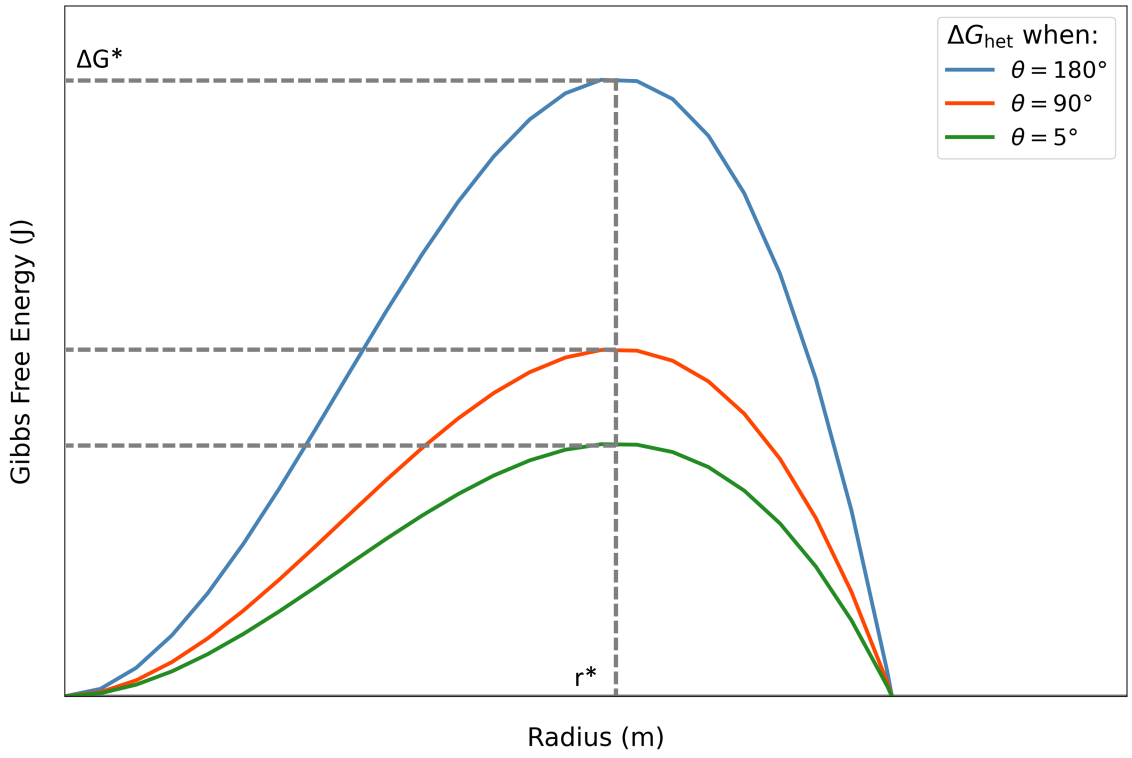

Figure 1.3: The change in Gibbs Free Energy (ΔG) for heterogeneous nucleation of ice from supercooled water. *showing the critical energy barrier for heterogeneous nucleation (ΔG^*) with different contact angles between the ice embryo and the nucleating surface (θ) and the critical radius (r^*).*

and the INP is important for determining the critical energy barrier for heterogeneous nucleation, with lower contact angles lowering the energy barrier to nucleation (Figure 1.3). For example, when θ is equal to 0°, ϕ is equal to 0, which would remove the free energy barrier to ice nucleation, indicating that the particle is the most efficient ice nucleator. On the other hand, if θ is equal to 180°, then the particle has practically no contact with the ice embryo, ϕ would be equal to 1 and the particle will have no effect on ice nucleation.

The heterogeneous nucleation rate, or J_{het} (cm^{-3} s^{-1}), can be calculated in a similar way to the homogeneous nucleation rate but with the addition of the reduction factor, ϕ, shown as follows:

$$J_{\text{het}} = A_{\text{het}} \exp\left(-\frac{\phi \Delta G^*}{k_{\text{B}} T}\right) \tag{9}$$

$$J_{\text{het}} = A_{\text{het}} \exp\left(-\frac{16\pi v^2 \gamma^3}{3 k_{\text{B}}^3 T^3 \ln {S_{\text{i}}}^2}\right) \cdot \frac{1}{4}(2 + \cos\theta)(1 - \cos\theta)^2 \tag{10}$$

where A_{het} is a pre-exponential factor mostly related to the self-diffusion of water. In reality, heterogeneous ice nucleation is a lot more complex than what is described in

Eq. 10. CNT uses the assumption that the surface of the particle is uniform and its ice-nucleating ability is distributed evenly across the surface. However, this assumption is an oversimplification when applied to real atmospheric INPs. The ice-nucleating ability of individual INPs is not distributed evenly across the surface. Instead, the surface of each INP is made up of individual ice-active sites meaning that the nucleation rate varies across the surface.

1.2.3 Types and Sources of Ice-Nucleating Particles

As discussed above, INPs consist of only a small subset of atmospheric aerosol particles (Rogers et al., 1998; DeMott et al., 2010), although, the exact nature of INPs and what constitutes an efficient ice nucleator remains unknown. The surface of the particles plays an important role as it acts as a template for ice formation (Ickes et al., 2015). It is known that on insoluble INPs, specific sites activate ice formation at specific temperatures. Therefore, we need to understand the nature of particles that act as INP in the atmosphere.

One of the most important and abundant INPs in the atmosphere, active below $-10\,^{\circ}\mathrm{C}$, is mineral dust (DeMott et al., 2003; Atkinson et al., 2013; Niemand et al., 2012). There are many sources of natural mineral dust, including soils and volcanoes (Maters et al., 2020), but the most significant sources of mineral dust in the atmosphere are from deserts (DeMott et al., 2003; Boose et al., 2016). In 2001, the emission rate of desert dust was determined to be between 1604 to 1960 Tg yr^{-1} (Ginoux et al., 2001). Since then, climate change has only led to further increases in these emission rates, with desertification drastically increasing the primary sources of mineral dust in the atmosphere and changes in weather patterns leading to more intense droughts which increase dust emissions. The high emissions and larger spread of desert dust across the globe means that its ice-nucleating ability is important for many regions. Since it is so important to cloud glaciation, the ice-nucleating ability of mineral dust has been investigated extensively (DeMott et al., 2003; Niemand et al., 2012; Niedermeier et al., 2015; Harrison et al., 2016). Of the different minerals commonly found in mineral dust, potassium-feldspar (K-feldspar) is the most effective ice nucleator (Atkinson et al., 2013; Harrison et al., 2016; Boose et al., 2016). Other minerals, such as clay and quartz, have been investigated for their ice-nucleating abilities. Still, clay minerals tend to nucleate ice at lower temperatures and the active sites on quartz are sensitive to ageing in air and water (Harrison et al., 2019). Therefore, it is thought that the ice-nucleating activity from mineral dust is dominated by K-feldspar.

Many other INP types have been identified with a variety of different ice-nucleating abilities. For example, in more remote, marine locations sea spray and biogenic marine aerosol tend to dominate ice nucleation (Wilson et al., 2015; Si et al., 2018). Furthermore, some primary biological particles, such as bacteria, fungi and pollen, have been identified as ice-active (Möhler et al., 2008; Morris et al., 2013; Augustin et al., 2013). Other organic substances, mostly from the breakdown of plant material like cellulose and lignin, can also nucleate ice (Vali et al., 1976; Steinke et al., 2020). Additionally, some organic biomass-burning aerosols are very effective ice nucleators (Prenni et al., 2012; McCluskey et al., 2014). It is thought that, although combustion aerosol may not contribute significantly to atmospheric INP concentrations (Schill et al., 2020; Adams et al., 2021), certain particles released from combustion events may influence ice formation in clouds close to the combustion source (Grawe et al., 2016; Schill et al., 2016). Given the uncertainties in the relative contributions of different aerosol sources to INP concentrations in the atmosphere, more observations are needed to better understand the nature and abundance of different INP sources.

1.2.4 Ice-Nucleating Particle Size Distributions and Atmospheric Lifetimes

The size of an aerosol particle contributes to its atmospheric lifetime. Large aerosol particles tend to fall out of the atmosphere rapidly by sedimentation, whereas exceedingly small particles rapidly grow by coagulation (Feichter and Leisner, 2009), this is particularly important in the free troposphere. Therefore, it is the mid-range size particles that tend to have the longest atmospheric lifetimes, on the order of days to tens of days compared to minutes to hours for much smaller and much larger particles (Figure 1.4). These mid-range sized particles are known as accumulation mode aerosols and they range in size from approximately 0.01 to 10 µm (Figure 1.4). Accumulation mode aerosols tend to be the size range of particles that accumulate in the atmosphere and are the most important for the long-range transport of ice-nucleating material and therefore, are the most important for cloud glaciation. In some cases other size ranges can be important for cloud glaciation, like in deep convective clouds where large amounts of air are drawn from the boundary layer, so larger particles become more relevant.

Only a few studies have investigated the size distribution of INPs in the atmosphere and the majority of these studies have focused on the analysis of ambient dust samples (DeMott et al., 2010; Mason et al., 2016; Reicher et al., 2019; Porter et al., 2020). In

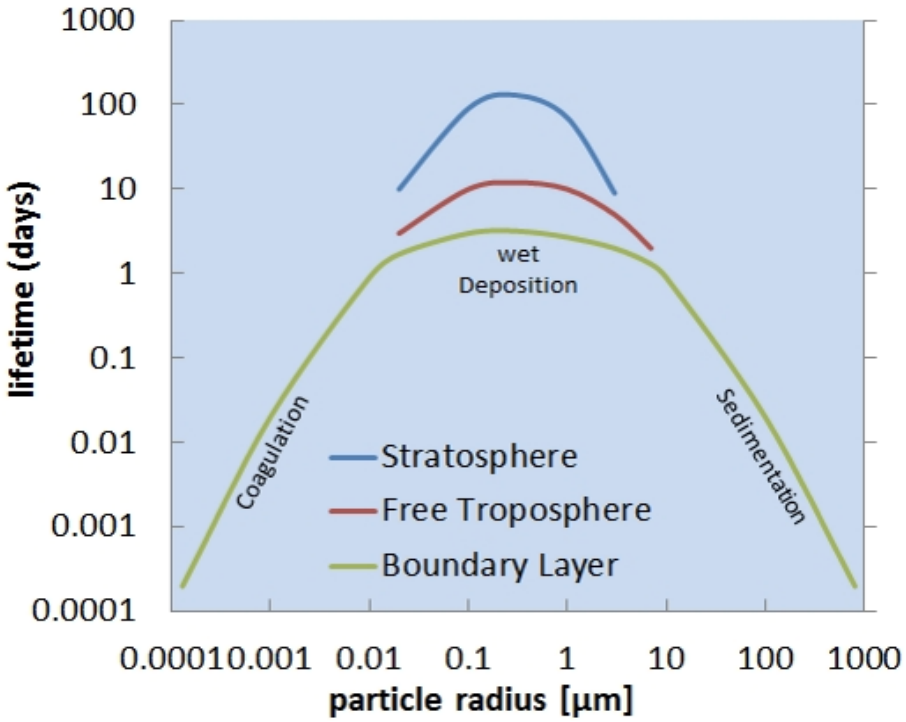

Figure 1.4: The size dependence of the lifetime of aerosol particles in the atmosphere. *Figure taken from Feichter and Leisner (2009).*

pure mineral dust aerosol, the number of ice-active sites scales with surface area, meaning that larger particles tend to be associated with greater ice-nucleating activities. Reicher et al. (2019) examined the size distribution of INP in atmospheric dust events in the Mediterranean and found that submicron particles (particles less than 1 µm) and supermicron particles (particles greater than 1 µm) had different ice-nucleating activities. They showed that supermicron particles had higher ice-active site densities per surface area (n_s) compared to submicron particles, which remained consistent across different dust events. Similarly, Mason et al. (2016), who examined size-segregated INP concentrations from ambient aerosol samples in six different locations across North America and Europe, also showed that supermicron particles have a greater ice-nucleating ability when compared to submicron particles. Porter et al. (2020) investigated the size-resolved concentration of INP whilst developing the SHARK instrument. They observed that the size distribution of INP varied by location and that submicron particles sometimes contributed more significantly to the INP concentration, such as in Hyytiälä in Finland, which is a boreal forest research station (Porter et al., 2020), suggesting that supermicron particles may not dominate in organic-rich aerosol samples.

1.3 Biological Aerosols as Ice-Nucleating Particles

Primary biological aerosol particles (PBAPs) are aerosol particles in the atmosphere that originate from the biosphere and consist of bacteria, pollen, fungi, algae, viruses, and biological fragments (e.g. leaf litter, insects etc.) and molecules (e.g. proteins, lipids and polysaccharides) (DeMott et al., 2010; Fröhlich-Nowoisky et al., 2015). These biological materials are found in various aerosol sources, including soil dust, marine aerosols, anthropogenic emissions and vegetation (Lindemann et al., 1982; Bigg, 1973; Wilson et al., 2015; Steinke et al., 2016; Knackstedt et al., 2018).

PBAPs are thought to contribute significantly to atmospheric aerosol concentrations, with cellular material and proteins potentially contributing up to 25% to global atmospheric aerosol concentrations (Jaenicke, 2005; Després et al., 2012). However, local emissions of biological aerosols have significant temporal and spatial variations (Jaenicke, 2005; Huffman et al., 2010), meaning that their overall contribution to global atmospheric aerosol and INP concentrations is hard to predict and may not be very significant when considering the annual average concentrations (Hoose et al., 2010; Spracklen and Heald, 2014). A subset of PBAPs can nucleate ice at temperatures above $-10\,^{\circ}\mathrm{C}$ (Möhler et al., 2008; Diehl et al., 2001; Hader et al., 2014), making them potentially important ice nucleators at relatively high atmospheric temperatures. However, a lack of measurements and knowledge of the mechanisms of ice nucleation in biological materials means that the exact importance of PBAPs as atmospheric ice nucleators remains poorly understood.

1.3.1 How do Biological Aerosols Nucleate Ice?

1.3.1.1 Bacteria

The ice-nucleating activity of bacteria was first discovered in the *Pseudomonas* genus in the 1970s (Maki et al., 1974; Arny et al., 1976; Vali et al., 1976; Maki and Willoughby, 1978). Maki et al. (1974) showed that the ice-nucleating ability of bacteria was lost when the cell was physically or chemically destroyed, leading to the conclusion that only whole cells could nucleate ice. However, later work revealed that the ice-nucleating ability of the bacteria cells was related to their ability to express certain ice-nucleating proteins (Phelps et al., 1986; Govindarajan and Lindow, 1988). These ice-nucleating proteins have active sites which template ice, allowing ice formation on their surface. The proteins are coded into the bacteria's genetic information as an ice nucleation active gene (*ina* gene), which can be detected using DNA sequencing techniques (Green and Warren, 1985; Wex

et al., 2015; Hill et al., 2016), allowing their ice-nucleating ability to remain associated with fragments of ice-active bacterial cells (Šantl Temkiv et al., 2015). The ability of ice-nucleating proteins to effectively nucleate ice is susceptible to heating and pH changes. When heated, the proteins become denatured and change shape, meaning that the active sites for ice nucleation are lost and the ice-nucleating ability of the bacteria is significantly reduced or lost completely (Christner et al., 2008; Conen et al., 2011).

The most well-characterised ice-active bacteria species is *Pseudomonas syringae*, which has been shown to have onset freezing temperatures of up to $-2\,^{\circ}\mathrm{C}$ (Maki et al., 1974; Maki and Willoughby, 1978). Due to its high levels of ice-nucleating ability, non-viable *P. syringae* bacteria and their fragments are the main constituents of Snomax, a commercially available material which is used for snow production. More recent studies have shown that aggregation of ice-nucleating proteins within the membranes of bacteria cells (either whole or fragments of the cell wall) is important for their ice-nucleating ability (Hartmann et al., 2022; Lukas et al., 2022). The size of the proteinaceous aggregates of *P. syringae* determines the temperature at which the protein can initiate freezing (Qiu et al., 2019). There are three different classes of aggregation associated with different freezing temperatures; Class A which triggers freezing at $-3\,^{\circ}\mathrm{C}$, Class B which triggers freezing at $-5\,^{\circ}\mathrm{C}$ and Class C which triggers freezing at $-8\,^{\circ}\mathrm{C}$ (Lukas et al., 2022). Aggregation of proteinaceous ice-nucleating macromolecules (INMs) is likely influenced by electrostatic and hydrophobic interactions between proteins and components of the bacterial membrane (Lukas et al., 2020; Schwidetzky et al., 2021).

Other bacteria have been examined for their ice-nucleating abilities and many active components have also been found to be proteinaceous in nature (Failor et al., 2017). Certain ice-active bacteria, however, are resistant to both heat treatments and digestion by lysosome or proteinase treatments. For example, the ice-nucleating ability of the *Lysinibacillus* genus has been shown to be heat and digestion stable (Failor et al., 2017). This observation suggests that the ice-nucleating ability of this bacteria genus is not associated with ice-nucleating proteins.

1.3.1.2 Fungal Material

Early investigations into the ice-nucleating activity of fungal species started with lichens, a composite organism consisting of algae and fungi in a symbiotic relationship. Since ice-active bacteria could not be isolated from lichen and its ice-nucleating activity was resistant to heat treatments, it was concluded that the ice-nucleating ability of lichens was

not associated with ice-active bacteria (Kieft, 1988; Kieft and Ruscetti, 1990).

Later work by Pouleur et al. (1992) aimed to investigate the ice-nucleating ability of fungal species by testing 20 genera of fungi for freezing at −5 °C. They highlighted two key species of fungi with the ability to nucleate ice above −5 °C, both of them were *Fusarium* species, a common soil fungus. Later, more species of *Fusarium* were investigated by Richard et al. (1996) and found more ice-active species. Further investigations into soil fungi, including *Fusarium* and *Mortierella* species, have found high ice-nucleating activities (Fröhlich-Nowoisky et al., 2015; Kunert et al., 2019). It was initially thought that the ice-nucleating ability of these fungal species was not proteinaceous, since Pouleur et al. (1992) showed that the ice-nucleating ability of *Fusarium acuminatum* and *Fusarium avenaceum* was more stable after heat treatments to 60 °C compared to ice-active bacteria. However, more recent research has indicated that the ice-nucleating activity of soil fungus is significantly reduced after exposure to heat treatments above 90 °C, suggesting this ice-nucleating ability is attributable to proteins (Fröhlich-Nowoisky et al., 2015; Kunert et al., 2019). Therefore, it is now thought that the ice-nucleating activity from *Fusarium* species, and other similar soil fungi, is proteinaceous. However, the nature of the fungal INPs is different to bacterial INPs since fungal INPs are more resistant to heat and pH treatments and the activity of these INPs is not dependent on membrane lipids (O'Sullivan et al., 2015).

Other fungal species have been investigated for their ice-nucleating abilities. Some fungal spores, such as those of *Cladosporium* species, a common plant fungus, have little to no ice-nucleating activity above −15 °C (Iannone et al., 2011; Haga et al., 2013). Iannone et al. (2011) concluded that the hydrophobic outer coating which is often found on fungal spores, called hydrophobins, limits the interaction of the spores with water, restricting their ability to form close lattice match for ice formation. On the other hand, further work by Morris et al. (2013) found that fungal spores of some species of rust fungi can nucleate ice above −10 °C, suggesting a higher ice-nucleating activity. However, the relative active-site density per spore was relatively low and atmospheric concentrations of these spores may not be high enough to contribute to atmospheric INP concentrations (Morris et al., 2013). Given all of this, it is unlikely that fungal spores contribute significantly to INP populations, but further work is needed to determine the relative importance of this material to atmospheric INP concentrations (Iannone et al., 2011; Haga et al., 2013; Morris et al., 2013).

1.3.1.3 Pollen

The ice-nucleating ability of pollen grains was first examined much later than that of bacteria and fungi (Diehl et al., 2001, 2002). Pollen was found to be an effective ice nucleator in itself, without any ice-nucleating ability from associated bacteria species (Diehl et al., 2001). However, it initiates the formation of ice at lower temperatures compared to the ice-nucleating proteins associated with most bacterial species (Diehl et al., 2001). Later, Pummer et al. (2012) found that the ice-nucleating ability of pollen grains was attributable to macromolecules that were easily washed off the pollen surface, into suspension. They also showed that these INMs were resistant to heat and lysosome treatments, indicating that they were not proteinaceous (Pummer et al., 2012).

Further studies by Augustin et al. (2013) found that birch pollen grains can produce two different types of INMs that initiate freezing at different temperatures. They classified these ice nucleation active (INA) macromolecules as INA-α and INA-β (Augustin et al., 2013). It has also been shown that aggregation of the polysaccharide molecules that contribute to the ice-nucleating ability of pollen is important for their ice-nucleating activity (Dreischmeier et al., 2017). Smaller polysaccharide molecules have been shown to act as ice-binding particles (IBPs), but when the same molecules form into larger aggregates, they then act as INPs (Dreischmeier et al., 2017).

1.3.1.4 Other Biological Materials

Other biological materials have also been investigated for their ice-nucleating abilities. For example, plant cell fragments such as cellulose, lignin and polysaccharides have all been shown to be ice-active compounds. Lignin is a biopolymer, most commonly found in woody plants and it forms a vital part of the structure of plant cells (Boerjan et al., 2003). The ice-nucleating activity of lignin is lower than other biological materials, with most freezing occurring below $-15\,^{\circ}\mathrm{C}$ (Bogler and Borduas-Dedekind, 2020). However, with lignin contributing up to 30% of the total organic carbon in the environment (Boerjan et al., 2003) along with its relative stability to atmospheric processing (Bogler and Borduas-Dedekind, 2020), the overall contribution of lignin to INP concentrations may be more significant than what models currently represent. Cellulose is also an important component of plant cells. The structure and composition of cellulose depend on its source and the environmental conditions the plant grows in. Cellulose is also present in the atmosphere on large temporal and spatial scales (Sánchez-Ochoa et al., 2007) and its ice-nucleating ability is similar to that of mineral dust and lignin, with freezing temperatures

mostly below −15 °C (Hiranuma et al., 2019).

Initial investigations into the ice-nucleating ability of viruses found little to no ice-nucleating activity (Junge and Swanson, 2008). However, further study by Cascajo-Castresana et al. (2020) showed that the tobacco mosaic virus, a common plant virus which infects many plants across the globe, can nucleate ice with an ice-active site density of 10^4 mg^{-1} at −20 °C. Furthermore, Adams et al. (2021) investigated a range of different virus types and found their ice-nucleating ability varied significantly. However, the overall ice-nucleating ability of viruses is much lower than that of other terrestrial and marine INP types, suggesting that they do not play a substantial role in cloud glaciation (Cascajo-Castresana et al., 2020; Adams et al., 2021).

1.3.2 Sources of Biological Ice-Nucleating Particles

The ice-active biological particles discussed above are found in a variety of different sources in the environment including soils, vegetation, and both fresh and ocean waters. Any of these environments can act as sources of biological INPs into the atmosphere, so many studies have investigated these potential sources to attempt to understand their relative contributions to atmospheric biological INP concentrations. The following section will discuss these different studies and sources of biological INPs in more detail.

1.3.2.1 Soils

Fertile soils are made up of a complex mix of mineral dust and small amounts of biological and organic material. This biogenic material consists of either microbes such as bacteria and fungi living within the soil or organic matter released during the breakdown of living organisms like plants, such as lignin, cellulose and polysaccharides. The presence of this biogenic material in soil dust can significantly enhance its ice-nucleating ability compared to pure mineral dust (Conen et al., 2011; O'Sullivan et al., 2014; Augustin-Bauditz et al., 2016). For example, a lab-based study conducted by Augustin-Bauditz et al. (2016) revealed that even a very small amount of biological material added to mineral particles was able to influence the freezing behaviour of the particles. Furthermore, analysis of soil samples collected in the field indicates that up to 90% of ice-nucleating activity at temperatures above −9 °C is attributable to heat-labile, likely biological materials (Conen et al., 2011; O'Sullivan et al., 2014; Hill et al., 2016). In particular, Steinke et al. (2016) showed that the ice-nucleating activity of soil samples collected from four different locations was greater than the ice-nucleating activity of mineral dust, particularly at temperatures over

−15 °C.

Heat-stable organic materials also contribute significantly to the ice-nucleating ability of fertile soils (Hill et al., 2016; Steinke et al., 2020). A study by Hill et al. (2016) found that 99% of the observed ice-nucleating activity at −18 °C was only removed after treatment with H_2O_2. The sensitivity of this material to hydrogen peroxide treatment suggests that the ice-nucleating ability was not attributable to minerals in the soil, indicating that other organic components such as lignin or cellulose must be responsible (Hill et al., 2016). A similar study by Steinke et al. (2020) investigated the ice-nucleating activity of organic compounds commonly found in fertile soils from the breakdown of plant materials, such as lignin, starch, and plant protein. They found that the ice-nucleating activity of the individual organic compounds was similar to or lower than the ice-nucleating activity of agricultural soils, indicating that these compounds make up a significant proportion of the ice-nucleating activity of these soils (Steinke et al., 2020).

Fungal proteins have also been identified as particularly important contributors to the ice-nucleating ability of fertile soils (Fröhlich-Nowoisky et al., 2015; O'Sullivan et al., 2015, 2016; Hill et al., 2016). For example, fungal INMs have been shown to adhere to clay minerals preferentially in soil suspensions, suggesting that the prevalence of biological material, particularly fungal INMs, in mineral dust is highly likely in many locations (O'Sullivan et al., 2016). The heat-labile portion of the ice-nucleating activity of soil samples investigated by Hill et al. (2016) was most likely associated with fungal proteins since no known ice-active bacteria were found during the study. The ice-nucleating activity of common soil fungi, such as *Fusarium* and *Mortierella* species, is widespread and frequent across different species and soil sample locations (Fröhlich-Nowoisky et al., 2015; O'Sullivan et al., 2015; Conen and Yakutin, 2018; Kunert et al., 2019). The ice-nucleating ability of these fungi is proteinaceous in origin but is slightly more stable to heat treatment than ice-active bacteria, suggesting that these INMs will have a higher stability in atmospheric conditions (Kunert et al., 2019).

Given all of the above, the complexity of soil makes it hard to predict its ice-nucleating abilities. A study by O'Sullivan et al. (2014) examined soil samples taken at four different locations across England and found that above −15 °C, the ice-nucleating ability of the samples were dominated by heat-labile, carbonaceous components and below this temperature, mineral dust seemed to dominate. However, they did not find a direct link between the organic carbon concentration and the ice-nucleating ability of the soils. The soil sam-

ple with the highest carbon fraction, at 12.7%, had very similar ice-nucleating activity as the soil samples with much lower carbon contents (2.5% and 2.9%), suggesting that the increased carbon content did not directly contribute to an increase in ice-nucleating activity (O'Sullivan et al., 2014). Therefore, it is hard to represent this increased ice-nucleating activity of fertile soils in atmospheric models and further investigations are required to break down the complexities of soil dust to improve the parameterisations of these INP sources in models.

1.3.2.2 Vegetation

Some of the earliest investigations into biological INPs found a high ice-nucleating ability in decaying leaf litter (Schnell and Vali, 1972, 1973; Schnell and Tan-Schnell, 1982) and found that its ice-nucleating ability was much greater than that of fresh or living leaves. This observation indicates that the ice nuclei were released as a result of active bacterial decomposition (Schnell and Vali, 1972). Furthermore, the ice-nucleating activity derived from decaying leaf litter was found to be consistent across many parts of the Northern Hemisphere (Schnell and Vali, 1973). For example, Conen et al. (2016) found that microbial activity in decaying leaf litter in the Arctic was an important source of INPs and Conen et al. (2017) found an increase in warm temperature INP concentrations associated with the shedding of leaves in autumn. Furthermore, the bacteria *Pseudomonas syringae* was found to be present in decaying leaf litter samples, indicating that ice-active bacteria contribute to the ice-nucleating ability of decaying leaves (Maki et al., 1974; Schnell and Vali, 1976).

The leaves of living plants are also a source of INPs. Some studies have successfully isolated ice-active bacteria species from the leaves, including *P. syringae*, of various plant species (Lindow et al., 1978; Maki and Willoughby, 1978; Lindemann et al., 1982). Lindemann et al. (1982) found ice-active bacteria were present on leaf samples collected from five different locations across the US in large enough quantities to induce frost damage to the plants. Leaves may also act as a source of INPs when infected with fungal pathogens. Some wind-dispersed fungal pathogens have been shown to be ice-active meaning they can be easily blown off the leaves of infected plants, releasing INPs into the atmosphere (Haga et al., 2013; Morris et al., 2013).

Trees can also act as a source of INMs from pollen and other similar plant compounds (Pummer et al., 2012; Hader et al., 2014). A study by Felgitsch et al. (2018) found INMs with similar freezing behaviour to those found in pollen washing waters in samples taken

from different parts of birch trees, including the leaves and bark. They argued that the observed ice-nucleating activity was not attributable to ice-active bacteria since they had filtered their samples to 0.22 µm removing bacterial cells and cell fragments, which they believed were required to maintain the ice-nucleating activity of the bacteria (Felgitsch et al., 2018).

1.3.2.3 Marine

In remote, marine locations, continental aerosol sources do not dominate aerosol or INP concentrations (Bigg, 1973). Sea Spray Aerosols (SSAs) are the dominant source of atmospheric particles in marine environments. SSAs are often enriched in organic material from the sea surface microlayer (SML), when debris from living organisms, such as phytoplankton and algae, collect at the sea-air interface (Wilson et al., 2015). At the surface of the ocean, wave action and bubble bursting create jet drops and film droplet aerosols that are enriched in organic material from the SML. It has been shown that the enrichment of these SSAs with organic material enhances their ability to nucleate ice (Burrows et al., 2013; Wilson et al., 2015; DeMott et al., 2016). In particular, Wilson et al. (2015) took sea samples from both the SML and from bulk seawater and found that the concentration of INPs was greater in the SML samples compared to the bulk seawater samples.

Some studies have been able to show a direct link between the presence of algal blooms and an increase in ice-nucleating activity of SSAs (Knopf et al., 2011; Wolf et al., 2019). Wolf et al. (2019) highlighted the potential importance of hydrophilic macromolecular compounds to the ice-nucleating ability of SSAs and hypothesised that the origin of these compounds was from polysaccharides, liposaccharides or proteins. McCluskey et al. (2018) conducted a mesocosm experiment to investigate the ice-nucleating ability of marine biological aerosols. They found that during phytoplankton blooms, there were two distinct populations of marine bioaerosol contributing to SSA ice-nucleating activity. Dissolved organic matter peaks in emissions in the middle of the dense phytoplankton blooms, whereas particular organics from intact or fragmented cells peak in emissions during the decline of the phytoplankton bloom (McCluskey et al., 2018). In contrast, however, studies investigating the ice-nucleating activity of the SML and bulk seawater in the Canadian Arctic did not observe an enrichment in biological INPs in the SML (Irish et al., 2017, 2019b). The exact reasons for these discrepancies in observations are not yet fully understood and more research is needed to better understand the relative importance of the SML to the ice-nucleating ability of SSAs.

1.3.2.4 Fresh Waters

In addition to seawater, freshwater sources including lakes, rivers and streams are also sources of INPs in the atmosphere. In a similar way to the ocean, bubble bursting in turbulent waters acts as an emission mechanism for aerosols from freshwater sources (Leifer et al., 2006). These freshwater sources have been shown to harbour bacteria, fungi, pollen, lichen and biogenic macromolecules that act as INP and are washed in runoff from river watersheds (Maki and Willoughby, 1978; Morris et al., 2008; Knackstedt et al., 2018; Moffett et al., 2018; Einbock et al., 2023). The relative abundance of ice-nucleating substances in freshwater sources is much greater than the abundance of INP in seawater (Irish et al., 2017; Moffett et al., 2018). For example, Moffett et al. (2018) found that the concentration of INP per mililitre (N_{INP}) at $-10\,^{\circ}\mathrm{C}$ for freshwater samples taken from surface waters in the US were on average 4950 mL^{-1}, which is nearly four orders of magnitude greater than the INP concentrations in seawater samples. They hypothesised that this high concentration of INPs found in freshwater sources was due to the accumulation of ice-nucleating material from freshwater runoff (Moffett et al., 2018).

Some previous studies, which specifically investigated the relative abundance of ice-active bacterial species in rivers and lakes, also found them to be present in large numbers (Maki and Willoughby, 1978; Morris et al., 2008). Furthermore, Knackstedt et al. (2018) investigated the ice-nucleating activity of freshwater samples from Lake Erie and the Maumee River and found a distinct correlation between the N_{INP} at $-10\,^{\circ}\mathrm{C}$ and the volume of the river discharge, or the amount of rainwater runoff from the river watershed (Knackstedt et al., 2018). Their findings suggest that the INP concentrations in freshwater are highly dependent on the river watershed and that many of the organic macromolecules contributing to the ice-nucleating ability of freshwater are from terrestrial origins. This link between the INP concentration of water and the terrestrial river runoff was also seen in studies in the Canadian Arctic (Irish et al., 2019a,b). They observed a strong link between the N_{INP} in SML and bulk seawater samples with the amount of precipitation and terrestrial runoff. These observations indicated that either the INPs found in Canadian Arctic waters originate from terrestrial locations, or that precipitation provides nutrients which enhance the production of marine biogenic INPs from marine organisms (Irish et al., 2019a).

1.3.3 Identifying Biological Ice-Nucleating Particles

Biological INPs are usually detected in samples by the observed reduction in ice-nucleating activity after degradation from physical, chemical or biological treatments (Conen et al., 2011; Conen and Yakutin, 2018; Felgitsch et al., 2018; Daily et al., 2022). As mentioned above, ice-active fungal proteins (like those found in *Fusarium* species) are more tolerable to heat than ice-active bacterial proteins. However, exposing either of these proteins to temperatures greater than 90 °C has been shown to completely remove their warm temperature freezing activity (as demostrated in Figure 1.5). Using heat treatments to test for the relative contribution of biological INPs to an environmental sample is, however, limited. Some biogenic INPs, such as polysaccharides, cellulose and others derived directly from plant cells, are very resistant to heat treatments. Therefore, it may not be correct to assume that all remaining ice-nucleating activity after heat treatment is attributable to mineral dust INPs. In addition, some studies have found that heating environmental samples can lead to an increase in ice-nucleating activity, but the exact reason for this increase remains unclear (McCluskey et al., 2018; Beall et al., 2020). It is hypothesised that the observed increases in ice-nucleating activity after heating are due to aggregates dissolving in the solution, releasing more ice-active sites, or from the degradation of plant cells also leading to the release of ice-nucleating substances into the solution. However, the exact mechanism of the increase in ice-nucleating activity after heating remains unknown and more studies are needed to better understand this response.

Other treatments can be used to identify the presence of biogenic INPs in environmental samples. The use of hydrogen peroxide to digest biological material has been used to determine if the remaining ice-nucleating activity after heat treatments is related to heat-stable organic material rather than minerals (O'Sullivan et al., 2014; Tobo et al., 2014; Suski et al., 2018; Tobo et al., 2019). This technique is useful because it digests all biogenic material so it can remove all ice-nucleating activity associated with biological INP within the sample. However, since it requires the addition of a reagent, this technique is not as convenient as heat treatment techniques.

There are other ways we can identify biological materials in ice-active samples, such as DNA sequencing (Garcia et al., 2012; Huffman et al., 2013), microscopy (Huffman et al., 2013; Sanchez-Marroquin et al., 2021) or culturing (Morris et al., 2013). These methods can be very useful, as they allow the identification of biological material without relying on heat treatments. For example, DNA sequencing has allowed us to identify the gene

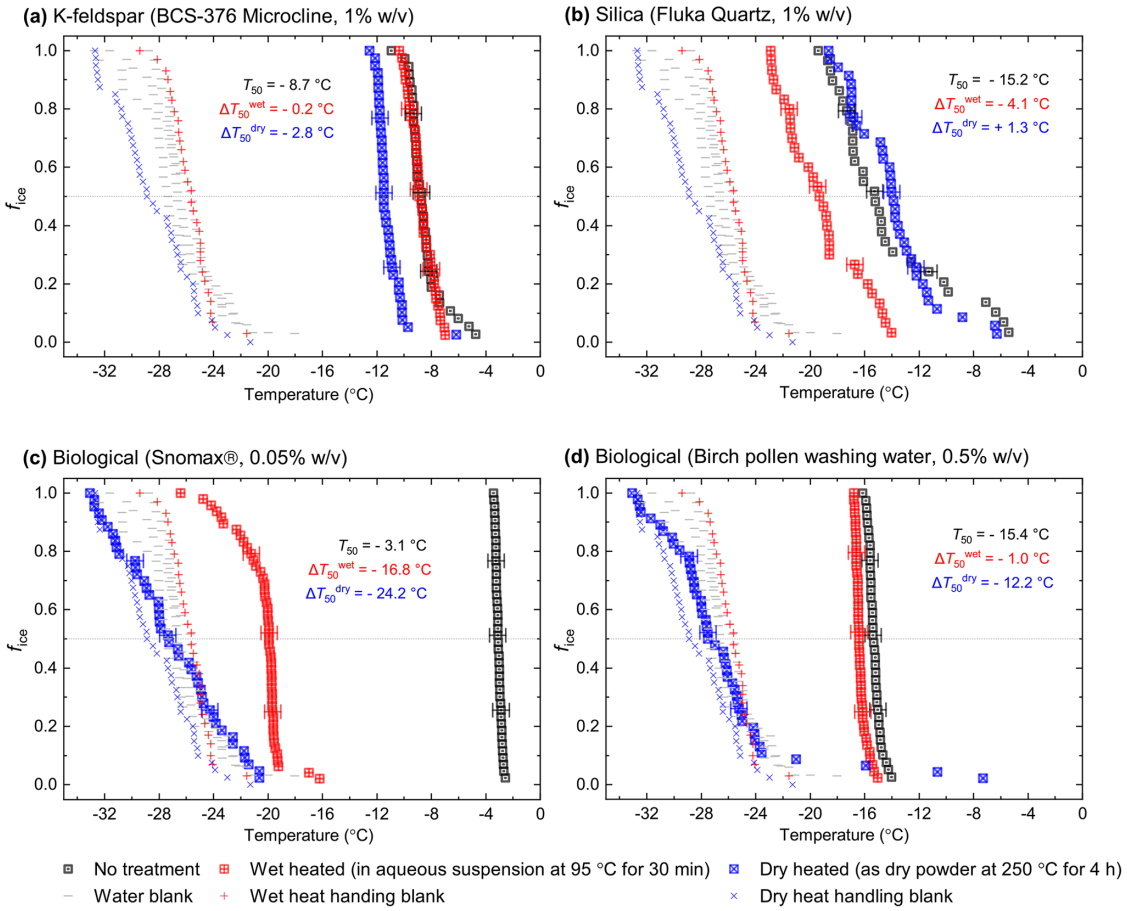

Figure 1.5: Fraction of frozen droplet ($f_{ice}(T)$) spectra illustrating characteristic heat treatment responses for (a) a dry heat-sensitive mineral INP (BCS-376 microcline), (b) a wet-heat-sensitive mineral INP (Fluka quartz), (c) a wet-heat-sensitive biological INP (Snomax®), and (d) a wet-heat-insensitive biological INP (birch pollen washing water). *Figure taken from Daily et al. (2022).*

responsible for the expression of ice-active proteins in bacterial cells (Garcia et al., 2012; Hill et al., 2016). This means that the number of *ina* genes in a sample helps us to determine the number of ice-active bacteria present, providing the *ina* gene sequence has not been damaged. The drawback of this approach is that the presence of the *ina* gene does not guarantee the presence of the *ina* protein and the protein may be present if the DNA sequence has been damaged (Garcia et al., 2012). The use of microscopy images can help us to better characterise the types of biological material present in our samples. For example, the use of fluorescence microscopy allows us to determine the number fraction of fluorescent bioparticles and distinguish them from mineral particles, which do not fluoresce (Huffman et al., 2013). However, these fluorescence microscopy techniques are not always able to detect all bioparticles and the presence of the bioparticles does not guarantee their ice-nucleating ability. Similarly, culturing techniques allow us to identify the number of colony-forming units (CFUs) in an environmental sample (Morris et al., 2013). However,

the ice-nucleating ability of bacteria and fungi is not dependent on its culturability and not all culturable species are ice-active.

1.4 Agricultural Sources of Ice-Nucleating Particles

The focus of this thesis will be on agricultural sources of INPs. Almost half of the Earth's habitable land is used for agriculture (Ellis et al., 2010), yet the potential of these soils as a source of atmospheric INP is still poorly understood. Crop agriculture is an important source of aerosolised soil dust and organic matter (such as bacteria, fungi, etc.) due to a combination of crop density and standard farming practises, such as harvesting and tilling, which inject large amounts of dust into the atmosphere (Lee et al., 2006). In addition, after harvest, the increase in the exposure of bare soil also leads to an increase in soil dust emissions. Animal agriculture has also been shown to increase soil dust emissions since overgrazing and animal manure release biological components into the atmosphere (Hiranuma et al., 2011). Agricultural dust emissions contribute up to 25% to the global dust emissions budget (Ginoux et al., 2012), making it a potentially important source of INPs in the atmosphere (Steinke et al., 2016; Sanchez-Marroquin et al., 2021). Furthermore, it has been shown that agricultural soil dust is easily washed into nearby rivers and lakes, enhancing the ice-nucleating abilities of these water bodies and creating an additional source of INPs in the atmosphere (see Section 1.3.2.4) (Knackstedt et al., 2018; Einbock et al., 2023). The presence of biogenic material may be key to the high ice-nucleating abilities observed in both rivers and soil dust associated with agriculture.

As described in Section 1.3.2, fertile soils are made up of a complex mix of both mineral dust and biological materials. Agricultural soils are fertile soils that originate from agricultural sources and may have additional biological material added to them, such as manure or other fertilisers, which may further enhance the organic matter within these soils. Due to the potential contribution of agricultural dust emissions to INP populations on a global scale, previous work has investigated the ice-nucleating activity of agricultural soil dust (Garcia et al., 2012; Tobo et al., 2014; Steinke et al., 2016; Suski et al., 2018; Hiranuma et al., 2021; Pereira et al., 2022). Agricultural soil dust has been shown to be highly ice-active above $-10\,^{\circ}\mathrm{C}$ (O'Sullivan et al., 2014; Suski et al., 2018) and heat treatments lead to a significant loss of this ice-nucleating activity, suggesting the relative importance of biological components such as ice-active bacteria and fungi in these agricultural soil dusts (O'Sullivan et al., 2015; Steinke et al., 2016).

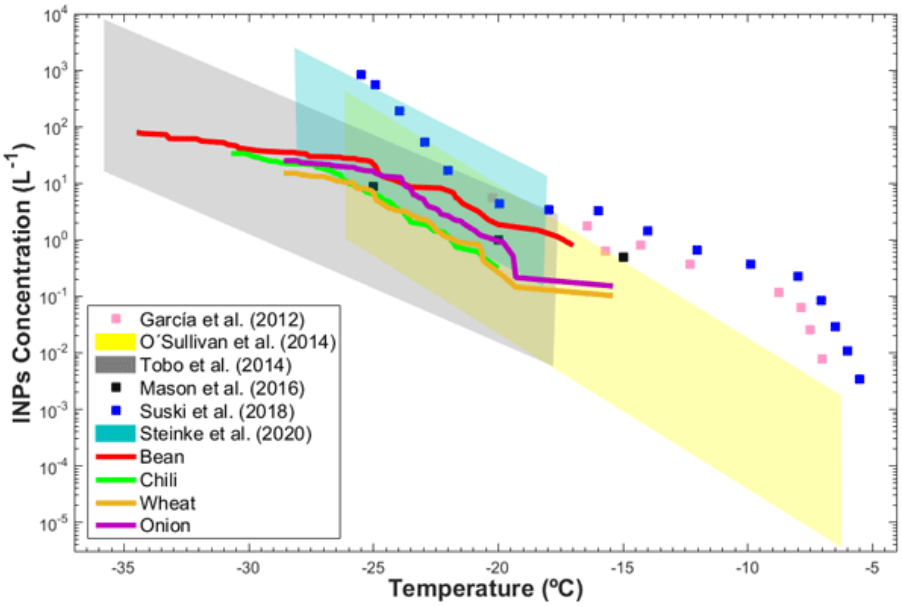

Figure 1.6: Comparison of the INP concentrations per litre (N_{INP}) as a function of temperature of sampled air from agricultural locations in different literature studies. *Figure taken from Pereira et al. (2022).*

Since agricultural soils are made up of such a complex mix of both mineral and organic components, recent work has been unable to determine exactly what is responsible for the observed ice-nucleating activity of these soils. For example, Garcia et al. (2012) investigated the ice-nucleating ability of agricultural soil dust emissions and used DNA analysis to identify the presence of the *ina* gene. They found that the presence of ice-active bacteria was not always required for ice-nucleating activity to be observed, suggesting that other components were responsible for the observed ice-nucleating activity. Similarly, Jimenez-Sanchez et al. (2018) examined the relative contribution of ice-active bacteria to the ice-nucleating ability of agricultural dust emissions. In this study, however, they only examined the ice-nucleating ability of culturable bacteria collected onto agar plates above an agricultural field and found that only a very small portion of the CFUs were ice-active. Since ice-active bacteria do not need to be viable to maintain their ice-nucleating ability, these observations most likely underestimate the relative contribution of bacteria to the ice-nucleating ability of agricultural soils.

Other key studies have shown that the presence of organic components makes it difficult to determine the ice-nucleating ability of agricultural soil dust. In particular, Conen et al. (2011) analysed the ice-nucleating activity of agricultural soils from Mongolia, Germany, Hungary and Yakutia and found that the ice-active mass site density (n_{m}) varied by about 200 μg^{-1} across the different soil samples. Steinke et al. (2016) investigated the ice-nucleating activity of agricultural soil samples collected from four different regions and

found that the variability in the ice-nucleating activity of different soil dust is much greater than that of mineral dust. They concluded that the observed variation is likely due to differences in soil organic matter but were unable to examine this directly (Steinke et al., 2016). Similarly, Suski et al. (2018) took aerosol samples of agricultural soil dust during harvesting activities in four different agricultural fields. They found that both heat-stable and heat-labile INPs were present in their samples, suggesting that a variety of different organic components were contributing to the ice-nucleating ability of the soil (Suski et al., 2018).

More recent work by Hiranuma et al. (2021) examined the ice-nucleating activity of animal agriculture by collecting aerosol samples both upwind and downwind of open animal feeding lots. They found a distinct increase in INP concentrations downwind of open animal lots, particularly at freezing temperatures above $-15\,^{\circ}\mathrm{C}$, suggesting that animal agriculture is also a substantial source of INP. Additionally, a study focused on the ice-nucleating activity of agricultural soil dust in Mexico highlighted that the observed high ice-nucleating activity of these soils is consistent across different regions of Mexico (Pereira et al., 2022), highlighting the need to better understand and characterise the ice-nucleating ability of these soils. Overall, we know that biological components contribute significantly to the ice-nucleating activity of agricultural soils and that the ice-nucleating activity of these soils varies significantly as a result (Figure 1.6). However, more work is needed to better understand the relative importance of these components and better predict the ice-nucleating activity from these anthropogenic sources.

1.5 Project Objectives

The overall aim of this thesis was to investigate the sources of INPs from agricultural locations to determine the extent to which agriculture influences INP populations on both regional and global scales. We characterised the ice-nucleating activity of agricultural soils and fungal crop pathogens with a focus on aiming to better understand the complex biological relationship that influences the ice-nucleating activity of agricultural emissions. We achieved this by addressing three main areas in three results chapters as follows:

1. The first results chapter investigates the importance of surfactant-like macromolecules as INPs and their relative contribution to the ice-nucleating ability of agricultural soils. We extracted the soluble fraction from different soil samples to answer the following questions:

- How does the ice-nucleating ability of agricultural soil relate to its surface activity?
- How does this relationship between surface and ice-nucleating activities in soil samples differ from that of two common soil subcomponents?
- What is the relative contribution of surfactant macromolecules to the ice-nucleating ability of anthropogenic soils?

2. The second results chapter quantifies the ice-nucleating activity of two different species of fungal crop pathogens. We examined the ice-nucleating activity of fungal spores from both field-collected samples and those grown in the lab to answer the following questions:

   - What is the ice-nucleating activity of fungal spores from Yellow Rust and Light Leaf Spot?
   - How do external stressors such as storage time and cold exposure impact the observed ice-nucleating ability of these fungal spores?
   - What is the relative contribution of ice-active bacteria to their ice-nucleating activity?

3. The third results chapter examines the size-resolved ice-nucleating activity of agricultural soils. We aerosolised soil samples collected at the University of Leeds research farm in our aerosol chamber to answer the following questions:

   - What is the size distribution of agricultural dust aerosols?
   - How is the ice-nucleating material distributed across the aerosol size distribution for agricultural dust?
   - What do the size-segregated INP concentrations tell us about the ice-nucleating activity of agricultural dust?

References

Adams, M. P., Atanasova, N. S., Sofieva, S., Ravantti, J., Heikkinen, A., Brasseur, Z., Duplissy, J., Bamford, D. H., and Murray, B. J. (2021). Ice nucleation by viruses and their potential for cloud glaciation. *Biogeosciences*, 18(14):4431–4444.

Arny, D. C., Lindow, S. E., and Upper, C. D. (1976). Frost sensitivity of Zea mays increased by application of Pseudomonas syringae. *Nature*, 262(5566):282–284.

Atkinson, J. D., Murray, B. J., Woodhouse, M. T., Whale, T. F., Baustian, K. J., Carslaw, K. S., Dobbie, S., O'Sullivan, D., and Malkin, T. L. (2013). The importance of feldspar for ice nucleation by mineral dust in mixed-phase clouds. *Nature*, 498(7454):355–358.

Augustin, S., Wex, H., Niedermeier, D., Pummer, B., Grothe, H., Hartmann, S., Tomsche, L., Clauss, T., Voigtländer, J., Ignatius, K., and Stratmann, F. (2013). Immersion freezing of birch pollen washing water. *Atmospheric Chemistry and Physics*, 13(21):10989–11003.

Augustin-Bauditz, S., Wex, H., Denjean, C., Hartmann, S., Schneider, J., Schmidt, S., Ebert, M., and Stratmann, F. (2016). Laboratory-generated mixtures of mineral dust particles with biological substances: characterization of the particle mixing state and immersion freezing behavior. *Atmospheric Chemistry and Physics*, 16(9):5531–5543.

Beall, C. M., Lucero, D., Hill, T. C., DeMott, P. J., Stokes, M. D., and Prather, K. A. (2020). Best practices for precipitation sample storage for offline studies of ice nucleation in marine and coastal environments. *Atmospheric Measurement Techniques*, 13(12):6473–6486.

Bigg, E. K. (1973). Ice Nucleus Concentrations in Remote Areas. *Journal of the Atmospheric Sciences*, 30(6):1153–1157.

Boerjan, W., Ralph, J., and Baucher, M. (2003). Lignin Biosynthesis. *Annual Review of Plant Biology*, 54(1):519–546.

Bogler, S. and Borduas-Dedekind, N. (2020). Lignin's ability to nucleate ice via immersion freezing and its stability towards physicochemical treatments and atmospheric processing. *Atmospheric Chemistry and Physics*, 20(23):14509–14522.

Boose, Y., Sierau, B., García, M. I., Rodríguez, S., Alastuey, A., Linke, C., Schnaiter, M., Kupiszewski, P., Kanji, Z. A., and Lohmann, U. (2016). Ice nucleating particles in the Saharan Air Layer. *Atmospheric Chemistry and Physics*, 16(14):9067–9087.

Burrows, S. M., Hoose, C., Pöschl, U., and Lawrence, M. G. (2013). Ice nuclei in marine air: biogenic particles or dust? *Atmospheric Chemistry and Physics*, 13(1):245–267.

Cascajo-Castresana, M., David, R. O., Iriarte-Alonso, M. A., Bittner, A. M., and Marcolli, C. (2020). Protein aggregates nucleate ice: the example of apoferritin. *Atmospheric Chemistry and Physics*, 20(6):3291–3315.

Ceppi, P., Brient, F., Zelinka, M. D., and Hartmann, D. L. (2017). Cloud feedback mechanisms and their representation in global climate models. *WIREs Climate Change*, 8(4):e465.

Christner, B. C., Morris, C. E., Foreman, C. M., Cai, R., and Sands, D. C. (2008). Ubiquity of Biological Ice Nucleators in Snowfall. *Science*, 319(5867):1214–1214.

Conen, F., Morris, C. E., Leifeld, J., Yakutin, M. V., and Alewell, C. (2011). Biological residues define the ice nucleation properties of soil dust. *Atmospheric Chemistry and Physics*, 11(18):9643–9648.

Conen, F., Stopelli, E., and Zimmermann, L. (2016). Clues that decaying leaves enrich Arctic air with ice nucleating particles. *Atmospheric Environment*, 129:91–94.

Conen, F. and Yakutin, M. V. (2018). Soils rich in biological ice-nucleating particles abound in ice-nucleating macromolecules likely produced by fungi. *Biogeosciences*, 15(14):4381–4385.

Conen, F., Yakutin, M. V., Yttri, K. E., and Hüglin, C. (2017). Ice Nucleating Particle Concentrations Increase When Leaves Fall in Autumn. *Atmosphere*, 8(10):202.

Daily, M. I., Tarn, M. D., Whale, T. F., and Murray, B. J. (2022). An evaluation of the heat test for the ice-nucleating ability of minerals and biological material. *Atmospheric Measurement Techniques*, 15(8):2635–2665.

David, R. O., Marcolli, C., Fahrni, J., Qiu, Y., Perez Sirkin, Y. A., Molinero, V., Mahrt, F., Brühwiler, D., Lohmann, U., and Kanji, Z. A. (2019). Pore condensation and freezing is responsible for ice formation below water saturation for porous particles. *Proceedings of the National Academy of Sciences*, 116(17):8184–8189.

DeMott, P. J., Hill, T. C. J., McCluskey, C. S., Prather, K. A., Collins, D. B., Sullivan, R. C., Ruppel, M. J., Mason, R. H., Irish, V. E., Lee, T., Hwang, C. Y., Rhee, T. S., Snider, J. R., McMeeking, G. R., Dhaniyala, S., Lewis, E. R., Wentzell, J. J. B., Abbatt, J., Lee, C., Sultana, C. M., Ault, A. P., Axson, J. L., Diaz Martinez, M., Venero, I., Santos-Figueroa, G., Stokes, M. D., Deane, G. B., Mayol-Bracero, O. L., Grassian, V. H., Bertram, T. H., Bertram, A. K., Moffett, B. F., and Franc, G. D. (2016). Sea spray aerosol as a unique source of ice nucleating particles. *Proceedings of the National Academy of Sciences*, 113(21):5797–5803.

DeMott, P. J., Prenni, A. J., Liu, X., Kreidenweis, S. M., Petters, M. D., Twohy, C. H., Richardson, M. S., Eidhammer, T., and Rogers, D. C. (2010). Predicting global atmospheric ice nuclei distributions and their impacts on climate. *Proceedings of the National Academy of Sciences*, 107(25):11217–11222.

DeMott, P. J., Sassen, K., Poellot, M. R., Baumgardner, D., Rogers, D. C., Brooks, S. D., Prenni, A. J., and Kreidenweis, S. M. (2003). African dust aerosols as atmospheric ice nuclei. *Geophysical Research Letters*, 30(14).

Després, V. R., Huffman, J. A., Burrows, S. M., Hoose, C., Safatov, A. S., Buryak, G., Fröhlich-Nowoisky, J., Elbert, W., Andreae, M. O., Pöschl, U., and Jaenicke, R. (2012). Primary biological aerosol particles in the atmosphere: a review. 64(1):15598.

Diehl, K., Matthias-Maser, S., Jaenicke, R., and Mitra, S. K. (2002). The ice nucleating ability of pollen:: Part II. Laboratory studies in immersion and contact freezing modes. *Atmospheric Research*, 61(2):125–133.

Diehl, K., Quick, C., Matthias-Maser, S., Mitra, S. K., and Jaenicke, R. (2001). The ice nucleating ability of pollen: Part I: Laboratory studies in deposition and condensation freezing modes. *Atmospheric Research*, 58(2):75–87.

Dreischmeier, K., Budke, C., Wiehemeier, L., Kottke, T., and Koop, T. (2017). Boreal pollen contain ice-nucleating as well as ice-binding 'antifreeze' polysaccharides. *Scientific Reports*, 7(1):41890.

Einbock, A., Burtscher, E., Frey, C., and Conen, F. (2023). Export of ice-nucleating particles from watersheds: results from the Amazon and Tocantins river plumes. *Royal Society Open Science*, 10(2):220878.

Ellis, E. C., Klein Goldewijk, K., Siebert, S., Lightman, D., and Ramankutty, N. (2010). Anthropogenic transformation of the biomes, 1700 to 2000. *Global Ecology and Biogeography*, 19(5):589–606.

Failor, K. C., Schmale, D. G., Vinatzer, B. A., and Monteil, C. L. (2017). Ice nucleation active bacteria in precipitation are genetically diverse and nucleate ice by employing different mechanisms. *The ISME Journal*, 11(12):2740–2753.

Feichter, J. and Leisner, T. (2009). Climate engineering: A critical review of approaches to modify the global energy balance. *The European Physical Journal Special Topics*, 176(1):81–92.

Felgitsch, L., Baloh, P., Burkart, J., Mayr, M., Momken, M. E., Seifried, T. M., Winkler, P., Schmale III, D. G., and Grothe, H. (2018). Birch leaves and branches as a source of ice-nucleating macromolecules. *Atmospheric Chemistry and Physics*, 18(21):16063–16079.

Forster, P., Storelvmo, T., Armour, K., Collins, W., Dufresne, J.-L., Frame, D., Lunt, D. J., Mauritsen, T., Palmer, M. D., Watanabe, M., Wild, M., and Zhang, H. (2021). The Earth's Energy Budget, Climate Feedbacks, and Climate Sensitivity. In *Climate Change 2021: The Physical Science Basis. Contribution of Working Group I to the Sixth Assessment Report of the Intergovernmental Panel on Climate Change.*, pages 923–1054. Cambridge University Press, Cambridge, United Kingdom and New York, NY, USA.

Fröhlich-Nowoisky, J., Hill, T. C. J., Pummer, B. G., Yordanova, P., Franc, G. D., and Pöschl, U. (2015). Ice nucleation activity in the widespread soil fungus *Mortierella alpina*. *Biogeosciences*, 12(4):1057–1071.

Garcia, E., Hill, T. C. J., Prenni, A. J., DeMott, P. J., Franc, G. D., and Kreidenweis, S. M. (2012). Biogenic ice nuclei in boundary layer air over two U.S. High Plains agricultural regions. *Journal of Geophysical Research: Atmospheres*, 117(D18).

Ginoux, P., Chin, M., Tegen, I., Prospero, J. M., Holben, B., Dubovik, O., and Lin, S.-J. (2001). Sources and distributions of dust aerosols simulated with the GOCART model. *Journal of Geophysical Research: Atmospheres*, 106(D17):20255–20273.

Ginoux, P., Prospero, J. M., Gill, T. E., Hsu, N. C., and Zhao, M. (2012). Global-scale attribution of anthropogenic and natural dust sources and their emission rates based on MODIS Deep Blue aerosol products. *Reviews of Geophysics*, 50(3).

Govindarajan, A. G. and Lindow, S. E. (1988). Size of bacterial ice-nucleation sites measured in situ by radiation inactivation analysis. *Proceedings of the National Academy of Sciences*, 85(5):1334–1338. Publisher: Proceedings of the National Academy of Sciences.

Grawe, S., Augustin-Bauditz, S., Hartmann, S., Hellner, L., Pettersson, J. B. C., Prager, A., Stratmann, F., and Wex, H. (2016). The immersion freezing behavior of ash particles from wood and brown coal burning. *Atmospheric Chemistry and Physics*, 16(21):13911–13928.

Green, R. L. and Warren, G. J. (1985). Physical and functional repetition in a bacterial ice nucleation gene. *Nature*, 317(6038):645–648. Number: 6038 Publisher: Nature Publishing Group.

Hader, J. D., Wright, T. P., and Petters, M. D. (2014). Contribution of pollen to atmospheric ice nuclei concentrations. *Atmospheric Chemistry and Physics*, 14(11):5433–5449.

Haga, D. I., Iannone, R., Wheeler, M. J., Mason, R., Polishchuk, E. A., Fetch Jr., T., van der Kamp, B. J., McKendry, I. G., and Bertram, A. K. (2013). Ice nucleation properties of rust and bunt fungal spores and their transport to high altitudes, where they can cause heterogeneous freezing. *Journal of Geophysical Research: Atmospheres*, 118(13):7260–7272.

Harrison, A. D., Lever, K., Sanchez-Marroquin, A., Holden, M. A., Whale, T. F., Tarn, M. D., McQuaid, J. B., and Murray, B. J. (2019). The ice-nucleating ability of quartz immersed in water and its atmospheric importance compared to K-feldspar. *Atmospheric Chemistry and Physics*, 19(17):11343–11361.

Harrison, A. D., Whale, T. F., Carpenter, M. A., Holden, M. A., Neve, L., O'Sullivan, D., Vergara Temprado, J., and Murray, B. J. (2016). Not all feldspars are equal: a survey of ice nucleating properties across the feldspar group of minerals. *Atmospheric Chemistry and Physics*, 16(17):10927–10940.

Hartmann, D. L., Ockert-Bell, M. E., and Michelsen, M. L. (1992). The Effect of Cloud Type on Earth's Energy Balance: Global Analysis. *Journal of Climate*, 5(11):1281–1304.

Hartmann, S., Ling, M., Dreyer, L. S. A., Zipori, A., Finster, K., Grawe, S., Jensen, L. Z., Borck, S., Reicher, N., Drace, T., Niedermeier, D., Jones, N. C., Hoffmann, S. V., Wex, H., Rudich, Y., Boesen, T., and Šantl Temkiv, T. (2022). Structure and Protein-Protein Interactions of Ice Nucleation Proteins Drive Their Activity. *Frontiers in Microbiology*, 13:872306.

Haywood, J. and Boucher, O. (2000). Estimates of the direct and indirect radiative forcing due to tropospheric aerosols: A review. *Reviews of Geophysics*, 38(4):513–543. _eprint: https://onlinelibrary.wiley.com/doi/pdf/10.1029/1999RG000078.

Herbert, R. J., Murray, B. J., Dobbie, S. J., and Koop, T. (2015). Sensitivity of liquid clouds to homogenous freezing parameterizations. *Geophysical Research Letters*, 42(5):1599–1605.

Hill, T. C. J., DeMott, P. J., Tobo, Y., Fröhlich-Nowoisky, J., Moffett, B. F., Franc, G. D., and Kreidenweis, S. M. (2016). Sources of organic ice nucleating particles in soils. *Atmospheric Chemistry and Physics*, 16(11):7195–7211.

Hiranuma, N., Adachi, K., Bell, D. M., Belosi, F., Beydoun, H., Bhaduri, B., Bingemer, H., Budke, C., Clemen, H.-C., Conen, F., Cory, K. M., Curtius, J., DeMott, P. J., Eppers, O., Grawe, S., Hartmann, S., Hoffmann, N., Höhler, K., Jantsch, E., Kiselev, A., Koop, T., Kulkarni, G., Mayer, A., Murakami, M., Murray, B. J., Nicosia, A., Petters, M. D., Piazza, M., Polen, M., Reicher, N., Rudich, Y., Saito, A., Santachiara, G., Schiebel, T., Schill, G. P., Schneider, J., Segev, L., Stopelli, E., Sullivan, R. C., Suski, K., Szakáll, M., Tajiri, T., Taylor, H., Tobo, Y., Ullrich, R., Weber, D., Wex, H., Whale, T. F., Whiteside, C. L., Yamashita, K., Zelenyuk, A., and Möhler, O. (2019). A comprehensive characterization of ice nucleation by three different types of cellulose particles immersed in water. *Atmospheric Chemistry and Physics*, 19(7):4823–4849.

Hiranuma, N., Auvermann, B. W., Belosi, F., Bush, J., Cory, K. M., Georgakopoulos, D. G., Höhler, K., Hou, Y., Lacher, L., Saathoff, H., Santachiara, G., Shen, X., Steinke, I., Ullrich, R., Umo, N. S., Vepuri, H. S. K., Vogel, F., and Möhler, O. (2021). Laboratory and field studies of ice-nucleating particles from open-lot livestock facilities in Texas. *Atmospheric Chemistry and Physics*, 21(18):14215–14234.

Hiranuma, N., Brooks, S. D., Gramann, J., and Auvermann, B. W. (2011). High concentrations of coarse particles emitted from a cattle feeding operation. *Atmospheric Chemistry and Physics*, 11(16):8809–8823.

Hoose, C., Kristjansson, J. E., Chen, J. P., and Hazra, A. (2010). A Classical-Theory-Based Parameterization of Heterogeneous Ice Nucleation by Mineral Dust, Soot, and Biological Particles in a Global Climate Model in: Journal of the Atmospheric Sciences Volume 67 Issue 8 (2010). *Journal of the Atmospheric Sciences*, 67(8):2483–2503.

Huffman, J. A., Prenni, A. J., DeMott, P. J., Pöhlker, C., Mason, R. H., Robinson, N. H., Fröhlich-Nowoisky, J., Tobo, Y., Després, V. R., Garcia, E., Gochis, D. J., Harris, E., Müller-Germann, I., Ruzene, C., Schmer, B., Sinha, B., Day, D. A., Andreae, M. O., Jimenez, J. L., Gallagher, M., Kreidenweis, S. M., Bertram, A. K., and Pöschl, U. (2013). High concentrations of biological aerosol particles and ice nuclei during and after rain. *Atmospheric Chemistry and Physics*, 13(13):6151–6164.

Huffman, J. A., Treutlein, B., and Pöschl, U. (2010). Fluorescent biological aerosol particle concentrations and size distributions measured with an Ultraviolet Aerodynamic Particle Sizer (UV-APS) in Central Europe. *Atmospheric Chemistry and Physics*, 10(7):3215–3233. Publisher: Copernicus GmbH.

Iannone, R., Chernoff, D. I., Pringle, A., Martin, S. T., and Bertram, A. K. (2011). The ice nucleation ability of one of the most abundant types of fungal spores found in the atmosphere. *Atmospheric Chemistry and Physics*, 11(3):1191–1201.

Ickes, L., Welti, A., Hoose, C., and Lohmann, U. (2015). Classical nucleation theory of homogeneous freezing of water: thermodynamic and kinetic parameters. *Physical Chemistry Chemical Physics*, 17(8):5514–5537.

Irish, V. E., Elizondo, P., Chen, J., Chou, C., Charette, J., Lizotte, M., Ladino, L. A., Wilson, T. W., Gosselin, M., Murray, B. J., Polishchuk, E., Abbatt, J. P. D., Miller, L. A., and Bertram, A. K. (2017). Ice-nucleating particles in Canadian Arctic sea-surface microlayer and bulk seawater. *Atmospheric Chemistry and Physics*, 17(17):10583–10595.

Irish, V. E., Hanna, S. J., Willis, M. D., China, S., Thomas, J. L., Wentzell, J. J. B., Cirisan, A., Si, M., Leaitch, W. R., Murphy, J. G., Abbatt, J. P. D., Laskin, A., Girard, E., and Bertram, A. K. (2019a). Ice nucleating particles in the marine boundary layer in the Canadian Arctic during summer 2014. *Atmospheric Chemistry and Physics*, 19(2):1027–1039.

Irish, V. E., Hanna, S. J., Xi, Y., Boyer, M., Polishchuk, E., Ahmed, M., Chen, J., Abbatt, J. P. D., Gosselin, M., Chang, R., Miller, L. A., and Bertram, A. K. (2019b). Revisiting properties and concentrations of ice-nucleating particles in the sea surface microlayer and bulk seawater in the Canadian Arctic during summer. *Atmospheric Chemistry and Physics*, 19(11):7775–7787.

Jaenicke, R. (2005). Abundance of Cellular Material and Proteins in the Atmosphere. *Science*, 308(5718):73–73.

Jimenez-Sanchez, C., Hanlon, R., Aho, K. A., Powers, C., Morris, C. E., and Schmale, D. G. (2018). Diversity and Ice Nucleation Activity of Microorganisms Collected With a Small Unmanned Aircraft System (sUAS) in France and the United States. *Frontiers in Microbiology*, 9.

Junge, K. and Swanson, B. D. (2008). High-resolution ice nucleation spectra of sea-ice bacteria: implications for cloud formation and life in frozen environments. *Biogeosciences*, 5(3):865–873.

Kanji, Z. A., Ladino, L. A., Wex, H., Boose, Y., Burkert-Kohn, M., Cziczo, D. J., and Krämer, M. (2017). Overview of Ice Nucleating Particles. *Meteorological Monographs*, 58(1):1.1–1.33.

Kieft, T. L. (1988). Ice Nucleation Activity in Lichens. *Applied and Environmental Microbiology*, 54(7):1678–1681.

Kieft, T. L. and Ruscetti, T. (1990). Characterization of biological ice nuclei from a lichen. *Journal of Bacteriology*, 172(6):3519–3523.

Knackstedt, K. A., Moffett, B. F., Hartmann, S., Wex, H., Hill, T. C. J., Glasgo, E. D., Reitz, L. A., Augustin-Bauditz, S., Beall, B. F. N., Bullerjahn, G. S., Fröhlich-Nowoisky, J., Grawe, S., Lubitz, J., Stratmann, F., and McKay, R. M. L. (2018). Terrestrial Origin for Abundant Riverine Nanoscale Ice-Nucleating Particles. *Environmental Science & Technology*, 52(21):12358–12367.

Knopf, D. A., Alpert, P. A., Wang, B., and Aller, J. Y. (2011). Stimulation of ice nucleation by marine diatoms. *Nature Geoscience*, 4(2):88–90.

Korolev, A. (2007). Limitations of the Wegener–Bergeron–Findeisen Mechanism in the Evolution of Mixed-Phase Clouds. *Journal of the Atmospheric Sciences*, 64(9):3372–3375.

Kunert, A. T., Pöhlker, M. L., Tang, K., Krevert, C. S., Wieder, C., Speth, K. R., Hanson, L. E., Morris, C. E., Schmale III, D. G., Pöschl, U., and Fröhlich-Nowoisky, J. (2019). Macromolecular fungal ice nuclei in *Fusarium*: effects of physical and chemical processing. *Biogeosciences*, 16(23):4647–4659.

Lee, S.-A., Adhikari, A., Grinshpun, S. A., McKay, R., Shukla, R., and Reponen, T. (2006). Personal Exposure to Airborne Dust and Microorganisms in Agricultural Environments. *Journal of Occupational and Environmental Hygiene*, 3(3):118–130.

Leifer, I., Caulliez, G., and de Leeuw, G. (2006). Bubbles generated from wind-steepened breaking waves: 2. Bubble plumes, bubbles, and wave characteristics. *Journal of Geophysical Research: Oceans*, 111(C6).

Lindemann, J., Constantinidou, H. A., Barchet, W. R., and Upper, C. D. (1982). Plants as Sources of Airborne Bacteria, Including Ice Nucleation-Active Bacteria. *Applied and Environmental Microbiology*, 44(5):1059–1063.

Lindow, S. E., Arny, D. C., and Upper, C. D. (1978). Distribution of ice nucleation-active bacteria on plants in nature. *Applied and Environmental Microbiology*, 36(6):831–838.

Lohmann, U. and Diehl, K. (2006). Sensitivity Studies of the Importance of Dust Ice Nuclei for the Indirect Aerosol Effect on Stratiform Mixed-Phase Clouds. *Journal of the Atmospheric Sciences*, 63(3):968–982.

Lohmann, U. and Feichter, J. (2005). Global indirect aerosol effects: a review. *Atmospheric Chemistry and Physics*, 5(3):715–737.

Lukas, M., Schwidetzky, R., Eufemio, R. J., Bonn, M., and Meister, K. (2022). Toward Understanding Bacterial Ice Nucleation. *The Journal of Physical Chemistry B*, 126(9):1861–1867.

Lukas, M., Schwidetzky, R., Kunert, A. T., Pöschl, U., Fröhlich-Nowoisky, J., Bonn, M., and Meister, K. (2020). Electrostatic Interactions Control the Functionality of Bacterial Ice Nucleators. *Journal of the American Chemical Society*, 142(15):6842–6846.

Maki, L. R., Galyan, E. L., Chang-Chien, M.-M., and Caldwell, D. R. (1974). Ice Nucleation Induced by Pseudomonas syringae. *Applied Microbiology*, 28(3):456–459.

Maki, L. R. and Willoughby, K. J. (1978). Bacteria as Biogenic Sources of Freezing Nuclei. *Journal of Applied Meteorology and Climatology*, 17(7):1049–1053. Publisher: American Meteorological Society Section: Journal of Applied Meteorology and Climatology.

Marcolli, C. (2014). Deposition nucleation viewed as homogeneous or immersion freezing in pores and cavities. *Atmospheric Chemistry and Physics*, 14(4):2071–2104.

Mason, R. H., Si, M., Chou, C., Irish, V. E., Dickie, R., Elizondo, P., Wong, R., Brintnell, M., Elsasser, M., Lassar, W. M., Pierce, K. M., Leaitch, W. R., MacDonald, A. M., Platt, A., Toom-Sauntry, D., Sarda-Estève, R., Schiller, C. L., Suski, K. J., Hill, T. C. J., Abbatt, J. P. D., Huffman, J. A., DeMott, P. J., and Bertram, A. K. (2016). Size-resolved measurements of ice-nucleating particles at six locations in North America and one in Europe. *Atmospheric Chemistry and Physics*, 16(3):1637–1651.

Maters, E. C., Cimarelli, C., Casas, A. S., Dingwell, D. B., and Murray, B. J. (2020). Volcanic ash ice-nucleating activity can be enhanced or depressed by ash-gas interaction in the eruption plume. *Earth and Planetary Science Letters*, 551:116587.

Matus, A. V. and L'Ecuyer, T. S. (2017). The role of cloud phase in Earth's radiation budget. *Journal of Geophysical Research: Atmospheres*, 122(5):2559–2578.

McCluskey, C. S., DeMott, P. J., Prenni, A. J., Levin, E. J. T., McMeeking, G. R., Sullivan, A. P., Hill, T. C. J., Nakao, S., Carrico, C. M., and Kreidenweis, S. M. (2014). Characteristics of atmospheric ice nucleating particles associated with biomass burning in the US: Prescribed burns and wildfires. *Journal of Geophysical Research: Atmospheres*, 119(17):10458–10470.

McCluskey, C. S., Hill, T. C. J., Sultana, C. M., Laskina, O., Trueblood, J., Santander, M. V., Beall, C. M., Michaud, J. M., Kreidenweis, S. M., Prather, K. A., Grassian, V., and DeMott, P. J. (2018). A Mesocosm Double Feature: Insights into the Chemical Makeup of Marine Ice Nucleating Particles. *Journal of the Atmospheric Sciences*, 75(7):2405–2423.

Moffett, B. F., Hill, T. C. J., and DeMott, P. J. (2018). Abundance of Biological Ice Nucleating Particles in the Mississippi and Its Major Tributaries. *Atmosphere*, 9(8):307.

Morris, C. E., Sands, D. C., Glaux, C., Samsatly, J., Asaad, S., Moukahel, A. R., Gonçalves, F. L. T., and Bigg, E. K. (2013). Urediospores of rust fungi are ice nucleation active at > -10 °C and harbor ice nucleation active bacteria. *Atmospheric Chemistry and Physics*, 13(8):4223–4233.

Morris, C. E., Sands, D. C., Vinatzer, B. A., Glaux, C., Guilbaud, C., Buffière, A., Yan, S., Dominguez, H., and Thompson, B. M. (2008). The life history of the plant pathogen Pseudomonas syringae is linked to the water cycle. *The ISME Journal*, 2(3):321–334.

Mullin, J. W. (2001). 5 - Nucleation. In Mullin, J. W., editor, *Crystallization (Fourth Edition)*, pages 181–215. Butterworth-Heinemann, Oxford.

Murray, B. J., Carslaw, K. S., and Field, P. R. (2021). Opinion: Cloud-phase climate feedback and the importance of ice-nucleating particles. *Atmospheric Chemistry and Physics*, 21(2):665–679.

Murray, B. J., O'Sullivan, D., D. Atkinson, J., and Webb, M. (2012). Ice nucleation by particles immersed in supercooled cloud droplets. *Chemical Society Reviews*, 41(19):6519–6554.

Möhler, O., Benz, S., Saathoff, H., Schnaiter, M., Wagner, R., Schneider, J., Walter, S., Ebert, V., and Wagner, S. (2008). The effect of organic coating on the heterogeneous ice nucleation efficiency of mineral dust aerosols. *Environmental Research Letters*, 3(2):025007.

Niedermeier, D., Augustin-Bauditz, S., Hartmann, S., Wex, H., Ignatius, K., and Stratmann, F. (2015). Can we define an asymptotic value for the ice active surface site density for heterogeneous ice nucleation? *Journal of Geophysical Research: Atmospheres*, 120(10):5036–5046.

Niemand, M., Möhler, O., Vogel, B., Vogel, H., Hoose, C., Connolly, P., Klein, H., Bingemer, H., DeMott, P., Skrotzki, J., and Leisner, T. (2012). A Particle-Surface-Area-Based Parameterization of Immersion Freezing on Desert Dust Particles. *Journal of the Atmospheric Sciences*, 69(10):3077–3092.

O'Sullivan, D., Murray, B. J., Malkin, T. L., Whale, T. F., Umo, N. S., Atkinson, J. D., Price, H. C., Baustian, K. J., Browse, J., and Webb, M. E. (2014). Ice nucleation by fertile soil dusts: relative importance of mineral and biogenic components. *Atmospheric Chemistry and Physics*, 14(4):1853–1867.

O'Sullivan, D., Murray, B. J., Ross, J. F., and Webb, M. E. (2016). The adsorption of fungal ice-nucleating proteins on mineral dusts: a terrestrial reservoir of atmospheric ice-nucleating particles. *Atmospheric Chemistry and Physics*, 16(12):7879–7887.

O'Sullivan, D., Murray, B. J., Ross, J. F., Whale, T. F., Price, H. C., Atkinson, J. D., Umo, N. S., and Webb, M. E. (2015). The relevance of nanoscale biological fragments for ice nucleation in clouds. *Scientific Reports*, 5(1):8082.

Pereira, D. L., Gavilán, I., Letechipía, C., Raga, G. B., Puig, T. P., Mugica-Álvarez, V., Alvarez-Ospina, H., Rosas, I., Martinez, L., Salinas, E., Quintana, E. T., Rosas, D., and Ladino, L. A. (2022). Mexican agricultural soil dust as a source of ice nucleating particles. *Atmospheric Chemistry and Physics*, 22(10):6435–6447.

Phelps, P., Giddings, T. H., Prochoda, M., and Fall, R. (1986). Release of cell-free ice nuclei by Erwinia herbicola. *Journal of Bacteriology*, 167(2):496–502.

Porter, G. C. E., Sikora, S. N. F., Adams, M. P., Proske, U., Harrison, A. D., Tarn, M. D., Brooks, I. M., and Murray, B. J. (2020). Resolving the size of ice-nucleating particles with a balloon deployable aerosol sampler: the SHARK. *Atmospheric Measurement Techniques*, 13(6):2905–2921.

Pouleur, S., Richard, C., Martin, J.-G., and Antoun, H. (1992). Ice Nucleation Activity in Fusarium acuminatum and Fusarium avenaceum. *Applied and Environmental Microbiology*, 58(9):2960–2964.

Prenni, A. J., DeMott, P. J., Sullivan, A. P., Sullivan, R. C., Kreidenweis, S. M., and Rogers, D. C. (2012). Biomass burning as a potential source for atmospheric ice nuclei: Western wildfires and prescribed burns. *Geophysical Research Letters*, 39(11).

Pruppacher, H. R. and Klett, J. D. (2010). *Microphysics of clouds and precipitation*. Atmospheric and oceanographic sciences library ; v. 18. Springer, Dordrecht ;.

Pummer, B. G., Bauer, H., Bernardi, J., Bleicher, S., and Grothe, H. (2012). Suspendable macromolecules are responsible for ice nucleation activity of birch and conifer pollen. *Atmospheric Chemistry and Physics*, 12(5):2541–2550.

Qiu, Y., Hudait, A., and Molinero, V. (2019). How Size and Aggregation of Ice-Binding Proteins Control Their Ice Nucleation Efficiency. *Journal of the American Chemical Society*, 141(18):7439–7452.

Reicher, N., Budke, C., Eickhoff, L., Raveh-Rubin, S., Kaplan-Ashiri, I., Koop, T., and Rudich, Y. (2019). Size-dependent ice nucleation by airborne particles during dust events in the eastern Mediterranean. *Atmospheric Chemistry and Physics*, 19(17):11143–11158.

Richard, C., Martin, J.-G., and Pouleur, S. (1996). Ice nucleation activity identified in some phytopathogenic Fusarium species. *Phytoprotection*, 77(2):83–92.

Rogers, D. C., DeMott, P. J., Kreidenweis, S. M., and Chen, Y. (1998). Measurements of ice nucleating aerosols during SUCCESS. *Geophysical Research Letters*, 25(9):1383–1386.

Rosinski, J., Haagenson, P. L., Nagamoto, C. T., and Parungo, F. (1986). Ice-forming nuclei of maritime origin. *Journal of Aerosol Science*, 17(1):23–46.

Sanchez-Marroquin, A., S. West, J., T. Burke, I., B. McQuaid, J., and J. Murray, B. (2021). Mineral and biological ice-nucleating particles above the South East of the British Isles. *Environmental Science: Atmospheres*, 1(4):176–191.

Schill, G. P., DeMott, P. J., Emerson, E. W., Rauker, A. M. C., Kodros, J. K., Suski, K. J., Hill, T. C. J., Levin, E. J. T., Pierce, J. R., Farmer, D. K., and Kreidenweis, S. M. (2020). The contribution of black carbon to global ice nucleating particle concentrations relevant to mixed-phase clouds. *Proceedings of the National Academy of Sciences*, 117(37):22705–22711.

Schill, G. P., Jathar, S. H., Kodros, J. K., Levin, E. J. T., Galang, A. M., Friedman, B., Link, M. F., Farmer, D. K., Pierce, J. R., Kreidenweis, S. M., and DeMott, P. J. (2016). Ice-nucleating particle emissions from photochemically aged diesel and biodiesel exhaust. *Geophysical Research Letters*, 43(10):5524–5531.

Schnell, R. C. and Tan-Schnell, S. N. (1982). Kenyan tea litter: A source of ice nuclei. 34(1):92.

Schnell, R. C. and Vali, G. (1972). Atmospheric Ice Nuclei from Decomposing Vegetation. *Nature*, 236(5343):163–165.

Schnell, R. C. and Vali, G. (1973). World-wide Source of Leaf-derived Freezing Nuclei. *Nature*, 246(5430):212–213.

Schnell, R. C. and Vali, G. (1976). Biogenic Ice Nuclei: Part I. Terrestrial and Marine Sources. *Journal of the Atmospheric Sciences*, 33(8):1554–1564.

Schwidetzky, R., Sudera, P., Backes, A. T., Pöschl, U., Bonn, M., Fröhlich-Nowoisky, J., and Meister, K. (2021). Membranes Are Decisive for Maximum Freezing Efficiency of Bacterial Ice Nucleators. *The Journal of Physical Chemistry Letters*, 12(44):10783–10787.

Seinfeld, J. H. and Pandis, S. (2016). *Atmospheric chemistry and physics: from air pollution to climate change*. Wiley, Hoboken, New Jersey, third edition.

Si, M., Irish, V. E., Mason, R. H., Vergara-Temprado, J., Hanna, S. J., Ladino, L. A., Yakobi-Hancock, J. D., Schiller, C. L., Wentzell, J. J. B., Abbatt, J. P. D., Carslaw, K. S., Murray, B. J., and Bertram, A. K. (2018). Ice-nucleating ability of aerosol particles and possible sources at three coastal marine sites. *Atmospheric Chemistry and Physics*, 18(21):15669–15685.

Spracklen, D. V. and Heald, C. L. (2014). The contribution of fungal spores and bacteria to regional and global aerosol number and ice nucleation immersion freezing rates. *Atmospheric Chemistry and Physics*, 14(17):9051–9059.

Steinke, I., Funk, R., Busse, J., Iturri, A., Kirchen, S., Leue, M., Möhler, O., Schwartz, T., Schnaiter, M., Sierau, B., Toprak, E., Ullrich, R., Ulrich, A., Hoose, C., and Leisner, T. (2016). Ice nucleation activity of agricultural soil dust aerosols from Mongolia, Argentina, and Germany. *Journal of Geophysical Research: Atmospheres*, 121(22):13,559–13,576.

Steinke, I., Hiranuma, N., Funk, R., Höhler, K., Tüllmann, N., Umo, N. S., Weidler, P. G., Möhler, O., and Leisner, T. (2020). Complex plant-derived organic aerosol as ice-nucleating particles – more than the sums of their parts? *Atmospheric Chemistry and Physics*, 20(19):11387–11397.

Storelvmo, T. (2017). Aerosol Effects on Climate via Mixed-Phase and Ice Clouds. *Annual Review of Earth and Planetary Sciences*, 45(1):199–222.

Storelvmo, T., Tan, I., and Korolev, A. V. (2015). Cloud Phase Changes Induced by CO2 Warming—a Powerful yet Poorly Constrained Cloud-Climate Feedback. *Current Climate Change Reports*, 1(4):288–296.

Suski, K. J., Hill, T. C. J., Levin, E. J. T., Miller, A., DeMott, P. J., and Kreidenweis, S. M. (2018). Agricultural harvesting emissions of ice-nucleating particles. *Atmospheric Chemistry and Physics*, 18(18):13755–13771.

Sánchez-Ochoa, A., Kasper-Giebl, A., Puxbaum, H., Gelencser, A., Legrand, M., and Pio, C. (2007). Concentration of atmospheric cellulose: A proxy for plant debris across a west-east transect over Europe. *Journal of Geophysical Research: Atmospheres*, 112(D23).

Tobo, Y., Adachi, K., DeMott, P. J., Hill, T. C. J., Hamilton, D. S., Mahowald, N. M., Nagatsuka, N., Ohata, S., Uetake, J., Kondo, Y., and Koike, M. (2019). Glacially sourced dust as a potentially significant source of ice nucleating particles. *Nature Geoscience*, 12(4):253–258.

Tobo, Y., DeMott, P. J., Hill, T. C. J., Prenni, A. J., Swoboda-Colberg, N. G., Franc, G. D., and Kreidenweis, S. M. (2014). Organic matter matters for ice nuclei of agricultural soil origin. *Atmospheric Chemistry and Physics*, 14(16):8521–8531.

Vali, G., Christensen, M., Fresh, R. W., Galyan, E. L., Maki, L. R., and Schnell, R. C. (1976). Biogenic Ice Nuclei. Part II: Bacterial Sources. *Journal of the Atmospheric Sciences*, 33(8):1565–1570.

Vali, G., DeMott, P. J., Möhler, O., and Whale, T. F. (2015). Technical Note: A proposal for ice nucleation terminology. *Atmospheric Chemistry and Physics*, 15(18):10263–10270.

Wex, H., Augustin-Bauditz, S., Boose, Y., Budke, C., Curtius, J., Diehl, K., Dreyer, A., Frank, F., Hartmann, S., Hiranuma, N., Jantsch, E., Kanji, Z. A., Kiselev, A., Koop, T., Möhler, O., Niedermeier, D., Nillius, B., Rösch, M., Rose, D., Schmidt, C., Steinke, I., and Stratmann, F. (2015). Intercomparing different devices for the investigation of ice nucleating particles using Snomax® as test substance. *Atmospheric Chemistry and Physics*, 15(3):1463–1485.

Wilson, T. W., Ladino, L. A., Alpert, P. A., Breckels, M. N., Brooks, I. M., Browse, J., Burrows, S. M., Carslaw, K. S., Huffman, J. A., Judd, C., Kilthau, W. P., Mason, R. H., McFiggans, G., Miller, L. A., Nájera, J. J., Polishchuk, E., Rae, S., Schiller, C. L., Si, M., Temprado, J. V., Whale, T. F., Wong, J. P. S., Wurl, O., Yakobi-Hancock, J. D., Abbatt, J. P. D., Aller, J. Y., Bertram, A. K., Knopf, D. A., and Murray, B. J. (2015). A marine biogenic source of atmospheric ice-nucleating particles. *Nature*, 525(7568):234–238.

Wolf, M. J., Coe, A., Dove, L. A., Zawadowicz, M. A., Dooley, K., Biller, S. J., Zhang, Y., Chisholm, S. W., and Cziczo, D. J. (2019). Investigating the Heterogeneous Ice Nucleation of Sea Spray Aerosols Using Prochlorococcus as a Model Source of Marine Organic Matter. *Environmental Science & Technology*, 53(3):1139–1149.

Šantl Temkiv, T., Sahyoun, M., Finster, K., Hartmann, S., Augustin-Bauditz, S., Stratmann, F., Wex, H., Clauss, T., Nielsen, N. W., Sørensen, J. H., Korsholm, U. S., Wick, L. Y., and Karlson, U. G. (2015). Characterization of airborne ice-nucleation-active bacteria and bacterial fragments. *Atmospheric Environment*, 109:105–117.

2 Methods

Throughout this thesis, a variety of methods have been used. Each results chapter that follows will detail the unique methodology used, however, some methods will be common throughout. This chapter will include some general methods that are common across all three chapters of this thesis. I will discuss the droplet-freezing techniques used in this thesis and describe how the ice nucleation analysis was carried out.

2.1 Droplet Freezing Assays

Droplet freezing assays are laboratory instruments designed for investigating the immersion freezing activity of ice-nucleating particles (INPs) and ice-nucleating macromolecules (INMs). A variety of different droplet freezing assay instruments have been designed and developed, all with slightly different methods of cooling, droplet generation, and freezing detection. There are three main cooling methods, with instruments typically using a cold stage (Whale et al., 2015; Chen et al., 2018; Tarn et al., 2020), a cooling bath (David et al., 2019; Miller et al., 2021) or a cooled block (Hill et al., 2016; Kunert et al., 2019; Steinke et al., 2020). Droplets can be generated either by using a micropipette (Whale et al., 2015; Chen et al., 2018; David et al., 2019; Miller et al., 2021), creating an emulsion with oil (Pummer et al., 2012) or using microfluidic droplet generation (Reicher et al., 2018; Tarn et al., 2020). Each setup also uses different droplet sizes, and droplet numbers and have different limits of detection and uncertainties. The droplet size varies from tens of microlitres to a few nanolitres and determines the temperature range of the freezing detection since larger droplet volumes have a higher statistical chance of contamination being present. Regardless of the technique used, each droplet freezing assay has the same function; to determine the freezing activity of the desired sample. In this thesis, two different droplet freezing techniques were used and are described in more detail below.

2.1.1 Microlitre NIPI

The Microlitre Nucleation by Immersed Particle Instrument (or µL-NIPI) is a cold stage droplet freezing technique designed and set up at the University of Leeds, in the UK, as described by Whale et al. (2015). The setup (shown in Figure 2.1) uses either a Grant-Asymptote EF600 cold stage or a custom-built Peltier cold stage, both of which can cool the droplets to below $-35\,^{\circ}\mathrm{C}$. A clean, siliconised glass slide (Hampton Research, HR3-

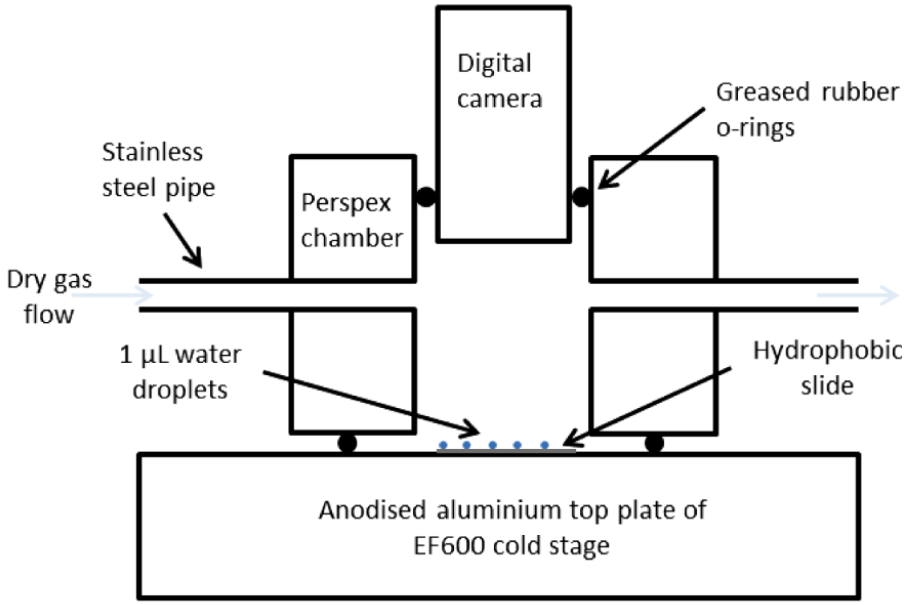

Figure 2.1: Schematic showing the key components of the* µL*-NIPI. *Image taken from Whale et al. (2015).*

233) provides a hydrophobic surface to minimise the contact angle between the droplets and the cold stage. For each freezing assay, between 40 and 50 droplets (of 1 µL in volume) are pipetted onto the hydrophobic glass slide and are covered by a Perspex chamber. The Perspex chamber contains the lighting and the camera for observing the droplet freezing, it is also connected to a supply of gas (either nitrogen gas or clean, dry air from a compressor) so the level of humidity can be controlled and no frost forms over the glass slide during the freezing experiment. Once the experiment is set up, the cold stage is cooled at a rate of 1 °C min^{-1} until all of the droplets are frozen, this rate is chosen as it is the best approximation of the cooling rates observed in moderate updraft convective clouds (Hader et al., 2014), without the analysis process taking too long. The raw data outputs are the temperature file, taken from the EF600 with the recorded temperatures over the time of the experiment, and the video file, which consists of all the images taken throughout the experiment.

From the µL-NIPI setup, droplet freezing is detected by the change in the light interaction by the droplet upon freezing. Since the light is situated above the droplets, they initially appear dark. Upon freezing, the increase in light scatter from the frozen droplet changes its appearance so that it appears light (Figure 2.2). The temperature at which the droplet colour change occurs is recorded as the freezing temperature for each droplet in the assay. This temperature is then used to calculate the fraction frozen, f_{ice}, as shown

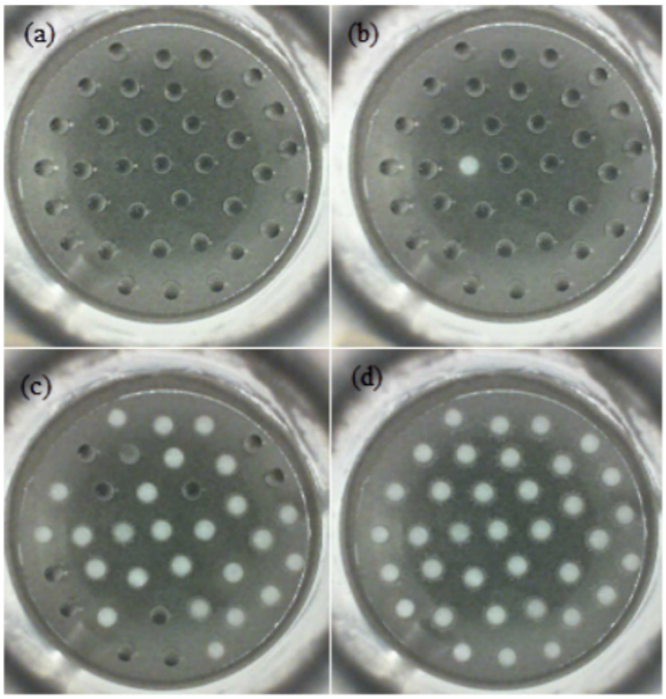

Figure 2.2: The progression of a freezing experiment within the* µL*-NIPI. *Image taken from Whale et al. (2015).*

below in Section 2.2.

2.1.2 FINC

The Freezing Ice Nuclei Counter (FINC) is a custom-built ice nucleation freezing assay technique, used to investigate heterogeneous ice nucleation by immersion freezing, as described by Miller et al. (2021). FINC was designed and built at ETH Zurich and its design was based on the DRoplet Ice Nuclei Counter Zurich (DRINCZ) (David et al., 2019). The setup consists of an ethanol bath (LAUDA Proline RP 845, Lauda-Königshofen) used to cool the sample, with a mounted camera and LED lights for detecting freezing based on changes in light intensity (Figure 2.3). Each cooling experiment consists of three 96-well Piko PCR trays, with each well containing 10 µL aliquots of the desired sample solution. The custom-built frame is designed to hold the PCR trays so that the wells are fully submerged in the ethanol cooling bath without any ethanol contaminating the solutions. Due to density changes in ethanol as it cools, a reservoir of ethanol tops up the levels in the bath during the freezing experiment. This top-up mechanism ensures that the wells remain fully submerged in the ethanol throughout the duration of the freezing experiment (David et al., 2019; Miller et al., 2021). The sample solutions are pipetted into the PCR trays inside a laminar flow hood to reduce contamination. The PCR trays are then care-

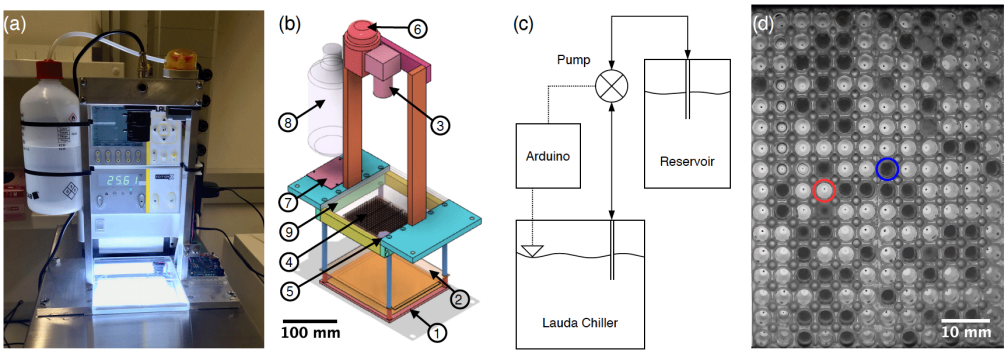

Figure 2.3: Image taken from Miller et al. (2021) with different aspects of the FINC setup *including; (a) a photograph of FINC, (b) a model of custom-built frame which is inserted into the Lauda bath, (c) a schematic of the bath leveller setup and (d) an image of the PCR trays from the FINC camera showing the change in light intensity between liquid (red circle) and ice (blue circle) in the wells.*

fully transferred into the ethanol bath and cooled at a rate of 1 °C min^{-1} until an endpoint of −32 °C, and the camera takes an image every 0.2 °C (Miller et al., 2021).

Droplet freezing events from FINC are detected by monitoring the light intensity and recording the temperature at which the greatest change in light intensity occurred. In this case, the LED lights are underneath the droplets meaning that they initially appear light and turn dark when they freeze (see Figure 2.3d). These freezing temperatures were then corrected to take into account the observed differences in the recorded bath temperatures and the temperatures experienced by the wells, as demonstrated by Miller et al. (2021). The details of the corrections used are given in the relevant chapters (see Chapter 3).

2.2 Ice Nucleation Analysis

For each droplet freezing assay, the fraction of droplets frozen as a function of temperature, or $f_{\text{ice}}(T)$, was calculated using the recorded and corrected droplet freezing temperatures. This calculation is shown in Eq. 11, where $N(T)$ is the number of droplets frozen at temperature T, and N_{total} is the total number of droplets in the given droplet freezing technique. The temperature at which 50% of the droplets were frozen (i.e. where $f_{\text{ice}}(T)$ is equal to 0.5) is referred to as the average freezing temperature, or T_{50}, and is used to summarise the average freezing behaviour of a droplet freezing assay.

$$f_{\text{ice}}(T) = \frac{N(T)}{N_{\text{total}}} \tag{11}$$

The total number of active sites above a given temperature, T, per unit sample volume, also known as the cumulative concentration of ice nuclei, or $K(T)$, was calculated based on

calculations derived by Vali (2019). This $K(T)$ value, as shown in Eq. 12, was calculated as a function of $f_{\mathrm{ice}}(T)$, where V_{d} is the volume of each droplet (in cm^3).

$$K(T) = -\frac{ln(1 - f_{\mathrm{ice}}(T))}{V_{\mathrm{d}}} \tag{12}$$

To further quantify the ice-nucleating activity, it is possible to normalise the $K(T)$ by the volume of sampled air, the mass concentration of particles, the surface area concentration of particles or the number concentration of particles depending on what information is available. Across this thesis, I will use all these methods to analyse the ice-nucleating ability of my samples, so I will describe them generally here. For filter-collected samples, the concentration of INPs per volume of sample air, N_{INP} (L^{-1}), was calculated using the volume of wash-off suspension, V_{w} (cm^{-3}), and the volume of sampled air at standard temperature and pressure, V_{a} (cm^{-3}), as shown in Eq. 13.

$$N_{\mathrm{INP}}(T) = K(T) \cdot \frac{V_{\mathrm{w}}}{V_{\mathrm{a}}} \tag{13}$$

The other samples in this thesis were analysed in different ways depending on the information available. Where the mass of the sample in suspension was known or could be estimated, the active site density per unit mass, n_{m} (g^{-1}), was calculated as a function of temperature using the mass concentration within the suspension, C_{m} (g), as shown in Eq. 14.

$$n_{\mathrm{m}}(T) = \frac{K(T)}{C_{\mathrm{m}}} \tag{14}$$

If the surface area concentration of the sample in suspension was known or could be estimated, the active site density per unit surface area, n_{s} (m^{-2}), was calculated as a function of temperature using the total collected aerosol surface area, A_{s} (m^2), as shown in Eq. 15.

$$n_{\mathrm{s}}(T) = \frac{N_{\mathrm{INP}}(T)}{A_{\mathrm{s}}} \tag{15}$$

Finally, where the number concentration of particles within the suspension was known, the ice-active site density per particle, n_{n} ($\mathrm{particle}^{-1}$), was calculated as a function of temperature using the total number of particles per droplet, C_{n}, as shown in Eq. 16.

$$n_{\mathrm{n}}(T) = \frac{ln(1 - f_{\mathrm{ice}}(T))}{C_{\mathrm{n}}} \tag{16}$$

2.3 Soil Sample Locations

Throughout this thesis, soil samples have been collected from three different agricultural locations in the UK and Canada. The sites were chosen based on practically and accessibilty, however, we also wanted to capture a range of different agricultural locations. The collection and use of each the collected samples are detailed in the respective results chapters later in this thesis (see Sections 3.2 and 5.2). Here, I will provide a brief description of each sampling location.

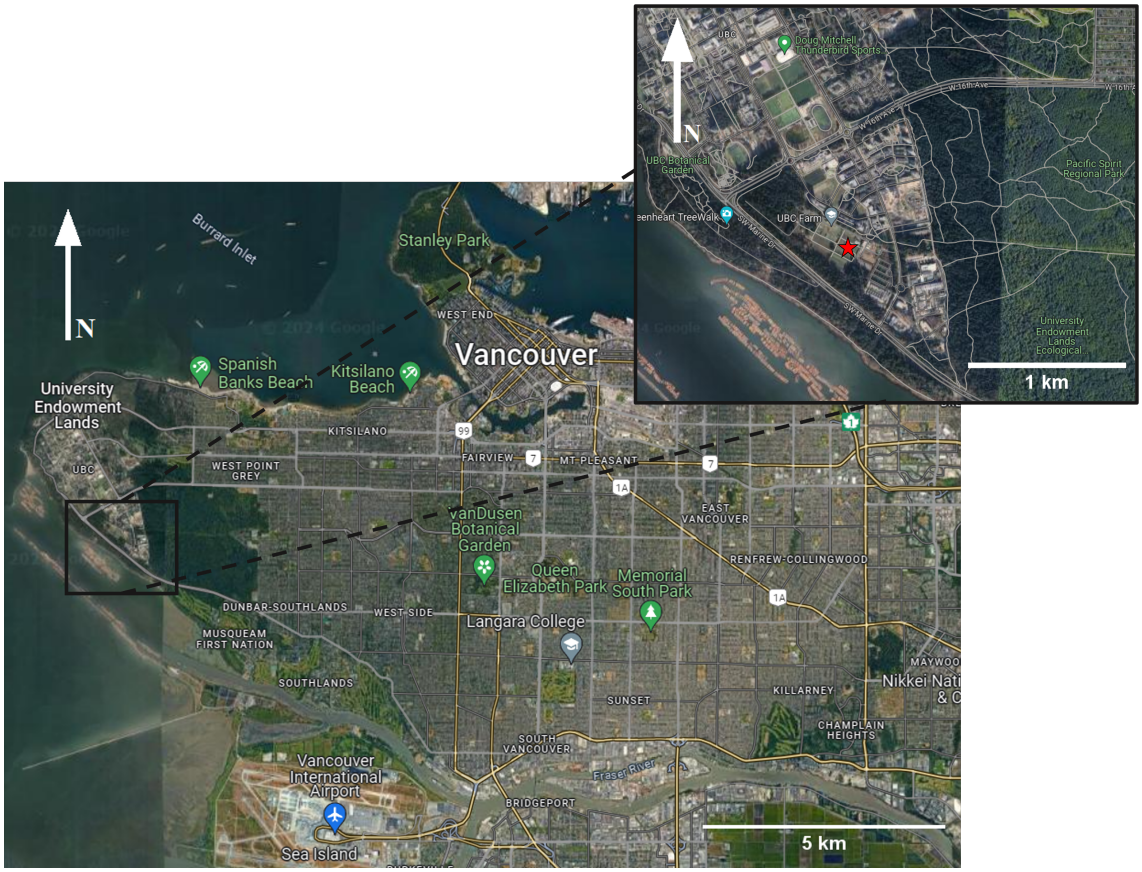

Figure 2.4: A map indicating the location of the soil samples taken from the University of British Columbia Farm, situated west of Vancouver, Canada. *The red star indicates the rough sampling location.*

The University of British Columbia (UBC) Farm (49.3°N, 123.2°W) is situated to the south of the UBC campus, which is west of Vancouver, Canada (see Figure 2.4). It is therefore located right by the coast of the Pacific Ocean, within the 90-year-old coastal hemlock forest which surrounds much of the UBC campus. The farm is a small-scale research farm which is part of the Centre for Sustainable Food Systems and it is located

on the traditional, ancestral and unceded territory of the Musqueam people. It comprises 24 hectares of organic farmland and forest ecosystems, growing mostly fruits, vegetables and herbs.

Figure 2.5: A map indicating the location of the soil samples taken from the University of Leeds Research Farm, situated east of Leeds, West Yorkshire. *The red star indicates the rough sampling location.*

The University of Leeds (UoL) Research Farm (53.9°N, 1.3°W) is situated to the north east of Leeds City Centre, near Tadcaster in West Yorkshire (see Figure 2.5). The farm consists of 317 hectares, spanning across four different farmsteads. It's position at the intersection between the A1(M), a motorway which runs north to south between Edinburgh and London, and the A64, a major road between Leeds and York, means the farm is likely heavily influenced by traffic pollution. The majority of the land at UoL Farm is dedicated to arable land, with some agroforestry plots spread throughout. Soils found at the UoL Farm are typically very shallow, loamy soils and the site ranges from 42 to 70 metres above sea level in elevation. The farm is also home to the National Pig Centre, which is part of the Centre Innovation Excellence in Livestock.

Rothamsted Research is located in Harpenden (51.8°N, 0.36°W), just north of St. Alban's in Hertfordshire, UK (see Figure 2.6). This sampling location is more rural than the other two sampling locations, however, the farm is located just east of the M1 motorway meaning there may be some influence from traffic pollution at this location. Rothamsted is home to the oldest continuing agricultural field experiment in the world. The farm consists of 330 hectares and the majority of the land is dedicated to growing a variety of

Figure 2.6: A map indicating the location of the soil samples taken from Rothamsted Research Farm, situated in Harpenden, Hertfordshire. *The red star indicates the rough sampling location.*

agricultural crops. The soils at the Rothamsted Farm site typically consist of heavy clay loam with good drainage.

References

Chen, W., Hambleton, S., Seifert, K. A., Carisse, O., Diarra, M. S., Peters, R. D., Lowe, C., Chapados, J. T., and Lévesque, C. A. (2018). Assessing Performance of Spore Samplers in Monitoring Aeromycobiota and Fungal Plant Pathogen Diversity in Canada. *Applied and Environmental Microbiology*, 84(9):e02601–17.

David, R. O., Cascajo-Castresana, M., Brennan, K. P., Rösch, M., Els, N., Werz, J., Weichlinger, V., Boynton, L. S., Bogler, S., Borduas-Dedekind, N., Marcolli, C., and Kanji, Z. A. (2019). Development of the DRoplet Ice Nuclei Counter Zurich (DRINCZ): validation and application to field-collected snow samples. *Atmospheric Measurement Techniques*, 12(12):6865–6888. Publisher: Copernicus GmbH.

Hader, J. D., Wright, T. P., and Petters, M. D. (2014). Contribution of pollen to atmospheric ice nuclei concentrations. *Atmospheric Chemistry and Physics*, 14(11):5433–5449.

Hill, T. C. J., DeMott, P. J., Tobo, Y., Fröhlich-Nowoisky, J., Moffett, B. F., Franc, G. D., and Kreidenweis, S. M. (2016). Sources of organic ice nucleating particles in soils. *Atmospheric Chemistry and Physics*, 16(11):7195–7211.

Kunert, A. T., Pöhlker, M. L., Tang, K., Krevert, C. S., Wieder, C., Speth, K. R., Hanson, L. E., Morris, C. E., Schmale III, D. G., Pöschl, U., and Fröhlich-Nowoisky, J. (2019). Macromolecular fungal ice nuclei in *Fusarium*: effects of physical and chemical processing. *Biogeosciences*, 16(23):4647–4659.

Miller, A. J., Brennan, K. P., Mignani, C., Wieder, J., David, R. O., and Borduas-Dedekind, N. (2021). Development of the drop Freezing Ice Nuclei Counter (FINC), intercomparison of droplet freezing techniques, and use of soluble lignin as an atmospheric ice nucleation standard. *Atmospheric Measurement Techniques*, 14(4):3131–3151.

Pummer, B. G., Bauer, H., Bernardi, J., Bleicher, S., and Grothe, H. (2012). Suspendable macromolecules are responsible for ice nucleation activity of birch and conifer pollen. *Atmospheric Chemistry and Physics*, 12(5):2541–2550.

Reicher, N., Segev, L., and Rudich, Y. (2018). The WeIzmann Supercooled Droplets Observation on a Microarray (WISDOM) and application for ambient dust. *Atmospheric Measurement Techniques*, 11(1):233–248.

Steinke, I., Hiranuma, N., Funk, R., Höhler, K., Tüllmann, N., Umo, N. S., Weidler, P. G., Möhler, O., and Leisner, T. (2020). Complex plant-derived organic aerosol as ice-nucleating particles – more than the sums of their parts? *Atmospheric Chemistry and Physics*, 20(19):11387–11397.

Tarn, M. D., Sikora, S. N. F., Porter, G. C. E., Wyld, B. V., Alayof, M., Reicher, N., Harrison, A. D., Rudich, Y., Shim, J.-u., and Murray, B. J. (2020). On-chip analysis of atmospheric ice-nucleating particles in continuous flow. *Lab on a Chip*, 20(16):2889–2910. Publisher: The Royal Society of Chemistry.

Vali, G. (2019). Revisiting the differential freezing nucleus spectra derived from drop-freezing experiments: methods of calculation, applications, and confidence limits. *Atmospheric Measurement Techniques*, 12(2):1219–1231.

Whale, T. F., Murray, B. J., O'Sullivan, D., Wilson, T. W., Umo, N. S., Baustian, K. J., Atkinson, J. D., Workneh, D. A., and Morris, G. J. (2015). A technique for quantifying heterogeneous ice nucleation in microlitre supercooled water droplets. *Atmospheric Measurement Techniques*, 8(6):2437–2447.

3 The relationship between surface tension and atmospheric ice-nucleating activity of agricultural soils

3.1 Introduction

Recent focus has been on understanding the mechanisms of ice formation in mineral dust ice-nucleating particles (INPs) (Harrison et al., 2016, 2019; Holden et al., 2021), with few studies investigating the mechanisms of the ice-nucleating activity in biological material. Many organic macromolecules, such as fatty acids, have surfactant properties which make them important for atmospheric processes such as cloud droplet formation (Gérard et al., 2016, 2019) and these properties may also play a role in their ice-nucleating ability. Surface active compounds, also known as surfactants, are amphiphilic macromolecules, meaning they have both hydrophobic and hydrophilic moieties present (Rosen and Kunjappu, 2012). Due to their amphiphilic nature, surfactant molecules partition to the surface of atmospheric aerosol droplets, reducing the surface tension of growing cloud droplets at the air-water interface. Therefore, surfactants reduce the barrier for further droplet growth from the condensation of water vapour onto the aerosol droplet, increasing the efficiency of cloud droplet formation (Gérard et al., 2016; Ovadnevaite et al., 2017). The partitioning of surfactant droplets to the surface and the subsequent hydrophobic interactions at the air-water interface could also impact atmospheric ice nucleation since the location of the ice-nucleating material within the droplet may impact its ice-nucleating ability (Fornea et al., 2009). In this chapter, we investigated the role of surfactants in ice nucleation in atmospheric cloud droplets.

On solid aerosol particles, surfactant coatings, such as fatty acids and alcohols, may interfere with ice-active sites to either enhance ice nucleation (Hiranuma et al., 2013; Kupiszewski et al., 2016; China et al., 2017) or inhibit it (Kuwabara et al., 2014; Boose et al., 2019). In aqueous droplets, surfactant macromolecules form a monolayer at the air-water interface of a droplet (Nesměrák and Němcová, 2006; Rosen and Kunjappu, 2012). Fornea et al. (2009) found that ice-nucleating substances tend to freeze at warmer temperatures when placed at the air-water interface of droplets instead of being immersed within the droplet bulk. These findings suggest that the formation of surfactant monolayers at the droplet air-water interface could enhance the ice-nucleating ability of these substances. Furthermore, at higher concentrations, the surfactant macromolecules become saturated at the surface of cloud droplets, so the surfactants begin to aggregate together

to partition the hydrophobic moiety out of the aqueous solution (Rosen and Kunjappu, 2012). This behaviour results in the formation of concentration-dependent aggregates, called micelles, which could create new sites for ice nucleation or could block ice nucleation sites (Gavish et al., 1990; DeMott et al., 2018). The structure of micelles formed in atmospheric aerosol droplets can vary depending on the temperature, humidity, saturation, pH and composition of the droplet itself (Pfrang et al., 2017). These observations suggest that multiple potential structures could form from organic macromolecules and that some may have more ice-nucleating potential than others. In addition, Bogler and Borduas-Dedekind (2020) found that the ice-nucleating ability of lignin cannot be normalized to the amount of material in the solution. These results may suggest the formation of concentration-dependent aggregates, or micelles, with different ice nucleating abilities.

Aggregates can form in droplet solutions in ways other than surfactant saturation and micelle formation. For many organic macromolecules, their ice-nucleating ability is closely linked to their aggregation and there is usually a critical size for aggregates to form to optimise their ice-nucleating ability (Dreischmeier et al., 2017; Qiu et al., 2017; Schwidetzky et al., 2023). As discussed in Section 1.3.1, proteinaceous aggregates of the bacteria *Pseudomonas syringae* nucleate ice at three different temperatures depending on the size of the aggregates (Hartmann et al., 2022; Qiu et al., 2019; Lukas et al., 2022). The nucleation mechanisms due to different aggregate sizes can be classified as class A, class B, or class C, triggering freezing at $-3\,^{\circ}\mathrm{C}$, $-5\,^{\circ}\mathrm{C}$ or $-8\,^{\circ}\mathrm{C}$, respectively (Lukas et al., 2022). Aggregation of proteinaceous ice-nucleating macromolecules (INMs) is likely influenced by electrostatic and hydrophobic interactions between proteins and components of the bacterial membrane (Lukas et al., 2020; Schwidetzky et al., 2021a). The importance of aggregation has also been found to be important for polysaccharides in pollen washing waters (Section 1.3.1), which has been shown to exhibit ice-binding properties when aggregates are smaller than 100 kDa, and only exhibit ice-nucleating properties when aggregates are larger than 100 kDa (Dreischmeier et al., 2017). In more complex solutions, like fertile soils, dissolved organic material can adsorb onto larger particles or reactions can take place, leading to coagulation and formation of complex particles and aggregates (Jackson and Burd, 1998). Although aggregation may form sites for ice nucleation, there is also evidence that it may cover ice-active sites. McCluskey et al. (2018) found that heating organic samples sometimes leads to an increase in their ice-nucleating ability. They suggested that this observed increase in ice-nucleating activity was due to aggregates being dissolved and redistribution

in the solution, opening up ice-active sites for nucleation (McCluskey et al., 2018). Other studies have shown that surfactant coatings reduce the ice-nucleating ability of mineral dust particles (Boose et al., 2019). Therefore, the pathways and drivers of aggregation for organic INMs remain elusive, and an accurate description of the ice nucleation ability of organic matter requires further investigation.

In this chapter, we investigated the potential relationship between the ice-nucleating ability and surface activity of agricultural soil extracts, meaning the aqueous solutions containing organic material extracted from soil and filtered to 200 nm. We also compared these observations of the surface tension and ice-nucleating activity of two soil subcomponents; lignin and Snomax. The goal of this study was to gain an understanding of the contribution of surfactant macromolecules to the ice-nucleating ability of anthropogenic soils, by investigating the surface tension reduction and ice-nucleating activity of soil extracts and proxies of their subcomponents.

3.2 Experimental Methods

3.2.1 Organic matter Sample Collection and Preparation

3.2.1.1 Lignin

Lignin is a biopolymer found to make up 30% of organic carbon in the environment (Section 1.3.1). An aqueous series of lignin (471003, Batch 1, Sigma Aldrich) solutions, ranging in concentration from 10 mg L^{-1} to 2×10^3 mg L^{-1}, were prepared in glass vials and diluted using microbiology-free reagent water (hereafter termed *SA water*, W4502, Sigma Aldrich). For consistency and comparability with previous work, the batch of lignin used in our experiments was kept the same as those used previously to demonstrate the ice-nucleating ability of kraft lignin (Bogler and Borduas-Dedekind, 2020; Miller et al., 2021). Each lignin solution was analysed for its surface and ice-nucleating activities by the methods described below.

3.2.1.2 Snomax

Snomax is a commercial product consisting of dead and disintegrated cells of *Pseudomonas syringae*, a common ice-active bacteria found on plants and in soils (Wex et al., 2015). The ice-nucleating activity observed from Snomax is associated with ice-active proteins from the bacteria. Proteins are common in soils and originate from bacteria and fungi. Here, we used Snomax as a proxy for ice-active proteins in fertile soils. An aqueous stock solution

Table 1: Summary of the collected soil samples for analysis in this study. Including date sampled, location and crop type.

Sample	Location	Coordinates	Crop / Field Type	Sampling Date
UBC Farm	Vancouver, Canada	49.25, -123.24	unknown	31/03/2022
Leeds Research Farm	Tadcaster, UK	53.87, -1.32	wheat	12/10/2022
Rothamsted Research	Harpenden, UK	51.81, -0.36	linseed	29/09/2022

of Snomax (Snomax® International) was prepared at a concentration of 10^3 mg L^{-1} in a centrifugal tube (sterile, 50 mL, Basix, Fisher Scientific) with SA water. The Snomax solution was then filtered through a 0.22 µm syringe filter (PES membrane, sterile, Merck Millipore) to remove large aggregates and cellular fragments. This filtration step allowed us to the investigation on INMs. The filtered stock solution was diluted with SA water to obtain a dilution series, ranging in concentration from 10^{-2} mg L^{-1} to 10^3mg L^{-1}. All dilutions were analyzed for ice-nucleating activity with FINC and surface tension reduction with the tensiometer and this work was carried out by Paul Bieber.

3.2.1.3 Soils

Soil samples were collected from three different agricultural locations in the UK and in British Columbia, Canada (Table 1 and Figure 3.1); the University of British Columbia (UBC) Farm, the University of Leeds (UoL) Farm and Rothamsted Research. At each location, soil samples were taken from crop fields with bare soil, at least 1 m from the boundary of the field. 50 mL polypropylene centrifuge tubes (Sarstedt Inc.), which were purchased sterilised, were used to sample from the top 5 cm of soil, with at least three samples collected per location. Additionally, at each location, a clean 50 mL centrifuge tube was opened and exposed to ambient air, to examine the contamination of INPs from handling the samples (hereafter referred to as handling blanks). Aside from location, there were also two distinct sampling periods (Table 1). The samples taken in the UK were obtained a few weeks after harvest season, whereas the Canadian samples were taken a few hours after the soils were tilled in preparation for planting the next season's crops. Furthermore, three different fields were sampled at the UBC Farm, whereas only one field was sampled at each of the other two locations. For the ice nucleation analysis (described in Section 2.2), the handling blanks were treated the same as the soil samples to verify that the extracted soil solutions were above any contamination introduced during sample manipulation. All sample tubes and handling blanks were then frozen at −20 °C until analysis. This was to stop any biological evolution of the samples until they could be analysed.

Figure 3.1: Agricultural soil sampling collection from three different locations in the UK and Canada. *(a) University of British Columbia Farm, (b) University of Leeds Farm and (c) Rothamsted Research (sampled field is situated behind the pictured sampling station) and (d) samples being taken at UBC Farm. Images demonstrate the differences between the three different sampling locations and how the soil samples were taken. Images taken on the day of sampling.*

3.2.1.4 Organic Matter Soil Extraction

A sample preparation method was developed for analysing the ice nucleation activity and surface tension of the macromolecules in the soil samples. Previous soil sample preparation methods dry sieve the soils to 63 µm before using water to make up a soil suspension (Tobo et al., 2014; Suski et al., 2018). However, in this study, we developed a slightly different method which maximises the extraction of organic macromolecules into our soil extract solutions. First, 40 mL of MilliQ water was added to 40 g of the soil samples to create a 10^6 mg L^{-1} concentration suspension. A centrifuge (Sorvall RC5B) and a fixed-angle rotor (Thermo Scientific SS-34) separated the larger soil particles from the prepared suspension, spinning between 6,000 and 10,000 rpm for 1 hr. An average cut-off particle diameter of 0.4 µm for the extracted supernatant was calculated using Stoke's Law (Gomboš et al., 2018), assuming an average soil density of 1.3 g cm^{-3} (Rai et al., 2017). Following centrifugation, the supernatant was extracted and filtered through a 0.22 µm syringe filter to remove the larger remaining fragments. The filtered solution was diluted

to create a dilution series, then all solutions were analysed for ice-nucleating activity and surface tension.

3.2.1.5 Heat Treatment Experiments

Heat treatment experiments were carried out using the protocol described in Daily et al. (2022). For two soil sample extracts, 5 mL aliquots were transferred into 50 mL polypropylene centrifuge tubes (Basix, Fisher Scientific). A heating bath from a rotary evaporator (B-490, Buchi) was filled with deionized water, and a clamp stand was used to secure the centrifuge tubes in position to fully immerse the sample within the water bath at 98 °C for 30 mins. The tubes were tightly closed to prevent evaporation, which would lead to an increase in the solution concentration. After heating, the aliquots were left to cool down fully before taking further surface tension measurements and ice-nucleating analysis, to observe any changes resulting from the heat treatment.

3.2.2 Instrumentation and Sample Analysis

3.2.2.1 Surface Tension Measurements

The surface tensions of the extracted soil sample solutions were measured using the DataPhysics optical contact angle (OCA) 15 EC Tensiometer alongside the DataPhysics SCA software for OCA (Figure 3.2). The pendant droplet method, where an electronic dosing system dispenses a small amount of solution to form a droplet (with a volume of 24.1±1.1 (mean ± SD) μl) suspended from the tip of a needle, was used to calculate the surface tension of the solutions. The shape of the droplet is determined by the surface tension, which pulls the liquid into a spherical shape, and by gravity, which deforms and lengthens the droplet. The DataPhysics SCA software uses the given value for the needle's outer diameter as a reference to determine the size of the droplet. The surface tension is then calculated by fitting the Lapace-Young equation to the shape of the droplet (Berry et al., 2015). For each soil extract solution, three droplets were formed and three individual surface tension measurements were taken for each droplet. Then, the mean and the standard deviation for all surface tension measurements were calculated for each sample solution.

To acquire a surface tension measurement, the droplet needs time to equilibrate with the surrounding air. The required equilibrium time was determined by measuring the surface tension every 30 seconds for a MilliQ water droplet suspended for 5 minutes. This experiment was repeated twice to assess the variability of surface tension measurements of water droplets over time (Figure A.1 in Appendix A). For the first few surface tension

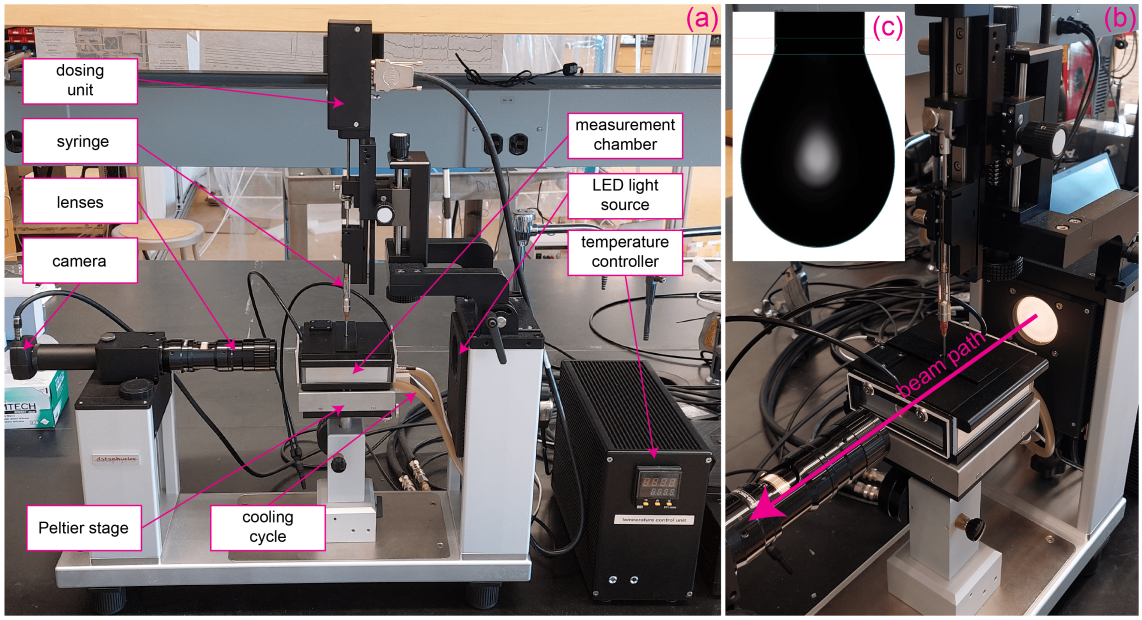

Figure 3.2: DataPhysics optical contact angle (OCA) 15 EC tensiometer *including; (a) side view with labelled components, (b) beam path, (c) example image of a pendant droplet.*

measurements, taken within the first 2 minutes of the experiment, the standard deviation was approximately 0.43±0.1 mN m^{-1}. After about 2 minutes, the accuracy and reproducibility of the surface tension measurements improved and remained steady for the next few minutes (Figure A.1 in Appendix A). Therefore, in this study, the droplet was left to equilibrate for two minutes before taking a surface tension measurement. The surface tension of pure water increases linearly with decreasing temperature (Gittens, 1969) (Figure A.2 in Appendix A). To address the role of temperature on surface tension, we used a Peltier temperature control unit (TPC 160, DataPhysics) to maintain a constant temperature of 22 °C with an uncertainty of ±0.3 °C during this study.

3.2.2.2 Dissolved Organic Carbon (DOC) Analysis

The dissolved organic carbon (DOC) of the soil extracts was measured in the lab to compare the ice-nucleating and surface activities of the different soil samples. The DOC analysis of the soil extracts was quantified using a high-temperature total organic carbon (TOC) analyser (Multi NC2100, Analytik Jena) and was carried out by Rachel Gasior. The analyser determines the amount of dissolved carbon (DC) by injecting 150 µL of the sample directly into a combustion tube set at a temperature of 800 °C, the carbon is digested and DC is measured from the detection of the generated carbon dioxide. Next, the analyser determines the amount of dissolved inorganic carbon (DIC) by injecting another 150 µL of the sample into the total inorganic carbon (TIC) condensation vessel, where

phosphoric acid is added and then the carbon dioxide is purged and detected. The software then calculates the DOC as the difference between DC and DIC. The TOC analyser was calibrated using standards diluted from commercially prepared stocks of 1000 ppm TOC (76067-250ML-F, Merck Life Science UK Ltd.) and 1000 ppm TIC (12003-250ML-F, Merck Life Science UK Ltd). After filtration to 0.22 µm, 2 mL of each soil extract solution was pipetted into glass auto-sampler vials and secured with a snap cap. A handling blank was analysed alongside the sample solutions. The difference in measured DOC between the sample and the blank was calculated to determine the organic carbon from the soil.

3.2.2.3 Immersion Freezing Analysis

The ice-nucleating ability of each sample solution was investigated here using FINC, as described in Section 2.1.2. For these experiments, 10 µL aliquots of the sample solution were pipetted into each of the 288 PCR wells. The average temperature in the well, T_{well}, was calculated from the measured bath temperature, T_{bath}, recorded by the Lauda bath thermometer. In this case, samples were analysed at two different time intervals, with some samples analysed in April 2022 and others analysed in March 2023. Therefore, the values of a and b in Eq. 17 were adjusted to account for the change in conditions between the two data analysis periods. So, for the measurements taken in April 2022, $a = 0.963$ and $b = 0.905$ and for measurements taken during March 2023, $a = 0.953$ and $b = 0.897$.

$$T_{well} = a \cdot T_{bath} + b \tag{17}$$

3.3 Results and Discussion

3.3.1 Ice-Nucleating Ability of Soil Extracts and their Subcomponents

3.3.1.1 Freezing Temperatures

In our analysis, we examined the ice-nucleating ability of soil aqueous extracts and two subcomponents using droplet freezing assays (Figures 3.3 and 3.4). The fraction frozen curves as a function of temperature for one soil extract sample and three dilutions at each of the three sampling locations are shown in Figure 3.3. The soil extract solutions from the three different locations displayed a range of freezing activity (Figure 3.3). Specifically, the average freezing temperature (T_{50}, see Section 2.2) of the undiluted soil extracts ranged from −15.5 °C to −6.3 °C, a difference of 11.2 °C. All of the freezing activities for the soil extracts were above the handling blanks (Figure 3.3), which were collected at the site

by exposing blank tubes to the ambient air. We noted that the handling blank from the University of British Columbia (UBC) showed higher freezing activity compared to the other handling blanks, with a T_{50} of $-18.2\,^{\circ}\mathrm{C}$, compared to an average T_{50} of $-24.1\,^{\circ}\mathrm{C}$ for all other handling blanks. This difference is possibly due to an increase in contamination of aerosols, which were deposited into the centrifuge tube whilst capturing this handling blank. Nevertheless, all of our samples remain above the background handling bank and our results demonstrate the breadth of freezing ability of a range of soil extracts across two continents.

To help break down some of the complexity of the ice-nucleating activity of our soil samples, we compared the freezing of our soil extracts with that of two soil subcomponents; an aqueous dilution series lignin and filtered Snomax (Figure 3.4). The two dilution series remain above but approach the freezing curves of the handling blanks, demonstrating that lignin and Snomax are both acting as ice-nucleating substances. The lignin solutions tended to initiate freezing at lower temperatures compared to the Snomax solutions; the T_{50} for the 1000 mg L^{-1} concentration solutions of lignin and Snomax was $-18\,^{\circ}\mathrm{C}$ and $-5.8\,^{\circ}\mathrm{C}$, respectively. These freezing temperatures are what we would expect when compared with previous work from Bogler and Borduas-Dedekind (2020) and Wex et al. (2015). To quantitatively compare the freezing activity of these two subcomponents with our soil extracts, we needed to normalise the freezing activity of all our samples.

3.3.1.2 Normalised INM Spectra

The freezing activity of each extract was normalised by (1) the organic carbon content of the solution after extraction, measured by TOC termed n_{mC} (Figure 3.5a), and (2) the mass of soil before any extraction taking place n_{m} (Figure 3.5b). The dilution series for the soil extracts from UBC and the University of Leeds (UoL) align to within $2\,^{\circ}\mathrm{C}$ as a function of temperature for both n_{mC} and n_{m}. However, for the Rothamsted Research (herein referred to as Rothamsted) sample, the dilution series is somewhat aligned as a function of temperature, except for the last dilution (10^{-3} mg L^{-1}) which is up to an order of magnitude higher than the rest of the dilution series. This could be due to the aggregation of macromolecules which is known to influence the ice-nucleating activity of ice-active proteins, with larger aggregates triggering nucleation at higher temperatures (Hartmann et al., 2022; Lukas et al., 2020, 2022). This finding suggests that the aggregation is hindering ice-active sites since we observed an increase in ice-nucleating activity after the aggregates were dissolved at lower concentrations of soil extract solution.

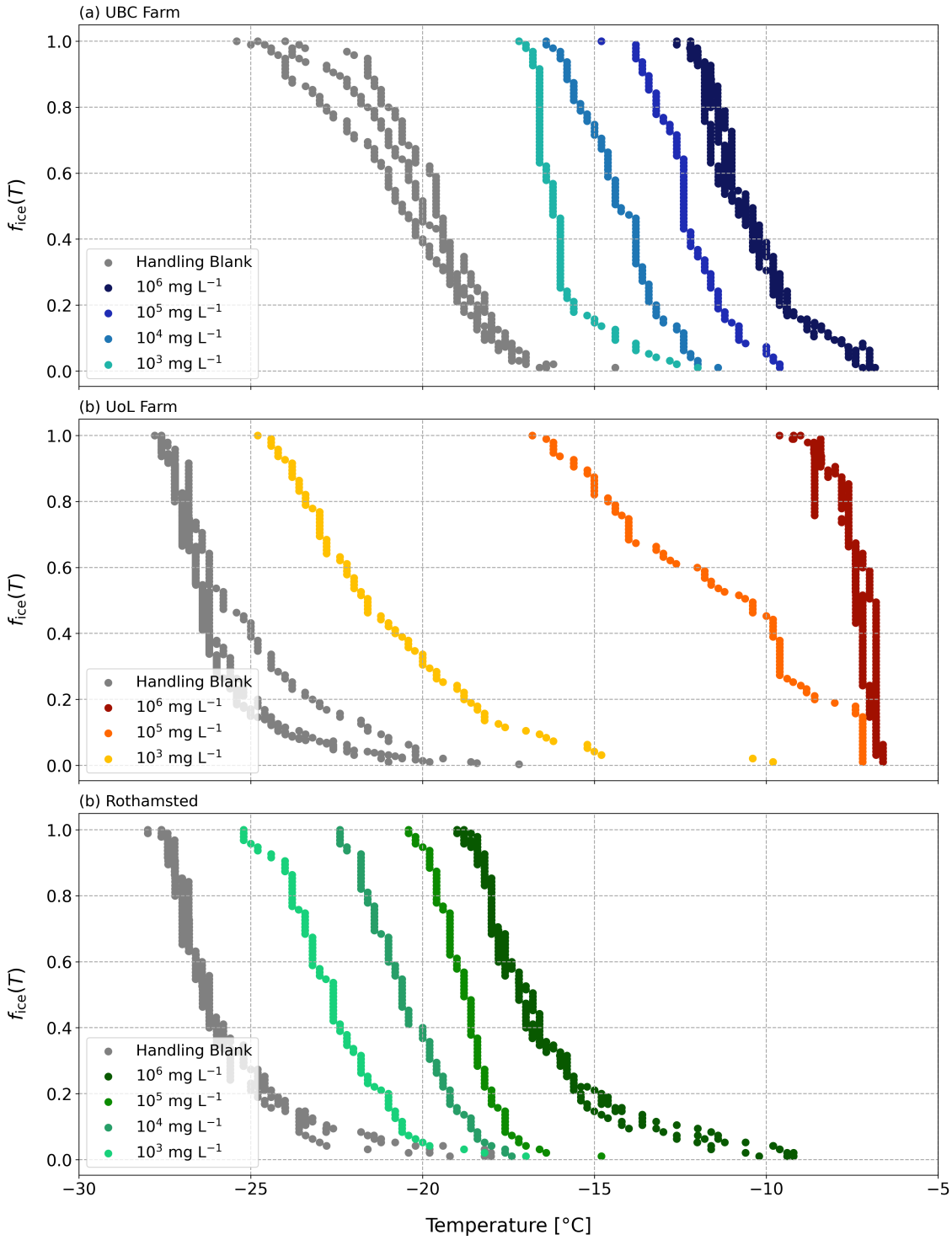

Figure 3.3: Fraction frozen ($f_{ice}(T)$) curves as a function of temperature for the three soil extract solutions and their dilutions *from (a) UBC Farm, (b) UoL Farm and (c) Rothamsted.*

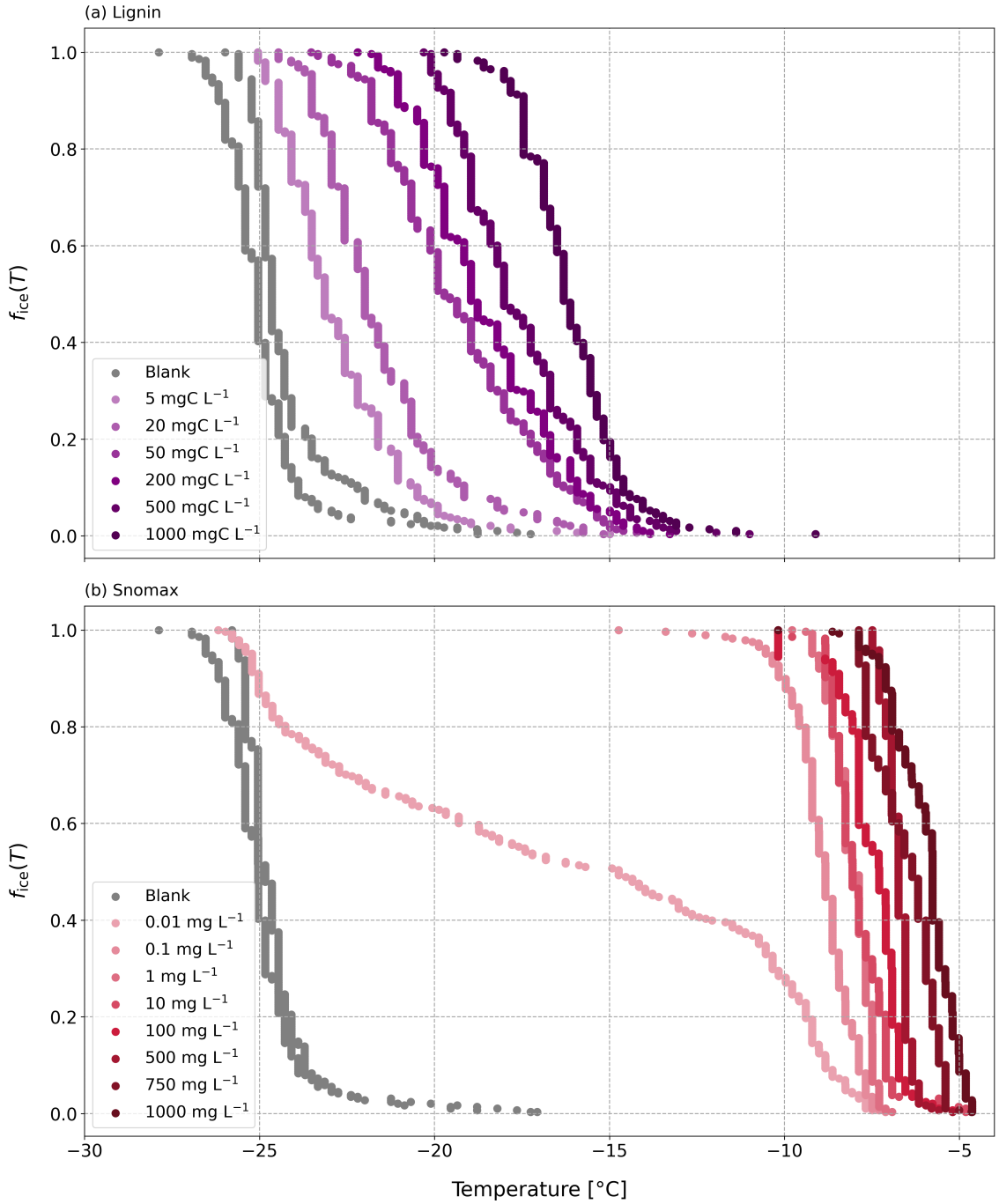

Figure 3.4: Fraction frozen ($f_{ice}(T)$) curves as a function of temperature for the two soil subcomponents and their dilutions *(a) lignin and (b) Snomax.*

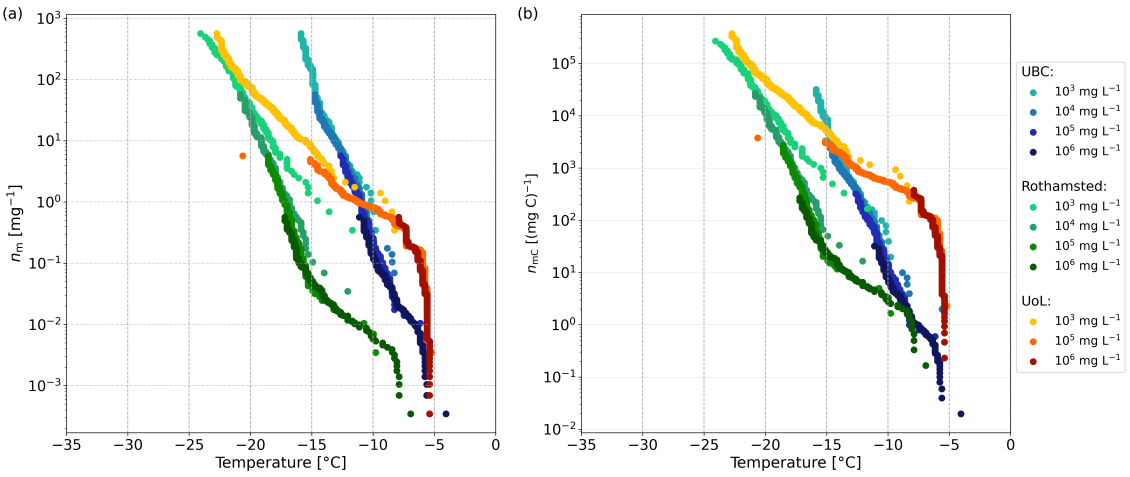

Figure 3.5: Ice-active mass site density (n_{mC} and n_m) as a function of temperature for the three soil extracts and their dilutions from the UBC Farm (Vancouver, Canada), the UoL Farm (Tadcaster, UK) and Rothamsted (Harpenden, UK) *calculated from (a) the mass of carbon in the soil extracts (n_{mC}) and (b) the mass of soil used for the extracts (n_m).*

By normalising the freezing activity of the soil extracts, we hoped to examine whether the ice-nucleating activity scales with the organic carbon content or the mass of the soils. For example, if the higher ice-nucleating activity observed in the UoL sample was explained by the higher carbon content, then we would expect to see the three different soil samples also align as a function of temperature. However, this is not the case and there is a large spread in the n_{mC} of the soil extracts (Figure 3.5a). Previous work by O'Sullivan et al. (2014) also found no correlation between the ice-nucleating activity and the dissolved organic carbon content of fertile soil extracts. For the n_{m} values, we did not expect to see the different soil samples align as a function of temperatures since the mass of soil used for extraction was used to calculate this mass site density. Since we used the same mass for each sample in the extraction process, we knew this mass concentration would not explain the range of freezing activities between the three soil samples. However, we were unable to investigate the mass concentration after extraction for these soil extract solutions.

We also examined the normalised ice-nucleating activity of the lignin and Snomax dilutions series (Figure 3.6). The observed freezing activity for the lignin solutions normalised to the carbon content (n_{mC}) aligns with previous work done by Bogler and Borduas-Dedekind (2020) and Miller et al. (2021) (Figure 3.6a). The n_{mC} tended to increase with decreasing concentration of lignin solution, a trend that was also observed by Bogler and Borduas-Dedekind (2020). The aggregation of lignin molecules at higher solution concentrations may obscure ice-active sites, therefore, once the aggregates are dissolved at lower concentrations, the ice-nucleating activity increases as the ice-active sites are released into

solution. The freezing activity of the filtered Snomax solutions, normalised by the mass of Snomax added into solution (n_{m}), shows a similar freezing behaviour as the Snomax parameterisation from Wex et al. (2015), however the values of n_{m} are on an order of magnitude lower (discussed in more detail in Section 3.3.2). We also observed that the normalised ice-nucleating activity of the Snomax solutions did not align well as a function of temperature (Figure 3.6b). This, again, could indicate that aggregation is playing a role in the ice-nucleating activity of these solutions. The aggregation is likely blocking sites for ice nucleation, which explains why the ice-nucleating activity increases at lower concentrations, where aggregates will have dissolved into solution.

The INM spectra for the soil extract solutions were compared with the INM spectra of the lignin and Snomax solutions to analyse the ice-nucleating activity and relative contributions from lignin and ice-active proteins (Figure 3.7). The n_{mC} of the soil extracts was compared with the lignin n_{mC} values and with data from Wilson et al. (2015) and Miller et al. (2021) (Figure 3.7a). The majority of the ice-nucleating activity of the soil extracts is greater than that of lignin solutions of 20 mg C L^{-1} (Miller et al., 2021) but varies due to the spread of our data. For example, at $-15\,^{\circ}\mathrm{C}$, the n_{mC} of the Rothamsted sample is the same as that of lignin, whereas, the n_{mC} of the UoL sample is a factor of 10 to 100 greater than lignin. This observation suggests that lignin's potential contribution to the investigated soils' overall ice-nucleating activity varies across different samples, which we will explore further in the following section. In contrast, the ice-nucleating activity of the extracted soil solutions is lower than that of the sea surface microlayer (Figure 3.7a).

The n_{m} of the soil extracts was compared with the Snomax n_{m} values and with data from Conen et al. (2011), Wex et al. (2015) and O'Sullivan et al. (2014) (Figure 3.7b). The large increase in n_{m}, from $3.5 \times 10^{-4}\,\mathrm{mg}^{-1}$ to $1.5 \times 10^{-1}\,\mathrm{mg}^{-1}$ in the UoL Farm samples occurring at $-6\,^{\circ}\mathrm{C}$ correlates with a sharp increase in ice-nucleating activity in the Snomax data. This increase in ice-nucleating activity was also observed in the UBC soil extract solutions, as the n_{m} increased by two orders of magnitude at around $-6\,^{\circ}\mathrm{C}$. This correlating increase in n_{m} suggests that proteinaceous INMs are contributing to the ice-nucleating activity of the UoL and UBC soil extracts at these high freezing temperatures, although smaller concentrations are present in the soil extracts compared with our pure, filtered Snomax solutions. Additionally, the high ice-nucleating activity of the soil extracts was observed even though the soil extract solutions were filtered to 0.22 µm, consistent with other studies that have also shown ice-nucleating activities remain high

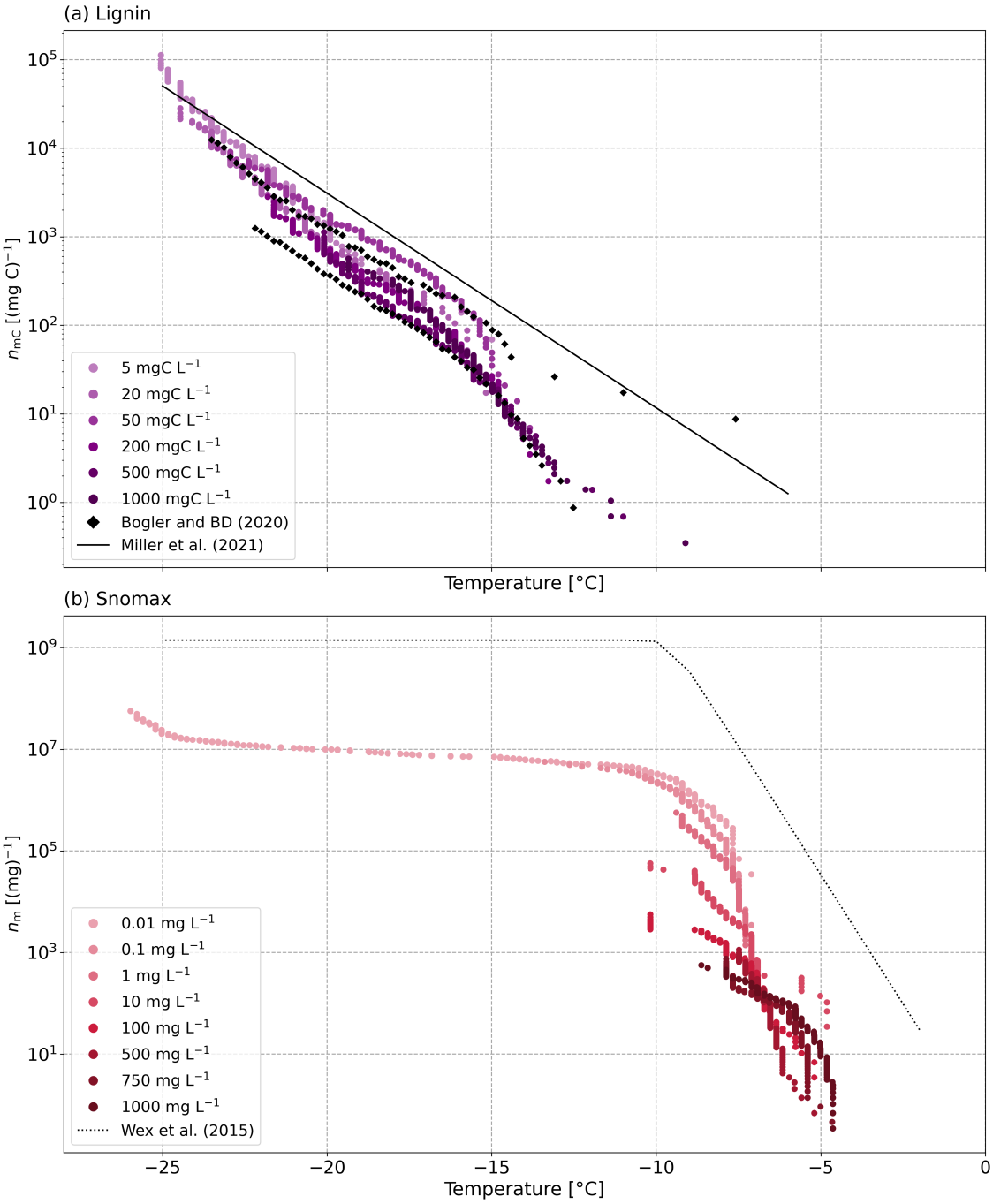

Figure 3.6: Ice-active mass site density (n_{mC} and n_m) as a function of temperature for the soil subcomponents and their dilutions *including (a) the ice-active mass density of carbon (n_{mC}) in the lignin dilutions and (b) the ice-active mass site density (n_m) for the filtered Snomax solutions.*

despite filtration (Pummer et al., 2012; O'Sullivan et al., 2015). These two observations suggest that biogenic macromolecules are contributing significantly to the ice-nucleating ability of all the soil extracts examined here. We also compare the n_{m} of the extracted soil solutions with that of other agricultural soils (Conen et al., 2011; O'Sullivan et al., 2014). Interestingly, our n_{m} values compare well with the n_{m} values from O'Sullivan et al. (2014), which was sampled from similar agricultural fields in the UK. Some of the n_{m} values from Conen et al. (2011) were also within the range of our soil extracts, particularly those from UoL and UBC. However, the ice-nucleating activity from our Rothamsted extracts was up to two orders of magnitude lower than that of Conen et al. (2011) and O'Sullivan et al. (2014). We also compared the ice-nucleating activity of our soil extracts with that of montmorillonite, a type of clay mineral, which was analysed by Conen et al. (2011), as a comparison to pure mineral dust. We observed that the ice-nucleating activity of the UBC and UoL soil extracts mostly remains above that of the montmorillonite, however, the ice-nucleating activity of the Rothamsted sample remained below the ice-nucleating activity of montmorillonite (Figure 3.7b). This observation suggests that the ice-nucleating activity of the Rothamsted soil extract was dominated by minerals, like clay, with little influence of biological materials such as ice-active proteins.

The spread of freezing activities observed here suggests that the ice-nucleating ability of agricultural soils could be dependent on their location, crop type, or land management. Each of our soil sampling locations was associated with a different crop type (Table 1), which likely created unique environments for the development of biological communities on the crops and within the soils (Redford et al., 2010) (see Figure 3.1). The different sampling locations affect the abundance and diversity of microbes, such as bacteria and fungi, in our samples. Since not all bacteria and fungi nucleate ice at the same efficiency, the overall abundance of microbial species may not directly correlate with the ice-nucleating ability of the soil (Bowers et al., 2011). However, the relative abundance of certain bacteria and fungi species will impact the overall ice-nucleating activity of the soil (Bowers et al., 2009). Hence, changes in the environments with crop type and location are likely important for the differences observed in this study. Specifically, our results indicate that a greater proportion of highly ice-active proteinaceous INMs were present in the UoL soil samples, contributing to its increased ice-nucleating activity at $-6\,^{\circ}\mathrm{C}$. This observation is consistent with other studies, which found that proteins can contribute to the ice-nucleating ability of agricultural soils (O'Sullivan et al., 2015; Hill et al., 2016).

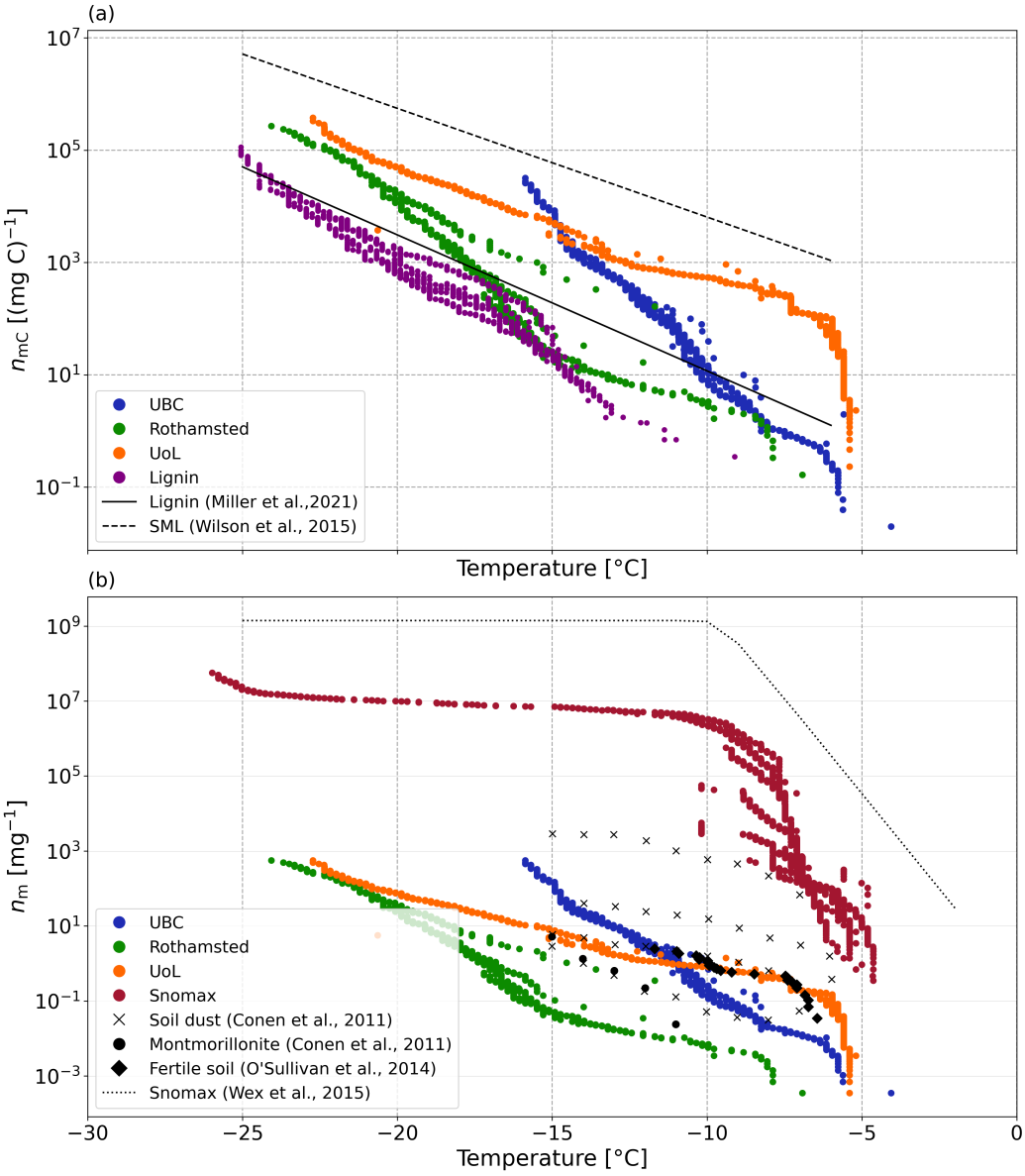

Figure 3.7: Ice-active mass site density (n_{mC} and n_m) as a function of temperature for the soil extracts, the soil subcomponents and literature comparisons. *(a) Ice-active Carbon mass site density as a function of temperature for the dilution series of the three soil extracts from the University of British Columbia Farm (Vancouver, Canada), the University of Leeds Farm (Tadcaster, UK) and Rothamsted Research (Harpenden, UK) and for our aqueous dilution series of lignin. For comparison, a parameterisation of sea spray aerosols containing biogenic material from Wilson et al. (2015); a parameterisation of lignin based on lignin solutions of 20 mg C L^{-1} from Miller et al. (2021); and n_m values of an aqueous dilution series of lignin produced by Bogler and Borduas-Dedekind (2020) are all included. (b) Ice-active mass site density as a function of temperature for the dilution series of the three soil extracts and for the aqueous dilution series of filtered Snomax.For comparison, n_m values from Conen et al. (2011) and O'Sullivan et al. (2015) are included; as well as a parameterisation for Snomax as described by Wex et al. (2015).*

Differences in location may contribute to variations in the organic content in the soil, which may contribute to the ice-nucleating ability of the soil. The wide range of freezing temperatures observed in our soil samples aligns with previous studies that found large variability in the ice-nucleating activity of agricultural soils, likely linked to a range in organic matter and biological content (O'Sullivan et al., 2015; Hiranuma et al., 2021; Hamzehpour et al., 2022a,b; Pereira et al., 2022). Conen et al. (2011) analysed the ice-nucleating activity of agricultural soils from Mongolia, Germany, Hungary and Yakutia. They found a variation of two orders of magnitude in the n_{m} of the different soil samples (Figure 3.7b). While some studies showed that fertile soils are distinctly more active than desert dust, particularly at higher freezing temperatures (Garcia et al., 2012; O'Sullivan et al., 2015; Steinke et al., 2016; Hiranuma et al., 2021), other studies found the ice-nucleating activity for these soils to be more comparable to that of desert dust (Tobo et al., 2014; O'Sullivan et al., 2014). Therefore, the range of ice-nucleating activities found in our extracted soil samples fits the range of activities expected for these kinds of soils.

3.3.2 Filtration of Snomax Samples

The Snomax solutions were filtered to more accurately compare the freezing activity of the Snomax solutions with the soil extract solutions since we were specifically interested in the soluble content of the soils. After filtration to 0.22 µm, we observed a shift in freezing temperatures of up to 3 °C (Figure 3.8). In addition, we observed up to an order of magnitude loss in n_{m} after filtration. However, despite these observations, the overall ice-nucleating activity of the Snomax solutions remained relatively high after filtering to 0.22 µm (Figure 3.8). Previous studies have assumed that filtering to 0.22 µm removes all ice-nucleating activity from bacteria because ice-active bacterial proteins are bound to either whole cells or cell fragments (Maki et al., 1974; Felgitsch et al., 2018; Ickes et al., 2020). Our observations suggest that filtering bacterial ice-nucleating does not completely remove its ice-nucleating activity, suggesting that we cannot rule out bacterial ice-nucleating after filtration to 0.22 µm.

The ice-nucleating activity of our Snomax solutions was also compared with the parameterization by Wex et al. (2015) (Figure 3.8b). The ice-nucleating activity of both the filtered and unfiltered solutions is lower than the ice-nucleating activity predicted by Wex et al. (2015). Storage of Snomax samples has been shown to reduce their ice-nucleating

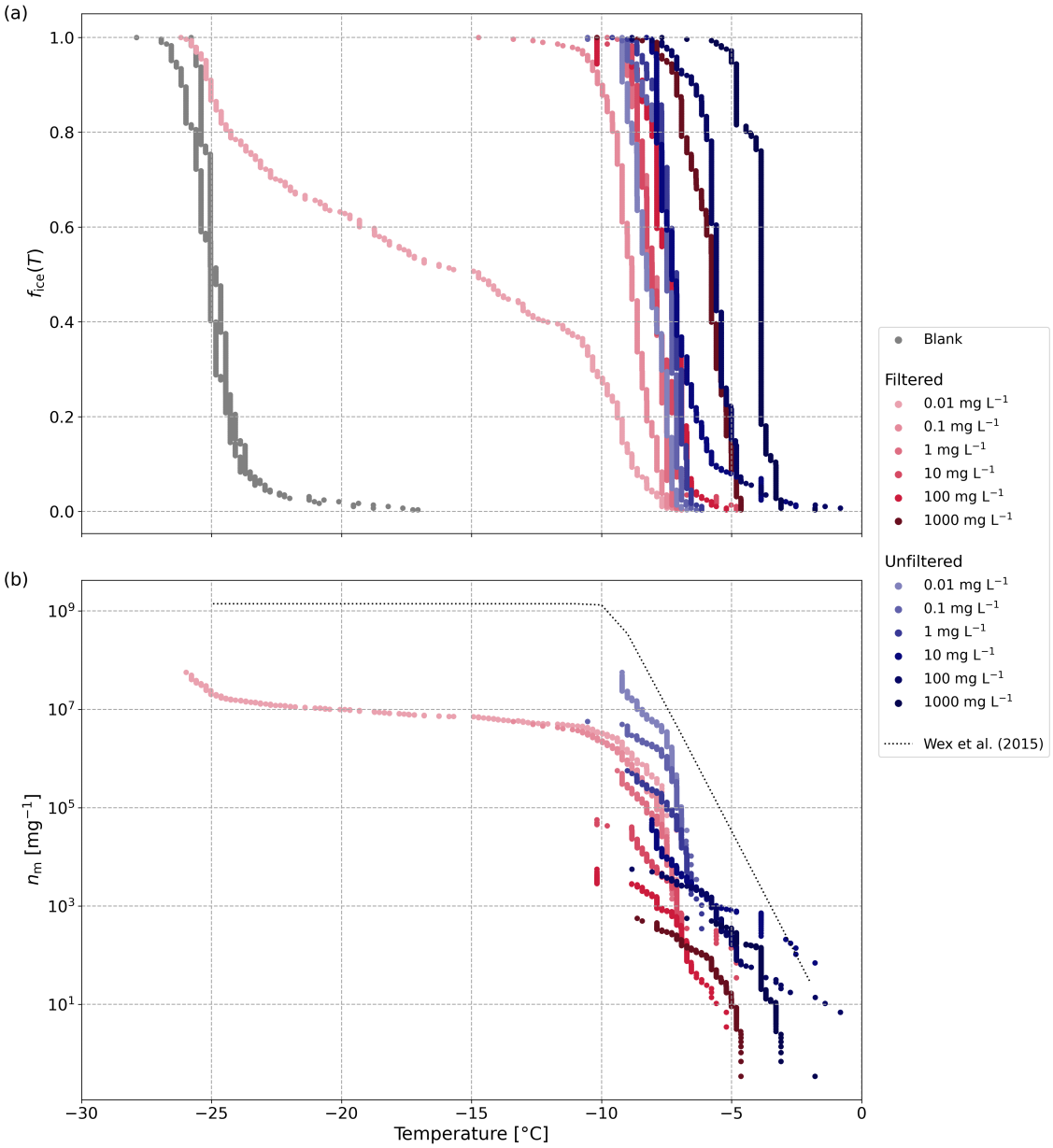

Figure 3.8: The ice-nucleating activity of Snomax before and after filtration. *(a) Fraction frozen ($f_{ice}(T)$) as a function of temperature for the filtered (red) and unfiltered Snomax dilution series. (b) Ice-active mass site density (n_m) for the same filtered and unfiltered Snomax dilutions series. For comparison, a parameterization of Snomax as described by Wex et al. (2015) is also plotted.*

activity over time (Polen et al., 2016), which could explain the lower ice-nucleating activity shown here. Furthermore, ice nucleation up to $-2\,^{\circ}\mathrm{C}$ is caused by large aggregates (Class A freezing mechanism) and is known to fluctuate between different Snomax samples (Polen et al., 2016; Lukas et al., 2022).

3.3.3 Surface Tension of Soil Extracts

To investigate whether surfactant-like macromolecules play an important role in the ice-nucleating ability of soils, we compared the ice-nucleating activity of the soil extracts with their measured surface tensions (Figures 3.9). In general, the T_{50} values of our soil extracts indicate that their ice-nucleating ability is dependent on the mass concentration of soil before filtration (Figure 3.9). However, the surface tension measurements for the soil extracts do not scale directly with the mass concentration of the soil. Some of the soil extracts show a slight surface tension reduction from pure water (which is 72.8 mN m^{-1} (Kalová and Mareš, 2015)) of up to 2.2 mN m^{-1}. However, even small reductions in surface tension did not correlate with the ice-nucleating activity of the soil extracts. We hypothesise that not every ice-nucleating substance in the soil extracts is a surfactant and that not every surfactant is ice-active. Thus, we do not observe a correlation between the ice-nucleating abilities of the soil extracts and their surface tension reductions. In addition, the fact that we observed little surface tension reduction in our soil extracts suggests that there is likely no micelle formation within these solutions.

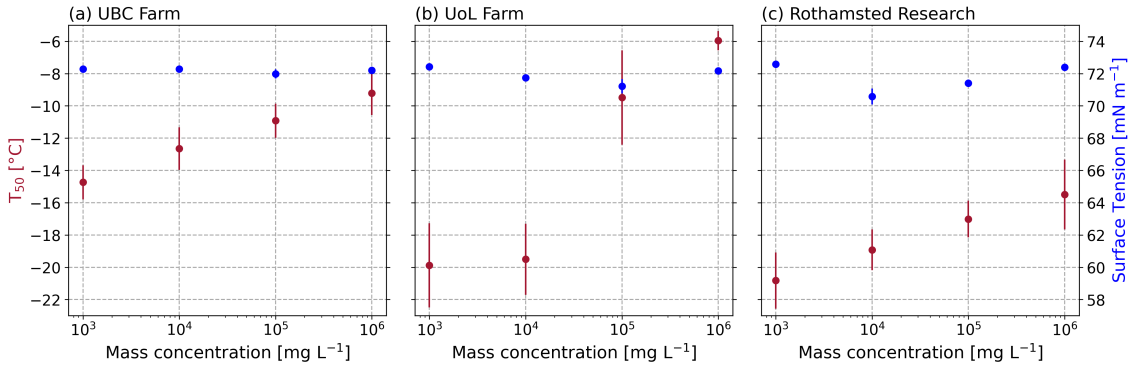

Figure 3.9: Surface tension and average freezing temperature (T_{50}) plotted against the mass concentration of the soil extracts *from (a) UBC Farm, (b) UoL Farm and (c) Rothamsted and each of their corresponding dilution series.*

3.3.4 Surface Tension of the Subcomponents

In contrast, surface tension reductions for the soil subcomponents correlated with increased freezing temperatures (Figure 3.10). For the 2.0×10^3 mg L^{-1} lignin solution and the 10^3 mg L^{-1} Snomax solution, the highest concentrations analysed in this study, the greatest surface tension reductions were observed, of 5.0 mN m^{-1} and 9.1 mN m^{-1}, respectively. However, the concentration of Snomax needed to pass the threshold of 100 mg L^{-1} before the measured surface tension reductions exceed 0.5 mN m^{-1} (Figure 3.10b). This result indicates that these soil subcomponents are surface active, accumulating at the air-water interface of the suspended droplet on the tensiometer. We also observed a general increase in T_{50} values with increasing surface tension reductions for both of the analysed subcomponents (Figure 3.10). However, for the Snomax solutions, we observed that the ice-nucleating activity remained at $-14.7\,°C$, even at the lowest mass concentration of 10^{-2} mg L^{-1} (Figure 3.10b). This trend indicates that the surface tension reduction was a function of the concentration of surfactants, whereas a significant decrease was only observed above a minimal surface coverage. In contrast, heterogeneous ice nucleation at moderate supercooling temperatures ($-9\,°C$) was only observed when trace amounts of INM were present (10^{-4} mg ml^{-1}) for Snomax solutions. Overall, the observed correlation between measured surface tension reduction and ice-nucleating activity of the soil subcomponents (in particular, for the lignin dilution series) indicates that the formation of a surfactant monolayer may be important for ice nucleation, but simply the presence of surfactants was unlikely to be an indicator of INA in any given solution.

The observed surface tension reductions also indicate the potential for micelle formation within the solutions (Mabrouk et al., 2022). As surfactants become saturated at the surface of a droplet, the macromolecules that remain in solution in the bulk cluster together into micelles to minimise the exposure of the hydrophobic moieties to the water (Rosen and Kunjappu, 2012). The concentration of surfactants needed to initiate micelle formation is called the critical micelle concentration (Rosen and Kunjappu, 2012). Once micelle formation is initiated, further increases in concentration do not lead to further decreases in surface tension since the surface is saturated (Nesměrák and Němcová, 2006). In our observations, it became difficult to create solutions with higher concentrations of lignin and of Snomax, so the critical micelle concentration, if it exists for these substances could not be measured. Nevertheless, we can state that the critical micelle concentrations for lignin and Snomax would be above 10^4 mg L^{-1} and above 10^3 mg L^{-1}, respectively.

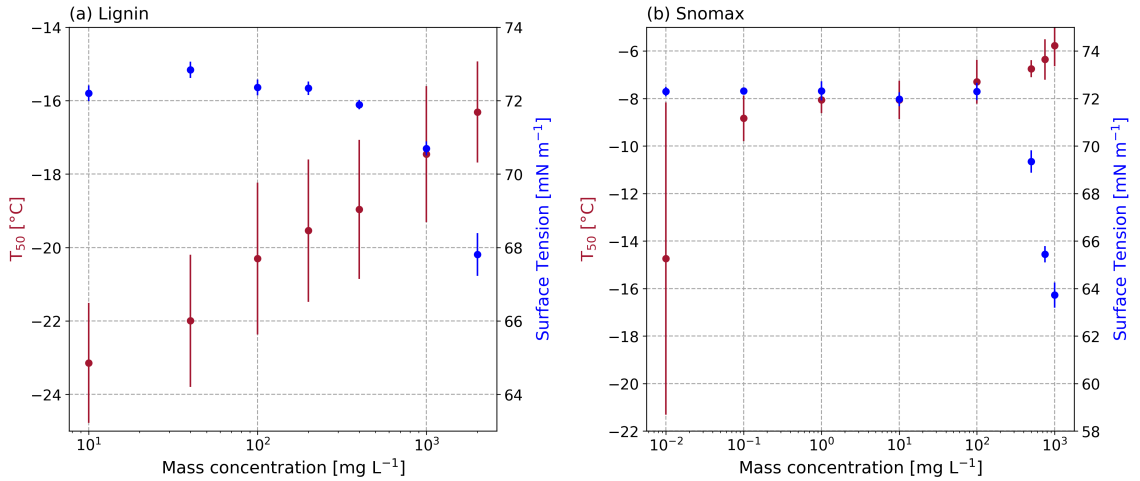

Figure 3.10: Surface tension and average freezing temperature (T_{50}) plotted against the mass concentration of the analysed soil subcomponents. *(a) Lignin and (b) Snomax for each of their corresponding dilution series*

We can therefore conclude that the formation of micelles was not necessary for lignin or Snomax to nucleate ice.

The T_{50} values for lignin are linear to the log of the mass concentration in both our work and the work of Bogler and Borduas-Dedekind (2020) (Figure 3.10a). This relationship leads to a dilution effect after normalisation to the carbon content of the lignin solutions (Bogler and Borduas-Dedekind, 2020). The surface tension reduction of lignin solutions observed in this study suggests that lignin acts as a surfactant and that aggregation of lignin macromolecules at the air-water interface could be a possible explanation for this observed concentration dependence in lignin's ice-nucleating activity.

3.3.5 Does Surface Tension Relate to Ice-Nucleating Ability?

The observed reduction in surface tension for our lignin and Snomax solutions indicates the presence of surface active components within these solutions. We also observed a correlation between the surface tension reduction and the freezing temperature for our lignin and Snomax solutions (Figure 3.11). However, the reason for this observed correlation remains unclear. One possible explanation could be that at higher solution concentrations, a greater quantity of material leads to more INPs within the solution and a greater number of surfactants with no direct link between the two. Another possible explanation is that the presence of surfactants within the solution helps to enhance the ice-nucleating activity of the component. Previous studies have indicated that the presence of surfactants can enhance the observed ice-nucleating activity (Hiranuma et al., 2013; China et al., 2017;

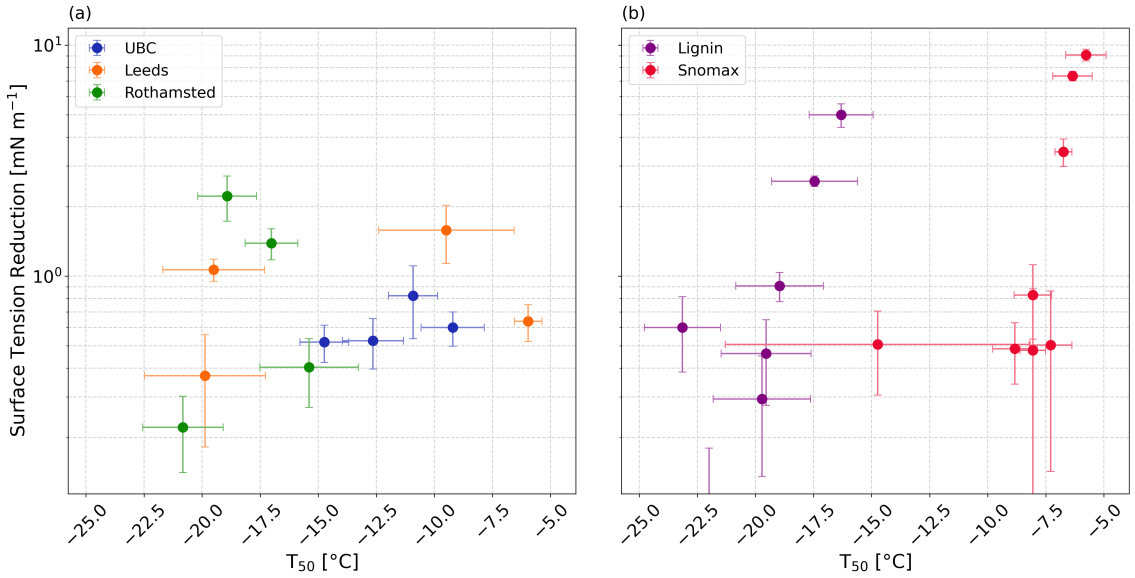

Figure 3.11: Relationship between the average freezing temperature (T_{50}) and surface tension for the dilution series of (a) our soil extracts and (b) subcomponent solutions.

Qiu et al., 2017; DeMott et al., 2018; Perkins et al., 2020; Schwidetzky et al., 2021b). It is therefore possible that there is a direct link between the ice-nucleating ability of our solutions and their surfactant concentrations as the structure of surfactant macromolecules is thought to be a good lattice match for ice formation (Qiu et al., 2017; DeMott et al., 2018). More recent work by Bieber and Borduas-Dedekind (2024) indicates that ice-nucleating proteins may need to accumulate at the air-water interface of the droplet for ice nucleation to occur, therefore this observed correlation between surfactant concentration and freezing activity may indicate a mechanism of ice formation by surfactant macromolecules. However, more work would be needed to confirm the importance of this relationship.

For our soil extract solutions, there was no clear relationship between the ice-nucleating activity and the surface tension reduction (Figure 3.11), indicating that the concentration of surfactants in these solutions was too low to impact the surface tension of our droplets. This result indicates that other biological macromolecules or components that are not surfactants are likely responsible for the ice-nucleating activity of our soil samples. The complexity of our soil samples means that many different components are likely to be present, such as bacteria, fungi, plant debris and even inorganic mineral components (Conen et al., 2011; Steinke et al., 2016, 2020), any of which may be contributing to the high ice-nucleating activities observed in this study. Aggregation other than micelle formation may be playing a role in the ice-nucleating ability of the soil extracts, particularly for the Rothamsted samples, where we observed some discrepancies in the normalised dilution

series as a function of temperature. Furthermore, it is possible that the aggregation of macromolecules impacted the filtration process in this study. For example, aggregates larger than 0.22 µm may have been removed during filtration, leading to the loss of ice-nucleating material from the analysed soil extracts.

In our experiments, the surface tension measurements were taken at room temperature, higher than the subzero temperatures experienced by the freezing droplets in FINC. Surface tension is temperature dependent (see Figure A.2); the surface tension of pure water increases with decreasing temperature (Gittens, 1969). Furthermore, the formation of micelles depends on the concentration of surfactants and the temperature of the solutions (Zieliński et al., 1989), which makes predictions of micelle formations in supercooled microscopic droplets challenging.

3.3.6 Sensitivity of Soil Extracts to Heat Treatment

To identify heat-liable biological material in the soil extracts (Hill et al., 2016; O'Sullivan et al., 2018; Daily et al., 2022), heat tests were performed on the two extracted soil dilution series as well as the samples with the highest ice-nucleating activities from UoL Farm and UBC Farm (Figure 3.12). We observed a loss of ice-nucleating activity, particularly at around −5 °C in the normalised INM spectra, suggesting that some ice-active proteins are destroyed as a result of the heat treatment (Steinke et al., 2016; Suski et al., 2018; Daily et al., 2022). In the undiluted extracted soil solution for the UoL sample 1, we observed a shift in the T_{50} from −7.2 °C to −11 °C and for the undiluted UBC sample 1, there was a decrease in the T_{50} from −9.2 °C to −10.6 °C. We also took measurements of the surface tension reduction for the heated soil extracts before and after heating. For both the UoL and UBC samples, we observed no significant change in the surface tension reduction after heating. However, in the dilutions, where freezing occurs at lower temperatures, the reduction in activity was much smaller or even negligible, indicating that there is a population of heat-stable ice nucleating entities.

In general, the ice-nucleating ability of the soil extracts remains high, despite exposure to heat treatment. The ice-nucleating activity was higher than expected for mineral dust, as shown by the n_{m} values for montmorillonite from Conen et al. (2011) shown in Figure 3.12, indicating the presence of heat-stable organics within the soil samples. Previous studies have investigated heat-stable organics which can help us to identify what might be causing freezing in these soils. Some high-temperature freezing can be lost after heat-

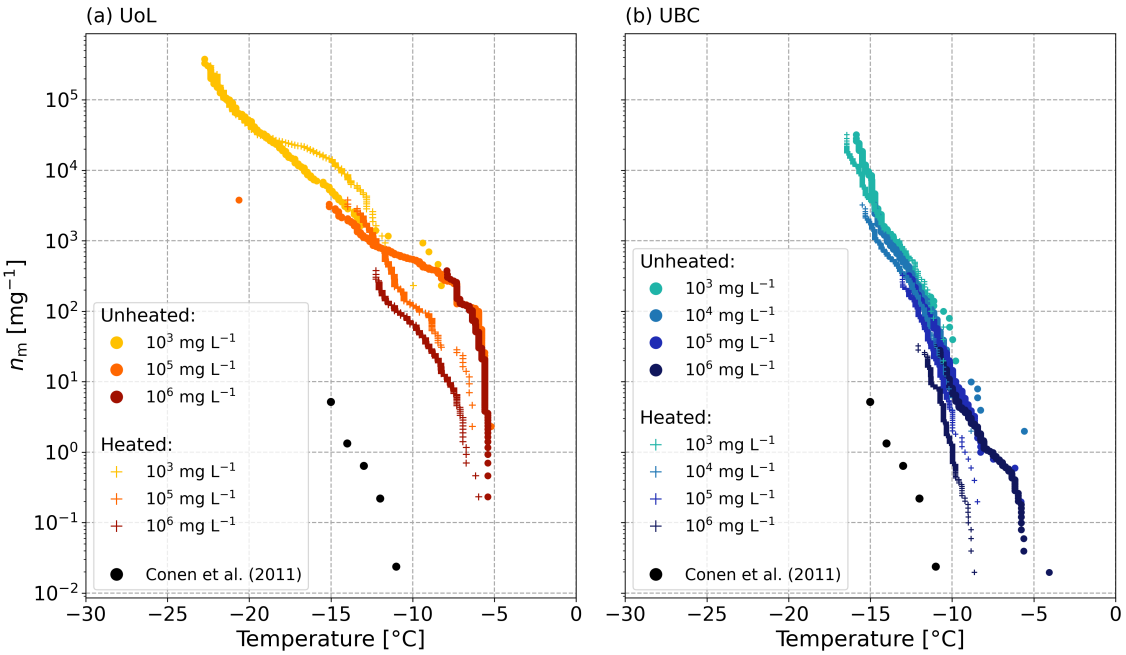

Figure 3.12: Ice active mass site density (n_m) as a function of the temperature of the dilution series for soil extracts before and after heat treatments. *(a) The UoL Farm and (b) the UBC Farm. For comparison, n_m values for montmorillonite from Conen et al. (2011) are also included.*

treating agricultural soils (Garcia et al., 2012; Suski et al., 2018), as observed in our data. Heat-stable INMs have been observed previously in soil samples, which subsequently broke down after treatment with hydrogen peroxide (O'Sullivan et al., 2014; Suski et al., 2018). Hill et al. (2016) found a large fraction of the ice-nucleating ability of agricultural soils was resistant to all tests except oxidation by hydrogen peroxide. They concluded that this ice-nucleating ability was likely attributed to plant material, such as lignin (Hill et al., 2016). These findings are similar to those in our study, where a large portion of the freezing activity remained unaffected by the heating, suggesting that the majority of the ice-nucleating activity was attributable to heat-stable INMs from the breakdown of plant material, such as lignin, cellulose, starch or pectin (Borduas-Dedekind et al., 2019; Steinke et al., 2020; Chen et al., 2021).

In addition, after heating the UoL soil extracts, we observed an increase of up to half an order of magnitude in the ice-nucleating activity below about $-12\,°C$. We saw a shift to warmer freezing temperatures after heating by $2\,°C$ at $1.5 \times 10^4\,mg^{-1}$. McCluskey et al. (2018) investigated the ice-nucleating ability of marine bioaerosols in a mesocosm experiment. They also observed increases in ice-nucleating activity after heating their samples. They hypothesised that this observed increase in ice-nucleating activity was due to the breakdown of cell walls and the release of INMs into suspension. This was likely not

the case in our extracted solutions since we filtered our samples to 0.22 µm, which likely removes whole cells. They also suggested that the observed increase in ice-nucleating activity could be due to the heating dissolving aggregates in suspension, redistributing macromolecules and exposing new ice-active sites (McCluskey et al., 2018). Therefore, the observed increase in ice-nucleating activity after heating our UoL soil extracts suggests that (a) there are aggregates present in the soil suspension which are not micelles and that (b) these aggregates are inhibiting ice nucleation at temperatures below about −12 °C.

3.4 Conclusions

In this chapter, we investigated the ice-nucleating activity of submicron entities in three different agricultural soil samples. This study aimed to better understand the ice-nucleating activity of fertile soils by breaking down the complexity of these soils to their submicron components and comparing these activities to that of two common soil subcomponents; lignin and ice-active proteins. We found that the ice-nucleating activity of agricultural soils varies widely between different sampling locations, which could be impacted by a variety of factors such as crop type, land management and environmental differences. We found that ice-active proteins (when Snomax was used as a proxy) seemed to contribute to the ice-nucleating activity of the analysed agricultural soils, in particular the UBC and UoL soil samples. However, when these soil samples were heated, we only observed a small reduction in ice-nucleating activity, which suggests that a large proportion of the ice-nucleating activity was attributable to heat-stable compounds such as lignin and cellulose. Despite this, the relative contribution of lignin remains unclear, although it may have contributed more to the observed ice-nucleating activity of the Rothamsted soil samples.

We also investigated the relative contribution of surfactant macromolecules to the ice-nucleating activity of our soil samples and their subcomponents. We achieved this by examining the relationship between surface tension reduction in relation to pure water and the ice-nucleating activity of the soil extract solutions and the solutions of lignin and Snomax. We found that the surface tension reduction caused by organic components within the soil extracts does not correlate with its ice-nucleating activity. This observation indicates that surfactants are not contributing significantly to the ice-nucleating activity of our soil extracts. Despite this observation in the soil extracts, we did observe a relationship between surface tension reduction and ice-nucleating activity for the soil

subcomponents analysed in this study, lignin and Snomax. This observed surface tension reduction indicates the presence of surfactants within these highly ice-active solutions. However, we were unable to confirm in this study whether this correlation indicated that the surfactants were acting as ice-nucleating material within these solutions.

Our results suggest that aggregation may play a role in the ice-nucleating ability of agricultural soils. For example, the n_{m} of the Rothamsted did not align as a function of temperature indicating that possible aggregation of macromolecules at higher concentrations was blocking nucleation sites. We also observed a slight increase in ice-nucleating activity after heat treatment for our UoL sample, which indicates that aggregates are dissolving and releasing ice-active sites into the solution. This aggregation, however, was not linked to the saturation of surfactants at the surface and the formation of micelles. Our findings also suggest that other, non-aggregating substances may be controlling the ice-nucleating ability of agricultural soils. To better understand if the formation of aggregates within soil extract solutions aids in their ability to nucleate ice, or hinders it, future work could investigate aggregates of organic macromolecules in more detail to determine what aggregate formations may be ideal to template ice formation.

References

Berry, J. D., Neeson, M. J., Dagastine, R. R., Chan, D. Y. C., and Tabor, R. F. (2015). Measurement of surface and interfacial tension using pendant drop tensiometry. *Journal of Colloid and Interface Science*, 454:226–237.

Bieber, P. and Borduas-Dedekind, N. (2024). High-speed cryo-microscopy proves that ice-nucleating proteins of Pseudomonas syringae trigger freezing at hydrophobic interfaces.

Bogler, S. and Borduas-Dedekind, N. (2020). Lignin's ability to nucleate ice via immersion freezing and its stability towards physicochemical treatments and atmospheric processing. *Atmospheric Chemistry and Physics*, 20(23):14509–14522.

Boose, Y., Baloh, P., Plötze, M., Ofner, J., Grothe, H., Sierau, B., Lohmann, U., and Kanji, Z. A. (2019). Heterogeneous ice nucleation on dust particles sourced from nine deserts worldwide – Part 2: Deposition nucleation and condensation freezing. *Atmospheric Chemistry and Physics*, 19(2):1059–1076.

Borduas-Dedekind, N., Ossola, R., David, R. O., Boynton, L. S., Weichlinger, V., Kanji, Z. A., and McNeill, K. (2019). Photomineralization mechanism changes the ability of dissolved organic matter to activate cloud droplets and to nucleate ice crystals. *Atmospheric Chemistry and Physics*, 19(19):12397–12412.

Bowers, R. M., Lauber, C. L., Wiedinmyer, C., Hamady, M., Hallar, A. G., Fall, R., Knight, R., and Fierer, N. (2009). Characterization of Airborne Microbial Communities at a High-Elevation Site and Their

Potential To Act as Atmospheric Ice Nuclei. *Applied and Environmental Microbiology*, 75(15):5121–5130.

Bowers, R. M., McLetchie, S., Knight, R., and Fierer, N. (2011). Spatial variability in airborne bacterial communities across land-use types and their relationship to the bacterial communities of potential source environments. *The ISME Journal*, 5(4):601–612.

Chen, J., Wu, Z. J., Zhao, X., Wang, Y. J., Chen, J. C., Qiu, Y. T., Zong, T. M., Chen, H. X., Wang, B. B., Lin, P., Liu, W., Guo, S., Yao, M. S., Zeng, L. M., Wex, H., Liu, X., Hu, M., and Li, S. M. (2021). Atmospheric Humic-Like Substances (HULIS) Act as Ice Active Entities. *Geophysical Research Letters*, 48(14):e2021GL092443.

China, S., Alpert, P. A., Zhang, B., Schum, S., Dzepina, K., Wright, K., Owen, R. C., Fialho, P., Mazzoleni, L. R., Mazzoleni, C., and Knopf, D. A. (2017). Ice cloud formation potential by free tropospheric particles from long-range transport over the Northern Atlantic Ocean. *Journal of Geophysical Research: Atmospheres*, 122(5):3065–3079.

Conen, F., Morris, C. E., Leifeld, J., Yakutin, M. V., and Alewell, C. (2011). Biological residues define the ice nucleation properties of soil dust. *Atmospheric Chemistry and Physics*, 11(18):9643–9648.

Daily, M. I., Tarn, M. D., Whale, T. F., and Murray, B. J. (2022). An evaluation of the heat test for the ice-nucleating ability of minerals and biological material. *Atmospheric Measurement Techniques*, 15(8):2635–2665.

DeMott, P. J., Mason, R. H., McCluskey, C. S., Hill, T. C. J., Perkins, R. J., Desyaterik, Y., Bertram, A. K., Trueblood, J. V., Grassian, V. H., Qiu, Y., Molinero, V., Tobo, Y., Sultana, C. M., Lee, C., and Prather, K. A. (2018). Ice nucleation by particles containing long-chain fatty acids of relevance to freezing by sea spray aerosols. *Environmental Science: Processes & Impacts*, 20(11):1559–1569.

Dreischmeier, K., Budke, C., Wiehemeier, L., Kottke, T., and Koop, T. (2017). Boreal pollen contain ice-nucleating as well as ice-binding 'antifreeze' polysaccharides. *Scientific Reports*, 7(1):41890.

Felgitsch, L., Baloh, P., Burkart, J., Mayr, M., Momken, M. E., Seifried, T. M., Winkler, P., Schmale III, D. G., and Grothe, H. (2018). Birch leaves and branches as a source of ice-nucleating macromolecules. *Atmospheric Chemistry and Physics*, 18(21):16063–16079.

Fornea, A. P., Brooks, S. D., Dooley, J. B., and Saha, A. (2009). Heterogeneous freezing of ice on atmospheric aerosols containing ash, soot, and soil. *Journal of Geophysical Research: Atmospheres*, 114(D13).

Garcia, E., Hill, T. C. J., Prenni, A. J., DeMott, P. J., Franc, G. D., and Kreidenweis, S. M. (2012). Biogenic ice nuclei in boundary layer air over two U.S. High Plains agricultural regions. *Journal of Geophysical Research: Atmospheres*, 117(D18).

Gavish, M., Popovitz-Biro, R., Lahav, M., and Leiserowitz, L. (1990). Ice Nucleation by Alcohols Arranged in Monolayers at the Surface of Water Drops. *Science*, 250(4983):973–975. Publisher: American Association for the Advancement of Science.

Gittens, G. J. (1969). Variation of surface tension of water with temperature. *Journal of Colloid and Interface Science*, 30(3):406–412.

Gomboš, M., Tall, A., Trpčevská, J., Kandra, B., Pavelkova, D., and Balejčíková, L. (2018). Sedimentation rate of soil microparticles. *Arabian Journal of Geosciences*, 11(20):635.

Gérard, V., Noziere, B., Fine, L., Ferronato, C., Singh, D. K., Frossard, A. A., Cohen, R. C., Asmi, E., Lihavainen, H., Kivekäs, N., Aurela, M., Brus, D., Frka, S., and Cvitešić Kušan, A. (2019). Concentrations and Adsorption Isotherms for Amphiphilic Surfactants in PM1 Aerosols from Different Regions of Europe. *Environmental Science & Technology*, 53(21):12379–12388.

Gérard, V., Nozière, B., Baduel, C., Fine, L., Frossard, A. A., and Cohen, R. C. (2016). Anionic, Cationic, and Nonionic Surfactants in Atmospheric Aerosols from the Baltic Coast at Askö, Sweden: Implications for Cloud Droplet Activation. *Environmental Science & Technology*, 50(6):2974–2982.

Hamzehpour, N., Marcolli, C., Klumpp, K., Thöny, D., and Peter, T. (2022a). The Urmia playa as a source of airborne dust and ice-nucleating particles – Part 2: Unraveling the relationship between soil dust composition and ice nucleation activity. *Atmospheric Chemistry and Physics*, 22(22):14931–14956.

Hamzehpour, N., Marcolli, C., Pashai, S., Klumpp, K., and Peter, T. (2022b). Measurement report: The Urmia playa as a source of airborne dust and ice-nucleating particles – Part 1: Correlation between soils and airborne samples. *Atmospheric Chemistry and Physics*, 22(22):14905–14930.

Harrison, A. D., Lever, K., Sanchez-Marroquin, A., Holden, M. A., Whale, T. F., Tarn, M. D., McQuaid, J. B., and Murray, B. J. (2019). The ice-nucleating ability of quartz immersed in water and its atmospheric importance compared to K-feldspar. *Atmospheric Chemistry and Physics*, 19(17):11343–11361.

Harrison, A. D., Whale, T. F., Carpenter, M. A., Holden, M. A., Neve, L., O'Sullivan, D., Vergara Temprado, J., and Murray, B. J. (2016). Not all feldspars are equal: a survey of ice nucleating properties across the feldspar group of minerals. *Atmospheric Chemistry and Physics*, 16(17):10927–10940.

Hartmann, S., Ling, M., Dreyer, L. S. A., Zipori, A., Finster, K., Grawe, S., Jensen, L. Z., Borck, S., Reicher, N., Drace, T., Niedermeier, D., Jones, N. C., Hoffmann, S. V., Wex, H., Rudich, Y., Boesen, T., and Šantl Temkiv, T. (2022). Structure and Protein-Protein Interactions of Ice Nucleation Proteins Drive Their Activity. *Frontiers in Microbiology*, 13:872306.

Hill, T. C. J., DeMott, P. J., Tobo, Y., Fröhlich-Nowoisky, J., Moffett, B. F., Franc, G. D., and Kreidenweis, S. M. (2016). Sources of organic ice nucleating particles in soils. *Atmospheric Chemistry and Physics*, 16(11):7195–7211.

Hiranuma, N., Auvermann, B. W., Belosi, F., Bush, J., Cory, K. M., Georgakopoulos, D. G., Höhler, K., Hou, Y., Lacher, L., Saathoff, H., Santachiara, G., Shen, X., Steinke, I., Ullrich, R., Umo, N. S., Vepuri, H. S. K., Vogel, F., and Möhler, O. (2021). Laboratory and field studies of ice-nucleating particles from open-lot livestock facilities in Texas. *Atmospheric Chemistry and Physics*, 21(18):14215–14234.

Hiranuma, N., Brooks, S. D., Moffet, R. C., Glen, A., Laskin, A., Gilles, M. K., Liu, P., Macdonald, A. M., Strapp, J. W., and McFarquhar, G. M. (2013). Chemical characterization of individual particles and

residuals of cloud droplets and ice crystals collected on board research aircraft in the ISDAC 2008 study. *Journal of Geophysical Research: Atmospheres*, 118(12):6564–6579.

Holden, M. A., Campbell, J. M., Meldrum, F. C., Murray, B. J., and Christenson, H. K. (2021). Active sites for ice nucleation differ depending on nucleation mode. *Proceedings of the National Academy of Sciences*, 118(18):e2022859118. Publisher: Proceedings of the National Academy of Sciences.

Ickes, L., Porter, G. C. E., Wagner, R., Adams, M. P., Bierbauer, S., Bertram, A. K., Bilde, M., Christiansen, S., Ekman, A. M. L., Gorokhova, E., Höhler, K., Kiselev, A. A., Leck, C., Möhler, O., Murray, B. J., Schiebel, T., Ullrich, R., and Salter, M. E. (2020). The ice-nucleating activity of Arctic sea surface microlayer samples and marine algal cultures. *Atmospheric Chemistry and Physics*, 20(18):11089–11117.

Jackson, G. A. and Burd, A. B. (1998). Aggregation in the Marine Environment. *Environmental Science & Technology*, 32(19):2805–2814.

Kalová, J. and Mareš, R. (2015). Reference Values of Surface Tension of Water. *International Journal of Thermophysics*, 36(7):1396–1404.

Kupiszewski, P., Zanatta, M., Mertes, S., Vochezer, P., Lloyd, G., Schneider, J., Schenk, L., Schnaiter, M., Baltensperger, U., Weingartner, E., and Gysel, M. (2016). Ice residual properties in mixed-phase clouds at the high-alpine Jungfraujoch site. *Journal of Geophysical Research: Atmospheres*, 121(20):12,343–12,362.

Kuwabara, C., Terauchi, R., Tochigi, H., Takaoka, H., Arakawa, K., and Fujikawa, S. (2014). Analysis of supercooling activities of surfactants. *Cryobiology*, 69(1):10–16.

Lukas, M., Schwidetzky, R., Eufemio, R. J., Bonn, M., and Meister, K. (2022). Toward Understanding Bacterial Ice Nucleation. *The Journal of Physical Chemistry B*, 126(9):1861–1867.

Lukas, M., Schwidetzky, R., Kunert, A. T., Pöschl, U., Fröhlich-Nowoisky, J., Bonn, M., and Meister, K. (2020). Electrostatic Interactions Control the Functionality of Bacterial Ice Nucleators. *Journal of the American Chemical Society*, 142(15):6842–6846.

Mabrouk, M. M., Hamed, N. A., and Mansour, F. R. (2022). Physicochemical and electrochemical methods for determination of critical micelle concentrations of surfactants: a comprehensive review. *Monatshefte für Chemie - Chemical Monthly*, 153(2):125–138.

Maki, L. R., Galyan, E. L., Chang-Chien, M.-M., and Caldwell, D. R. (1974). Ice Nucleation Induced by Pseudomonas syringae. *Applied Microbiology*, 28(3):456–459.

McCluskey, C. S., Hill, T. C. J., Sultana, C. M., Laskina, O., Trueblood, J., Santander, M. V., Beall, C. M., Michaud, J. M., Kreidenweis, S. M., Prather, K. A., Grassian, V., and DeMott, P. J. (2018). A Mesocosm Double Feature: Insights into the Chemical Makeup of Marine Ice Nucleating Particles. *Journal of the Atmospheric Sciences*, 75(7):2405–2423.

Miller, A. J., Brennan, K. P., Mignani, C., Wieder, J., David, R. O., and Borduas-Dedekind, N. (2021). Development of the drop Freezing Ice Nuclei Counter (FINC), intercomparison of droplet freezing tech-

niques, and use of soluble lignin as an atmospheric ice nucleation standard. *Atmospheric Measurement Techniques*, 14(4):3131–3151.

Nesměrák, K. and Němcová, I. (2006). Determination of Critical Micelle Concentration by Electrochemical Means. *Analytical Letters*, 39(6):1023–1040.

O'Sullivan, D., Adams, M. P., Tarn, M. D., Harrison, A. D., Vergara-Temprado, J., Porter, G. C. E., Holden, M. A., Sanchez-Marroquin, A., Carotenuto, F., Whale, T. F., McQuaid, J. B., Walshaw, R., Hedges, D. H. P., Burke, I. T., Cui, Z., and Murray, B. J. (2018). Contributions of biogenic material to the atmospheric ice-nucleating particle population in North Western Europe. *Scientific Reports*, 8(1):13821.

O'Sullivan, D., Murray, B. J., Malkin, T. L., Whale, T. F., Umo, N. S., Atkinson, J. D., Price, H. C., Baustian, K. J., Browse, J., and Webb, M. E. (2014). Ice nucleation by fertile soil dusts: relative importance of mineral and biogenic components. *Atmospheric Chemistry and Physics*, 14(4):1853–1867.

O'Sullivan, D., Murray, B. J., Ross, J. F., Whale, T. F., Price, H. C., Atkinson, J. D., Umo, N. S., and Webb, M. E. (2015). The relevance of nanoscale biological fragments for ice nucleation in clouds. *Scientific Reports*, 5(1):8082.

Ovadnevaite, J., Zuend, A., Laaksonen, A., Sanchez, K. J., Roberts, G., Ceburnis, D., Decesari, S., Rinaldi, M., Hodas, N., Facchini, M. C., Seinfeld, J. H., and O' Dowd, C. (2017). Surface tension prevails over solute effect in organic-influenced cloud droplet activation. *Nature*, 546(7660):637–641.

Pereira, D. L., Gavilán, I., Letechipía, C., Raga, G. B., Puig, T. P., Mugica-Álvarez, V., Alvarez-Ospina, H., Rosas, I., Martinez, L., Salinas, E., Quintana, E. T., Rosas, D., and Ladino, L. A. (2022). Mexican agricultural soil dust as a source of ice nucleating particles. *Atmospheric Chemistry and Physics*, 22(10):6435–6447.

Perkins, R. J., Vazquez de Vasquez, M. G., Beasley, E. E., Hill, T. C. J., Stone, E. A., Allen, H. C., and DeMott, P. J. (2020). Relating Structure and Ice Nucleation of Mixed Surfactant Systems Relevant to Sea Spray Aerosol. *The Journal of Physical Chemistry A*, 124(42):8806–8821.

Pfrang, C., Rastogi, K., Cabrera-Martinez, E. R., Seddon, A. M., Dicko, C., Labrador, A., Plivelic, T. S., Cowieson, N., and Squires, A. M. (2017). Complex three-dimensional self-assembly in proxies for atmospheric aerosols. *Nature Communications*, 8(1):1724.

Polen, M., Lawlis, E., and Sullivan, R. C. (2016). The unstable ice nucleation properties of Snomax® bacterial particles. *Journal of Geophysical Research: Atmospheres*, 121(19):11,666–11,678.

Pummer, B. G., Bauer, H., Bernardi, J., Bleicher, S., and Grothe, H. (2012). Suspendable macromolecules are responsible for ice nucleation activity of birch and conifer pollen. *Atmospheric Chemistry and Physics*, 12(5):2541–2550.

Qiu, Y., Hudait, A., and Molinero, V. (2019). How Size and Aggregation of Ice-Binding Proteins Control Their Ice Nucleation Efficiency. *Journal of the American Chemical Society*, 141(18):7439–7452.

Qiu, Y., Odendahl, N., Hudait, A., Mason, R., Bertram, A. K., Paesani, F., DeMott, P. J., and Molinero, V. (2017). Ice Nucleation Efficiency of Hydroxylated Organic Surfaces Is Controlled by Their Structural Fluctuations and Mismatch to Ice. *Journal of the American Chemical Society*, 139(8):3052–3064.

Rai, R. K., Singh, V. P., and Upadhyay, A. (2017). Chapter 17 - Soil Analysis. In Rai, R. K., Singh, V. P., and Upadhyay, A., editors, *Planning and Evaluation of Irrigation Projects*, pages 505–523. Academic Press.

Redford, A. J., Bowers, R. M., Knight, R., Linhart, Y., and Fierer, N. (2010). The ecology of the phyllosphere: geographic and phylogenetic variability in the distribution of bacteria on tree leaves. *Environmental Microbiology*, 12(11):2885–2893.

Rosen, M. J. and Kunjappu, J. T. (2012). *Surfactants and Interfacial Phenomena*. John Wiley & Sons, 4th edition.

Schwidetzky, R., Ribeiro, I. d. A., Bothen, N., Backes, A., DeVries, A. L., Bonn, M., Frhlich-Nowoisky, J., Molinero, V., and Meister, K. (2023). E Pluribus Unum: Functional Aggregation Enables Biological Ice Nucleation.

Schwidetzky, R., Sudera, P., Backes, A. T., Pöschl, U., Bonn, M., Fröhlich-Nowoisky, J., and Meister, K. (2021a). Membranes Are Decisive for Maximum Freezing Efficiency of Bacterial Ice Nucleators. *The Journal of Physical Chemistry Letters*, 12(44):10783–10787.

Schwidetzky, R., Sun, Y., Fröhlich-Nowoisky, J., Kunert, A. T., Bonn, M., and Meister, K. (2021b). Ice Nucleation Activity of Perfluorinated Organic Acids. *The Journal of Physical Chemistry Letters*, 12(13):3431–3435.

Steinke, I., Funk, R., Busse, J., Iturri, A., Kirchen, S., Leue, M., Möhler, O., Schwartz, T., Schnaiter, M., Sierau, B., Toprak, E., Ullrich, R., Ulrich, A., Hoose, C., and Leisner, T. (2016). Ice nucleation activity of agricultural soil dust aerosols from Mongolia, Argentina, and Germany. *Journal of Geophysical Research: Atmospheres*, 121(22):13,559–13,576.

Steinke, I., Hiranuma, N., Funk, R., Höhler, K., Tüllmann, N., Umo, N. S., Weidler, P. G., Möhler, O., and Leisner, T. (2020). Complex plant-derived organic aerosol as ice-nucleating particles – more than the sums of their parts? *Atmospheric Chemistry and Physics*, 20(19):11387–11397.

Suski, K. J., Hill, T. C. J., Levin, E. J. T., Miller, A., DeMott, P. J., and Kreidenweis, S. M. (2018). Agricultural harvesting emissions of ice-nucleating particles. *Atmospheric Chemistry and Physics*, 18(18):13755–13771.

Tobo, Y., DeMott, P. J., Hill, T. C. J., Prenni, A. J., Swoboda-Colberg, N. G., Franc, G. D., and Kreidenweis, S. M. (2014). Organic matter matters for ice nuclei of agricultural soil origin. *Atmospheric Chemistry and Physics*, 14(16):8521–8531.

Wex, H., Augustin-Bauditz, S., Boose, Y., Budke, C., Curtius, J., Diehl, K., Dreyer, A., Frank, F., Hartmann, S., Hiranuma, N., Jantsch, E., Kanji, Z. A., Kiselev, A., Koop, T., Möhler, O., Niedermeier, D., Nillius, B., Rösch, M., Rose, D., Schmidt, C., Steinke, I., and Stratmann, F. (2015). Intercomparing

different devices for the investigation of ice nucleating particles using Snomax® as test substance. *Atmospheric Chemistry and Physics*, 15(3):1463–1485.

Wilson, T. W., Ladino, L. A., Alpert, P. A., Breckels, M. N., Brooks, I. M., Browse, J., Burrows, S. M., Carslaw, K. S., Huffman, J. A., Judd, C., Kilthau, W. P., Mason, R. H., McFiggans, G., Miller, L. A., Nájera, J. J., Polishchuk, E., Rae, S., Schiller, C. L., Si, M., Temprado, J. V., Whale, T. F., Wong, J. P. S., Wurl, O., Yakobi-Hancock, J. D., Abbatt, J. P. D., Aller, J. Y., Bertram, A. K., Knopf, D. A., and Murray, B. J. (2015). A marine biogenic source of atmospheric ice-nucleating particles. *Nature*, 525(7568):234–238.

Zieliński, R., Ikeda, S., Nomura, H., and Kato, S. (1989). Effect of temperature on micelle formation in aqueous solutions of alkyltrimethylammonium bromides. *Journal of Colloid and Interface Science*, 129(1):175–184.

4 Investigating the ice-nucleating ability of fungal plant pathogens.

4.1 Introduction

Few studies have investigated local sources of ice-nucleating particles (INP) in the UK and even fewer have focused on biological material as an important component of INP sources (O'Sullivan et al., 2018; Sanchez-Marroquin et al., 2021). As discussed in Section 1.4, agriculture is potentially a key source due to emissions of fertile soils and plant matter, as well as microorganisms associated with soils and plants (Steinke et al., 2016; Sanchez-Marroquin et al., 2021). The natural landscape of the UK consists of mostly grassland and woodland. However, 20% of the land in the UK has now been adapted into cropland (Graves et al., 2016). Despite a slight decrease in the total area of land used for agriculture in the UK, from 19.8 million ha in 1961 to 17 million ha in 2005 (Graves et al., 2016), the overall intensity in agricultural practises has increased, including the extensive use of monocultures in crop production. Crop agriculture has also grown on a global scale and intense farming practices inject large amounts of biological material, including bacteria and fungi (Lymperopoulou et al., 2016; Calderón-Ezquerro et al., 2020), potentially creating a significant source of INPs. In particular, agricultural soils may act as a reservoir for ice-nucleating biological particles, accumulating overtime and releasing large quantities into the atmosphere. This chapter aims to investigate the impact of agricultural fungal pathogens on regional INP populations by investigating the ice-nucleating (IN) abilities of two important fungal plant pathogens in the UK.

Yellow Rust (*Puccinia striiformis*) and Light Leaf Spot (*Pyrenopeziza brassicae*) spores were chosen for analysis in this study because the crops they infect (wheat, barley and oilseed rape) are common across the UK and their ice-nucleating activity is poorly understood. As discussed in Section 1.3.1, previous work has focused on common soil fungi, such as species of *Fusarium*. These studies have shown that *Fusarium* species are highly ice-active and likely proteinaceous in origin (Pouleur et al., 1992; Kunert et al., 2019; O'Sullivan et al., 2015). On the other hand, studies of other common plant fungal species, such as *Cladosporium* species, suggest that their hydrophobic properties make them poor ice nucleators (Iannone et al., 2011). Only one study has examined the ice-nucleating ability of Yellow Rust spores (Morris et al., 2013), whereas Light Leaf Spot spores have not been analysed for their ice-nucleating ability. Additionally, rust spores are known to

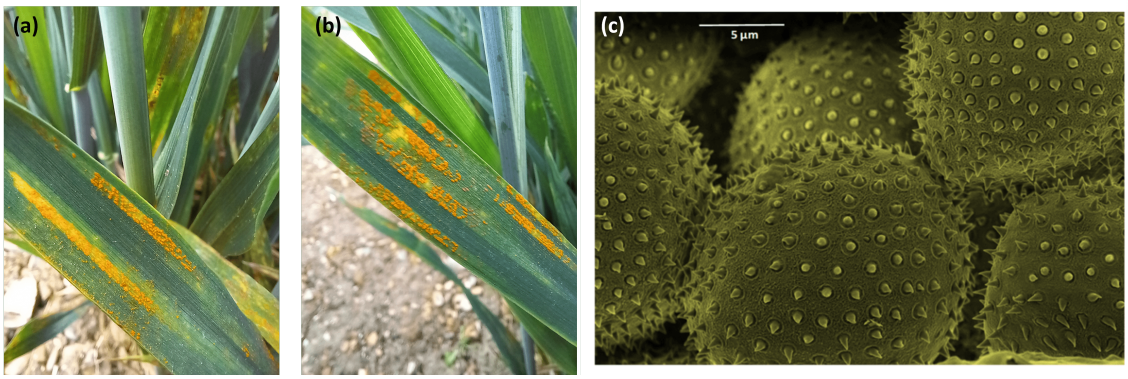

Figure 4.1: Yellow Rust (Puccinia striiformis) infection and fungal spores. *Yellow Rust infection on wheat leaves (a) and (b) showing yellow-coloured pustules that release urediniospores (photos taken by Jon West, Rothamsted Research). (c) False colour scanning electron microscopy image of Yellow Rust urediniospores taken from Bouvet et al. (2022).*

be widespread and evidence has shown they can travel at least 800 km in distance (Ingold, 1971). Therefore, the ice-nucleating ability of these spores may be important for atmospheric ice formation, transported at high concentrations to cloud-relevant altitudes by deep convection.

Yellow Rust (herein referred to as YR) is a disease which infects wheat, barley and grasses and is caused by a fungus called *Puccinia striiformis* (Bouvet et al., 2022). The YR infection appears as stripes of yellow pustules on the leaves of infected plants which release urediniospores, which are fungal spores with relatively thick, pigmented walls (Ingold, 1971), hence its other common name; stripe rust (Figure 4.1a and b). Over the winter months, YR mycelium lies dormant and can survive temperatures as low as $-5\,^{\circ}$C. As temperatures begin to increase in the spring months, YR begins to cultivate and the infection can take hold. Temperatures between 10°C and 15°C, with relative humidities of 100% in April and May are the optimal conditions for the growth and spread of this disease. YR spores are spread by wind, meaning they can disperse at large regional scales and infect large areas of cropland (Bouvet et al., 2022). YR urediniospores are spherical and approximately 22 µm in diameter with small spikes covering their surface (Figure 4.1c). The spikes help to anchor the spores once they land on the leaf of a plant (Lacey and West, 2006). The YR urediniospores also secrete mucilage, a thick secretion of compounds such as polysaccharides, glycoproteins and amino acids, to their surface (Ramadoss et al., 1985; Qu et al., 2017), the thickness of which depends on the environmental relative humidity. This mucilage production allows the spores to stick together and avoids dispersal at the wrong time (Rapilly, 1979; Geagea et al., 1999).

Light Leaf Spot (herein referred to as LLS) is a fungal pathogen which infects oilseed

Figure 4.2: Light Leaf Spot (Pyrenopeziza brassicae) infection and fungal spores. *Light Leaf Spot infection on oilseed rape leaves showing (a) early sporulation and (b) the later stage of infection with pale sites of the established infection (photos taken by Jon West, Rothamsted Research). (c) Microscope image of Light Leaf Spot conidia spores stained blue, taken by Jon West.*

rape plants and is caused by the fungus *Pyrenopeziza brassicae*. The infection appears as light spots on the leaves of the infected plant (see Figure 4.2a and b). LLS uses two different methods of dispersal; conidia spores are dispersed, usually only very short distances, by rain splash, whereas ascospores are released through wind dispersal, which usually involves long-distance transportation of fungal spores (Gilles et al., 2000). The LLS infection starts in the autumn months but tends to develop into a full infection in the spring when temperatures are between 4°C and 20°C. Warm, wet weather creates an optimal environment for the growth of LLS on plant leaves, meaning the infection tends to peak in the spring or summer months. For LLS, both the conidia spores and the ascospores are rod-shaped with an average length of around 14 µm (see Figure 4.2c), the difference between the two spores is that the conidia spores are reproduced asexually, whereas ascospores are sexually reproduced by multiple fungi.

This chapter focuses on the effects of storage length and exposure to cold stress on the ice-nucleating ability of fungal spores. Experiments with YR spores considered the impact of long-term storage and whether their ice-nucleating ability was associated with their viability. The aim of this was to establish the potential of these fungal spores to accumulate in agricultural soils, increasing their relative contribution to atmospheric INP concentrations. Previous work on ice-active bacteria identified an ageing effect where the ice-nucleating activity was lost over months of storage (Polen et al., 2016). However, the ice-nucleating ability of these ice-active bacteria is not dependent on their culturability as even cell fragments can harbour the important ice-nucleating proteins (Hartmann et al., 2022). So, here we explored if these observations hold for fungal ice-nucleating macromolecules (INMs). YR can only grow on living plants and so cannot be cultured in a lab. Therefore, the YR spores used in this study were collected directly from plants and stored dry in the fridge.

For LLS spores, we investigated whether cold stress would induce ice-nucleating activity in the fungal spores. Previous work done on ice-active bacteria from permafrost environments showed a distinct increase in ice-nucleating ability after exposure to low temperatures (4 °C and −10 °C) and that a greater cold shock caused a larger increase in ice-nucleating activity (Ponder et al., 2005). Additionally, the impact of cold stress has been shown to hold true for ice-binding proteins (Bredow and Walker, 2017). So, in this study, we investigated whether cold stress could induce ice-nucleating activity in LLS fungal spores. Bacteria species associated with fungal spores may help to contribute to their ice-nucleating activity, but so far this contribution is believed to be very small (Morris et al., 2013). In this chapter, we examined the potential contribution of ice-active bacteria species associated with fungal spores to determine the true nature of the ice-nucleating activity from fungal spores.

4.2 Experimental Methods

We started by collecting different samples of YR and LLS from different locations, some were grown in a clean laboratory environment and others were sampled directly from infected plants in the field. In this case, both field and lab-grown samples were examined to determine how different factors influence the ice-nucleating ability of the fungal spores. During the collection of field-based fungal samples, it's likely that other ice-active substances will be collected alongside the fungal spores themselves. For example, Morris et al. (2013) found highly ice-active bacteria (*P. syringae*) on urediniospores of rust collected in the field. The presence of highly ice-active bacteria, such as *P. syringae*, could enhance the ice-nucleating activity of the analysed fungal spores leading to the overestimation of the ice-nucleating ability of the fungal spores. Therefore, by growing fungal isolates in the lab, we could ensure that contamination by highly ice-active components such as bacteria could be minimised, allowing us to identify the ice-nucleating ability of the fungal spores themselves. On the other hand, natural environmental growth conditions, such as temperature and humidity, may influence the expression of ice-active substances on the surface of fungal spores. Therefore, growing isolates in controlled and sterile conditions may lead to the underestimation of their ice-nucleating ability, hence we decided to also examine samples collected from the field. Once the different samples of YR and LLS spores were collected, we created fungal suspensions with pure water to investigate the immersion freezing behaviour of the fungal spores using our droplet freezing assay technique (See

Methods).

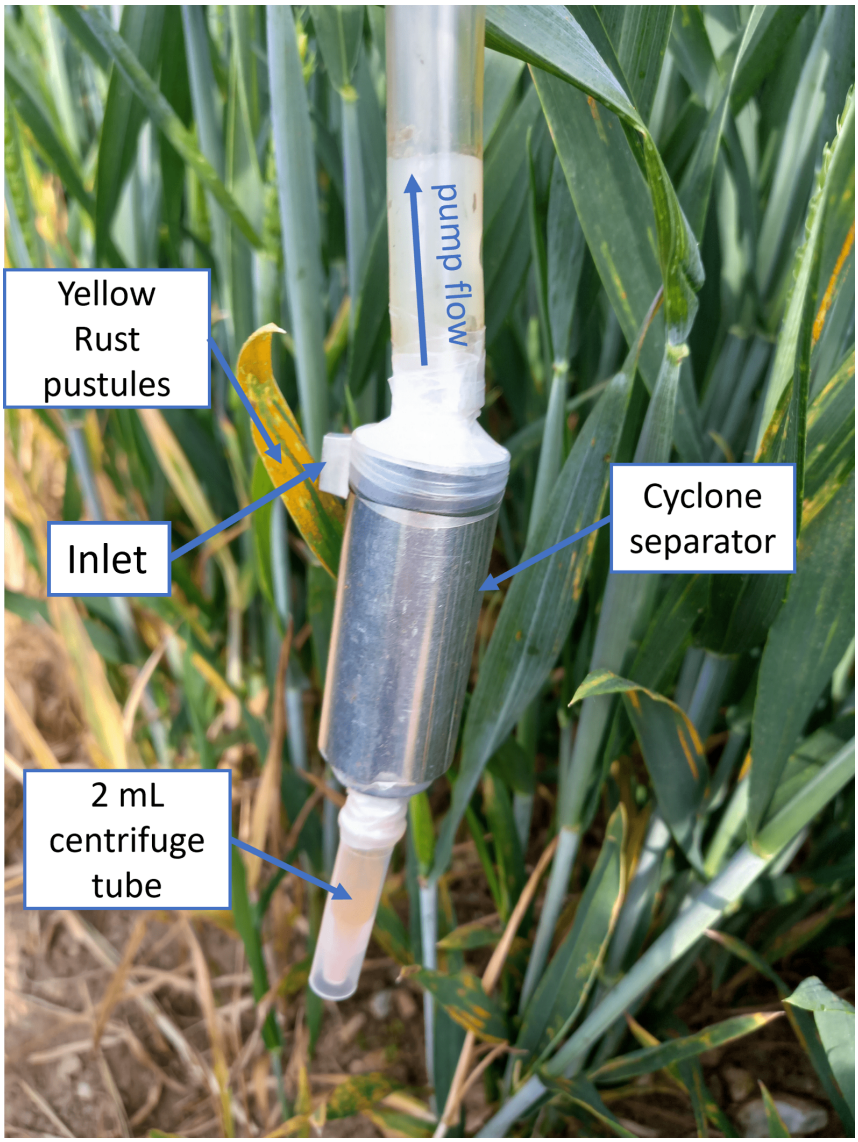

Figure 4.3: Cyclone separator used to collect YR fungal spores from pustules identified on infected wheat leaves.

4.2.1 Sample Collection and Preparation

4.2.1.1 Yellow Rust (YR)

The fungus that causes YR (*Puccinia striiformis*) cannot be isolated and grown in a lab on agar plates because the fungus does not grow past initial germination and must be grown on the leaves of plants. Therefore, YR spores were collected directly from the infected wheat leaves by Jon West. A cyclone separator (taken from a Burkard cyclone field sampler and adapted for portable use) was used to extract the fungal spores from the visible pustules on the leaves of infected plants directly into 2 mL centrifuge tubes, a similar technique was used in Macher et al. (2008). The cyclone separator was run until the 2 mL

Table 2: Overview of collected fungal samples. Including sampling date, location and coordinates.

Sample Type	Sample date	Location	Coordinates
YR spores	24th Apr 2022	Harpenden, Hertfordshire	51.8, -0.36
	25th May 2023	Harpenden, Hertfordshire	51.8, -0.39
LLS leaves	13th Apr 2023	Harlaxton, Lincolnshire	52.9, -0.68
LLS D02 isolate	30th Mar 2023	Kincaroine, Scotland	N/A*
LLS B08 isolate	7th Feb 2023	Carlow, Ireland	N/A*

*exact location unknown for data protection reasons

tubes were two-thirds full. In this study, we examined the ice-nucleating abilities of two different samples of YR spores. The first sample was collected from wheat (Fielder variety) grown in a polytunnel (a controlled but not sterile environment) at Rothamsted Research in Harpenden and inoculated with YR spores (Table 2). A sample of these YR spores was collected on the 24th of April 2022 and stored at 4 °C before analysis. The sample collected in April 2022 (herein referred to as 2022 sample) was initially analysed in October 2022, then was stored again at 4 °C until analysis was repeated in May 2023. The second sample of YR spores was collected from wheat (variety unknown) infected with YR in a field in Harpenden, Hertfordshire on the 25th of May 2023 (Table 2) and analysed immediately (herein referred to as 2023 sample). It is possible that other INP types were collected through this method alongside the YR spores. However, we assumed that the fungal spores were dominating the freezing activities of these samples. Although the sample likely contains small amounts of other material, such as leaf fragments and bacteria, the quantities of these materials are assumed to be small, and therefore have a minimal impact on the ice-nucleating analysis. DNA analysis completed after ice-nucleating analysis did not find quantifiable amounts of bacteria in our YR fungal samples.

For each sample, a small subsample of the spores was added to 200 µL of High-Performance Liquid Chromatography (HPLC) grade water and mixed into suspension with a vortex mixer for 10 seconds. The fungal spores have a high hydrophobicity, meaning that they were visibly clumping together within the suspension. Clumping of the fungal spores within the suspension could mean that the spores are not evenly distributed across the microlitre droplets, for example, some of the droplets contain large clumps of fungal spores whereas others contain only one or two spores. We need the spores to be evenly distributed across the freezing assay to be able to see the full spectra of freezing. We found that by leaving the suspensions for 1 hour and mixing for a few more seconds on the vortex mixer, the clumping was visibly reduced.

4.2.1.2 Light Leaf Spot (LLS)

Isolates of LLS (*Pyrenopeziza brassicae*) were obtained from two different locations by a third party and sent to Rothamsted Research for analysis (Table 2). The first isolate (D02) was collected from Kincaroine in Scotland, where it was found growing on the Crome oilseed rape variety and the second isolate (B08) was collected from Carlow, Ireland, where it was found growing on the Ergo oilseed rape variety (further details of the collection of these isolates are unknown due to data protection). Colonies of LLS were grown from the isolates on 3% malt extract agar (MEA) in plastic Petri dishes by Kevin King. Each Petri dish was sealed with parafilm and incubated for 45 days at 18 °C before further analysis was carried out. Examples of the incubated isolates are shown in Figure 4.4. To subculture LLS, a small square of mycelium from the leading edge of the colony was spread onto the 3% MEA plate in a sterile-flow cabinet. After incubation, some of the Petri dishes were placed in the freezer at −20 °C overnight for 12 hours to investigate the impact of exposure to cold stress on the ice-nucleating ability of the fungal spores. After being exposed to −20 °C for 12 hours, the isolates were allowed to thaw and then left to incubate for another 2 days before extraction, to determine if spores grown after exposure to cold stress were more ice-nucleating active.

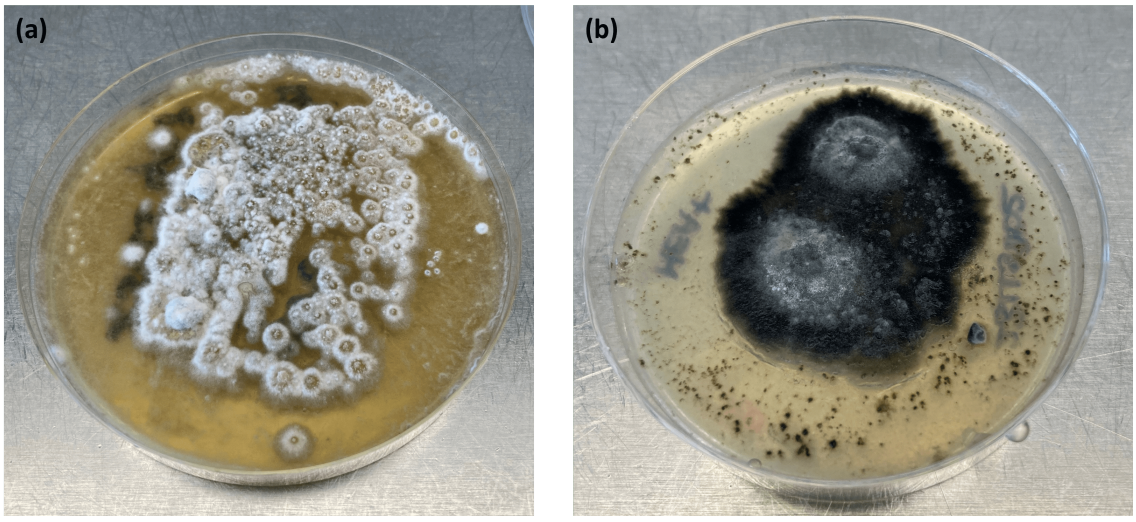

Figure 4.4: Two examples of the cultures of LLS grown in the lab (a) and (b).

To harvest the fungal spores from the agar plates, 1 mL of HPLC-grade water was pipetted onto the fungal culture. A plastic rod was used to gently agitate the culture and remove the spores from the surface of the agar. Then the suspension was pipetted from the Petri dish and filtered through some miracloth to remove any mycelium that may have been extracted, leaving a pure spore suspension. This process was completed for each extracted fungal isolate and is a similar process to that used by Fröhlich-Nowoisky et al.

(2015). On the 21st of April 2023, we harvested four fungal cultures; three of the D02 isolates (two of which had been exposed to subzero temperatures) and one B08 isolate. On the 9th of May 2023, we harvested four more fungal cultures; two of the D02 isolates and two of the B08 isolates where one of each had been exposed to subzero temperatures.

Leaves from oilseed rape crops which were infected with LLS (strain unknown) were collected by Jon West from a field near Harlaxton, Lincolnshire on 13th April 2023. The leaves were frozen until they could be analysed on 5th May 2023. Each leaf was placed into 10 mL of HPLC-grade water in a glass beaker. The leaf was left to soak for about two minutes and then the glass beaker was gently shaken to agitate the surface of the leaves and remove the spores until the suspension was visibly cloudy from the presence of fungal spores. We assumed that other ice-active substances, in addition to the LLS spores, would be washed into suspension during this process. To consider this potential contamination with our analysis, we wanted to compare the LLS leaf washings with washings from an uninfected oilseed rape leaf. However, the LLS disease starts very indistinct and can be hard to identify on leaves of oilseed rape (see Figure 4.2a), therefore it was difficult to find a leaf that was free from any fungal infections to use to assess the ice-nucleating activity washed from oilseed rape without LLS. Therefore, our sample freezing temperatures were compared to pure HPLC-grade water blanks instead of using handling blanks.

4.2.1.3 Isolation of Bacteria from LLS Field Samples

We also investigated a leaf-washed sample of LLS collected from the field in 1996, which had been kept in a freezer at $-20\,^{\circ}\mathrm{C}$ for 27 years. DNA extraction and PCR amplification techniques as described by Nicolaisen et al. (2017) were used to identify species of bacteria within the 1996 leaf-washed sample and were carried out by Gail Canning. After DNA extraction, four identified bacteria species were isolated and cultured on 3% potato dextrose agar (PDA) plates (Figure 4.5). Once grown, the bacteria was extracted from the agar plates by scrapping a small amount off the top using a sterile plastic loop and mixing with 200 µm of HPLC-grade water. The bacteria suspensions were then tested for their ice-nucleating ability.

4.2.1.4 Spore Concentration Calculations

The concentration of spores in each spore suspension was quantified using an Improved Neubauer Haemocytometer (Weber Scientific International, Lancing, UK) with an Olympus BH-2 laboratory microscope (using a times 10 eyepiece and a times 20 objective lens

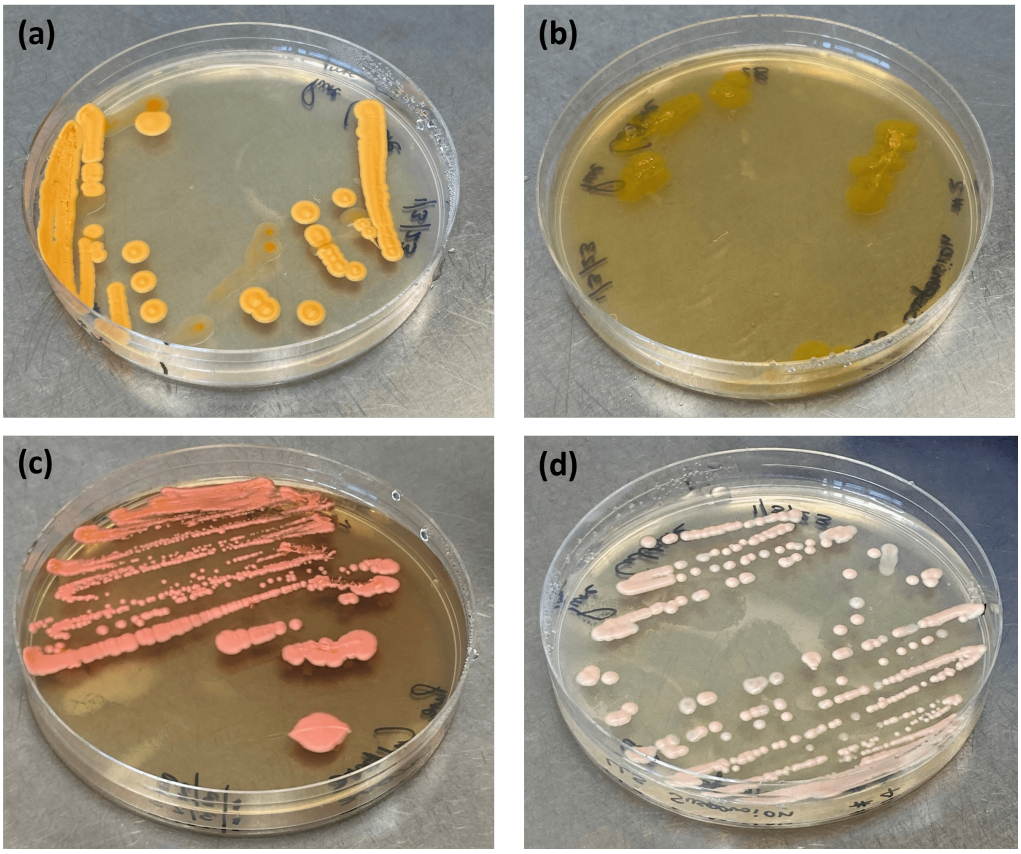

Figure 4.5: Cultures of bacteria isolated from the 1996 field sample of LLS infected leaves. *(a) No. 2 Yellow, (b) No. 2 Orange, (c) No. 3 and (d) No. 4.*

for counting spores). The haemocytometer is a counting chamber originally designed for counting blood cells (Waller et al., 1998). The counting chamber of the haemocytometer is designed so that it is exactly 0.1 mm deep and has grids ruled onto the top to portion out the chamber into 1 mm squares (Figure 4.6). The central 1 mm grid is subdivided into 25 smaller squares, which are each subdivided again into 16 even smaller squares (Waller et al., 1998). This design means that we can determine the average number of spores in one 0.0025 mm^2 grid cell of the haemocytometer and then scale up to determine the number of fungal spores in 1 mL of the fungal suspension. Since the YR and LLS spores were relatively large, at 22 µm and 14 µm respectively, and the concentrations of our fungal spore suspensions were relatively high, we counted five of the 0.0025 mm^2 grids and calculated an average count for one of those grids. We then multiplied the calculated average number of spores by 250,000 to calculate the average concentration of spores per cm^3 for the fungal spore suspension.

This estimation works on the assumption that the fungal spores are evenly distributed throughout the fungal spore suspension and that the concentration of sample used for the count is representative of the whole suspension. The YR spores were very hydrophobic and

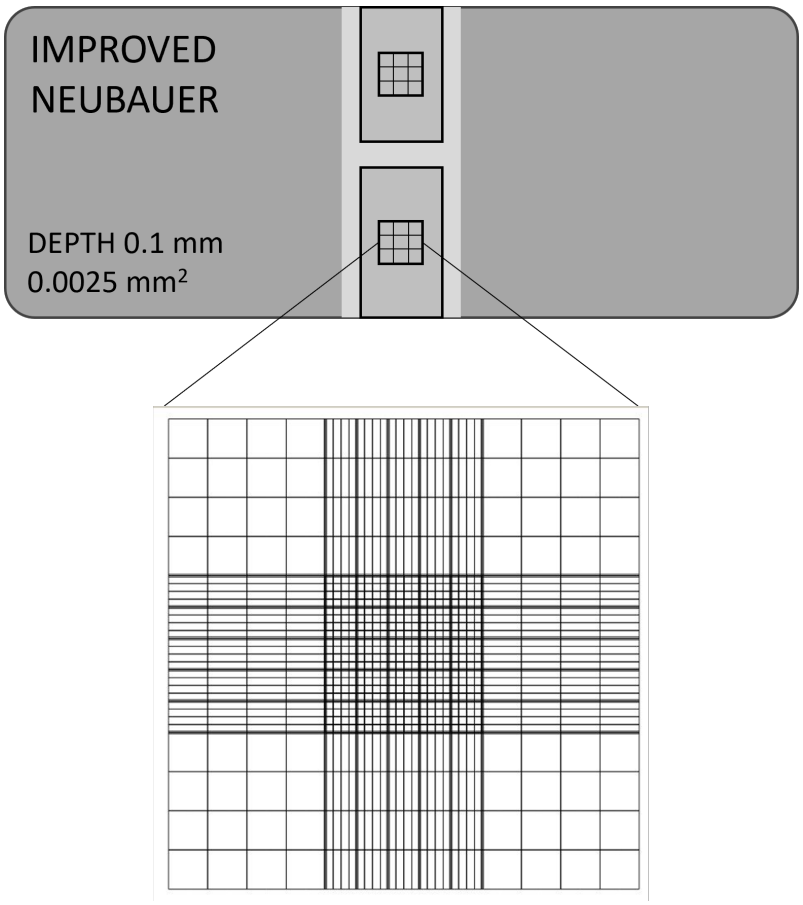

Figure 4.6: Schematic of the Improved Neubauer Haemocytometer used for estimating the concentration of fungal spores within each fungal spore suspension. *Showing the lined grids of the counting chamber, designed to break down the chamber and make the counting more efficient.*

although they seemed to be evenly distributed throughout the suspension, we noticed that the spores themselves were adhering to the inside of the pipette tips when pipetting out droplets for the freezing analysis. So, we decided to calculate the average number of spores per droplet after the freezing analysis to verify the concentration of spores in the analysed droplets. After the droplets had been frozen, they were allowed to thaw before being placed under a microscope to examine the level of mixing of spores within the droplets. First, we verified that the fungal spores were evenly distributed throughout the droplets (Figure 4.7). Then, the average number of spores per droplet was calculated by selecting five droplets at random and counting the total number of spores in each droplet (Figure 4.7).

4.2.2 Immersion Freezing Analysis

Droplet freezing experiments to measure the ice-nucleating activity of our spore suspensions were carried out using the Microlitre Nucleation by Immersed Particle Instrument

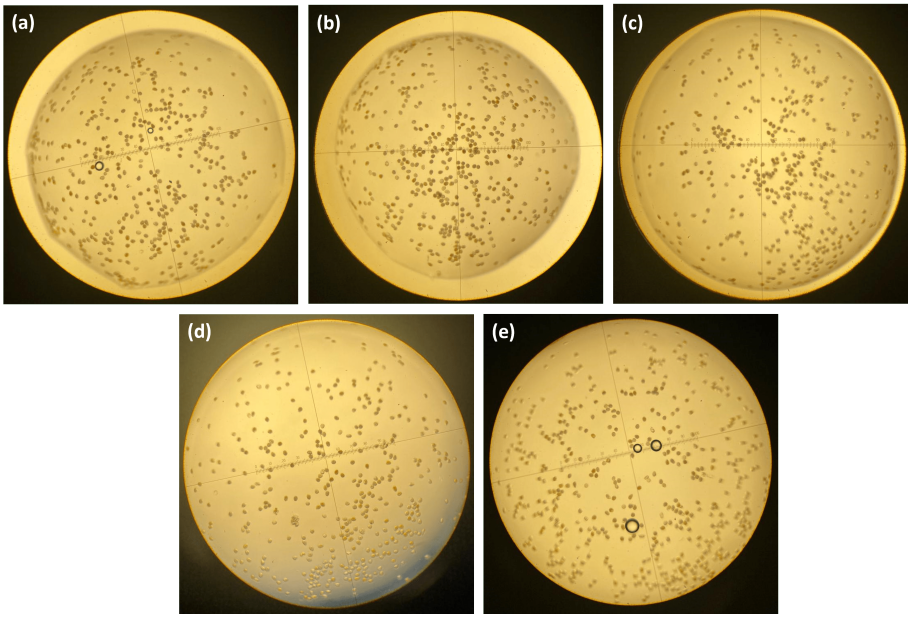

Figure 4.7: Microscope images of 1 µL ***droplets of YR spore suspensions taken after freezing assay (a) to (e).***

(µL-NIPI), as described in Section 2.1.1. Due to the portability of the Peltier cold stage, we chose this method for the droplet freezing analysis of the extracted fungal suspensions. As detailed in Section 2.2, the temperature at which each droplet froze was used to determine the fraction of droplets frozen as a function of temperature, or $f_{\mathrm{ice}}(T)$, for each fungal spore suspension (Eq. 11). The $f_{\mathrm{ice}}(T)$ was then used to calculate the total number of ice-active sites per spore, n_{n}, where C_{n} was the total number of fungal spores per droplet (Eq. 16).

To estimate the ice-active site density per mass of fungal spores, or n_{m} (in g^{-1}), for the YR samples, we used the average diameter of 22 µm and an average mass density of 1 $\mathrm{g\,cm}^{-3}$ (Lacey and West, 2006) to estimate the total mass of one fungal spore. Multiplying the mass of one fungal spore by the number concentration of spores per cubic centimetre, provided an estimate for the total mass concentration of spores in the analysed fungal suspension, or C_{m} (in $\mathrm{g\,cm}^{-3}$). This C_{m} and the volume of the droplet, V_{d} (in cm^{-3}), were then used to calculate n_{m} (as shown in Eq. 14).

4.2.3 Agar Analysis

It was important to test whether the MEA itself contributed to the ice-nucleating activity of our LLS fungal extracts. Agar consists of polysaccharides extracted from the cell walls of red algae species. Marine algae have been shown previously to be sources of ice-nucleating activity in sea surface aerosols (SSAs), meaning that the MEA is likely to

contain this ice-nucleating ability (Knopf et al., 2011; Wolf et al., 2019). To test if the MEA contributed to the ice-nucleating activity of our fungal extracts, we used a blank 3% MEA agar plate and completed the full extraction technique and ice-nucleating analysis without any fungal culture being added. To do this, 1 mL of HPLC-grade water was pipetted onto a blank agar plate and gently rubbed with a sterile plastic rod. The water was then carefully pipetted off the plate and filtered through miracloth. To examine the effect of freezing on the possible ice-nucleating activity of agar, two blank agar plates were also left in the freezer at $-20\,^{\circ}\mathrm{C}$ overnight, and the extracted process was repeated to see if any change in the ice-nucleating activity was observed. The freezing activity of the agar extracted solutions was compared with pure water which had been passed through the miracloth, to test if any observed contamination was attributable to the miracloth.

4.3 Results and Discussion

4.3.1 Yellow Rust (YR)

The YR fungal spores displayed significant ice-nucleating activity above the background (Figure 4.8). For the concentrations of fungal spore suspension examined here, the majority of freezing occurred below $-15\,^{\circ}\mathrm{C}$, with some sporadic freezing events occurring between $-10\,^{\circ}\mathrm{C}$ and $-15\,^{\circ}\mathrm{C}$. The average freezing temperature (T_{50}) of the undiluted fungal spore suspensions from the 2022 sample was $-20.3\,^{\circ}\mathrm{C}$, whereas the T_{50} for the spore suspensions from the 2023 sample was $-21.2\,^{\circ}\mathrm{C}$. Therefore, we observed a small amount of natural variation between the different collected samples, which was expected as the two samples were collected a year apart with different environmental growth conditions and in different crop fields. Additionally, the observed freezing temperatures suggest that the YR spores have a lower ice-nucleating activity compared to other biogenic material, in particular, proteinaceous INP which tends to nucleate ice at temperatures above $-10\,^{\circ}\mathrm{C}$. However, we would need to normalise the freezing to the concentration of spores in the analysed suspensions to compare to the ice-nucleating activity of other biogenic substances. Two dilutions of the original 2022 sample suspension were prepared and examined in May 2023. These dilutions were used to determine the full spread of the INP spectra for the 2022 sample and were prepared as a factor ten dilution each time. These dilutions are also shown to nucleate ice above the background freezing (Figure 4.8).

The first part of our analysis was to verify if the ice-nucleating activity of the YR spore dilutions scaled evenly as a function of temperature. We calculated the total number of ice-

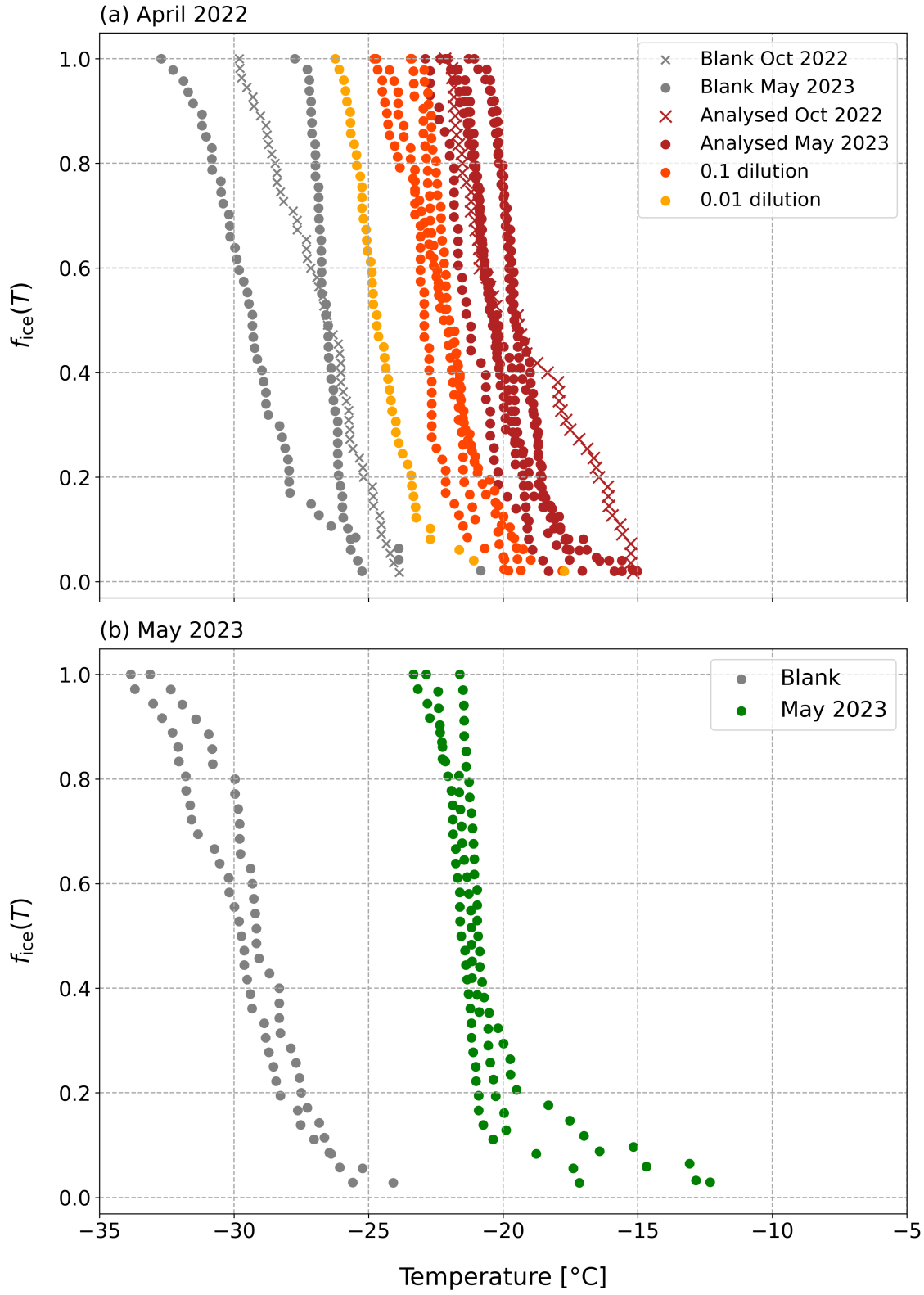

Figure 4.8: Fraction frozen ($f_{ice}(T)$) curves as a function of temperature for the YR spore suspensions. *(a) From the sample collected in April 2022, analysed in October 2022 (blue) and again in May 2023 (yellow). (b) From the sample collected in May 2023.*

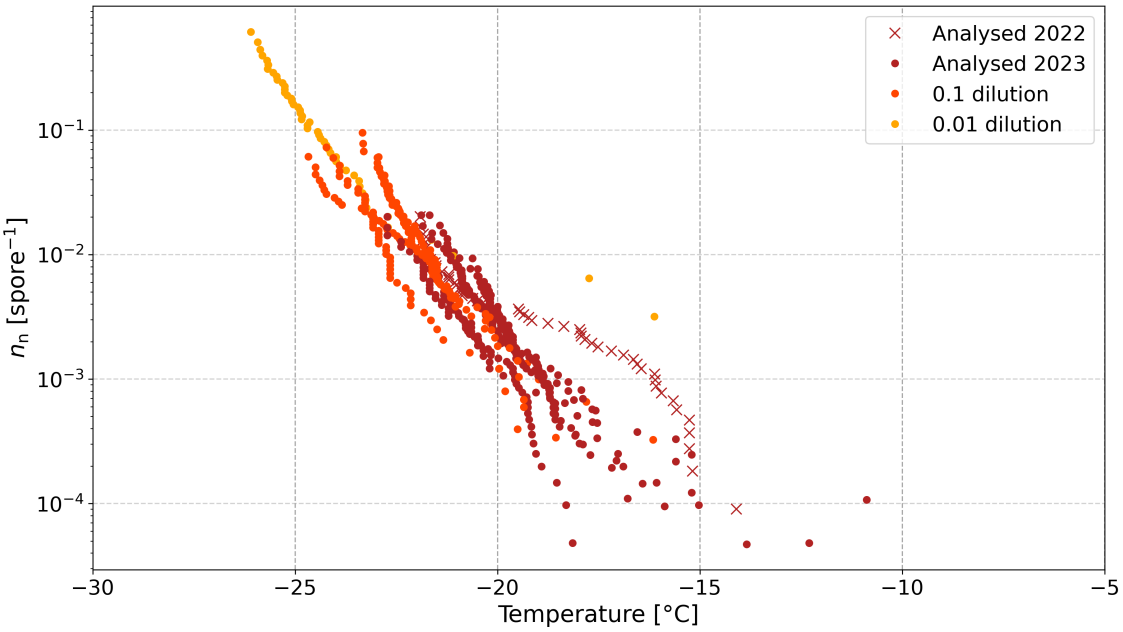

Figure 4.9: Total number of ice-active sites per spore (n_n) as a function of temperature for the YR spore suspension and dilutions collected in April 2022.

active sites per spore (n_n) from the estimated concentrations of our YR spore suspensions and then compared the ice-nucleating activity of the 2022 sample, which was analysed both in October 2022 and May 2023 (Figure 4.9). The dilution series which were analysed in May 2023 align well as a function of temperature. We expected to see a small degree of natural variability between the different dilutions and analysis runs since the ice-nucleating activity of individual spores is likely to vary significantly. Natural variation between fungal spores will impact the expression of ice-active substances at the surface of the spore and depends on growth conditions and genetic variations. The number of ice-active sites per spore continues to increase as we expect with decreasing freezing temperatures and that aggregation was likely not impacting the ice-nucleating ability of these spores (referring back to Section 3).

We also examined the impact of the length of storage on the ice-nucleating ability of the YR spores (Figure 4.9). Long-term storage of biological INP substances can either enhance or inhibit their ice-nucleating abilities, depending on the composition or source of the INP (Polen et al., 2016; Beall et al., 2020). To see how the length of storage impacts the ice-nucleating activity of YR spores, we completed two separate freezing analyses on the 2022 sample. We first analysed the ice-nucleating activity of the 2022 sample in October 2022, after five months of storage in a fridge at 4 °C. The 2022 sample was then analysed again in May 2023, after 13 months of storage at the same temperature. At temperatures below −20 °C, there was little to no change in the ice-nucleating activity

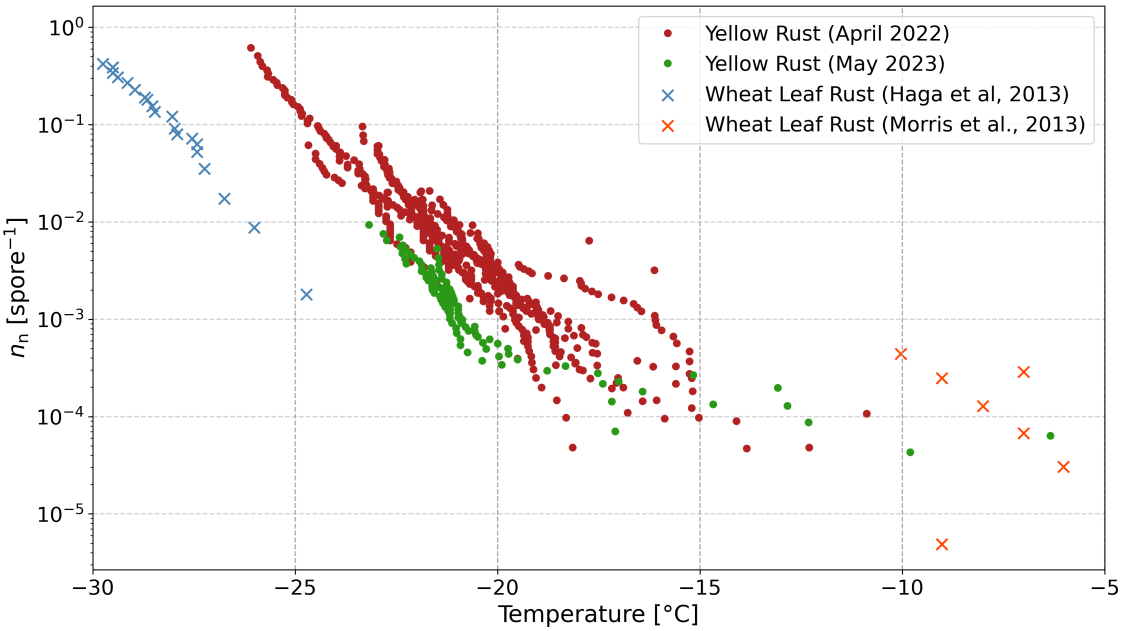

Figure 4.10: Total number of ice-active sites per spore (n_n) as a function of temperature for the rust spore suspensions and dilutions. *Showing both YR spores from this study collected in April 2022 and May 2023 and, for comparison, Wheat Leaf Rust spores analysed by Haga et al. (2013) and Morris et al. (2013).*

of the 2022 sample between October 2022 and May 2023. This observation suggests that long-term storage has little impact on the ice-nucleating activity of YR spores at these temperatures. However, the ice-nucleating activity between −15 °C and −20 °C decreased over this time by about 1.5×10^{-3} spore^{-1}. This observed change in the total number of ice-active sites per spore between −15 °C and −20 °C could indicate a loss of ice-nucleating activity due to the extra 8 months of storage, which is consistent with previous studies which found that larger aggregates, tending to freeze at higher temperatures, are more sensitive to the loss of ice-nucleating activity with storage length (Polen et al., 2016; Beall et al., 2020). However, it is worth noting that the analysis of the 2022 sample from October 2022 contains only one sample run, due to time constraints. As we would expect a large variation in the ice-nucleating activity of different spores within the sample, particularly at higher freezing temperatures. Therefore, we were unable to rule out natural variability as the cause of this observed difference.

We also analysed two different samples of YR spores, collected a year apart to better understand the impact of long-term storage on their ice-nucleating activity (Figure 4.10). Since the 2023 sample was collected and analysed on the same day, we expected the ice-nucleating activity of this sample to be higher than the 2022 sample, which was only analysed for the first time 5 months after collection. Therefore, we anticipated that the ice-nucleating activity of a fresh sample of YR spores would be higher since storage has

not yet degraded its activity. However, we observed that the ice-nucleating activity of the 2023 sample was, in fact, slightly lower than that of the 2022 sample. At −20 °C, the full spread of variation between the different samples spans an order of magnitude with much wider variation in the 2022 sample compared to the 2023 sample. This observation suggests that natural variability within samples of YR spores may play a bigger role in the ice-nucleating activity than storage length. Growth conditions, including temperature, humidity and moisture availability will have impacted the expression of ice-active material within the two different samples, and may be leading to the observed differences in ice-nucleating activity. The two samples were collected from different locations, with the 2023 sample from field-grown wheat and the 2022 sample from polytunnel-grown wheat, and were likely from different varieties of wheat and *P. striiformis*. Therefore, it is likely that these differences are contributing more significantly to the observed difference in ice-nucleating activity, rather than the length of storage of the sample. For example, it could be that in the slightly more controlled environment of the polytunnel, more mucilage was produced on the spores in the 2022 sample. The increased production of mucilage could result in the release of more INMs to the surface of the fungal spores, increasing their ice-nucleating activity per spore. Furthermore, the loss of activity observed in the 2022 sample was only seen for freezing temperatures above −20 °C, however, there is very little ice-nucleating activity above −20 °C at all in the 2023 sample. This observation suggests that the ice-nucleating activity of YR spores above −20 °C was more sensitive to long-term storage but that natural variability across different YR samples means that warmer temperature freezing was not always present.

Previous work by Morris et al. (2013) focused on the ice nucleation of fungal spores as a mechanism for the dispersal of fungal species in the environment. Before reanalysing the 2022 sample, we attempted to use some of the spores to infect a new wheat plant to test the viability of the spores. We were unable to induce spore germination of the YR spores, suggesting the spores were no longer viable. This potential loss of viability was not associated with a loss of ice-nucleating activity in these spores, suggesting that the ice-nucleating ability of the YR fungal spores was not associated with their viability. This observation may be in contrast with the theory presented by Morris et al. (2013) since the spores would need to maintain their viability for their ice-nucleating activity to be a mechanism of dispersal. Instead, this observation indicates that the ice-nucleating ability of YR spores was attributable to a substance with another function whose ice-

nucleating activity is coincidental. However, it is worth considering other reasons we were unable to induce germination with the YR spores, such as the environmental conditions of inoculation, and the spores may have remained viable during their time stored (Ingold, 1971).

We compared the total number of ice-active sites per spore for our YR spore suspensions with data from the literature (Figure 4.10). Since the ice-nucleating activity of YR spores have not previously been examined in detail, we compared its activity to a similar fungal species, *P. triticina* (Haga et al., 2013; Morris et al., 2013). Both of these fungal species are part of the same genus of plant pathogens, known as rust fungus. Therefore, the ice-nucleating activity of our collected YR spores, both the 2022 sample and the 2023 sample, were compared with the ice-nucleating activity of wheat leaf rust spores (Haga et al., 2013; Morris et al., 2013), to compare the ice-nucleating activity of different rust species (Figure 4.10). In general, the ice-nucleating activity of our YR spores spans the freezing temperature range between the activity identified by Haga et al. (2013) and Morris et al. (2013). At $-25\,^{\circ}\mathrm{C}$, the ice-nucleating activity of the YR spores from our 2022 sample is up to 2 orders of magnitude higher than that of Haga et al. (2013). The Morris et al. (2013) data, on the other hand, spans across the high temperature freezing and seems to overlap with some of the sporadic freezing observed in our YR samples. However, we cannot rule out contamination as the cause of this sporadic freezing in our YR samples, making comparison to Morris et al. (2013) very difficult.

We also wanted to compare the ice-nucleating activity of our YR samples with that of *Fusarium*, a fungi known to be an efficient ice nucleator. Literature values have estimated the ice-active mass site density of *Fusarium* species (O'Sullivan et al., 2015), so we estimated the ice-active mass site density (n_{m}) for our YR spore suspensions using the average density and diameter of YR spores (Figure 4.11). We were then able to compare this ice-nucleating activity with the ice-active mass site density of *Fusarium avenaceum*, as analysed by O'Sullivan et al. (2015). The ice-nucleating activity of YR spores was up to 5 orders of magnitude lower than the ice-nucleating activity of *Fusarium* (Figure 4.11). We also observed a distinct difference in the freezing behaviour of these two fungal species. The majority of the freezing activity of *Fusarium avenaceum* is above $-10\,^{\circ}\mathrm{C}$ and then the cumulative ice-nucleating activity of *Fusarium* plateaus at an ice-active mass site density of around 10^9 g^{-1}. However, the ice-nucleating activity of YR fungal spores occurs mostly below $-15\,^{\circ}\mathrm{C}$ with some sporadic freezing occurring above this temperature.

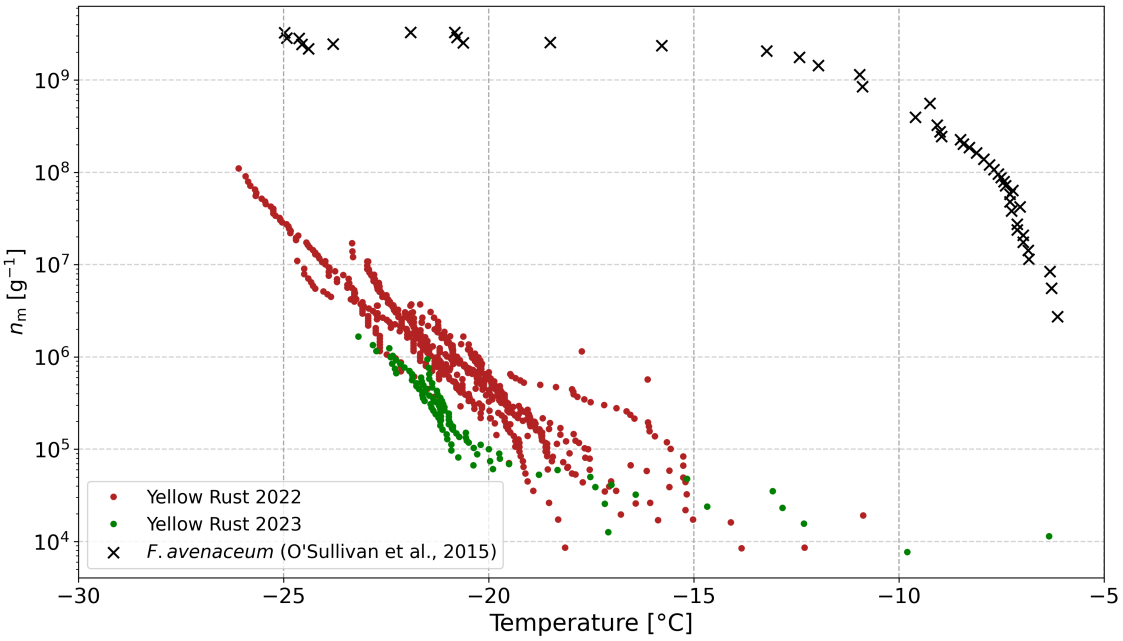

Figure 4.11: Ice-active mass site density (n_m) as a function of temperature for fungal spores. *Showing both YR spores examined in this study and the mycelium of Fusarium avenaceum analysed by O'Sullivan et al. (2015).*

These results suggest that the nature of the macromolecules responsible for freezing in *Fusarium* samples is different to the nature of the macromolecules responsible for the freezing activity of YR spores. *Fusarium* INMs are known to be proteinaceous, since heat tests of soil fungus species have shown a decrease in ice-nucleating activity most likely due to the denaturing of proteins (Pouleur et al., 1992; Fröhlich-Nowoisky et al., 2015). However, the ice-nucleating activity of rust spores may be attributable to other ice-nucleating substances. Morris et al. (2013) found that the ice-nucleating activity of rust spores remained unaffected by treatment with lysosome, an enzyme which digests proteins, indicating that polysaccharides are responsible for the ice-nucleating activity of rust spores. Given that mucilage released to the surface of fungal spores is often composed of polysaccharides and glycoproteins, these substances may be responsible for the observed ice-nucleating activity in YR spores. Also, we can apply knowledge from classical nucleation theory (CNT; Section 1.2.2) to determine the size of the macromolecules involved in the ice nucleation for each fungal species since the critical ice embryo size is temperature-dependent (Seinfeld and Pandis, 2016). The high-temperature freezing observed for *Fusarium avenaceum* is likely associated with large aggregates of macromolecules since larger ice embryos have higher nucleation rates. On the other hand, the freezing activity of the YR spores occurs at lower temperatures suggesting the INMs associated with freezing in YR spores are made up of smaller macromolecular aggregates which nucleate at a slower rate.

4.3.2 Light Leaf Spot (LLS)

4.3.2.1 Lab-Grown Cultures

First, we investigated the ice-nucleating activity of LLS spores extracted from lab-grown cultures of LLS. The range of freezing observed in the malt extract agar handling blanks was much larger than the usual range for handling blanks (Figure 4.12a). This meant that the freezing for our LLS spore suspensions was within the range of our contaminated blanks (Figure 4.12b). Since the freezing activity of the LLS spores was indistinguishable from that of the baseline, we can confirm that the ice-nucleating ability of these spores is not higher than the freezing observed within our handling blanks of this study. We also exposed some of the fungal isolates to subzero temperatures to determine if cold stress could trigger the release of INMs. The fungal isolates that were exposed to subzero temperatures were also extracted and analysed for their ice-nucleating ability, however, the freezing was still within the range of the background handling blank (Figure 4.12b). Therefore, despite the exposure to subzero temperatures, the ice-nucleating ability of the LLS fungal spores remained below our limit of detection.

4.3.2.2 Field Samples

We also examined the ice-nucleating ability of LLS spores extracted directly from infected oilseed rape crops. Despite seeing no evidence of ice-nucleating activity in LLS spores grown in the lab, we wanted to investigate if these spores express INMs when exposed to environmental factors. The fungal spores were removed from the oilseed rape leaves by washing into the suspension. The leaf-washing suspensions were then tested for their ice-nucleating ability, which was shown to be higher than the lab-grown fungal suspensions (Figure 4.13). We also tested the ice-nucleating activity of an old leaf washing from 1996, which had been left stored in the freezer. All of the leaf wash samples collected in 2023 had a similar pattern of freezing behaviour. However, we observed a distinct natural variation between the different sampled leaves, with a spread in T_{50} of 1.3 °C. Given that many different factors could be impacting the ice-nucleating activity of these leaf-washed samples, such as levels of contamination, concentration of spores washed into suspension and specific growth conditions, we concluded that this level of natural variation seemed reasonable for these samples. For the 1996 sample, only one freezing analysis run was completed due to time constraints, but we were still able to compare this sample with our 2023 samples. We observed that there was more of a tail of freezing for the 1996 sample at

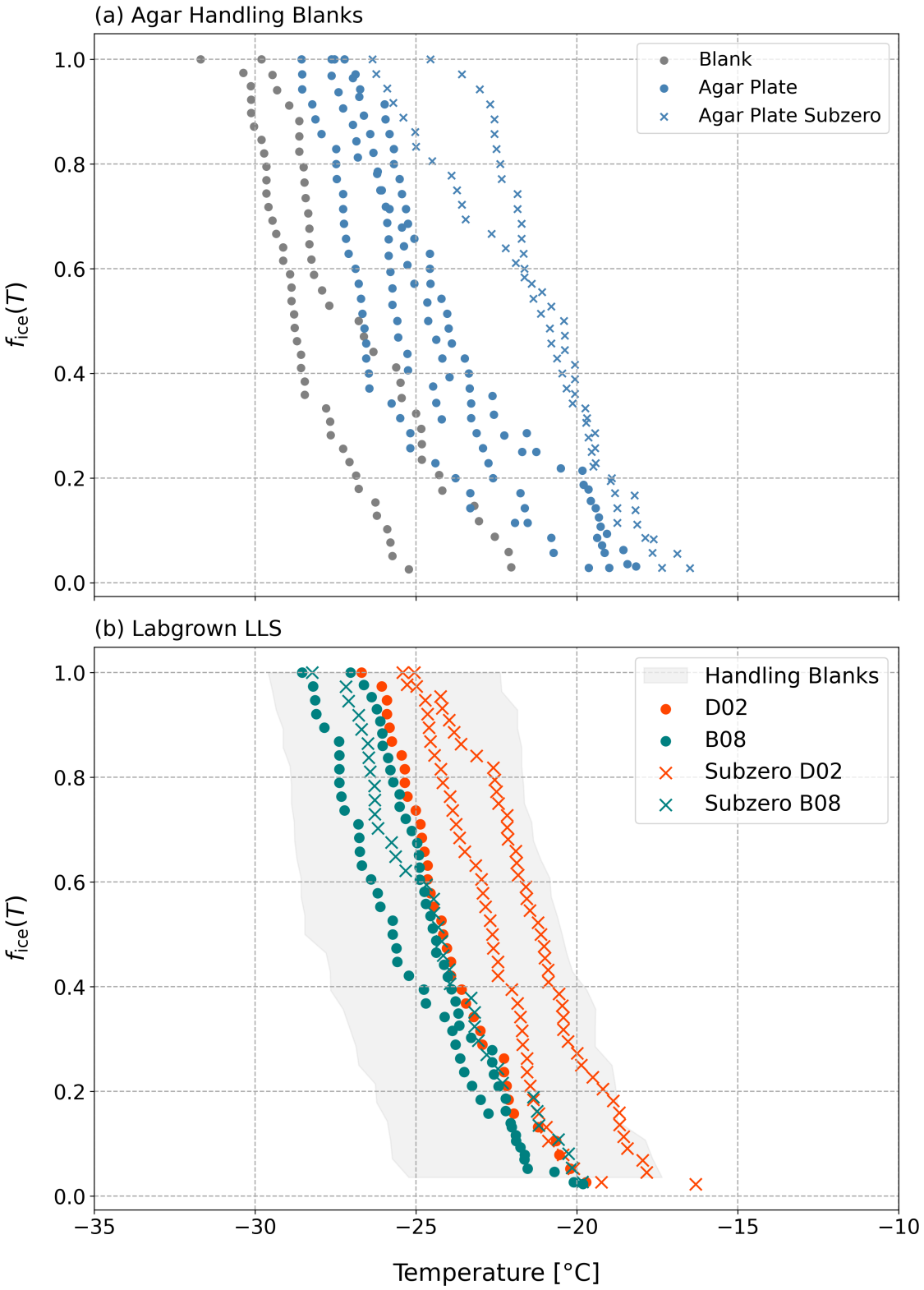

Figure 4.12: Fraction frozen ($f_{ice}(T)$) curves as a function of temperature for lab-grown analysis *including (a) agar plate handling blanks and (b) the two different isolates of LLS.*

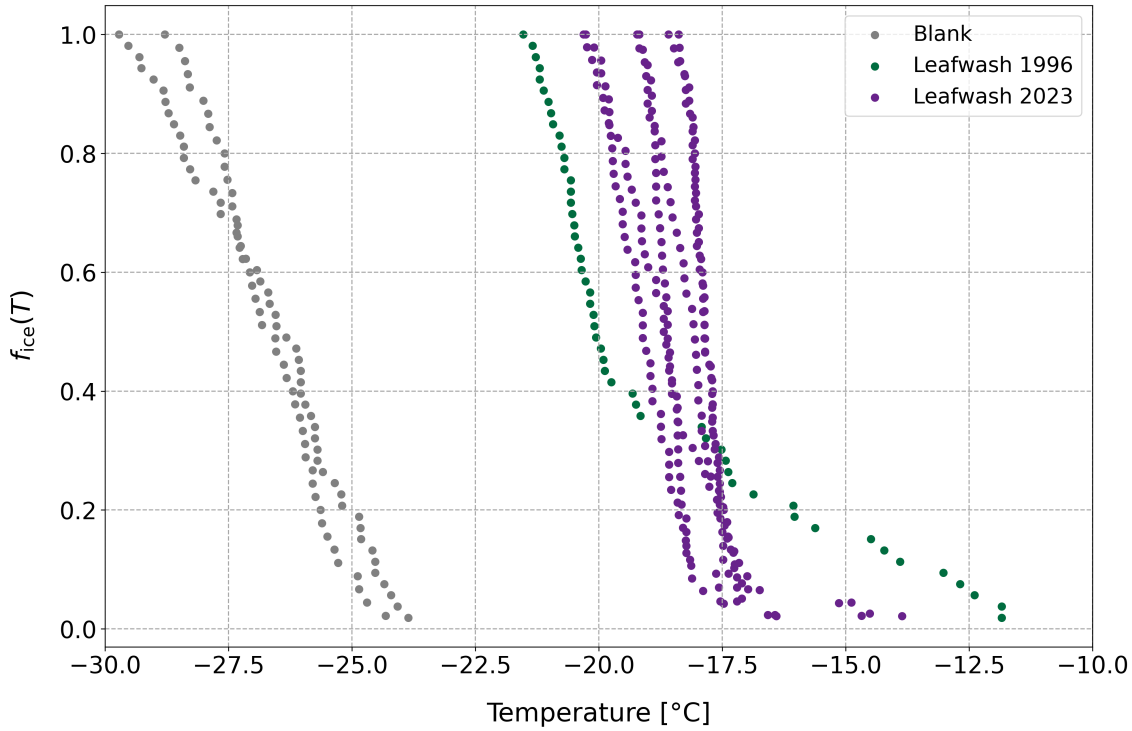

Figure 4.13: Fraction frozen ($f_{ice}(T)$) curves as a function of temperature for LLS spore suspensions from field samples collected in 1996 and 2023.

greater freezing temperatures and that the majority of freezing occurs at around −20 °C. We hypothesise that the higher freezing temperatures observed in the 1996 sample were due to a greater level of contamination from other sources compared to our samples collected in 2023.

The freezing activity of the 1996 sample remained relatively high despite it being stored in a freezer for 27 years. Although we have no previous measurements of the ice-nucleating activity of this sample, its ice-nucleating activity has not been completely lost over this time. Previous work by Beall et al. (2020) suggests that the length of storage of samples at room temperature has little impact on their INP concentrations, concluding that the majority of changes to INP concentrations occur in the first 24 hours of storage or upon freezing the sample. They also suggest that warm-temperature INPs, which are more sensitive to heat treatment, are also more sensitive to storage (Beall et al., 2020). Therefore the ice-nucleating activity of the 1996 sample containing freezing above −10 °C originally, but that activity may have since been lost due to freezing and storage.

The freezing activity from the LLS leaf washings was normalised by the average number of ice-active sites per spore so comparisons could be made to other fungal species (Figure 4.14). At −20 °C, the number of ice-active sites per spore varied across 2 orders of magnitude (3×10^{-4} spore^{-1} to 3×10^{-2} spore^{-1}) across the different spore types, with

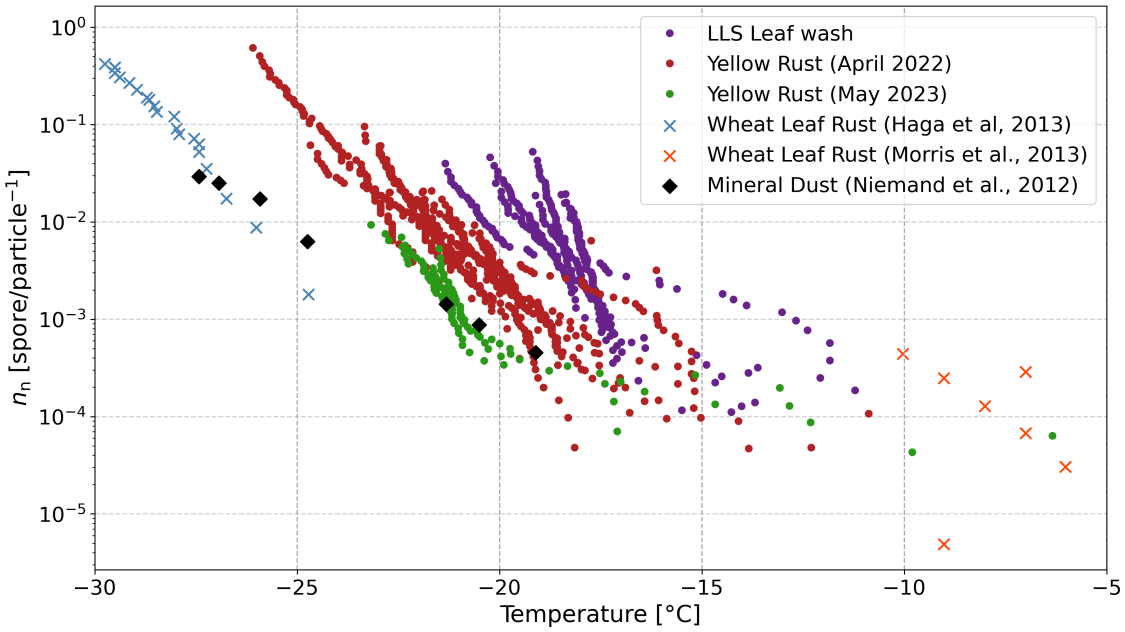

Figure 4.14: Total number of ice-active sites per spore (n_n) as a function of temperature for LLS spore suspensions extracted from oilseed rape leaves. *For comparison, the total number of ice-active sites per spore (n_n) for YR (this study) and wheat leaf rust (Haga et al., 2013; Morris et al., 2013)*

the LLS leaf washings being at the upper end of this range. Despite this large variation, the ice-nucleating activity of the LLS leaf wash and the YR collected spores both fit well with the observed range of freezing observed in other rust species (Haga et al., 2013; Morris et al., 2013). To compare the freezing activity of rust spores with that of mineral dust, Haga et al. (2013) calculated the average ice-active site density per particle from data collected by Niemand et al. (2012) using the average diameter measured by Niemand and others and assuming the mineral dust particles were spherical (Haga et al., 2013). This converted data from Haga et al. (2013) is plotted in Figure 4.14 so we can compare the ice-nucleating activity of our YR and LLS samples with the ice-nucleating activity of mineral dust. The ice-nucleating ability of the YR and LLS spores analysed in this study seems to be up to an order of magnitude higher than that of mineral dust. However, the atmospheric concentrations of mineral dust in the atmosphere are known to dominate ice nucleation in mixed-phase clouds due to high concentrations of mineral dust aerosols, therefore, mineral dust likely outcompetes the fungal spores analysed here as INPs in the atmosphere.

Since there was no evidence of any ice-nucleating activity in the lab-grown LLS samples, but a distinct freezing activity above the blank for the field-collected samples, we investigated whether the ice-nucleating ability of the LLS fungal spores could be attributed to bacteria associated with the spores or collected with the leaf washings. Bacterial species

were isolated from the leaf washing which had been collected in 1996. These bacteria were cultured on agar, extracted into suspension using a sterile plastic loop and then examined for their ice-nucleating ability, shown in Figure 4.15. Out of the four bacteria species analysed, only one had a freezing activity greater than that of the 1996 LLS leaf-washing sample. DNA analysis of the bacterial isolates revealed their identity to the genus level as there were too many similar sequences to determine the species. However, we were able to identify that the most ice-active bacteria isolate (No.2 Yellow) was of the genus *Pseudomonas*, a genus of bacteria which contains many known ice-active bacteria species (Morris et al., 2008). For example, *Pseudomonas syringae* is a bacterial species which is well known for its ability to nucleate ice at high temperatures (Maki and Willoughby, 1978; Möhler et al., 2007).

Previous work has investigated the potential that the ice-nucleating ability of rust spores may be attributable to ice-active bacteria associated with the spores, rather than the spores themselves (Morris et al., 2013). Morris et al. (2013) collected urediniospores of various rust species from infected plants that had been grown both in natural and greenhouse environments. To test for the presence of ice-active bacteria on the fungal spores, they made up cultures from the fungal suspension used for freezing analysis. This technique allowed them to determine the number of culturable bacteria present on the fungal spores. Still, it did not rule out any non-culturable ice-active bacteria that were non-viable or fragmented but had maintained their ice-nucleating ability. However, they were able to further confirm that ice-active bacteria were not contributing to the observed ice-nucleating ability of the rust spores by showing that treatment with lysosome did not reduce the observed ice-nucleating activity, which normally removes proteinaceous ice-nucleating such as bacteria (Morris et al., 2013). The results of our analysis of LLS spores indicate a possible difference in the origin of the ice-nucleating activity compared to rust spores. We observed little to no ice-nucleating activity in our lab-grown samples, but ice-nucleating activity was associated with the presence of bacteria in our leaf-washed samples. This suggests that the LLS fungal spores themselves cannot nucleate ice, but that the observed ice-nucleating ability was attributable to associated bacteria species. This finding counters that of Morris et al. (2013) but may highlight a distinct difference in the ice-nucleating ability of rust spores compared to fungal spores of LLS.

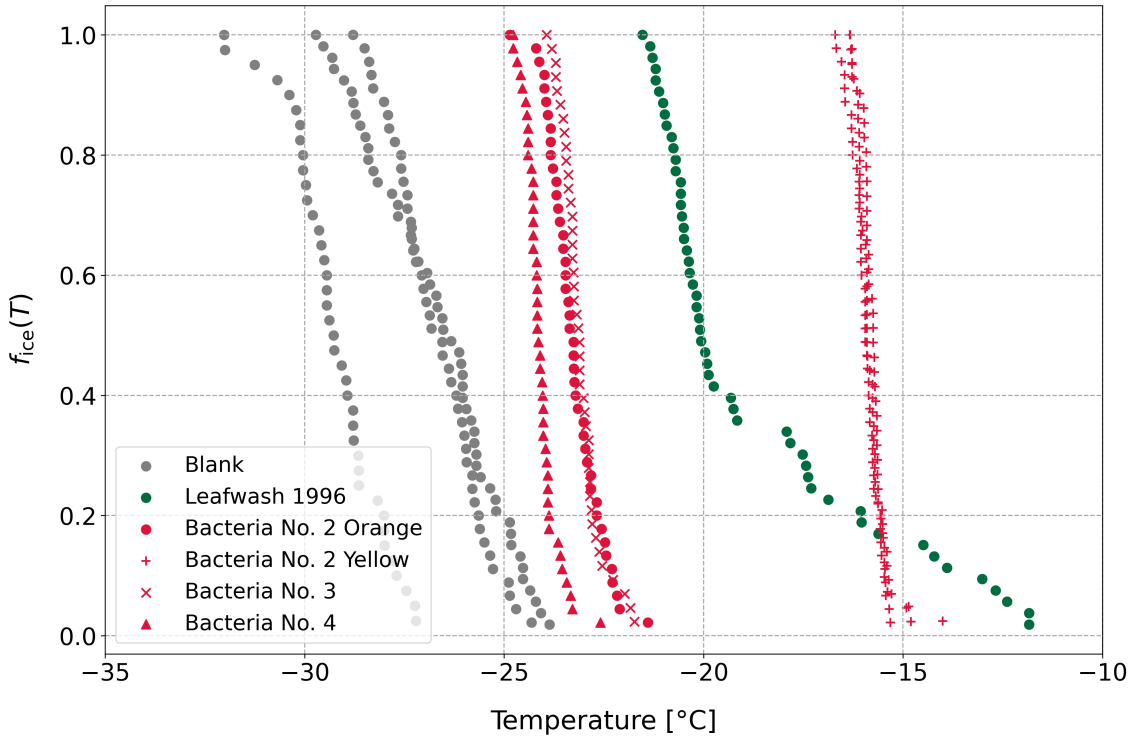

Figure 4.15: Fraction frozen, $f_{ice}(T)$, curves as a function of temperature for LLS spore suspensions extracted from oilseed rape leaves (1996 field sample) compared with the bacteria isolated from the suspension.

4.3.3 Ice-Nucleating Activity of Agar

To better understand the potential contamination of the extraction process for our LLS cultures, a set of handling blanks were investigated for their ice-nucleating ability. The freezing activity of the solution extracted from the blank MEA plate was above that of the pure water blanks and the other handling blanks (including filtering through the miracloth), suggesting that the agar has a distinct ice-nucleating ability which is causing contamination of our fungal suspensions after extraction from the MEA plates (Figure 4.12a). We also placed two of the blank MEA plates in a freezer overnight to clarify that any increases in ice-nucleating activity we observed were from the LLS spores, not from the agar itself. After exposure to subzero temperatures in the freezer, the blank MEA plates were extracted and analysed for their ice-nucleating ability again. There was an observable increase in the freezing temperatures of the MEA plate extraction solution after exposure to subzero temperatures. The reason for this increase in freezing activity remains unclear though.

It is possible, as was our hypothesis for fungal spores, that the exposure to cold stress initiated the release of ice-nucleating macromolecules, triggering an increase in the ice-nucleating ability of the agar itself. Previous work has shown that freezing can enhance

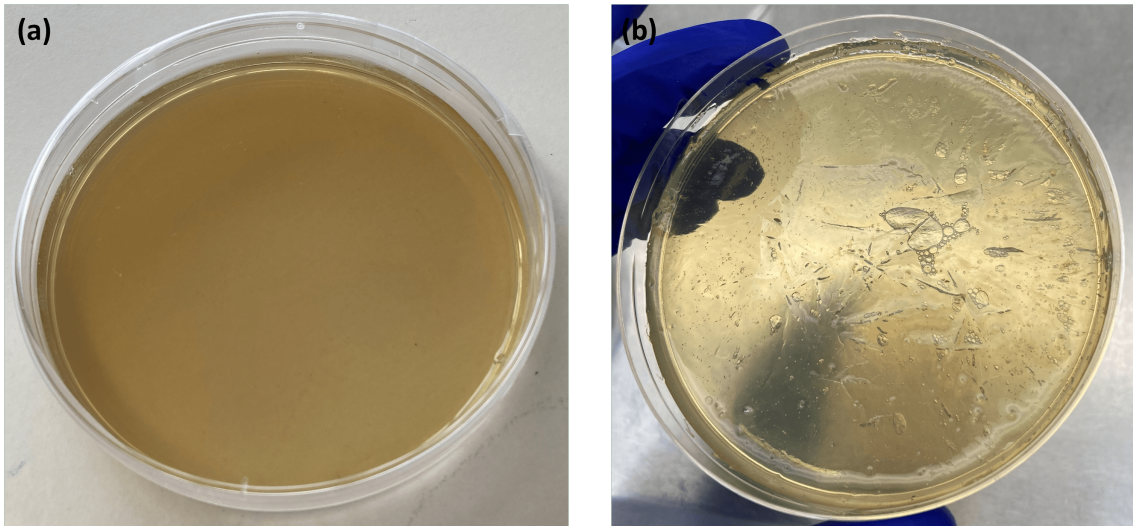

Figure 4.16: Blank malt extract agar plate used to analyse contamination by agar extraction process *(a) before and (b) after freezing at* $-20\,^{\circ}\mathrm{C}$ *for 6 hours.*

the ice-nucleating ability of certain biological samples, particularly for biological particles below 0.45 µm in diameter (Beall et al., 2020). It is thought that the observed increase in ice-nucleating activity after freezing of biological material could be a result of the enhancements in solution concentration as solutes are rejected from ice crystals during their growth (Butler, 2002; Beall et al., 2020). An increase in solute concentration is likely to lead to an increase in the aggregation of macromolecules, which could create more sites for ice nucleation to occur (Beall et al., 2020) (see Section 3). Furthermore, Perkins et al. (2020) studied the ice-nucleating ability of fatty acids and fatty alcohols in sea spray aerosols. They also found that after freezing, the ice-nucleating ability of these substances increased (Perkins et al., 2020). They suggested that the reason for this observed increase in ice-nucleating ability was due to the restructuring of the molecules into more crystalline structures, which acted as better templates for ice formation (Perkins et al., 2020). Furthermore, we noticed a change in the structure of the agar plate after being frozen overnight (Figure 4.16). The rupturing of the agar after being frozen (as shown in Figure 4.16b) could have led to the increased release of ice nuclei into suspension during the extraction process, meaning that the overall ice-nucleating ability of the agar remains the same, but the concentration of agar within the solution had increased. We were unable to measure the concentration of agar released into the solution, so it remains unclear if the observed increase in freezing activity was due to an increase in the concentration of INPs or an increase in the ice-nucleating activity of the agar.

These results indicate that the agar itself can nucleate ice. Since agar is made up of polysaccharides from the cell walls of red algae species, these findings suggest that these

polysaccharides are IN. Marine algae and phytoplankton have been identified as sources of ice-nucleating activity in SSAs (Knopf et al., 2011; Wolf et al., 2019). In particular, Wolf et al. (2019) found that organic macromolecules such as polysaccharides were enriching the sea surface microlayer and contributing most significantly to the observed increase in ice-nucleating ability of SSAs. Therefore, polysaccharides from algae (which are also found in agar) may be important ice nucleators. The agar used in this study also contained other organic substances from malt extract, which is added as a source of energy within the growth medium, meaning that other substances may be responsible for the observed ice-nucleating activity. Interestingly, Fröhlich-Nowoisky et al. (2015) discuss the use of malt extract agar in their fungal experiments, suggesting that they too observed contamination of ice-nucleating activity when using MEA as the growth medium for their fungal isolates. They observed that when they changed the growth medium from MEA to dextrose-peptone-yeast extract (DPY) agar instead, the level of contamination in their fungal isolates was reduced. This finding suggests that the observed ice-nucleating activity in our agar plates may be attributable to substances within the malt extract, rather than the polysaccharides of algae present. However, since the agar is autoclaved at 115 °C for sterilisation before use, it is unlikely that proteinaceous INPs are responsible for the ice-nucleating activity seen in this study. Our results also have important implications for future work with agar plate cultures. The ice-nucleating ability of agar could interfere with observations of bacterial or fungal cultures when extracted from agar plates and caution should be taken to reduce contamination from agar in ice-nucleating analysis of these cultures.

4.4 Conclusions

This chapter investigated the ice-nucleating ability of fungal spores from YR and LLS, fungal pathogens which infect wheat and oilseed rape crops, respectively. We found that both of these spores have a small ice-nucleating ability which is very similar to the ice-nucleating ability of other rust species such as wheat leaf rust. However, our lab-based experiments with LLS suggested that the ice-nucleating ability of the LLS spores found on the leaves of oilseed rape is likely to be attributable to bacteria also found on the leaves and may not be attributable to the fungal spores themselves. We were also able to show that the freezing behaviour of the YR fungal spores was distinctly different to the freezing behaviour of *Fusarium* fungal species.

We also examined the impact of freezing and storage length on the ice-nucleating ability of these fungal spore samples. Our findings were in agreement with previous studies which found that storage can lead to a decrease in ice-nucleating ability, particularly at temperatures above $-20\,^{\circ}\mathrm{C}$ (Polen et al., 2016; Beall et al., 2020). However, we also showed that this loss of ice-nucleating activity can be unpredictable, since the fungal spore suspension we tested from 1996, which had been frozen for the last 27 years, still showed a significant amount of freezing above $-20\,^{\circ}\mathrm{C}$, suggesting that ice-nucleating activity is not always lost during storage. This observed ice-nucleating activity may be a result of freezing enhancing ice-nucleating activity, as seen in previous studies (Beall et al., 2020; Perkins et al., 2020). Future work could investigate the impact of long-term storage and viability on the ice-nucleating activity of fungal spores in more detail as this could have implications for the distribution and monitoring of these INPs in the atmosphere.

Finally, we examined the ice-nucleating activity associated with blank MEA plates and found the presence of ice-active material from the MEA itself was impacting our ability to observe any ice-nucleating activity in our lab-grown LLS samples. This observation suggested that either the agar itself or the associated malt extract has an ice-nucleating activity which is released during the extraction of fungal spores from the MEA plate. Future work could examine the impact of agar as a source of ice-nucleating contamination when culturing fungus or other cultures in the lab and other extraction techniques may need to be considered to reduce this impact in the future.

References

Beall, C. M., Lucero, D., Hill, T. C., DeMott, P. J., Stokes, M. D., and Prather, K. A. (2020). Best practices for precipitation sample storage for offline studies of ice nucleation in marine and coastal environments. *Atmospheric Measurement Techniques*, 13(12):6473–6486.

Bouvet, L., Holdgate, S., James, L., Thomas, J., Mackay, I. J., and Cockram, J. (2022). The evolving battle between yellow rust and wheat: implications for global food security. *Theoretical and Applied Genetics*, 135(3):741–753.

Bredow, M. and Walker, V. K. (2017). Ice-Binding Proteins in Plants. *Frontiers in Plant Science*, 8:2153.

Butler, M. F. (2002). Freeze Concentration of Solutes at the Ice/Solution Interface Studied by Optical Interferometry. *Crystal Growth & Design*, 2(6):541–548.

Calderón-Ezquerro, M. C., Serrano-Silva, N., and Brunner-Mendoza, C. (2020). Metagenomic characterisation of bioaerosols during the dry season in Mexico City. *Aerobiologia*, 36(3):493–505.

Fröhlich-Nowoisky, J., Hill, T. C. J., Pummer, B. G., Yordanova, P., Franc, G. D., and Pöschl, U. (2015). Ice nucleation activity in the widespread soil fungus *Mortierella alpina*. *Biogeosciences*, 12(4):1057–1071.

Geagea, Huber, and Sache (1999). Dry-dispersal and rain-splash of brown (Puccinia recondita f.sp. tritici) and yellow (P. striiformis) rust spores from infected wheat leaves exposed to simulated raindrops. *Plant Pathology*, 48(4):472–482.

Gilles, T., Evans, N., Fitt, B. D., and Jeger, M. J. (2000). Epidemiology in Relation to Methods for Forecasting Light Leaf Spot (Pyrenopeziza brassicae) Severity on Winter Oilseed Rape (Brassica napus) in the UK. *European Journal of Plant Pathology*, 106(7):593–605.

Graves, A., Knox, J., Morris, J., Burgess, P., Weatherhead, K., and Holman, I. (2016). Agriculture & Forestry Report Card Paper 1. Technical report, Cranfield University, Cranfield, Bedford.

Haga, D. I., Iannone, R., Wheeler, M. J., Mason, R., Polishchuk, E. A., Fetch Jr., T., van der Kamp, B. J., McKendry, I. G., and Bertram, A. K. (2013). Ice nucleation properties of rust and bunt fungal spores and their transport to high altitudes, where they can cause heterogeneous freezing. *Journal of Geophysical Research: Atmospheres*, 118(13):7260–7272.

Hartmann, S., Ling, M., Dreyer, L. S. A., Zipori, A., Finster, K., Grawe, S., Jensen, L. Z., Borck, S., Reicher, N., Drace, T., Niedermeier, D., Jones, N. C., Hoffmann, S. V., Wex, H., Rudich, Y., Boesen, T., and Šantl Temkiv, T. (2022). Structure and Protein-Protein Interactions of Ice Nucleation Proteins Drive Their Activity. *Frontiers in Microbiology*, 13:872306.

Iannone, R., Chernoff, D. I., Pringle, A., Martin, S. T., and Bertram, A. K. (2011). The ice nucleation ability of one of the most abundant types of fungal spores found in the atmosphere. *Atmospheric Chemistry and Physics*, 11(3):1191–1201.

Ingold, C. T. (1971). *Fungal Spores: Their Liberation and Dispersal*. Clarendon Press, Oxford.

Knopf, D. A., Alpert, P. A., Wang, B., and Aller, J. Y. (2011). Stimulation of ice nucleation by marine diatoms. *Nature Geoscience*, 4(2):88–90.

Kunert, A. T., Pöhlker, M. L., Tang, K., Krevert, C. S., Wieder, C., Speth, K. R., Hanson, L. E., Morris, C. E., Schmale III, D. G., Pöschl, U., and Fröhlich-Nowoisky, J. (2019). Macromolecular fungal ice nuclei in *Fusarium*: effects of physical and chemical processing. *Biogeosciences*, 16(23):4647–4659.

Lacey, M. and West, J., editors (2006). *The Air Spora*. Springer, Boston, MA.

Lymperopoulou, D. S., Adams, R. I., and Lindow, S. E. (2016). Contribution of Vegetation to the Microbial Composition of Nearby Outdoor Air. *Applied and Environmental Microbiology*, 82(13):3822–3833.

Macher, J., Chen, B., and Rao, C. (2008). Field Evaluation of a Personal, Bioaerosol Cyclone Sampler. *Journal of Occupational and Environmental Hygiene*, 5(11):724–734. Publisher: Taylor & Francis _eprint: https://doi.org/10.1080/15459620802400159.

Maki, L. R. and Willoughby, K. J. (1978). Bacteria as Biogenic Sources of Freezing Nuclei. *Journal of Applied Meteorology and Climatology*, 17(7):1049–1053. Publisher: American Meteorological Society Section: Journal of Applied Meteorology and Climatology.

Morris, C. E., Sands, D. C., Glaux, C., Samsatly, J., Asaad, S., Moukahel, A. R., Gonçalves, F. L. T., and Bigg, E. K. (2013). Urediospores of rust fungi are ice nucleation active at > -10 °C and harbor ice nucleation active bacteria. *Atmospheric Chemistry and Physics*, 13(8):4223–4233.

Morris, C. E., Sands, D. C., Vinatzer, B. A., Glaux, C., Guilbaud, C., Buffière, A., Yan, S., Dominguez, H., and Thompson, B. M. (2008). The life history of the plant pathogen Pseudomonas syringae is linked to the water cycle. *The ISME Journal*, 2(3):321–334.

Möhler, O., DeMott, P. J., Vali, G., and Levin, Z. (2007). Microbiology and atmospheric processes: the role of biological particles in cloud physics. *Biogeosciences*, 4(6):1059–1071.

Nicolaisen, M., West, J. S., Sapkota, R., Canning, G. G. M., Schoen, C., and Justesen, A. F. (2017). Fungal Communities Including Plant Pathogens in Near Surface Air Are Similar across Northwestern Europe. *Frontiers in Microbiology*, 8.

Niemand, M., Möhler, O., Vogel, B., Vogel, H., Hoose, C., Connolly, P., Klein, H., Bingemer, H., DeMott, P., Skrotzki, J., and Leisner, T. (2012). A Particle-Surface-Area-Based Parameterization of Immersion Freezing on Desert Dust Particles. *Journal of the Atmospheric Sciences*, 69(10):3077–3092.

O'Sullivan, D., Adams, M. P., Tarn, M. D., Harrison, A. D., Vergara-Temprado, J., Porter, G. C. E., Holden, M. A., Sanchez-Marroquin, A., Carotenuto, F., Whale, T. F., McQuaid, J. B., Walshaw, R., Hedges, D. H. P., Burke, I. T., Cui, Z., and Murray, B. J. (2018). Contributions of biogenic material to the atmospheric ice-nucleating particle population in North Western Europe. *Scientific Reports*, 8(1):13821.

O'Sullivan, D., Murray, B. J., Ross, J. F., Whale, T. F., Price, H. C., Atkinson, J. D., Umo, N. S., and Webb, M. E. (2015). The relevance of nanoscale biological fragments for ice nucleation in clouds. *Scientific Reports*, 5(1):8082.

Perkins, R. J., Vazquez de Vasquez, M. G., Beasley, E. E., Hill, T. C. J., Stone, E. A., Allen, H. C., and DeMott, P. J. (2020). Relating Structure and Ice Nucleation of Mixed Surfactant Systems Relevant to Sea Spray Aerosol. *The Journal of Physical Chemistry A*, 124(42):8806–8821.

Polen, M., Lawlis, E., and Sullivan, R. C. (2016). The unstable ice nucleation properties of Snomax® bacterial particles. *Journal of Geophysical Research: Atmospheres*, 121(19):11,666–11,678.

Ponder, M. A., Gilmour, S. J., Bergholz, P. W., Mindock, C. A., Hollingsworth, R., Thomashow, M. F., and Tiedje, J. M. (2005). Characterization of potential stress responses in ancient Siberian permafrost psychroactive bacteria. *FEMS Microbiology Ecology*, 53(1):103–115.

Pouleur, S., Richard, C., Martin, J.-G., and Antoun, H. (1992). Ice Nucleation Activity in Fusarium acuminatum and Fusarium avenaceum. *Applied and Environmental Microbiology*, 58(9):2960–2964.

Qu, J., Zou, X., Yu, J., and Zhou, Y. (2017). The conidial mucilage, natural film coatings, is involved in environmental adaptability and pathogenicity of Hirsutella satumaensis Aoki. *Scientific Reports*, 7(1):1301. Number: 1 Publisher: Nature Publishing Group.

Ramadoss, C. S., Uhlig, J., Carlson, D. M., Butler, L. G., and Nicholson, R. L. (1985). Composition of the mucilaginous spore matrix of Colletotrichum graminicola, a pathogen of corn, sorghum, and other grasses. *Journal of Agricultural and Food Chemistry*, 33(4):728–732. Publisher: American Chemical Society.

Rapilly, F. (1979). Yellow Rust Epidemiology. *Annual Review of Phytopathology*, 17(1):59–73. _eprint: https://doi.org/10.1146/annurev.py.17.090179.000423.

Sanchez-Marroquin, A., S. West, J., T. Burke, I., B. McQuaid, J., and J. Murray, B. (2021). Mineral and biological ice-nucleating particles above the South East of the British Isles. *Environmental Science: Atmospheres*, 1(4):176–191.

Seinfeld, J. H. and Pandis, S. (2016). *Atmospheric chemistry and physics: from air pollution to climate change*. Wiley, Hoboken, New Jersey, third edition.

Steinke, I., Funk, R., Busse, J., Iturri, A., Kirchen, S., Leue, M., Möhler, O., Schwartz, T., Schnaiter, M., Sierau, B., Toprak, E., Ullrich, R., Ulrich, A., Hoose, C., and Leisner, T. (2016). Ice nucleation activity of agricultural soil dust aerosols from Mongolia, Argentina, and Germany. *Journal of Geophysical Research: Atmospheres*, 121(22):13,559–13,576.

Waller, J. M., Ritchie, B. J., and Holderness, M. (1998). *Plant clinic handbook*. CAB International, Wallingford, UK. Publisher: CAB INTERNATIONAL.

Wolf, M. J., Coe, A., Dove, L. A., Zawadowicz, M. A., Dooley, K., Biller, S. J., Zhang, Y., Chisholm, S. W., and Cziczo, D. J. (2019). Investigating the Heterogeneous Ice Nucleation of Sea Spray Aerosols Using Prochlorococcus as a Model Source of Marine Organic Matter. *Environmental Science & Technology*, 53(3):1139–1149.

5 Characterisation of the size distribution of ice-nucleating particles from fertile soils in the UK

5.1 Introduction

The size distribution of atmospheric aerosol evolves over time (see Section 1.2.4), making the size-resolved ice-nucleating particle (INP) concentration important for understanding cloud glaciation. For example, INPs larger than around 10 µm are less likely to impact cloud glaciation (except in deep convective clouds), since larger particles have faster sedimentation rates (Feichter and Leisner, 2009). Similarly, INPs which are smaller than 0.01 µm rapidly grow by coagulation, a process which likely leads to the covering of ice-active sites on the surface of particles, potentially reducing their ice-nucleating ability. In addition, as discussed in Section 1.4, we know that biological components play a key role in the ice-nucleating activity of agricultural soils (Conen et al., 2011; O'Sullivan et al., 2014, 2015; Augustin-Bauditz et al., 2016) but how these components are distributed through agricultural soil dust is important to understand how the ice-nucleating activity of the soil changes with transport in the atmosphere. However, only a few studies have investigated the size distribution of INPs (DeMott et al., 2010; Mason et al., 2016; Reicher et al., 2019; Porter et al., 2020).

In pure mineral dust aerosol, larger particles with larger surface areas, have a greater number of ice-active sites at the surface (Si et al., 2018). Using INP observations over 14 years, DeMott et al. (2010) showed that atmospheric INP concentrations could be explained as the number concentration of aerosol particles larger than 0.5 µm. Similarly, Reicher et al. (2019) studies INP concentrations from mineral dust sources in the Mediterranean, concluding that supermicron particles (aerosol particles larger than 1 µm) contributed the most to the observed ice-nucleating activity for mineral dust (Reicher et al., 2019). However, the size distribution of INPs in agricultural soil dust aerosols has not previously been investigated. Agricultural soils are complex and externally mixed with a variety of ice-active biological compounds in addition to mineral dust particles (see Section 1.4). Therefore, the size distribution of INPs across soil dust aerosols will be dependent on the type of biological material that dominates the ice-nucleating activity of these soils. If whole bacteria cells or fungal spores are important for the ice-nucleating activity of agricultural soil, then we would expect the majority of INPs to be within the large particle size range, around 1 µm or greater. However, ice-active biogenic macromolecules, such as

proteins, polysaccharides and compounds from the breakdown of plant material are known to maintain their ice-nucleating activity even when separated from living cells (Cascajo-Castresana et al., 2020; Bogler and Borduas-Dedekind, 2020; Steinke et al., 2020; Burkart et al., 2021). So if these ice-nucleating macromolecules dominate the ice-nucleating activity of agricultural soils, we would expect the size-segregated INP concentration to be more evenly distributed across the soil dust aerosol as the macromolecules become spread evenly across the dust and become associated with soil particles of all sizes.

In this chapter, we investigated the size distribution of ice-nucleating components throughout aerosolised soil dust samples collected from agricultural fields west of Leeds. We wanted to investigate the relative importance of submicron particles compared to larger biological INPs such as bacteria, fungal spores and pollen. To further understand the relative contribution of biogenic components at different size fractions compared to mineral components, we also use heat treatments to see how exposure to heat impacted the ice-nucleating activity of the filter suspensions.

5.2 Experimental

5.2.1 Sample Collection and Preparation

Soil samples were taken from two different agricultural fields at the University of Leeds Research Farm on the 12th of October 2022 (Figure 5.1). The samples were taken from adjacent fields, one at the top of a hill (herein referred to as the Upper Field sample) and the other at the bottom of a hill (herein referred to as the Lower Field sample). Both fields had been harvested before samples were taken, however, the Upper Field had contained wheat crops and the Lower Field had contained potato crops before the harvesting took place. At each sampling location, 50 mL polypropylene centrifuge tubes (Sarstedt Inc.) were used to sample from the top 5 cm of soil and three different samples were taken from slightly different locations to reduce bias from sampling in one location. Each soil sample was taken a minimum of 1 m from the boundary of the field and each chosen field consisted of bare soil with no crops present. Once collected, the soil samples were air-dried in an oven on foil-lined baking trays at about 27 °C for at least 2 hours. Once visibly dry, any large stones were removed. The dried soil samples were then aerosolised in an aerosol chamber setup at the University of Leeds (Figure 5.2).

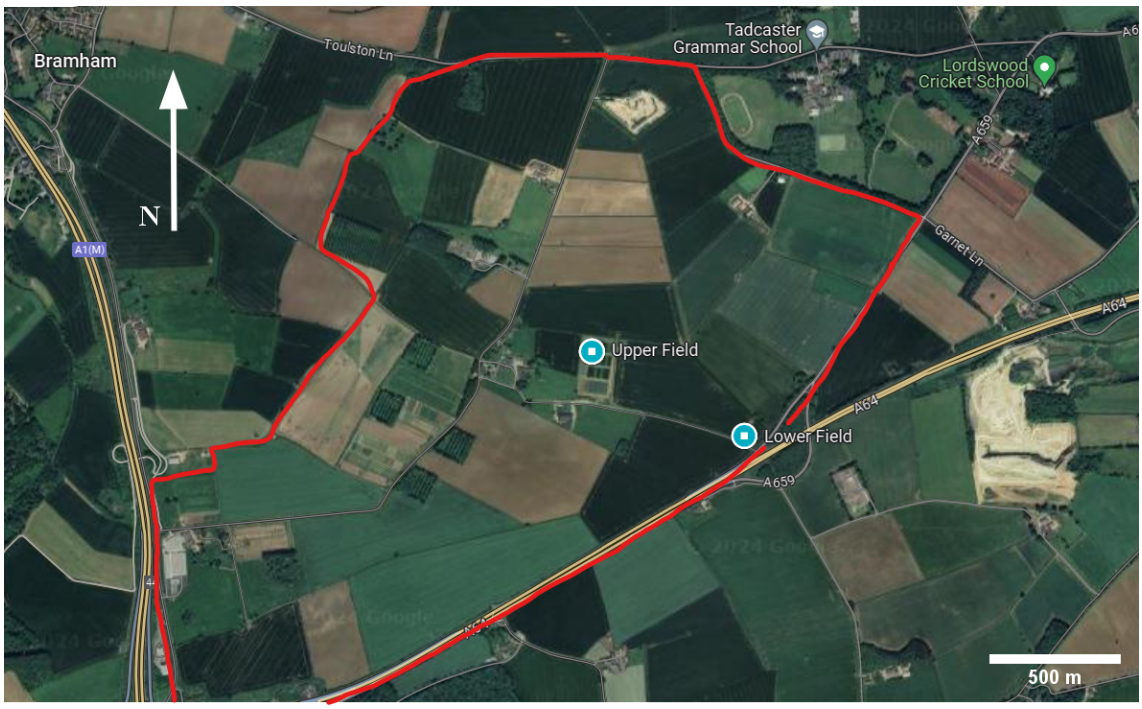

Figure 5.1: The University of Leeds Research Farm (outlined in red) with the two sampling locations from the 12th October 2022 labelled as Upper Field and Lower Field. Image taken from Google Maps.

5.2.2 Aerosol Chamber Setup

The aerosol chamber setup included an aerosol chamber of about 1 m^{-3}, similar to the setup used in Ponsonby et al. (2024). A flow of compressed air was passed through a charcoal filter (PN 12012, Carbon Capsule, Pall Life Sciences, UK) and a HEPA filter (Whatman, UK) to produce a clean airflow for our experiments in the aerosol chamber. The soil samples were injected into the aerosol chamber using two different aerosolisation techniques (as described below in Section 5.2.2.1). Two different methods of aerosolisation of the soil were used during this experiment, these are compared to observe the improved Dust Tower technique (see Section 5.2.2.1). An Aerodynamic Particle Sizer (APS; TSI Model 3321) was used to determine the size distribution of particles between 0.5 and 20 µm and a Scanning Mobility Particle Sizer (SMPS; TSI Model 3938) was used to determine the size distribution of smaller aerosol particles at the range of 1 to 1000 nm (described in more detail in Section 5.2.2.2). A cascade impactor (Sioutas Personal Cascade Impactor, SKC Ltd., UK) was also connected to the base of the aerosol chamber to collect a sample of the aerosolised dust for offline INP analysis (as described in Section 5.2.2.3).

Handling blanks were performed before each chamber run experiment by running the cleaned, compressed air through the aerosol chamber setup and analysing the filters in the same way as described below to test for any contamination from the airflow or the

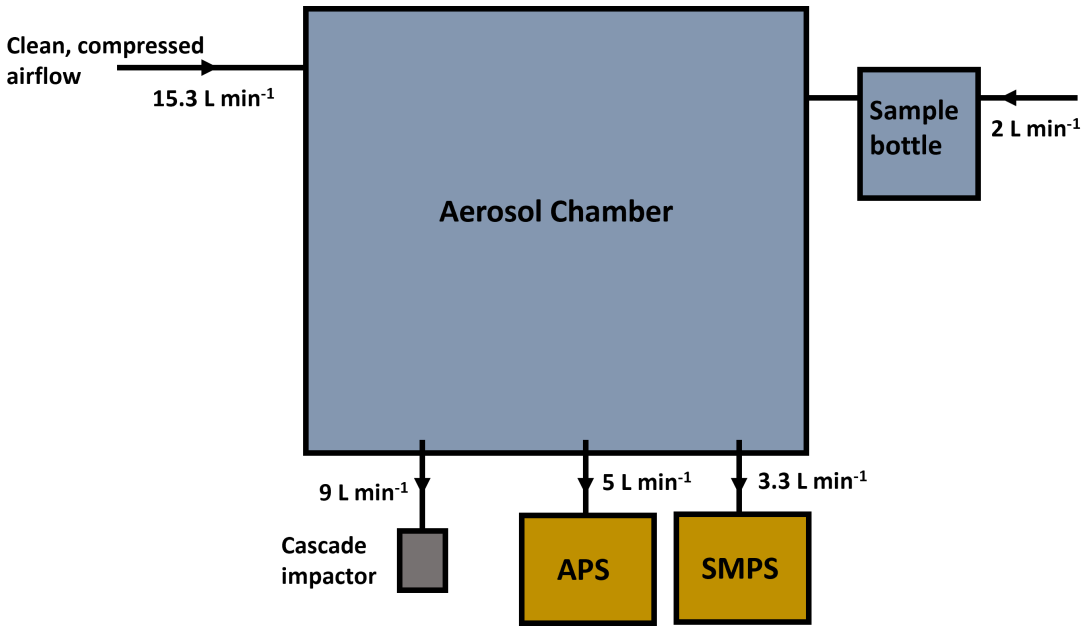

Figure 5.2: Schematic of the aerosol chamber setup used in this experiment. *This shows the manual aerosolisation technique.*

setup. Once the handling blank was complete, the sample was introduced into the aerosol chamber setup, the aerosol was produced and samples were taken for between 1 to 2 hours depending on the produced aerosol concentrations. After each sample run, the compressed airflow was left on overnight to flush out any soil sample remaining in the chamber.

5.2.2.1 Aerosolisation Techniques

During this study, we used two different aerosolisation techniques. For each collected sample, multiple runs were completed in the aerosol chamber to establish the variation in the handling of the sample and investigate different aerosol loadings within the chamber. We examined different aerosol loadings so we could examine more of the INP spectra and examine how the aerosol loading impacted the observed ice-nucleating activity. The first three aerosol chamber runs were completed using the Manual aerosolisation technique (Table 3). This technique involved placing the dried soil sample in a cleaned chemical bottle, which was manually agitated to generate an aerosol plume which was then passed into the main aerosol chamber as compressed airflow was passed through the sample bottle at a flow rate of 2.0 L min^{-1} (as shown in Figure 5.2). Although this technique allowed us to generate soil dust within the aerosol chamber effectively, the manual agitation required meant that we were not able to produce a consistent concentration of particles throughout the length of the experiment.

The second technique was an automatic aerosolisation technique using a Dust Tower (X78502, Grimm Aerosol Technik, Germany), a similar technique was used by Shi et al.

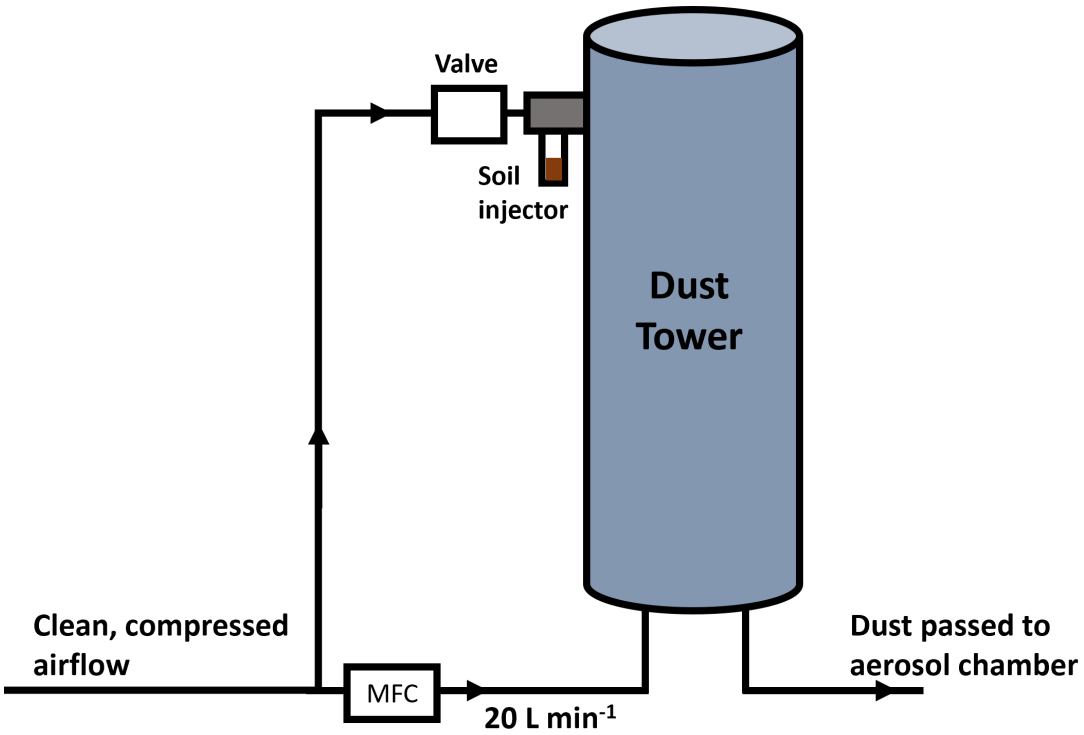

Figure 5.3: Schematic of the Dust Tower setup used for three of the aerosol chamber runs in this experiment.

(2011). For this setup, the clean, compressed airflow was injected into the bottom of the Dust Tower at 20 $\mathrm{L\,min^{-1}}$ to create turbulent flow within the tower (Figure 5.3). The dried soil sample was placed into a 15 mL centrifuge tube (352196, Falcon) which was attached to an injector at the top of the Dust Tower. The aerosolisation of the sample was completed by pulsing the compressed air through the sample injector at regular intervals (between 4 and 8 seconds), which injected the dust into the tower, where it was mixed with the turbulent air. The air was then drawn out of the Dust Tower and through into the aerosol chamber, where the same sampling and size distribution monitoring could take place as described below (Figure 5.2). As the air pulses through the aerosol injector, there is a potential for the fragmentation of larger soil aggregates as they fall and collide with other soil particles within the 15 mL Falcon tube. Therefore, this aerosolisation technique is similar to the natural saltation process of natural, wind-blown dust. Other aerosolisation techniques, including those used by Steinke et al. (2016), use a rotating brush to generate dust aerosol inside the chamber. This rotating brush generator is specifically designed to avoid breaking down aggregates within the soil, which is less representative of the natural saltation process so produces aerosol which is less representative of natural soil dust aerosol.

Table 3: Summary of aerosol chamber runs, samples and aerosolisation method used.

Chamber Run	Date	Sample	Aerosolisation Method	Sample Length (mins)
Run 1	08/11/2022	Upper Field	Manual	69.0
Run 2	11/01/2023	Lower Field	Manual	72.2
Run 3	01/02/2023	Lower Field	Manual	107.0
Run 4	24/01/2024	Upper Field	Dust Tower	94.1
Run 5	29/01/2024	Lower Field	Dust Tower	100.0
Run 6	30/01/2024	Upper Field	Dust Tower	90.0

5.2.2.2 Size-Distribution Intrumentation

The APS determines the aerodynamic diameter of the aerosolised dust particles within the chamber between 0.5 and 20 µm. As the particles enter the APS, they pass through an accelerating orifice and the rate of acceleration between two laser beams is observed by the instrument. The size of each particle will determine its rate of acceleration since larger particles will accelerate much slower due to increased inertia. As they pass through the lasers, scattered light is collected using an elliptical mirror and focused onto an avalanche photodetector. Each particle creates a two-peak signal and the time-of-flight between the two peaks is used to determine the size of the particle, with a longer time-of-flight indicating a larger particle.

The SMPS determines the mobility diameter of the aerosolised dust particles between 1 and 1000 nm. The SMPS consists of three main parts; a neutraliser, a Differential Mobility Analyser (DMA) and a Condensation Particle Counter (CPC). The neutraliser uses a radioactive source to expose the sampled aerosols to an electrically neutral ion cloud, allowing a steady-state charge distribution to be applied to the particles. This standard charge distribution enables the size of the particles to be determined purely on their electrical mobility. The DMA creates an electrical field by applying voltage to the central rod, which allows the particles to be pulled towards the central column at different rates depending on their electrical mobility. By selecting different voltage settings, the DMA can select a range of different particle sizes based on their electrical mobilities. Each scan of the SMPS spans across a voltage range to determine the concentration of particles across a range of particle sizes and electrical mobilities. Since the DMA relies on the assumption that the electrical mobility of the particle can be directly related to its size, the charge of the particles needs to be controlled for the DMA to accurately sort the particles. Once the particles have been size selected by the DMA, they are passed to the CPC to determine the particle concentration. The particles are grown through the condensation of butanol onto the particle surface, this allows the particles to grow large

enough to be counted optically. Once grown, the particles are passed through a laser, where they are counted based on the scattering of light.

5.2.2.3 Sample Collection

A cascade impactor was used to collect a size-resolved sample of the aerosolised dust (Figure 5.4). The impactor contains four impactor stages (labelled A to D) which sort the aerosol particles into four different size bins; > 2.5 µm (Stage A), 1.0-2.5 µm (Stage B), 0.5-1.0 µm (Stage C) and 0.25-0.5 µm (Stage D). A battery-powered pump (Leyland Legacy Pump, SKC Ltd., UK) was used to supply a flow rate of 9 L min^{-1} through the impactor and 25 mm diameter filters with 0.05 µm pore size (Nuclepore track-etched membrane polycarbonate filters, Whatman, UK) were used in each impactor stage to collect the aerosol particles. For some of the aerosol chamber runs, an after filter was attached to the bottom of the cascade impactor to collect the majority of the remaining particles (< 0.25 µm) using a filter holder containing a 45 mm diameter filter with 5 µm pore size (Nuclepore track-etched membrane polycarbonate filters, Whatman, UK).

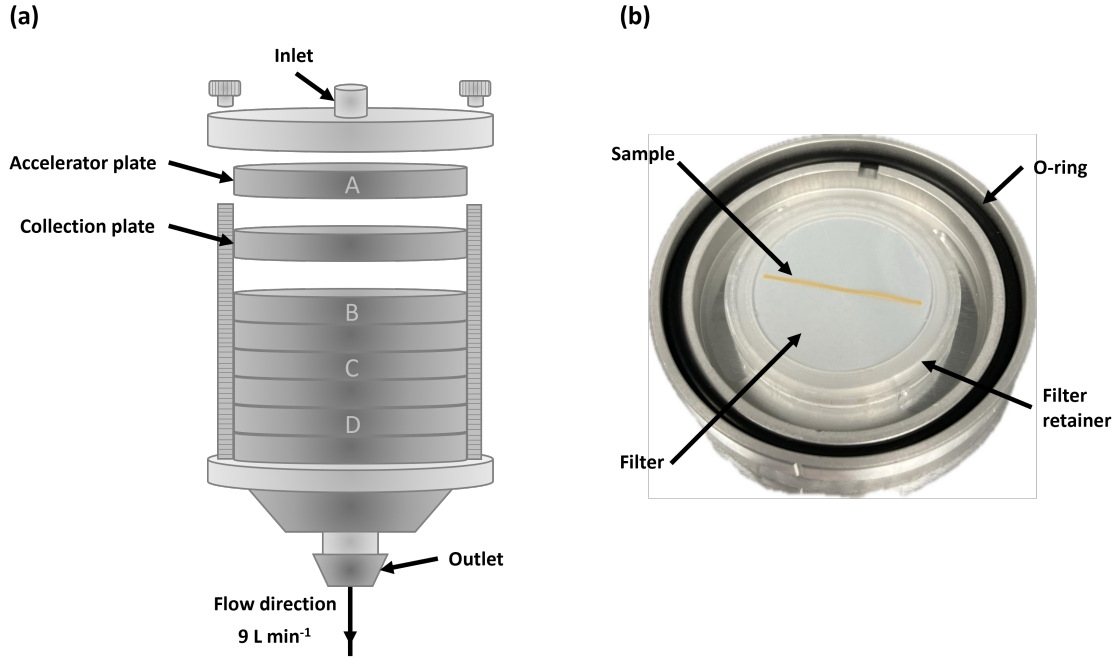

Figure 5.4: Illustration of the Sioutas Personal Cascade Impactor and an example of one of the collector plates. *(a) The four acceleration plates, A to D, are shown with collection plates placed between them. Air is pumped through the inlet at a rate of 9* $\mathrm{L\,min^{-1}}$ *and particles above the cut-off size for each accelerator plate are deposited onto the associated collector plate. (b) An example of a collector plate with a collected dust sample. Each collector plate consists of a 25 mm diameter filter, a plastic filter retainer and a nitrile O-ring to create an airtight seal.*

5.2.3 Immersion Freezing Analysis

Droplet freezing experiments were carried out using the Microlitre Nucleation by Immersed Particle Instrument (µL-NIPI), as described in Section 2.1.1. During these experiments, we used the Grant-Asymptote EF600 for the droplet freezing analysis (see Section 2.1.1). The filters from each impactor stage were removed and placed in 30 mL tubes (327150PP, SciLabware Ltd.), and then 3 mL of MilliQ water was added to wash the aerosol from the filter into suspension with water. The filter suspensions were placed on a vortex mixer for 10 minutes to ensure that all of the particles had been removed from the filter surface, similar to the technique used in O'Sullivan et al. (2018).

For each impactor stage filter suspension, 1 µL droplets were pipetted onto a clean glass slide which was placed onto the cold stage. As described in Section 2.2, the temperature at which each droplet froze was used to determine the fraction of droplets frozen as a function of temperature ($f_{\mathrm{ice}}(T)$) for each impactor stage of each aerosol chamber run (Eq. 11). The $f_{\mathrm{ice}}(T)$ was then used to calculate the concentration of INPs per volume of sampled air ($N_{\mathrm{INP}}(T)$) and the total number of ice-active sites per surface area of dust ($n_{\mathrm{s}}(T)$) for each impactor stage (Equations 13 and 15).

To estimate the total collected aerosol surface area, A_{s}, the particle number concentrations measured using the APS and SMPS instruments were used. To compare the results of these two instruments and to accurately calculate the total surface area loading onto each cascade impactor filter, the mobility-equivalent particle diameter (D_{me}) from the SMPS and the aerodynamic particle diameter (D_{ae}) from the APS, were converted into volume-equivalent particle diameters (D_{ve}) according to the following equations:

$$D_{\mathrm{ve}} = \frac{1}{\chi} D_{\mathrm{me}} \tag{18}$$

$$D_{\mathrm{ve}} = \sqrt{\frac{\chi \rho_0}{\rho}} D_{\mathrm{ae}} \tag{19}$$

where χ is the dynamic shape factor, which accounts for non-spherical particle shapes and is assumed to be equal to 1.3, a value typical for mineral dust (Möhler et al., 2008), ρ is the particle density, which is assumed to be 2.6 $\mathrm{g\,cm^{-3}}$ (Möhler et al., 2008) and ρ_0 is the unit density of 1 $\mathrm{g\,cm^{-3}}$. The number distributions calculated from the APS and SMPS instruments were used to calculate the surface area distribution for each aerosol chamber run (see Eq. 20). This surface area distribution was then used to determine the

surface area on each impactor stage by integrating within the size bin of each impactor stage. The total surface area on each impactor stage was then used to calculate the $n_s(T)$ as described in Section 2.2 (Eq. 15).

$$A_s = \pi D_{ve}^2 \tag{20}$$

5.2.4 Heat Treatment Experiments

Heat treatment experiments were carried out using the protocol described in Daily et al. (2022). Aliquots of the impactor filter suspensions were transferred into 1.5 mL centrifuge tubes (Safe-Lock, Eppendorf). The aliquots were suspended in a bath of water which was heated to boiling and left to sit in the boiling water for 30 mins. The tubes were tightly closed to prevent evaporation, which would lead to an increase in the solution concentration. After heating, the aliquots were left to cool down fully before taking further ice nucleation analysis to observe any changes in ice-nucleating activity resulting from the heat treatment.

5.3 Results and Discussion

5.3.1 Freezing Temperatures and INP Concentrations

For each aerosol chamber run, we analysed the freezing activity of each impactor stage (Figure 5.5). All of the freezing activity, except for the After Filter and Stage D in Upper Field Run 1 (Figure 5.5a), were above the observed background freezing, indicating that ice-active compounds are present in the aerosolised soil dust. For the After Filter and Stage D in Upper Field Run 1, no compounds were present that were more ice-active than the handling blanks, most likely due to low particle concentrations at these size ranges (below 0.5 µm), meaning that we were unable to detect an increase in freezing activity on these filters. The observed aerosol concentrations for Upper Filed Run 1 were the lowest of all the aerosol chamber runs for this study (Table 4), with a surface area concentration of 2.6×10^{-13} $m^2\,cm^{-3}$ on Stage C. Therefore, the freezing data for the After Filter and Stage D in Upper Field Run 1 was considered to be below the limit of detection for this study and no ice-nucleating activity was detected, the data from these impactor stages was not taken forward for further analysis.

A range in freezing was observed across the different aerosol chamber runs and impactor stages, with the average freezing temperature (or T_{50}, as described in Section 2.2) ranging

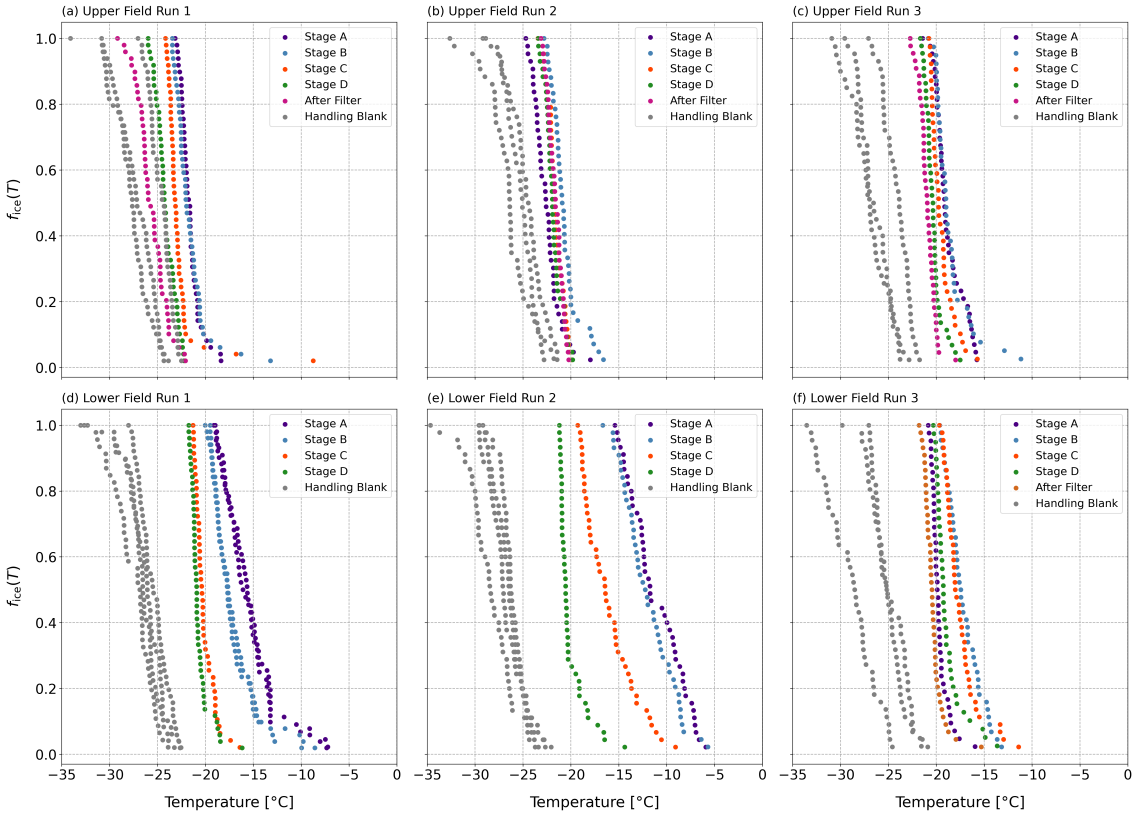

Figure 5.5: Fraction frozen ($f_{ice}(T)$) as a function of temperature for the aerosolised soil dust samples. *(a) to (c) are the Upper Field sample and (d) to (f) are the Lower Field sample.*

Table 4: Overview of each aerosol chamber run, including the volume of air sampled for each run and the surface area loading on each cascade impactor stage.

Chamber Run	Sample Vol. (L)	Surface Area Concentration per stage ($m^2\,cm^{-3}$)			
		A	B	C	D
Upper Field Run 1	621.0	1.7×10^{-11}	1.0×10^{-11}	2.6×10^{-13}	n/a
Upper Field Run 2	847.0	3.6×10^{-12}	1.2×10^{-11}	6.5×10^{-12}	4.4×10^{-12}
Upper Field Run 3	801.0	2.9×10^{-11}	7.9×10^{-11}	3.5×10^{-11}	1.6×10^{-11}
Lower Field Run 1	649.9	6.5×10^{-11}	8.4×10^{-11}	3.2×10^{-12}	n/a
Lower Field Run 2	965.8	8×10^{-10}	4.0×10^{-10}	3.8×10^{-12}	n/a
Lower Field Run 3	901.1	3.4×10^{-11}	1.9×10^{-10}	7.7×10^{-11}	3.0×10^{-11}

from −23.4 °C to −11.7 °C (Figure 5.5). This observed range in freezing temperatures was expected due to variations in the aerosol loading on the impactor stages due to different aerosol concentrations in the chamber and the size distribution of the aerosol particles (Table 4). For example, impactor Stage A in Lower Field Run 2 collected the highest surface area concentration at 8×10^{-10}, and also observed the highest freezing temperatures with a T_{50} of −11.7 °C. Additionally, higher freezing temperatures were observed for the impactor stages A and B, particles in the size range above 1.0 µm, compared to the impactor stages C and D, which contain particles between 0.25 and 1.0 µm. This observation shows that there is more ice-active material present in the particles larger than 1.0 µm, where the larger surface area loadings were also observed (see Table 4). To

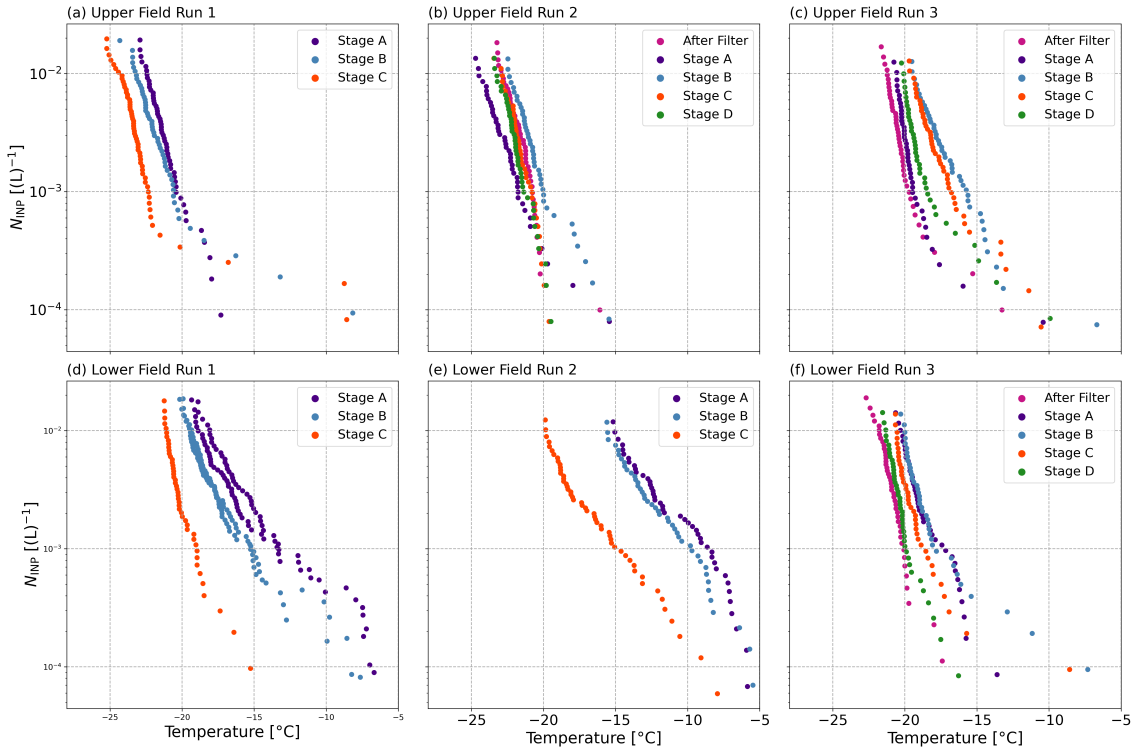

Figure 5.6: Concentration of INPs per volume of sampled air ($N_{INP}(T)$) as a function of temperature for the aerosolised soil dust samples. *(a) to (c) are the Upper Field sample and (d) to (f) are the Lower Field sample.*

further understand the relative ice-nucleating activity per surface area, further analysis was required.

We used the volume of air sampled to calculate the concentration of INPs as a function of temperature ($N_{\mathrm{INP}}(T)$) for each impactor stage (Figure 5.6). The $N_{\mathrm{INP}}(T)$ values for the larger impactor stages (Stages A and B) are up to an order of magnitude greater than the smaller size bins (Stages C and D and the After Filter) for four out of the six aerosol chamber runs. This observation shows that there is a greater proportion of ice-active material (per litre of sampled air) for particles larger than 1.0 µm, which is again due to a greater aerosol loading per surface area on these impactor stages (Table 4). Where the $N_{\mathrm{INP}}(T)$ of Stage C is greater than that of Stage A (for Upper Field Run 2 and Lower Field Run 3), the surface area loading for Stage C is also greater than Stage A (Table 4). This further demonstrates the need to normalise by the surface area loading on each impactor stage to compare the ice-nucleating activity across the different size bins.

5.3.2 Aerosol Size Distributions

The first three aerosol chamber runs, Upper Field Run 1 and Lower Field Run 1 and 2, were done using the manual aerosolisation technique (Section 5.2.2.1). During these runs,

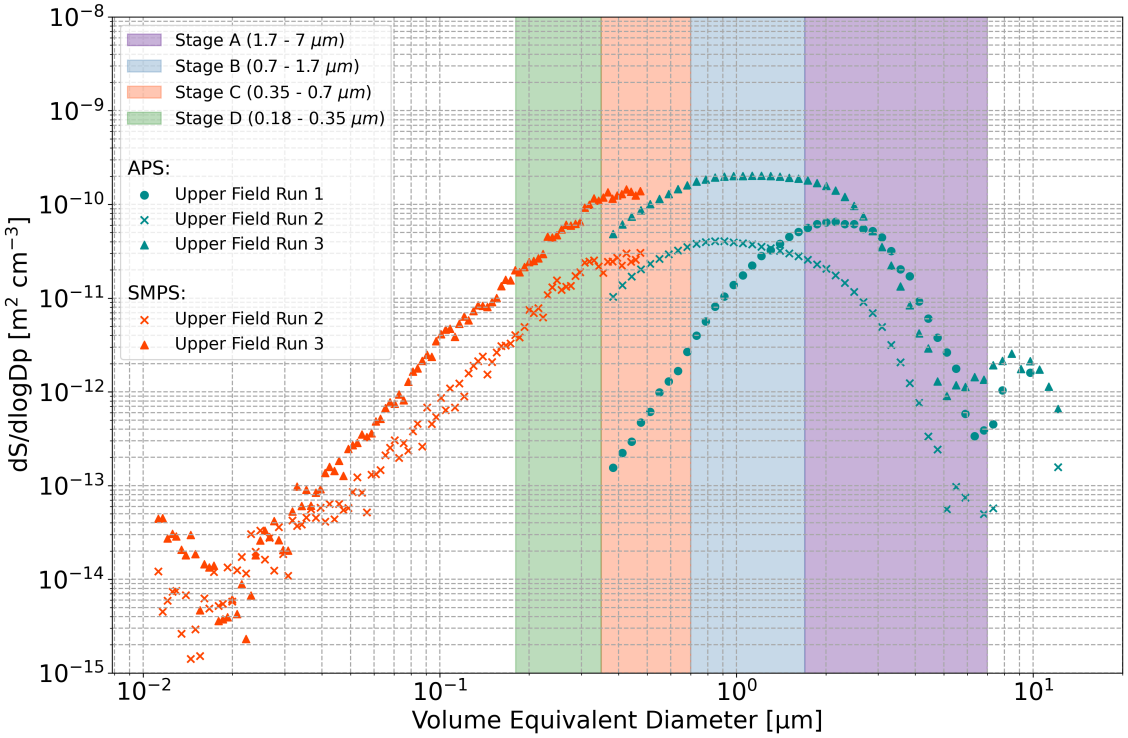

***Figure 5.7: Surface area size distribution** (dS/dlogDp) **of soil dust from the Upper Field sample,** as shown for the three different aerosol chamber runs. The shaded regions show the adjusted volume equivalent diameter size bins for the four stages of the cascade impactor calculated using Equation 19*

the neutraliser for the SMPS was not functioning, meaning that there was no standard charge applied to the aerosols. Therefore, the size segregation completed by the DMA was unreliable since it was unable to assume a standard charge across the particles. The other three aerosol chamber runs, Upper Field Run 2 and 3 and Lower Field Run 3, were done using the Dust Tower aerosolisation technique (Section 5.2.2.1). During these runs, the neutraliser was fully functioning, so the SMPS data was considered during the data analysis for these three runs but not for Upper Field Run 1 and Lower Field Run 1 and 2. The overlap between the two aerosol sizers was placed within the size range for Stage C (as shown in Figures 5.7 and 5.8). To derive the surface area loading for Stage C of each aerosol chamber run, the last few size bins from the APS were discarded and the surface area was taken from the SMPS data instead. The SMPS data was favoured at this overlap because the accuracy of detection for the lowest size bins of the APS drops significantly meaning that the APS tends to underestimate particle concentrations below about 0.8 µm.

The surface area size distributions of the different aerosol chamber runs were examined to identify the concentration of particles within each size bin of the cascade impactor (Figures 5.7 and 5.8). By examining the size distributions within the aerosol chamber, we

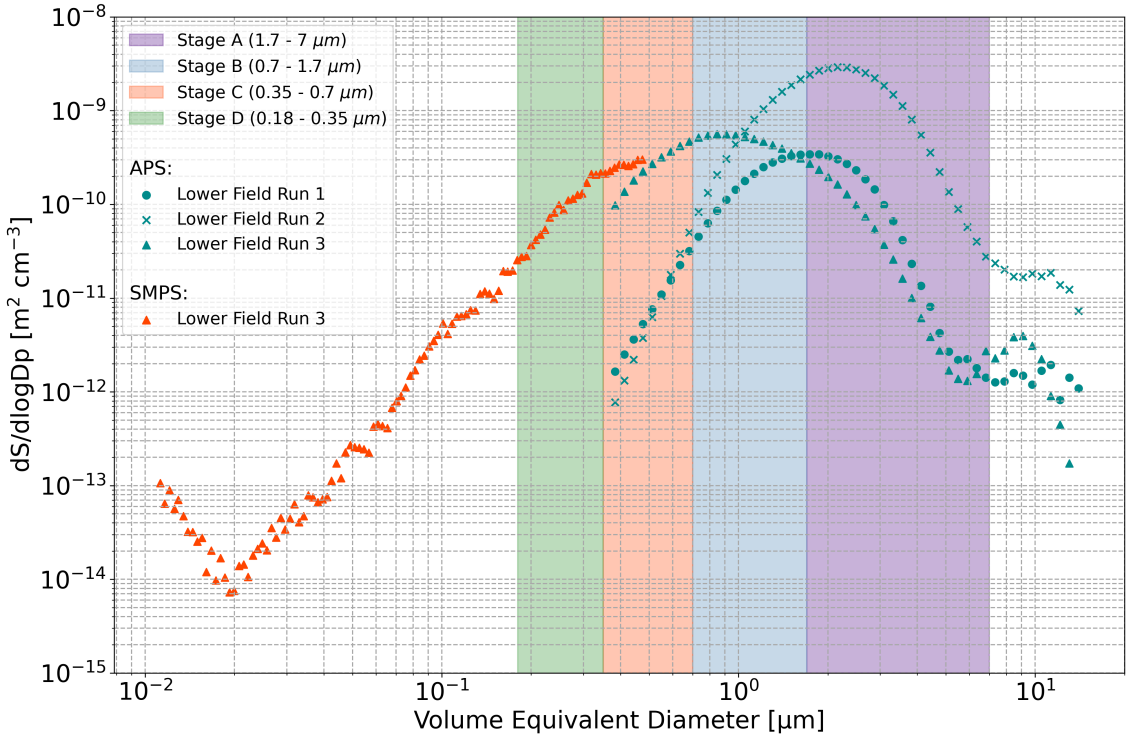

***Figure 5.8: Surface are size distribution** (dS/dlogDp) **of soil dust from the Lower Field sample,** as shown for the three different aerosol chamber runs. The shaded regions show the adjusted volume equivalent diameter size bins for the four stages of the cascade impactor calculated using Equation 19.*

were able to determine the difference in the aerosol loadings for all six chamber runs and the Upper and Lower Fields. For example, for the Upper Field soil sample, we completed three aerosol chamber runs, Upper Field Run 1 was achieved using the manual aerosol technique and Upper Field Runs 2 and 3 were done using the Dust Tower (Figure 5.7). A distinct shift in the mode diameter of the surface area concentration from around 2.5 µm to around 1 µm was observed between the manual aerosolisation technique and the Dust Tower for both the Upper Field and Lower Field samples (Figures 5.7 and 5.8). This observed shift in peak surface area concentration indicates that the Dust Tower technique leads to more fragmentation of aggregates within the soil compared to the manual bottle method. The pulse of air used in the Dust Tower method may create a higher input of energy which breaks down more aggregates leading to the production of more, smaller particles in the produced soil dust (Shao, 2001; Kok, 2011).

5.3.3 Ice-Active Site Density

The above surface area size distributions were used to calculate the ice-active site density per surface area (n_s) for each impactor stage of each aerosol chamber run, as described above in Section 5.2.3 (Figure 5.9). This normalisation was performed so that

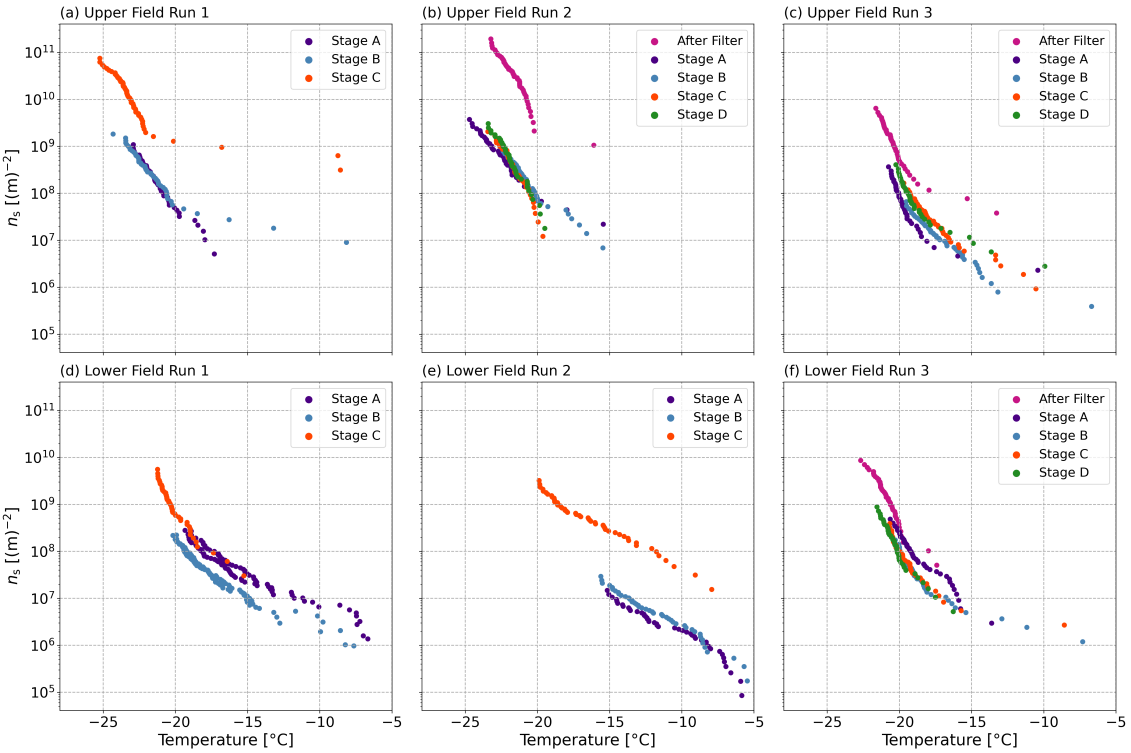

Figure 5.9: Ice-active site density per surface area (n_s) as a function of temperature for the aerosolised soil dust samples. *(a) to (c) are the Upper Field sample and (d) to (f) are the Lower Field sample.*

the differences in aerosol loading on each cascade impactor stage could be accounted for to determine the ice-nucleating activity within each size range examined. As anticipated, the differences in the surface area concentration collected on each impactor stage accounted for the observed differences in the droplet freezing temperatures. This observation indicates that the ice-active material is distributed evenly through the soil dust.

The n_s for impactor Stage C in Upper Field Run 1 and Lower Field Runs 1 and 2 were calculated using the surface area from the APS only since the SMPS data from these runs was unreliable. The size range for Stage C of the cascade impactor falls at the lower end of the range of sizes covered by the APS instrument, therefore the limit of detection for these lowest bin sizes is much lower than the rest of the size ranges for the APS. Therefore, the surface area collected onto Stage C was likely underestimated for these aerosol chamber runs, resulting in an overestimation of the n_s, so we decided to remove these runs from any further analysis. Additionally, the filter holder used for the After Filter runs was suspected to leak, meaning that the After Filter was subject to contamination from the lab air, also leading to an overestimation of the n_s. Therefore, the After Filter runs were also removed from all future analysis.

The n_s values from the Upper Field sample were compared with that of the Lower

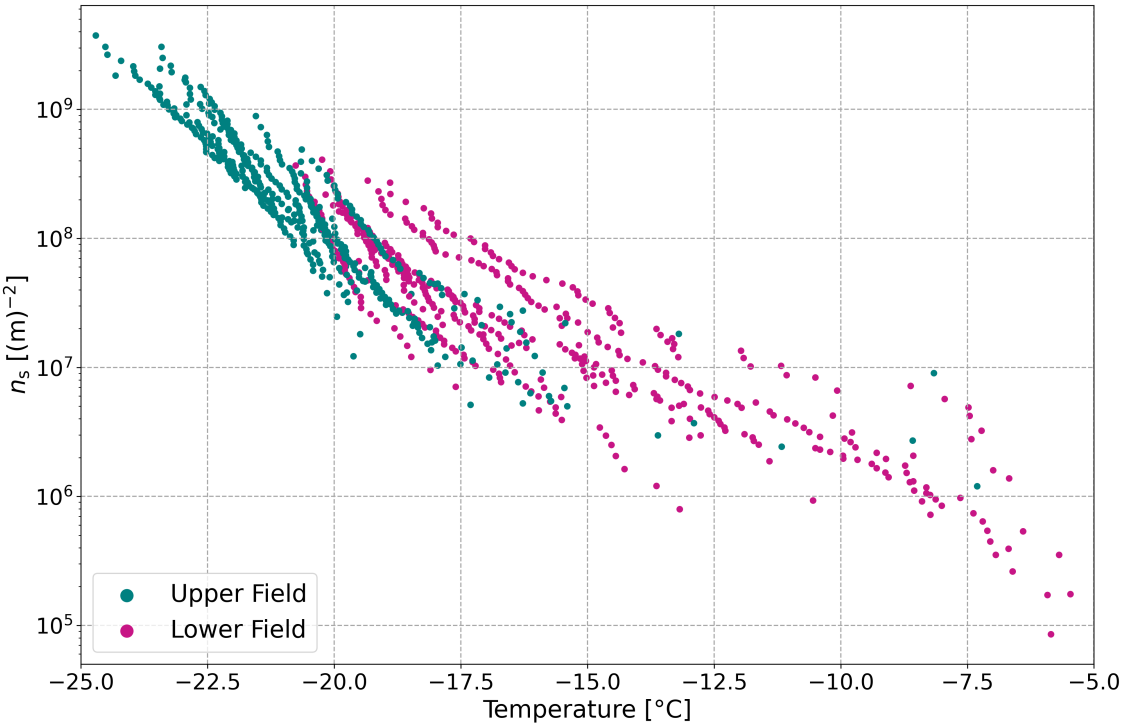

Figure 5.10: Ice-active site density per surface area (n_s) as a function of temperature for the Upper Field and Lower Field soil samples.

Field sample (Figure 5.10). Once normalised by surface area, the Upper and Lower Field samples aligned as a function of temperature to within 1 °C. Therefore, the observed range in $f_{\mathrm{ice}}(T)$ between the Upper and Lower Field samples can be explained by differences in aerosol loadings within the aerosol chamber runs. Higher aerosol concentrations were achieved during the Lower Field runs, meaning more of the INP spectra could be analysed.

It is commonly accepted that aerosol particles larger than 1 micron (supermicron particles) dominate the ice-nucleating activity of dust aerosols, particularly in mineral dust (DeMott et al., 2010; Mason et al., 2016; Reicher et al., 2019). For example, Reicher et al. (2019) sampled a variety of dust events in the Mediterranean to determine the size-resolved INP concentrations of mineral dust emissions. They found that supermicron particles had higher INP concentrations and n_{s} values compared to submicron particles, suggesting that supermicron particles dominate the ice-nucleating activity in mineral dust (Reicher et al., 2019). Although other studies have examined the ice-nucleating activity of agricultural soil dust, the size-resolved INP concentrations of soil dust have not previously been examined. Here, we were able to show that the ice-nucleating ability of soil dust is evenly distributed across its size distribution and that supermicron particles do not dominate ice nucleation in these aerosols. As shown in the previous chapters of this thesis (Sections 3 and 4), biological material plays an important role in the ice-nucleating ability

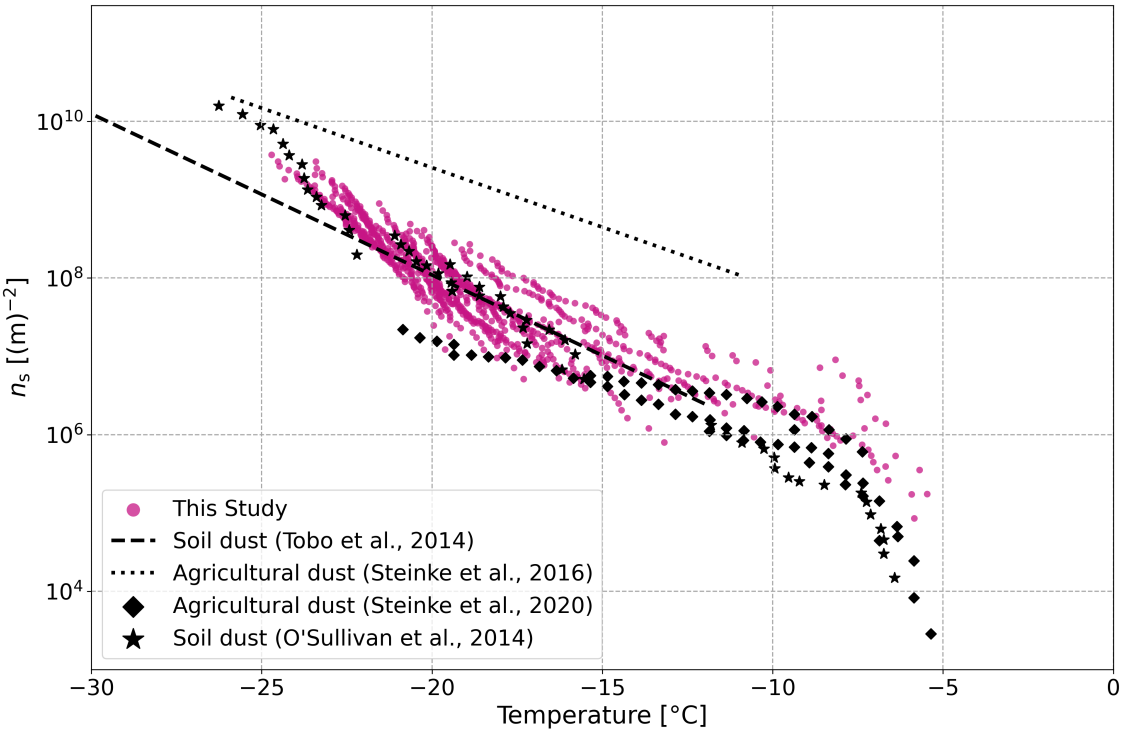

Figure 5.11: Ice-active site density per surface area (n_s) as a function of temperature for each aerosol chamber run for all of the analysed soil samples. *For comparison, n_s values from O'Sullivan et al. (2014), Tobo et al. (2014), Steinke et al. (2016) and Steinke et al. (2020).*

of agricultural soil dust. Therefore, the results of this chapter indicate that the biological material associated with the ice-nucleating activity of soil dust can adhere to soil particles of any size and that the size range of the ice-nucleating activity is not dependent on the size range of the material itself. This finding is supported by work from O'Sullivan et al. (2016), which showed that ice-active proteins adsorb onto clay particles effectively whilst maintaining their ice-nucleating activity, effectively passing their ice-nucleating activity to the mineral particles. Therefore, these observations suggest that biological nanoparticles with high ice-nucleating activity are distributed across the size ranges and are responsible for the overall ice-nucleating ability of agricultural soils. The observations also suggest that the ice-nucleating activity of agricultural soils is not attributable to material of specific size ranges, such as whole bacteria cells or bacterial fragments.

The n_s values from this study were compared to those of previous studies that also examined the ice-nucleating activity of agricultural soils (Figure 5.11). In general, the observed n_s values from this study fit well with the n_s parameterisation as derived from Tobo et al. (2014) but up to an order of magnitude lower than the parameterisation derived by Steinke et al. (2016). The n_s values aligned well with n_s values measured by O'Sullivan et al. (2016) and Steinke et al. (2020). The samples from O'Sullivan et al. (2014) were

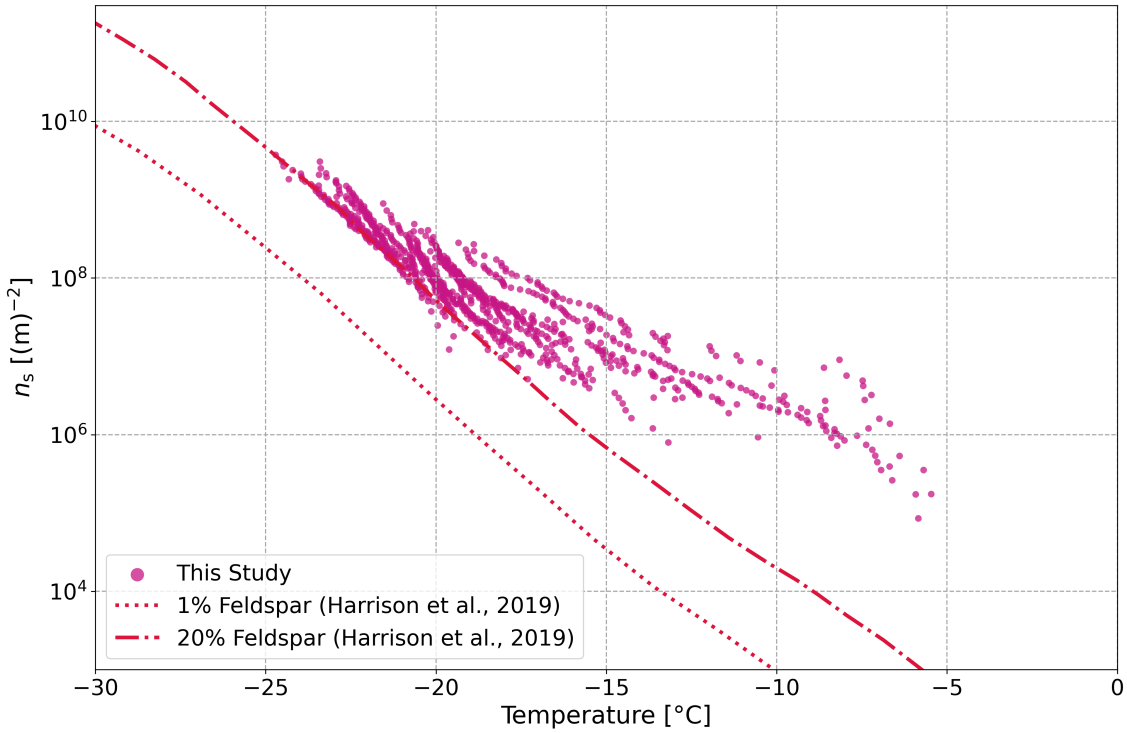

Figure 5.12: Comparison between ice-active site density per surface area (n_s) as a function of temperature for this study with parameterisations of n_s from the literature. *Including comparisons with O'Sullivan et al. (2014), Steinke et al. (2016) and parameterisations for 1% and 20% K-feldspar from Harrison et al. (2019)*

also collected from agricultural fields in the UK, therefore the consistency between the results shown in this chapter and the results from O'Sullivan et al. (2014) indicate that the ice-nucleating activity of agricultural soils remains consistent on local regional scales. On the other hand, the samples from Steinke et al. (2020) were collected from agricultural fields in Germany, so this further confirms the consistency of the ice-nucleating activity of agricultural soils on wider regional scales. However, more work would be required to determine the consistency of the ice-nucleating activity of these soils more closely. In addition, both the findings observed in this chapter and the findings from agricultural soils samples in Steinke et al. (2020) show a biological hump in n_s at around $-7\,°C$.

While biological materials are more highly ice-nucleating, mineral dust is prevalent at much higher atmospheric loadings, meaning that the ice-nucleating activity is often dominated by mineral dust aerosol. So, to better understand the relative contribution of mineral dust compared to biological material as ice-nucleating material within our soil samples, we also compared our measured n_s values with parameterisations for the n_s of mineral dust where 1% or 20% of the mineral surface area is made of K-feldspar, as characterised by Harrison et al. (2019) (Figure 5.12). We can see that the 20% K-felspar parameterisation suggests that K-feldspar is contributing to the ice-nucleating activity of

our soil dust at temperatures below −18 °C. However, a large fraction of the observed ice-nucleating activity, especially at warmer freezing temperatures, is much greater than that of 20% K-feldspar aerosol, indicating that the ice-nucleating activity of agricultural soils is not attributable to mineral dust particles above −18 °C, further indicating the potential contribution from biological nanoparticles.

5.3.4 Heat Sensitivity

Heat tests were performed on a representative chamber run from each of the sampled locations (Upper Field Run 1 and Lower Field Run 2), to identify heat-liable biological material within the aerosolised soil dust samples, as previously examined by Hill et al. (2016) and O'Sullivan et al. (2018). For Upper Field Run 1, $N_{\mathrm{INP}}(T)$ increases by up to 4.3×10^{-4} L^{-1} after heating Stage A and decreases by up to 4×10^{-4} L^{-1} after heating for Stage B (Figure 5.13). For Lower Field Run 2, $N_{\mathrm{INP}}(T)$ decreases by up to an order of magnitude after heating for freezing temperatures above −10 °C. Below −10 °C, the heat treatment increased the observed $N_{\mathrm{INP}}(T)$ by up to 7.5×10^{-3} L^{-1}.

As discussed in Section 1.3, if heat-sensitive biological material was present in our aerosolised soil dust, we would have expected to observe a decrease in the ice-nucleating activity. This is usually because proteinaceous ice-active substances become denatured when heated, resulting in a loss of their ice-nucleating ability (Daily et al., 2022). If heat-stable organics or mineral dust is present in our agricultural soils, we would expect heating to have no effect on the ice-nucleating ability of the soils (O'Sullivan et al., 2014; Suski et al., 2018). The observed increase in $N_{\mathrm{INP}}(T)$ after exposure to heat treatments in this study is unusual but has been observed before, by McCluskey et al. (2018) and in Section 3 of this thesis. Increases in freezing activity after heating is likely due to the breakdown of biological macromolecular aggregates, leading to the redistribution of the macromolecules and the exposure of ice-active sites. McCluskey et al. (2018) also hypothesised that heat treatments led to the breakdown of cell walls, which results in the release of ice-nucleating macromolecules into solution and an increase in ice-nucleating activity. The release of biological macromolecules into solution as a result of the heating experiments could explain the increase in INP concentrations observed in this study.

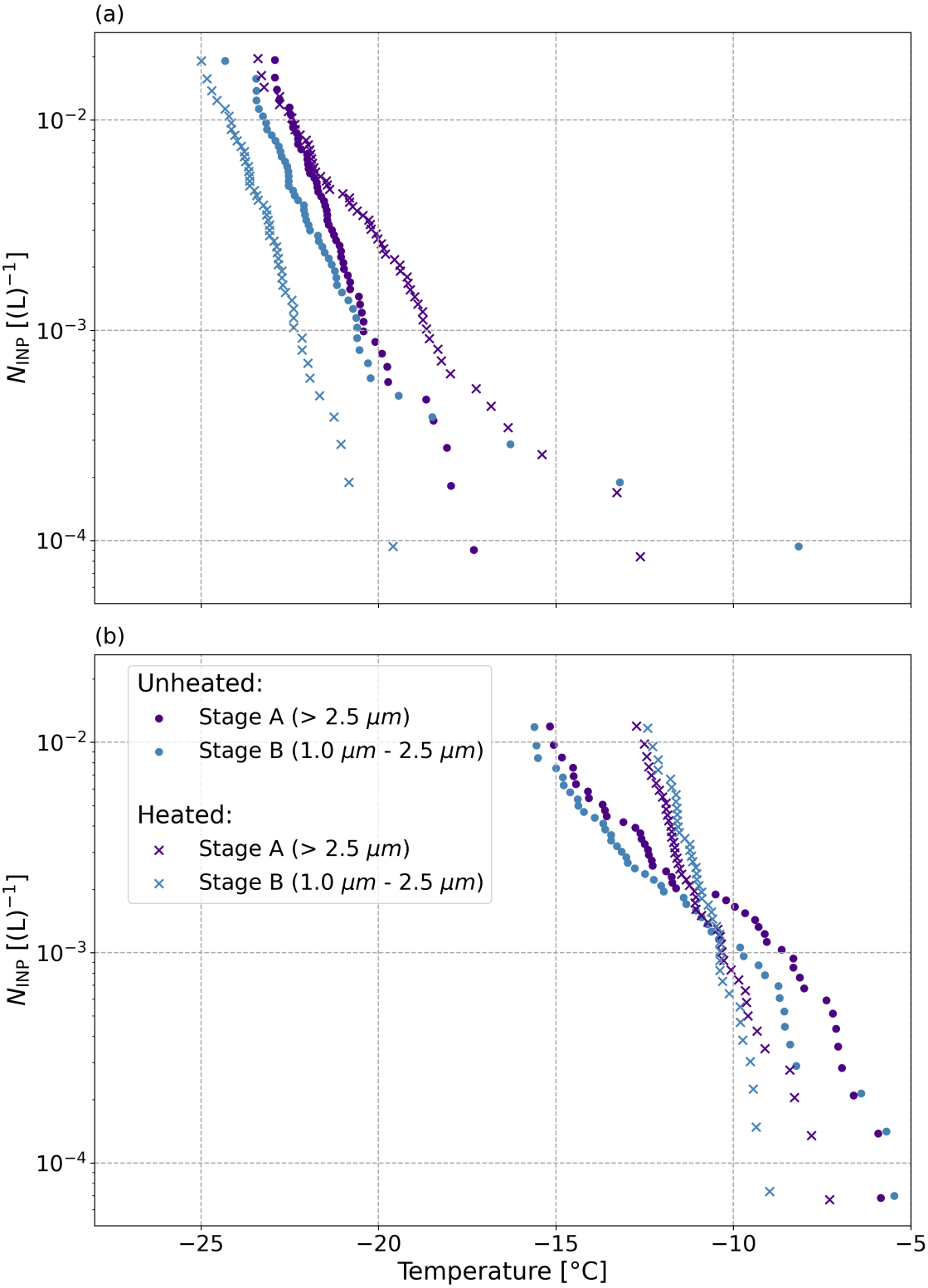

Figure 5.13: Concentration of INPs per volume of sampled air ($N_{INP}(T)$) as a function of temperature before and after heating for two of the aerosol chamber runs. *(a) is Upper Field Run 1 and (b) is Lower Field Run 2.*

5.4 Conclusions

This chapter investigated the size-segregated ice-nucleating activity within agricultural soil samples from two different agricultural fields west of Leeds in the UK. The ice-active site density per surface area was uniformly distributed across the analysed size ranges; 0.25-0.5 µm (Stage D), 0.5-1.0 µm (Stage C), 1.0-2.5 µm (Stage B) and $>$ 2.5 µm (Stage A). After heating the aerosolised soil samples, an increase in INP concentration was observed. These observations are consistent with biological macromolecules which become associated with soil particles, influencing their ice-nucleating activity. Our results align well with previous literature, indicating that the ice-nucleating activity of different agricultural soils remains consistent across different mid-latitude locations.

Heat tests confirmed the presence of heat-sensitive INPs within the analysed samples, indicating that at least some of the observed ice-nucleating activity was likely attributable to heat-sensitive biological components. We also observed some increases in freezing activity after exposure to heat. This also indicates the presence of biological macromolecules since the increase in freezing activity was likely due to the breakdown of aggregates or cell walls, leading to the release of ice-active sites for nucleation.

References

Augustin-Bauditz, S., Wex, H., Denjean, C., Hartmann, S., Schneider, J., Schmidt, S., Ebert, M., and Stratmann, F. (2016). Laboratory-generated mixtures of mineral dust particles with biological substances: characterization of the particle mixing state and immersion freezing behavior. *Atmospheric Chemistry and Physics*, 16(9):5531–5543.

Bogler, S. and Borduas-Dedekind, N. (2020). Lignin's ability to nucleate ice via immersion freezing and its stability towards physicochemical treatments and atmospheric processing. *Atmospheric Chemistry and Physics*, 20(23):14509–14522.

Burkart, J., Gratzl, J., Seifried, T. M., Bieber, P., and Grothe, H. (2021). Isolation of subpollen particles (SPPs) of birch: SPPs are potential carriers of ice nucleating macromolecules. *Biogeosciences*, 18(20):5751–5765.

Cascajo-Castresana, M., David, R. O., Iriarte-Alonso, M. A., Bittner, A. M., and Marcolli, C. (2020). Protein aggregates nucleate ice: the example of apoferritin. *Atmospheric Chemistry and Physics*, 20(6):3291–3315.

Conen, F., Morris, C. E., Leifeld, J., Yakutin, M. V., and Alewell, C. (2011). Biological residues define the ice nucleation properties of soil dust. *Atmospheric Chemistry and Physics*, 11(18):9643–9648.

Daily, M. I., Tarn, M. D., Whale, T. F., and Murray, B. J. (2022). An evaluation of the heat test for the ice-nucleating ability of minerals and biological material. *Atmospheric Measurement Techniques*, 15(8):2635–2665.

DeMott, P. J., Prenni, A. J., Liu, X., Kreidenweis, S. M., Petters, M. D., Twohy, C. H., Richardson, M. S., Eidhammer, T., and Rogers, D. C. (2010). Predicting global atmospheric ice nuclei distributions and their impacts on climate. *Proceedings of the National Academy of Sciences*, 107(25):11217–11222.

Feichter, J. and Leisner, T. (2009). Climate engineering: A critical review of approaches to modify the global energy balance. *The European Physical Journal Special Topics*, 176(1):81–92.

Harrison, A. D., Lever, K., Sanchez-Marroquin, A., Holden, M. A., Whale, T. F., Tarn, M. D., McQuaid, J. B., and Murray, B. J. (2019). The ice-nucleating ability of quartz immersed in water and its atmospheric importance compared to K-feldspar. *Atmospheric Chemistry and Physics*, 19(17):11343–11361.

Hill, T. C. J., DeMott, P. J., Tobo, Y., Fröhlich-Nowoisky, J., Moffett, B. F., Franc, G. D., and Kreidenweis, S. M. (2016). Sources of organic ice nucleating particles in soils. *Atmospheric Chemistry and Physics*, 16(11):7195–7211.

Kok, J. F. (2011). A scaling theory for the size distribution of emitted dust aerosols suggests climate models underestimate the size of the global dust cycle. *Proceedings of the National Academy of Sciences*, 108(3):1016–1021.

Mason, R. H., Si, M., Chou, C., Irish, V. E., Dickie, R., Elizondo, P., Wong, R., Brintnell, M., Elsasser, M., Lassar, W. M., Pierce, K. M., Leaitch, W. R., MacDonald, A. M., Platt, A., Toom-Sauntry, D., Sarda-Estève, R., Schiller, C. L., Suski, K. J., Hill, T. C. J., Abbatt, J. P. D., Huffman, J. A., DeMott, P. J., and Bertram, A. K. (2016). Size-resolved measurements of ice-nucleating particles at six locations in North America and one in Europe. *Atmospheric Chemistry and Physics*, 16(3):1637–1651.

McCluskey, C. S., Hill, T. C. J., Sultana, C. M., Laskina, O., Trueblood, J., Santander, M. V., Beall, C. M., Michaud, J. M., Kreidenweis, S. M., Prather, K. A., Grassian, V., and DeMott, P. J. (2018). A Mesocosm Double Feature: Insights into the Chemical Makeup of Marine Ice Nucleating Particles. *Journal of the Atmospheric Sciences*, 75(7):2405–2423.

Möhler, O., Benz, S., Saathoff, H., Schnaiter, M., Wagner, R., Schneider, J., Walter, S., Ebert, V., and Wagner, S. (2008). The effect of organic coating on the heterogeneous ice nucleation efficiency of mineral dust aerosols. *Environmental Research Letters*, 3(2):025007.

O'Sullivan, D., Adams, M. P., Tarn, M. D., Harrison, A. D., Vergara-Temprado, J., Porter, G. C. E., Holden, M. A., Sanchez-Marroquin, A., Carotenuto, F., Whale, T. F., McQuaid, J. B., Walshaw, R., Hedges, D. H. P., Burke, I. T., Cui, Z., and Murray, B. J. (2018). Contributions of biogenic material to the atmospheric ice-nucleating particle population in North Western Europe. *Scientific Reports*, 8(1):13821.

O'Sullivan, D., Murray, B. J., Malkin, T. L., Whale, T. F., Umo, N. S., Atkinson, J. D., Price, H. C., Baustian, K. J., Browse, J., and Webb, M. E. (2014). Ice nucleation by fertile soil dusts: relative importance of mineral and biogenic components. *Atmospheric Chemistry and Physics*, 14(4):1853–1867.

O'Sullivan, D., Murray, B. J., Ross, J. F., and Webb, M. E. (2016). The adsorption of fungal ice-nucleating proteins on mineral dusts: a terrestrial reservoir of atmospheric ice-nucleating particles. *Atmospheric Chemistry and Physics*, 16(12):7879–7887.

O'Sullivan, D., Murray, B. J., Ross, J. F., Whale, T. F., Price, H. C., Atkinson, J. D., Umo, N. S., and Webb, M. E. (2015). The relevance of nanoscale biological fragments for ice nucleation in clouds. *Scientific Reports*, 5(1):8082.

Ponsonby, J., King, L., Murray, B. J., and Stettler, M. E. J. (2024). Jet aircraft lubrication oil droplets as contrail ice-forming particles. *Atmospheric Chemistry and Physics*, 24(3):2045–2058. Publisher: Copernicus GmbH.

Porter, G. C. E., Sikora, S. N. F., Adams, M. P., Proske, U., Harrison, A. D., Tarn, M. D., Brooks, I. M., and Murray, B. J. (2020). Resolving the size of ice-nucleating particles with a balloon deployable aerosol sampler: the SHARK. *Atmospheric Measurement Techniques*, 13(6):2905–2921.

Reicher, N., Budke, C., Eickhoff, L., Raveh-Rubin, S., Kaplan-Ashiri, I., Koop, T., and Rudich, Y. (2019). Size-dependent ice nucleation by airborne particles during dust events in the eastern Mediterranean. *Atmospheric Chemistry and Physics*, 19(17):11143–11158.

Shao, Y. (2001). A model for mineral dust emission. *Journal of Geophysical Research: Atmospheres*, 106(D17):20239–20254. _eprint: https://onlinelibrary.wiley.com/doi/pdf/10.1029/2001JD900171.

Shi, Z. B., Woodhouse, M. T., Carslaw, K. S., Krom, M. D., Mann, G. W., Baker, A. R., Savov, I., Fones, G. R., Brooks, B., Drake, N., Jickells, T. D., and Benning, L. G. (2011). Minor effect of physical size sorting on iron solubility of transported mineral dust. *Atmospheric Chemistry and Physics*, 11(16):8459–8469. Publisher: Copernicus GmbH.

Si, M., Irish, V. E., Mason, R. H., Vergara-Temprado, J., Hanna, S. J., Ladino, L. A., Yakobi-Hancock, J. D., Schiller, C. L., Wentzell, J. J. B., Abbatt, J. P. D., Carslaw, K. S., Murray, B. J., and Bertram, A. K. (2018). Ice-nucleating ability of aerosol particles and possible sources at three coastal marine sites. *Atmospheric Chemistry and Physics*, 18(21):15669–15685.

Steinke, I., Funk, R., Busse, J., Iturri, A., Kirchen, S., Leue, M., Möhler, O., Schwartz, T., Schnaiter, M., Sierau, B., Toprak, E., Ullrich, R., Ulrich, A., Hoose, C., and Leisner, T. (2016). Ice nucleation activity of agricultural soil dust aerosols from Mongolia, Argentina, and Germany. *Journal of Geophysical Research: Atmospheres*, 121(22):13,559–13,576.

Steinke, I., Hiranuma, N., Funk, R., Höhler, K., Tüllmann, N., Umo, N. S., Weidler, P. G., Möhler, O., and Leisner, T. (2020). Complex plant-derived organic aerosol as ice-nucleating particles – more than the sums of their parts? *Atmospheric Chemistry and Physics*, 20(19):11387–11397.

Suski, K. J., Hill, T. C. J., Levin, E. J. T., Miller, A., DeMott, P. J., and Kreidenweis, S. M. (2018). Agricultural harvesting emissions of ice-nucleating particles. *Atmospheric Chemistry and Physics*, 18(18):13755–13771.

Tobo, Y., DeMott, P. J., Hill, T. C. J., Prenni, A. J., Swoboda-Colberg, N. G., Franc, G. D., and Kreidenweis, S. M. (2014). Organic matter matters for ice nuclei of agricultural soil origin. *Atmospheric Chemistry and Physics*, 14(16):8521–8531.

6 Conclusions

In this thesis, agricultural sources of INPs were investigated and characterised, with a focus on agricultural soils and fungal crop pathogens. The overall goal of this thesis was to determine the extent to which agriculture influences INP populations on both regional and global scales. A range of measurements and analysis techniques were used to address the gaps in our understanding of these agricultural INP sources and their potential impact on cloud microphysical properties. We started by examining the ice-nucleating activity of the submicron entities within agricultural soil samples. Then we investigated the ice-nucleating activity of two common fungal crop pathogens that were collected from the field and grown in the lab. Finally, we analysed the size-resolved concentrations of INPs in agricultural soil samples, aiming to understand how ice-active material was distributed across different particle sizes in agricultural soil dust.

6.1 Summary of Findings

6.1.1 Ice-Nucleating Macromolecules in Agricultural Soils

In Chapter 3, we investigated the contribution of surfactant macromolecules to the ice-nucleating activity of soil extracts and their subcomponents. Soil samples were collected from three different agricultural locations in the UK and Canada; the University of British Columbia Farm in Canada, the University of Leeds Farm in the UK and Rothamsted Research in Harpenden, UK. The submicron entities within each soil sample were extracted by filtering the soil solutions to 0.22 µm to analyse their ice-nucleating ability and surface activity. Two examples of common soil subcomponents, lignin and Snomax, were also analysed for their ice-nucleating and surface activities to compare to the extracted soil solutions.

The ice nucleation analysis of the extracted soil samples revealed a large variation in ice-nucleating activity across different sample locations which could not be explained by different levels of dissolved organic carbon or mass of material in the soil solutions. Similar studies have also shown a large variation in the ice-nucleating activity of agricultural soil from different locations without being able to link the observed variation to organic content or the presence of ice-active bacteria (Garcia et al., 2012; O'Sullivan et al., 2014). This study also aimed to investigate the relationship between surface and ice-nucleating abilities within extracted organic solutions. There was little to no reduction in surface

tension measurements observed from the soil extract solutions (relative to pure water), indicating that the concentration of surfactants in the extract solutions was insignificant. Therefore, we concluded that the observed range in freezing activity between the different soil samples would also not be explained by differences in surfactant concentrations within the solutions. For the soil subcomponents analysed during this study, there was an observed reduction in surface tension relative to pure water, indicating the presence of surfactant macromolecules. There was also an observed correlating increase in ice-nucleating activity with increasing surfactant concentrations, although other components within the solutions would also have been increasing in concentration so we were unable to determine that it was the surfactants themselves acting as ice-nucleating macromolecules within these subcomponent solutions. Further work is needed to further unpick the complexity of the ice-nucleating activity of agricultural soils.

Our results also suggested that aggregation may play a role in the ice-nucleating ability of agricultural soils. For example, the ice-active mass density (n_{m}) of the Rothamsted did not align as a function of temperature indicating that possible aggregation of macromolecules at higher concentrations was blocking nucleation sites. We also observed a slight increase in ice-nucleating activity after heat treatment for our UoL sample, which indicates that aggregates are dissolving and releasing ice-active sites into the solution. This aggregation, however, was not linked to the saturation of surfactants at the surface and the formation of micelles. Our findings also suggest that other, non-aggregating substances may be controlling the ice-nucleating ability of agricultural soils. To better understand if the formation of aggregates within soil extract solutions aids in their ability to nucleate ice, or hinders it, future work could investigate aggregates of organic macromolecules in more detail to determine what aggregate formations may be ideal to template ice formation.

We also examined the effect of filtration on the ice-nucleating activity of Snomax solutions. Our results show that filtering the Snomax solutions to 0.22 µm did not significantly reduce the observed ice-nucleating activity of the solutions. It was previously understood that the ice-active proteins responsible for the observed ice-nucleating activity of certain bacteria species (particularly *P. syringae*, the species found in Snomax) need to aggregate onto the surface of intact cells or cell fragments to maintain their ice-nucleating activity. Therefore, some previous studies have used filtration to assume the removal of bacterial ice-nucleating proteins so that other ice-nucleating materials can be examined (Maki et al., 1974; Felgitsch et al., 2018; Ickes et al., 2020). Our findings suggest that filtration

to 0.22 µm may not remove all ice-nucleating activity from bacterial proteins and therefore suggest that other techniques are required to remove the activity from bacterial proteins in field samples fully.

6.1.2 Fungal Crop Pathogens as Ice-Nucleating Particles

Chapter 4 investigated the ice-nucleating ability of two different species of fungal crop pathogen commonly found in agricultural fields in the UK. The ice-nucleating activity of the fungal spores of *P. striiformis*, which causes Yellow Rust (YR) infection on wheat crops, and *P. brassicae*, which causes Light Leaf Spot (LLS) infections on oilseed rape crops, were examined. Both the fungal spores of YR and the fungal spores of LLS have a small ice-nucleating ability which is very similar to the ice-nucleating ability of other rust species such as wheat leaf rust. This is a potentially important finding, especially because future climate warming will likely increase the presence of these fungal pathogens and soils may act as a reservoir for these INPs, creating a potentially significant source of INPs into the atmosphere.

However, lab-based experiments with LLS suggested that the ice-nucleating ability of the LLS spores found on the leaves of oilseed rape is attributable to bacteria also found in the leaves and may not be attributable to the fungal spores themselves. The normalised ice-active mass site density (n_{m}) of the YR spores was also compared with the n_{m} of *Fusarium* fungal material, showing that the freezing behaviour of *Fusarium* is distinctly different to that of YR spores. This observation indicates that the mechanism for ice nucleation in YR fungal spores is different from that of *Fusarium* fungal species, which have been shown to be proteinaceous.

The impact of freezing and storage length on the ice-nucleating ability of these fungal spore samples was also examined. Our findings were in agreement with previous studies which found that storage can lead to a decrease in ice-nucleating ability, particularly at temperatures above $-20\,^{\circ}\mathrm{C}$ (Polen et al., 2016; Beall et al., 2020). However, we also showed that this loss of ice-nucleating activity can be unpredictable, since the fungal spore suspension we tested from 1996, which had been frozen for the last 27 years, still showed a significant amount of freezing above $-20\,^{\circ}\mathrm{C}$, suggesting that ice-nucleating activity is not always lost during storage. This observed ice-nucleating activity may be a result of freezing enhancing ice-nucleating activity, as seen in previous studies (Beall et al., 2020; Perkins et al., 2020). Similarly, we observed an increase in ice-nucleating activity in the

agar plate extract solutions after freezing. This observed increase in ice-nucleating activity after freezing could indicate a mechanism by which ice-active molecules are released upon freezing, but further work would be required to better quantify this. The observed ice-nucleating activity of agar also indicated the potential for contamination from agar when culturing fungus (or potentially other species) in the lab. Other extraction techniques should be considered to reduce this contamination in the future.

6.1.3 Distribution of Ice-Nucleating Activity in Agricultural Soil Dust

Chapter 5 analysed the size-resolved INP concentrations across aerosolised agricultural soil dust samples from the University of Leeds Research Farm. When normalised by the total surface area on each cascade impactor, the ice-nucleating activity was uniformly distributed throughout the analysed size ranges across the aerosolised soil dust. These observations suggest that submicron particles may contribute more significantly to INP populations compared to pure mineral dust or other ambient dust aerosols (DeMott et al., 2010; Mason et al., 2016; Reicher et al., 2019). The nature of ice nucleation in agricultural soils is attributable to biological material within the soil, therefore, these findings indicate that this biological material is evenly distributed across the soil dust particle sizes and is most likely associated with macromolecules.

Heat tests confirmed the presence of heat-sensitive INPs within the analysed samples, indicating that at least some of the observed ice-nucleating activity was likely attributable to heat-sensitive biological components. We also observed some increases in freezing activity after exposure to heat. This also indicates the presence of biological macromolecules since the increase in freezing activity was likely due to the breakdown of aggregates or cell walls, leading to the release of ice-active sites for nucleation.

6.2 Limitations

The main limitation of the work presented in Chapter 3 was the transportation of the soil samples which were collected in the UK. The soil samples which were collected at the University of Leeds Farm and Rothamsted Research Farm were shipped frozen to the University of British Columbia so that the same analysis could be applied to all three soil samples. However, this meant that the UK soil samples were frozen and stored for up to five months before any analysis took place. As highlighted in Chapter 4 of this thesis, freezing and storage of biological INPs may impact their ice-nucleating potential. Since we

were unable to control the freezing and length of storage of the soil samples in this study, we cannot rule out the possibility that these factors significantly impacted the observed ice-nucleating activities.

In addition, the number and variety of soil samples were important limitations for both Chapter 3 and Chapter 5 of this thesis. Since we were only able to collect soil samples from three agricultural locations, we cannot confirm whether these samples are representative of mid-latitude agricultural locations. Many different factors may impact the content of the collected sample and their ability to nucleate ice, such as the type of soil, the crops grown, the fertilisers used and the weather conditions. For these reasons, the ice-nucleating activity of these agricultural soils likely changes with the season. Therefore, examining the seasonality of the ice-nucleating activity of these soils may be worthwhile.

6.3 Future Work

The thesis has furthered the knowledge and understanding of agricultural sources of INPs in the atmosphere but has also highlighted some key questions that remain unanswered. The work in this thesis has emphasised the complexity of the ice-nucleating activity of these fertile soils and our need to unpick this complexity to understand better why some agricultural soils nucleate ice more efficiently than others. Chapter 3 suggested that aggregation of macromolecules may play a role in the ice-nucleating activity of agricultural soils, but further work would be needed to understand the relative importance of aggregating macromolecules better. We know that aggregation is important when it comes to the ice-nucleating activity of ice-active proteins, such as those derived from bacteria (Qiu et al., 2019; Hartmann et al., 2022; Lukas et al., 2020), but few studies have investigated the aggregation of other ice-nucleating substances, which may also be important (Dreischmeier et al., 2017). In addition, surfactants have a higher impact on surface tension in small, more cloud-relevant droplet sizes (Bzdek et al., 2020), therefore, the relative importance of surfactant macromolecules to the ice-nucleating activity of agricultural soils may be greater for pico-litre sized droplets. I propose that a future study would investigate surfactant macromolecules and aggregation more closely to examine how the formation of aggregates impacts the ice-nucleating activity of different substances. One way to achieve this would be to use similar techniques to those used by Bzdek et al. (2020), which would mean implementing holographic optical tweezers to optically trap cloud-relevant sized droplets, then using different lab techniques to analyse the structure

of aggregates forming in the droplet and to measure the surface tension reductions. If possible, we could then freeze the droplets and observe the impact of these aggregates on the ice-nucleating activity of the solution.

The work in Chapter 4 highlighted the potential of agar growth medium used to grow fungi and bacteria in the lab. I propose future work would investigate this potential source of contamination and the ice-nucleating activity of red algae, which is the main component of most agar. Agar itself consists of polysaccharides derived from the cell walls of red algae. I hypothesise that it is these polysaccharides which are responsible for the ice-nucleating activity of the agar blanks, which would be in agreement with work completed by Fröhlich-Nowoisky et al. (2015), who discussed using agarose as a substitute to standard agar due to the presence of ice-nucleating activity found in agar. However, agar also consists of other components, which act as food for whatever is being grown in the agar plates. For example, in Chapter 4, the agar used also contained malt extract as an energy source for the growth of *P. brassicae* on the agar plate. Since malt extract is also made up of polysaccharides, it may also be a source of ice-nucleating contamination, which would again agree with Fröhlich-Nowoisky et al. (2015), who also found ice-nucleating activity in MEA. Some previous studies extracted the fungal spores using a flow cell, which aerosolises the spores and deposits them by impacting them straight onto a filter or a hydrophobic slide (Iannone et al., 2011; Haga et al., 2013). This extraction technique may reduce the ice-nucleating contamination from the agar compared to the extraction techniques described in Chapter 4. I propose that further work would investigate different types of agar growth mediums and different extraction techniques to understand the level of ice-nucleating contamination from each and how this may impact future lab-based studies of fungal and bacterial INPs. Working with known quantities of agar would allow us to identify the normalised ice-nucleating activity of the agar and to determine if the observed increase in freezing temperatures after exposure to cold stress was due to an increase in ice-nucleating activity or the release of ice-nucleating material. Additionally, it may highlight other potential sources of INPs and the nature of these INPs. If the agar itself is ice-nucleating active, this shows that the polysaccharides of red algae are ice-active. Future increases in algae blooms due to oceanic warming may create a significant source of atmospheric INP.

In Chapter 4, it was also demonstrated that YR and LLS fungal spores had a different ice-nucleating activity compared to species such as *Fusarium*, which are proteinaceous.

This observation suggests that there is another substance which is attributable to the ice-nucleating activity of these fungal species. We hypothesise that this ice-active substance could originate from the mucilage which is excreted at the surface of fungal spores. Previous work has attributed the ice-nucleating ability of pollen grains to polysaccharide macromolecules found at the surface of pollen grains (Augustin et al., 2013; Dreischmeier et al., 2017). Since polysaccharides are secreted as part of the mucilaginous material at the surface of fungal spores, they may also be responsible for the observed ice-nucleating activity of YR and LLS spores. However, other substances, such as glycoproteins and amino acids are also released within the mucilaginous material of fungal spores, meaning that the observed ice-nucleating activity could be attributable to some other substance present at the surface of the spores. I propose that future work could attempt to identify the ice-active material responsible for the ice-nucleating activity of these fungal species using spectroscopy techniques such as those demonstrated in Dreischmeier et al. (2017). This would allow the identification of compounds present on the surface of fungal spores, but would not identify which compounds are responsible for the observed freezing behaviour. I would propose that these experiments be coupled with a bottom-up approach, such as the approach used in Chapter 3, to examine pure suspensions of these compounds and analyse their ice-nucleating abilities in comparison with the fungal spore suspensions. Identifying the substance responsible for the observed ice-nucleating activity in these fungal species would allow better predictions of the ice-nucleating activities and how the changing climate may impact this ice-nucleating activity in the future.

Chapter 5 investigated the distribution of ice-nucleating material throughout aerosolised soil samples collected from the University of Leeds Farm. To further the conclusions of this study, I propose that future work would use the same Dust Tower aerosolisation technique to investigate a wider variety of agricultural soil samples, from various regions associated with different crop types, and test whether the conclusions hold across soils from different locations. Future work could also analyse different mineral dust aerosols using the same technique. Previous work, such as Reicher et al. (2019) and Mason et al. (2016), analysed the size distribution of ambient dust events; however, the aerosol chamber technique demonstrated in Chapter 5 allows for more controlled investigations of the size-segregated INP concentrations of various mineral dust aerosols. Using this technique to analyse dust samples collected in a variety of locations, including major dust sources, could provide significant insight into the ice-nucleating ability of different dust aerosols

and their impact on cloud glaciation.

A key finding in this thesis was the wide range of freezing activities observed across different samples of agricultural soils. Previous work has also shown a wide range in ice-nucleating activity across different soil samples which has not been explained by differences in organic matter content or the presence of ice-active proteins (Conen et al., 2011; Garcia et al., 2012; O'Sullivan et al., 2014; Steinke et al., 2016). I propose a more complex intercomparison study to better understand the similarities and differences in the composition and ice-nucleating activity of different agricultural soils. For example, this thesis highlighted the potential importance of ice-active proteins to the ice-nucleating activity of agricultural soils (Chapter 3), however, we were unable to confirm whether bacterial or fungal proteins may be contributing more to this ice-nucleating activity. Furthermore, we investigated the ice-nucleating activity of two fungal pathogens in Chapter 4 and found that their ice-nucleating activity per spore was greater than that of mineral dust. We also found that the ice-nucleating activity of these spores is fairly stable over time and despite the viability of the spores themselves, indicating that if these spores are present in agricultural soils, they could accumulate over time, building their relative contribution to the soil's ice-nucleating activity. So, a complex study would also investigate the relative contribution of fungal spores to the ice-nucleating activity of agricultural soils. Finally, in Chapter 5, we found that the ice-nucleating ability of agricultural soil is evenly distributed across the size range of the aerosolised dust. By investigating a wide range of samples, I would hope that we could identify what causes this even distribution of ice-nucleating activity and whether this activity is attributable to one type of substance found across the size distribution of the dust.

References

Augustin, S., Wex, H., Niedermeier, D., Pummer, B., Grothe, H., Hartmann, S., Tomsche, L., Clauss, T., Voigtländer, J., Ignatius, K., and Stratmann, F. (2013). Immersion freezing of birch pollen washing water. *Atmospheric Chemistry and Physics*, 13(21):10989–11003.

Beall, C. M., Lucero, D., Hill, T. C., DeMott, P. J., Stokes, M. D., and Prather, K. A. (2020). Best practices for precipitation sample storage for offline studies of ice nucleation in marine and coastal environments. *Atmospheric Measurement Techniques*, 13(12):6473–6486.

Bzdek, B. R., Reid, J. P., Malila, J., and Prisle, N. L. (2020). The surface tension of surfactant-containing, finite volume droplets. *Proceedings of the National Academy of Sciences*, 117(15):8335–8343.

Conen, F., Morris, C. E., Leifeld, J., Yakutin, M. V., and Alewell, C. (2011). Biological residues define the ice nucleation properties of soil dust. *Atmospheric Chemistry and Physics*, 11(18):9643–9648.

DeMott, P. J., Prenni, A. J., Liu, X., Kreidenweis, S. M., Petters, M. D., Twohy, C. H., Richardson, M. S., Eidhammer, T., and Rogers, D. C. (2010). Predicting global atmospheric ice nuclei distributions and their impacts on climate. *Proceedings of the National Academy of Sciences*, 107(25):11217–11222.

Dreischmeier, K., Budke, C., Wiehemeier, L., Kottke, T., and Koop, T. (2017). Boreal pollen contain ice-nucleating as well as ice-binding 'antifreeze' polysaccharides. *Scientific Reports*, 7(1):41890.

Felgitsch, L., Baloh, P., Burkart, J., Mayr, M., Momken, M. E., Seifried, T. M., Winkler, P., Schmale III, D. G., and Grothe, H. (2018). Birch leaves and branches as a source of ice-nucleating macromolecules. *Atmospheric Chemistry and Physics*, 18(21):16063–16079.

Fröhlich-Nowoisky, J., Hill, T. C. J., Pummer, B. G., Yordanova, P., Franc, G. D., and Pöschl, U. (2015). Ice nucleation activity in the widespread soil fungus *Mortierella alpina*. *Biogeosciences*, 12(4):1057–1071.

Garcia, E., Hill, T. C. J., Prenni, A. J., DeMott, P. J., Franc, G. D., and Kreidenweis, S. M. (2012). Biogenic ice nuclei in boundary layer air over two U.S. High Plains agricultural regions. *Journal of Geophysical Research: Atmospheres*, 117(D18).

Haga, D. I., Iannone, R., Wheeler, M. J., Mason, R., Polishchuk, E. A., Fetch Jr., T., van der Kamp, B. J., McKendry, I. G., and Bertram, A. K. (2013). Ice nucleation properties of rust and bunt fungal spores and their transport to high altitudes, where they can cause heterogeneous freezing. *Journal of Geophysical Research: Atmospheres*, 118(13):7260–7272.

Hartmann, S., Ling, M., Dreyer, L. S. A., Zipori, A., Finster, K., Grawe, S., Jensen, L. Z., Borck, S., Reicher, N., Drace, T., Niedermeier, D., Jones, N. C., Hoffmann, S. V., Wex, H., Rudich, Y., Boesen, T., and Šantl Temkiv, T. (2022). Structure and Protein-Protein Interactions of Ice Nucleation Proteins Drive Their Activity. *Frontiers in Microbiology*, 13:872306.

Iannone, R., Chernoff, D. I., Pringle, A., Martin, S. T., and Bertram, A. K. (2011). The ice nucleation ability of one of the most abundant types of fungal spores found in the atmosphere. *Atmospheric Chemistry and Physics*, 11(3):1191–1201.

Ickes, L., Porter, G. C. E., Wagner, R., Adams, M. P., Bierbauer, S., Bertram, A. K., Bilde, M., Christiansen, S., Ekman, A. M. L., Gorokhova, E., Höhler, K., Kiselev, A. A., Leck, C., Möhler, O., Murray, B. J., Schiebel, T., Ullrich, R., and Salter, M. E. (2020). The ice-nucleating activity of Arctic sea surface microlayer samples and marine algal cultures. *Atmospheric Chemistry and Physics*, 20(18):11089–11117.

Lukas, M., Schwidetzky, R., Kunert, A. T., Pöschl, U., Fröhlich-Nowoisky, J., Bonn, M., and Meister, K. (2020). Electrostatic Interactions Control the Functionality of Bacterial Ice Nucleators. *Journal of the American Chemical Society*, 142(15):6842–6846.

Maki, L. R., Galyan, E. L., Chang-Chien, M.-M., and Caldwell, D. R. (1974). Ice Nucleation Induced by Pseudomonas syringae. *Applied Microbiology*, 28(3):456–459.

Mason, R. H., Si, M., Chou, C., Irish, V. E., Dickie, R., Elizondo, P., Wong, R., Brintnell, M., Elsasser, M., Lassar, W. M., Pierce, K. M., Leaitch, W. R., MacDonald, A. M., Platt, A., Toom-Sauntry, D., Sarda-Estève, R., Schiller, C. L., Suski, K. J., Hill, T. C. J., Abbatt, J. P. D., Huffman, J. A., DeMott, P. J., and Bertram, A. K. (2016). Size-resolved measurements of ice-nucleating particles at six locations in North America and one in Europe. *Atmospheric Chemistry and Physics*, 16(3):1637–1651.

O'Sullivan, D., Murray, B. J., Malkin, T. L., Whale, T. F., Umo, N. S., Atkinson, J. D., Price, H. C., Baustian, K. J., Browse, J., and Webb, M. E. (2014). Ice nucleation by fertile soil dusts: relative importance of mineral and biogenic components. *Atmospheric Chemistry and Physics*, 14(4):1853–1867.

Perkins, R. J., Vazquez de Vasquez, M. G., Beasley, E. E., Hill, T. C. J., Stone, E. A., Allen, H. C., and DeMott, P. J. (2020). Relating Structure and Ice Nucleation of Mixed Surfactant Systems Relevant to Sea Spray Aerosol. *The Journal of Physical Chemistry A*, 124(42):8806–8821.

Polen, M., Lawlis, E., and Sullivan, R. C. (2016). The unstable ice nucleation properties of Snomax® bacterial particles. *Journal of Geophysical Research: Atmospheres*, 121(19):11,666–11,678.

Qiu, Y., Hudait, A., and Molinero, V. (2019). How Size and Aggregation of Ice-Binding Proteins Control Their Ice Nucleation Efficiency. *Journal of the American Chemical Society*, 141(18):7439–7452.

Reicher, N., Budke, C., Eickhoff, L., Raveh-Rubin, S., Kaplan-Ashiri, I., Koop, T., and Rudich, Y. (2019). Size-dependent ice nucleation by airborne particles during dust events in the eastern Mediterranean. *Atmospheric Chemistry and Physics*, 19(17):11143–11158.

Steinke, I., Funk, R., Busse, J., Iturri, A., Kirchen, S., Leue, M., Möhler, O., Schwartz, T., Schnaiter, M., Sierau, B., Toprak, E., Ullrich, R., Ulrich, A., Hoose, C., and Leisner, T. (2016). Ice nucleation activity of agricultural soil dust aerosols from Mongolia, Argentina, and Germany. *Journal of Geophysical Research: Atmospheres*, 121(22):13,559–13,576.

A Tensiometer Setup

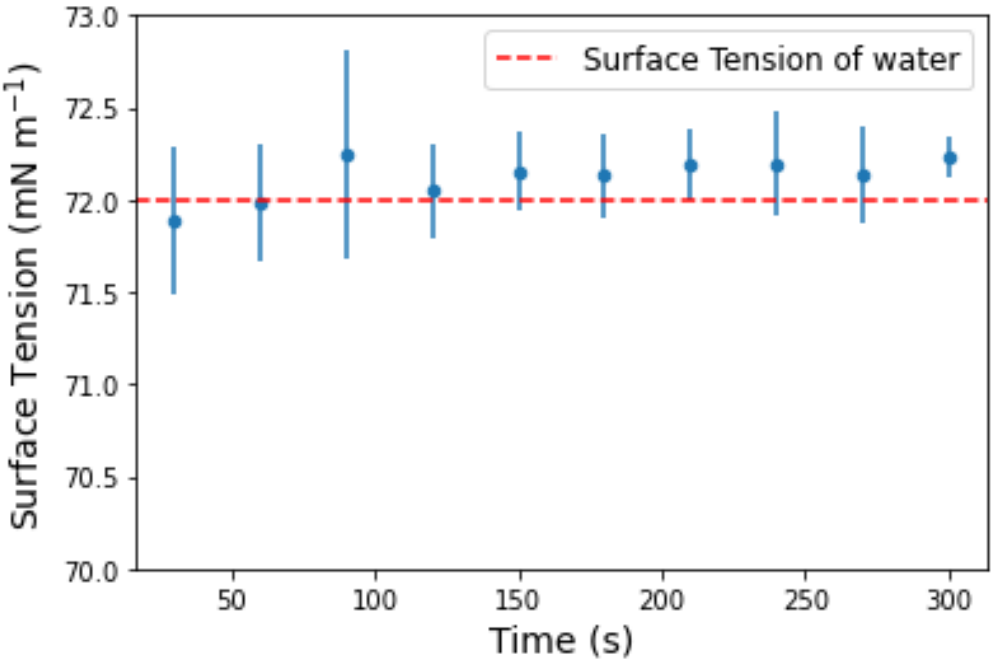

Figure A.1: Average surface tension measurement of MilliQ water droplet measured every 30 seconds over 5 minutes. *The error bars represent the standard deviation of three different experiments*

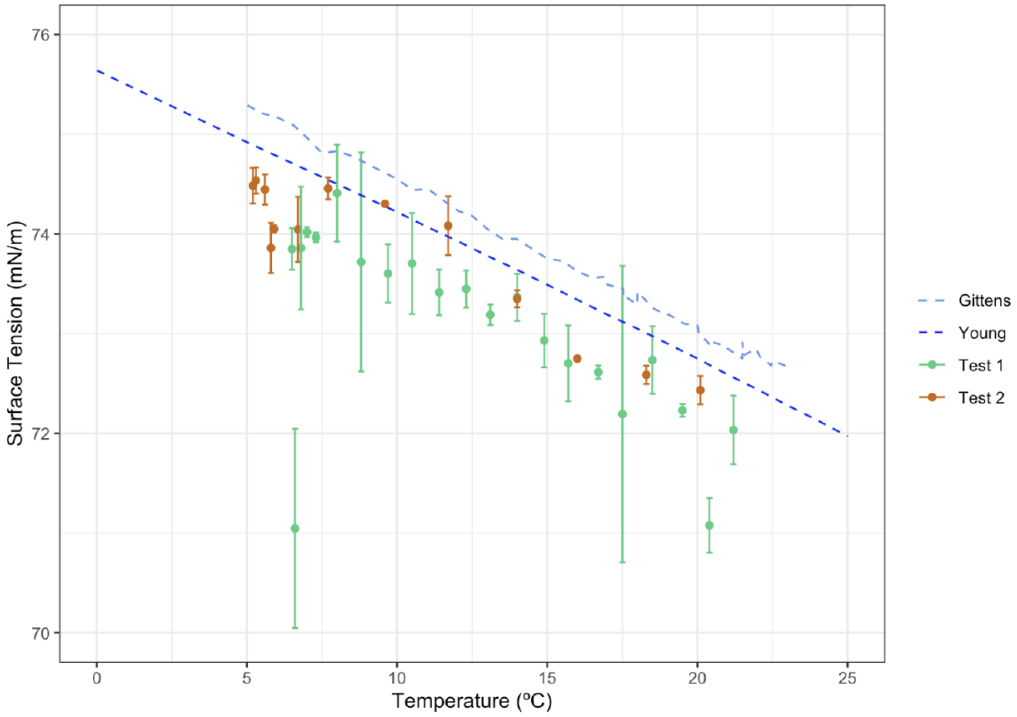

Figure A.2: Surface tension measurement of MilliQ water droplet with changing temperature. *Compared against literature data from Gittens (1969) and Young and Harkins (1928). Credit to Nicole Link.*